

LEVIDUCTION - A STUDY IN ELECTROMAGNETIC LEVITATION

by

Alan Attwood, B.Sc.(Eng.), A.C.G.I.

July 1978

A thesis submitted for the degree of Doctor of Philosophy
of the University of London and for the Diploma of Imperial College

Electrical Engineering Department,
Imperial College,
London SW7.

ABSTRACT OF THESIS

In 1972, by purely empirical methods, a new type of electromagnetic machine was discovered - a linear induction motor capable of producing levitating and laterally-guiding forces in addition to the normal axial propulsive force. The new machine was called an "electromagnetic river". This thesis describes some of the researches which followed the invention.

Firstly several circular and linear versions of the new machine were investigated. Their novel abilities offer some immediate possibilities for industrial exploitation, particular examples being a rotary version acting as a frictionless bearing and a linear version capable of operating in a back-to-back "shuttle" mode. The latter may make it practicable to replace the noisy, impulsive mechanical method for propulsion of a shuttle across a weaving loom by a silent electrical system. More generally the new principle could be applied both to low-speed situations where there is a need for support and guidance without physical contact, and to more dramatic possibilities at high speed where passenger-carrying vehicles could be lifted, guided and propelled by a single set of electromagnetic coils.

Secondly a series of experiments was performed on laboratory-scale models, with the aim of simulating the behaviour of a large-scale electromagnetic river. In an effort to understand the mechanism of stability a new experimental procedure was developed. This allows determination of the distribution of electromagnetic forces acting on a floating conducting plate, from a knowledge only of the surrounding magnetic field. Several theories are discussed concerning the stability mechanism; no single one however has yet succeeded in explaining every aspect of the phenomenon.

Finally a further new invention is described - a "Mark Two" electromagnetic river, superior to the original in all three axes of lift, guidance and propulsion. Time permitted only a preliminary investigation of this most recent class of machine.

A Note on "Leviduction"

Levitation by electromagnetic induction is but one of several distinct methods for the provision of lifting forces by the use of electric and magnetic phenomena. A few of the alternative methods are also capable of providing lateral stabilisation (which becomes guidance if the supported object is moving)..

The acronym "Maglev" was coined for one of the better known of these systems, more fully titled "levitation and stabilisation by means of magnetic forces of attraction". However there has been a tendency to apply this name to the whole subject of electromagnetic levitation, regardless of the particular system under discussion. Such use unfortunately tends to carry with it the implication that the recognised drawbacks to the Maglev system also apply in general.

To emphasise the difference between Maglev and the electromagnetic system that forms the subject of this thesis, it was decided to invent a name applicable only to the latter. The word coined was "leviduction", which is to be regarded as synonymous with "levitation and stabilisation by means of repelling forces between primary and induced secondary currents". There is, however, little call for use of the new word within the body of the thesis, since apart from a few well-defined exceptions the entire subject matter comes under the heading "leviduction". No confusion need arise.

ACKNOWLEDGMENTS

A large number of people were involved in the work that is described in this thesis. To acknowledge all would be impossible, but a particular debt is owed to three groups of personnel.

Firstly the academic staff in and around the laboratory at Imperial College. At the top of the list (in more ways than one) is Professor Eric Laithwaite, whose supervision, guidance and above all enthusiasm kept the work going throughout the three-year period with which this report is concerned. Also present at the time was Dr. J.F. Eastham (now Professor Eastham of Bath University), who with Professor Laithwaite was responsible for the research activities described in Chapter 1, and took much part in all that followed. Many thanks are due also to Dr. H. Bolton and Dr. E.M. Freeman for their invaluable contributions in the way of discussion and ideas, and special thanks to Elizabeth Boden for her help and her quiet and patient organisation of all administrative and secretarial affairs.

None of the work described could have been carried out without the support of the technical staff, headed by the ever-helpful Barry Owen in the laboratory and Colin Jones in the workshop. Particular thanks are due to Cliff Johnson who was responsible for building many of the machines described, and also to Jim McEwen who wound the coils for almost all of the machines, and whose effective but original coil-winding techniques sometimes led to even more permutations of the machines than had been anticipated!

Two people outside Imperial College who deserve special mention are Mr J.G. Steel of the Central Electricity Research Laboratories, Leatherhead, who took continued interest in the progress of the work and made a large number of helpful comments on the presentation of this report, and my father, now retired to the mountains of North Wales, whose attention to fine detail proved of immense value in the final presentation. Lastly appreciation should be expressed of the part played by Paul Jarvis, postgraduate student at Imperial College, and "Mirabel" the friendly college computer, without whose help the diagrams in their present form would not have been possible.

CONTENTS

<u>Chapter</u>	<u>Page</u>
INTRODUCTION	8
1. THE ORIGIN OF THE ELECTROMAGNETIC RIVER	9
1.1 Transpo '72	9
1.2 The Birth of the Electromagnetic River	13
1.3 The Washington Model	17
1.4 An Expanding Geometry	23
2. STABILITY IN ALL AXES	28
2.1 Longitudinal stabilisation	28
2.2 The Magic Carpet	30
2.3 Height, stability and efficiency of levitation	34
2.4 Sustained oscillations	38
3. ELECTROMAGNETIC SPRINGS, WHIRLPOOLS AND OTHER THINGS	43
3.1 The machine with long poles	43
3.2 The double-loop pattern	46
3.3 Circular levitators	50
3.4 The Electromagnetic Whirlpool	55
4. DISTRIBUTION OF FORCE ON FLOATING PLATES	59
4.1 Rotor surface voltage distribution	59
4.2 Rotor surface flux	65
4.3 An analytical approach	70
4.4 Forces by Maxwell Second Stress	75
4.5 Pictorial representation of force distribution	86
5. THE PHASE-MIXED ELECTROMAGNETIC RIVER	90
5.1 Improvements in propulsion	90
5.2 Lift and guidance "for free"	93
5.3 The seven-metre stator	97
5.4 The Electromagnetic Shuttle	102

<u>Chapter</u>	<u>Page</u>
6. LOW FLYING AIRCRAFT	110
6.1 Steel wheel upon steel rail	111
6.2 Contact-free systems	117
6.3 The Electromagnetic River for high-speed transport	126
6.4 Protection against loss of supply	130
6.5 Secondary support system and speed restrictions	133
6.6 Choice of linear motor design	135
7. LABORATORY SIMULATION OF LARGE-SCALE ELECTROMAGNETIC RIVERS	140
7.1 The "Catamaran" Machine	140
7.2 Variable stator core dimensions - use of gramme-ring wound stator blocks	146
7.3 Simulation of a wide electromagnetic river by gramme-ring wound blocks	151
7.4 Human levitation	156
7.5 Levitators turned "the right way up"	158
7.6 The Electromagnetic Track Joint	161
7.7 Electromagnetic Scale Modelling	166
7.8 Tests at high frequency	169
7.9 Tests on load-bearing rotors	175
7.10 Dynamic stability tests	178
7.11 Review of Chapter 7	180
8. THE LECTURE NOTE FLOATER	183
8.1 An Annular Magic Carpet	184
8.2 A square levitator	187
8.3 Return to gramme-ring wound stator blocks	193
8.4 Success at last	197
9. THEORY	200
9.1 A Hypothesis	200
9.2 The Jumping Ring	201
9.3 Arguments with limitations	208
9.4 Stability by attracting and repelling currents	212

<u>Chapter</u>	<u>Page</u>
9.5 Stability over a conventional linear motor	217
9.6 Stability by Shaded-Pole Action	219
9.7 Stability by Rules of Thumb	224
9.8 "Hills of Flux"	228
10. CONCLUSIONS AND RECOMMENDATIONS	234
10.1 Review and suggestions for further work	234
10.2 Addition of backing steel	237
11. POSTSCRIPT - THE XI-CORE MOTOR	240
11.1 Kilowatts per tonne	240
11.2 A new geometry	243
11.3 Design of the Xi-core motor	246
11.4 Performance of the Xi-core motor	250
11.5 Boundaries of stability	255
REFERENCES	263
APPENDIX A. Engineering details of four machines	268
<u>Volume II</u>	272
APPENDIX B. An Alternative Theoretical Approach	273
APPENDIX C. Analytical Derivations of the Mathematical Expressions Used in Appendix B	297
APPENDIX D. Computer Subroutines, Functions and Programs	309
APPENDIX E. Computer Source Code Listings	336

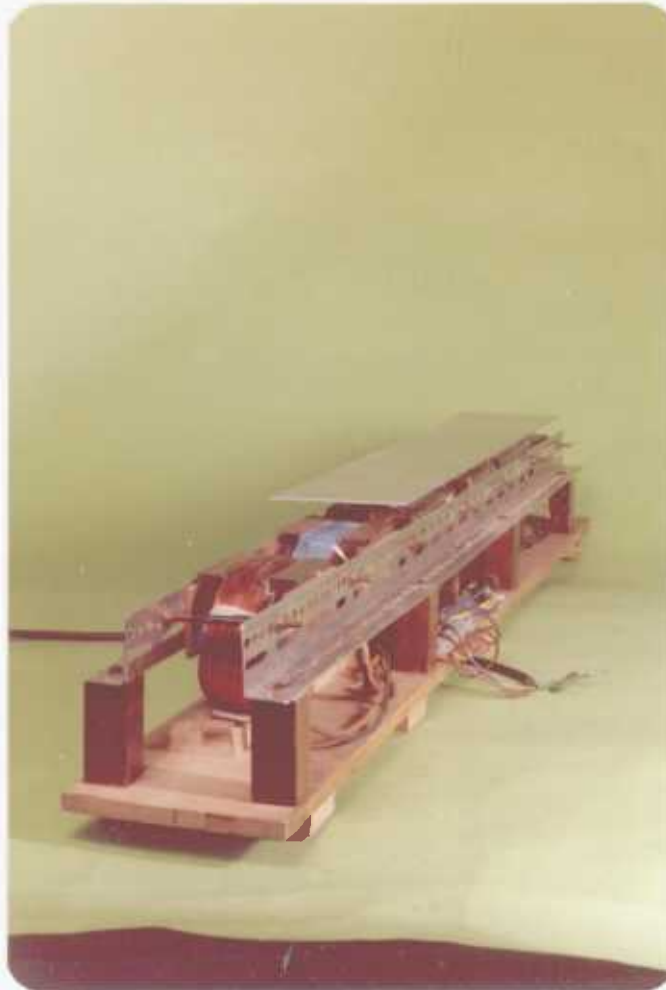
INTRODUCTION

Few inventions or discoveries are made by the direct process of defining a problem, setting out methodically to investigate all possible ideas for solution, gradually eliminating those which are unfruitful until the one remaining solution emerges as the perfect answer - and all in exactly three years, neatly to complete a higher degree! Equally, seldom is success achieved by continually pondering over a problem, turning it around and around until suddenly, in a flash of inspiration, the solution is clear - "Eureka" - in the manner of Archimedes. More often the process is one of fruitless lines of investigation, dead ends, turnings back, followed by an apparently fortuitous "grasshopper jump" into an entirely new plane and direction for no logical reason at all.

It is tempting when writing a final report of one's work to prune the account of these unfruitful branches, to cut off the dead ends and bridge the jumps, until the result is a straightforward path of logical reasoning from beginning to end. The danger in such an approach is that in cutting away the unprofitable sidelines, the fascinating and rewarding phenomena that sometimes lie within them are cut away also. Accordingly, in this thesis, the alternative approach will be adopted - every little sideline will be explored to its fullest extent - and it will be seen that it is in these sidelines that some of the most promising ideas for future research are found.

CHAPTER 1

THE ORIGIN OF THE ELECTROMAGNETIC RIVER



The Washington model (p 21). Ten metres of this design, suitably camouflaged, were sent to the Dulles exhibition.

CHAPTER 1. THE ORIGIN OF THE ELECTROMAGNETIC RIVER

1.1 Transpo '72

The story of the Electromagnetic River began in 1971, when the American Department of Transportation announced plans to hold an international exhibition and conference on systems for high-speed ground transport. "Transpo '72", as it was called, was to take place in May 1972, at Dulles (near Washington), and any company or consortium was welcome to exhibit their plans or working models.

At that time Professor Laithwaite and his linear motor research team at Imperial College were acting as consultants to Tracked Hovercraft Ltd. This was a company set up in 1966 by the National Research and Development Corporation to investigate possible high-speed transport systems using air-cushions for vehicle support and guidance, and linear motors for propulsion. Tracked Hovercraft Ltd. wished to exhibit at Transpo '72, but aware of the pollution-conscious atmosphere prevailing in America (particularly the recently formed opinion that sheer noise is a form of pollution just as objectionable as the many chemical forms), they were reluctant to send a model that depended on noisy air-cushions for support and air-screws for propulsion. Instead they wished to present an all-electromagnetic model - silent, reliable, easily controllable and totally pollution-free.

At this point the managing director of Tracked Hovercraft Ltd. approached Professor Laithwaite for assistance. The project demanded an electromagnetic system never before attempted - namely the provision of three sets of electromagnetic fields, one to lift the vehicle, one to guide it and one to propel; all to act simultaneously without interfering with one another. But as the managing director pointed out, there was already in existence in the heavy machines laboratory at Imperial College a machine which went some way towards achievement of the desired goal. This machine, illustrated in Fig 1, had been shown to float and stabilise rectangular aluminium plates of a variety of sizes between 10 and 30 cm wide. Indeed its performance had led

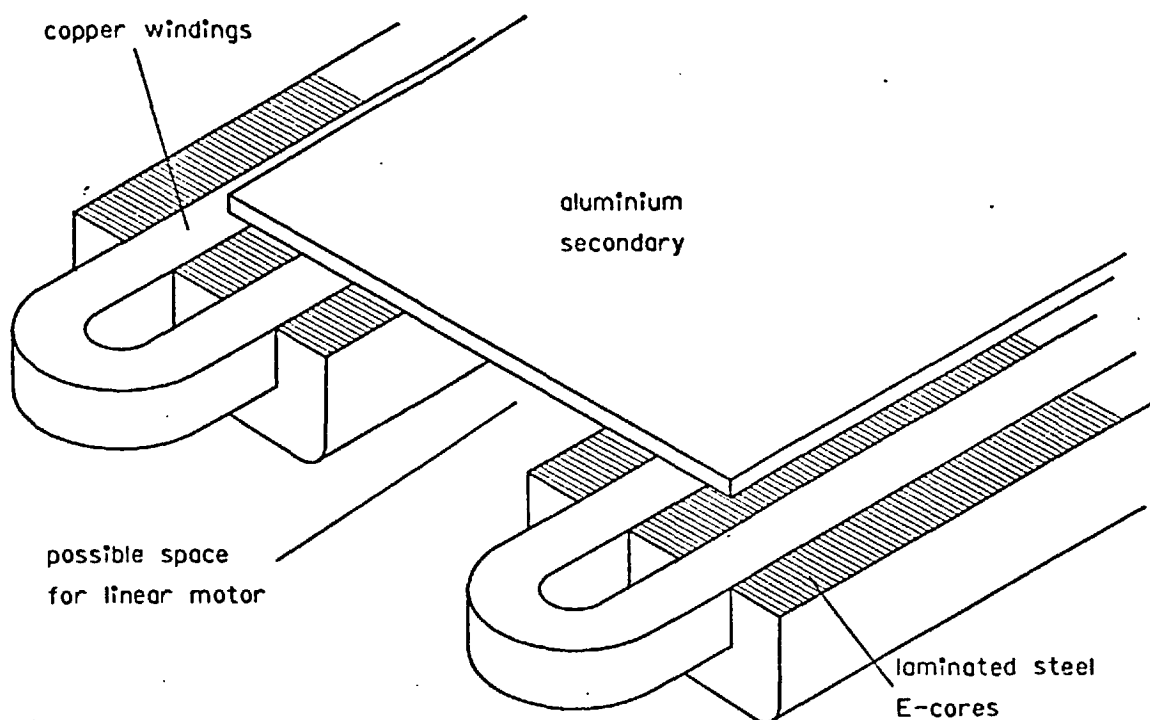


Fig 1. "Flat-plate floater" - the beginnings of the electromagnetic river.

to its being christened "the world's most perfect spirit level", since, as can be seen from the plan view of Fig 2, longitudinal movement of the plate results in no change in magnetic flux linkage, and hence no force tending to increase or reduce the motion. Thus the plate, provided it remains remote from the ends of the machine, floats on a "cushion" of magnetism, with strong guidance laterally and zero resistance to motion longitudinally. The "spirit level" effect turned into a mildly irritating habit when the machine was set up for demonstrations, for no matter how carefully the supporting table was levelled, the plate would always find which end of the machine was the lower, and would gently slide that way. (The irritation was eventually removed by slightly dishing the whole machine to make the centre the lowest point.)

It will be seen that the stator of the machine consists of two separate coils, wound on independent sets of iron laminations.

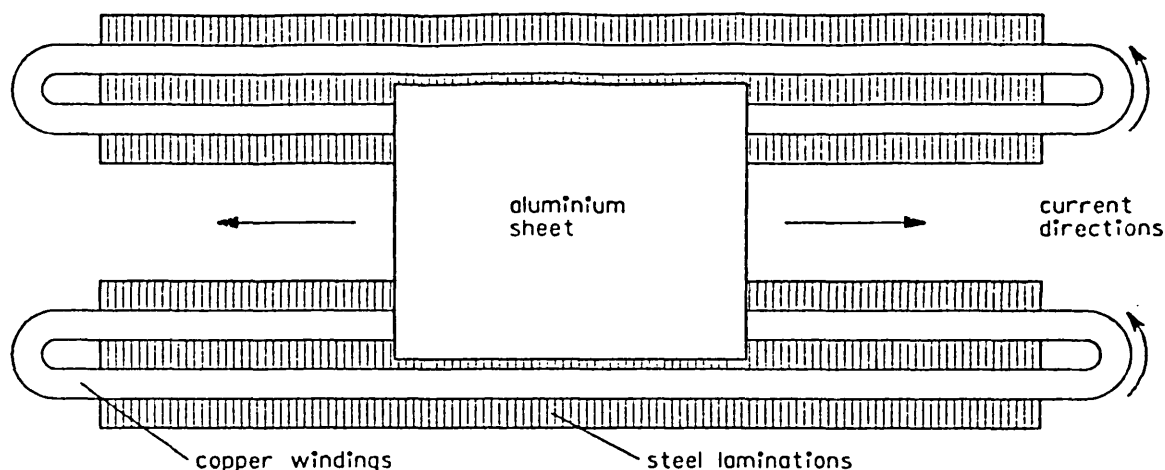


Fig 2. Plan view of the flat-plate floater. The plate is free to move in the directions indicated by the arrows.

The gap between the blocks of laminations can be varied to accommodate various sizes of aluminium plate - there was found, however, a minimum value of the gap (about 5 cm) below which plates cannot be stabilised. It was assumed when considering the machine for a model at the Dulles exhibition that it would be possible to mount a linear motor in this gap to provide the propulsion force.

But first of all there was another problem to be tackled. It has been known for many years that electromagnetic devices become steadily less effective and ultimately impossible as they are made smaller. Now the organisers in Dulles had specified a maximum area per exhibit of 6 m by 10 m, and in order to make a vehicle of correct proportions "look right" on a track only ten metres long it was necessary to restrict its width, and that of the track, to a maximum of ten centimetres. The flat-plate floater was 30 cm wide, and a particular cause for concern was that it could be operated for only about five minutes before overheating - a feature likely to become even more restrictive on a smaller machine. Indeed so acute is the problem of scaling down electromagnetic devices that considerable

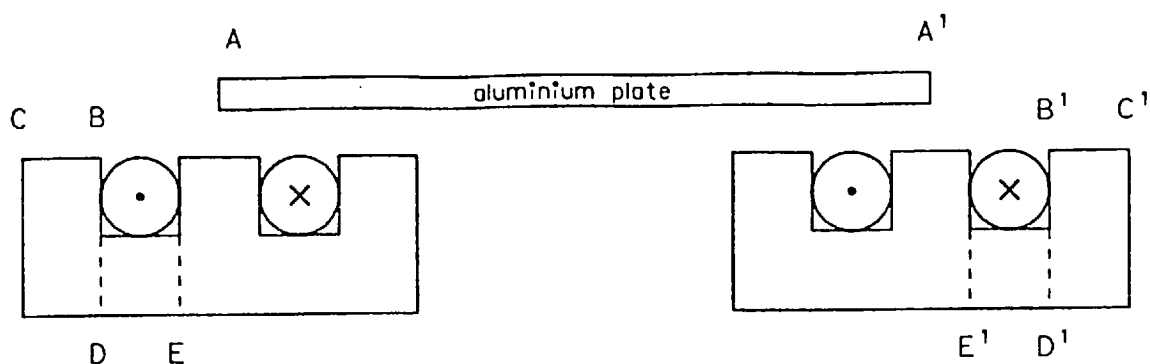


Fig 3. Cross-section through plate floater.

doubt was expressed as to whether it would even be possible to make a working laboratory model only 10 cm wide, let alone a model capable of continuous demonstration in an exhibition.

First ideas for modifications were based on purely intuitive reasoning. Although at the time the mechanism of the lateral stabilising forces was not fully understood, there was a general feeling that it was all a matter of edges - a question of whether a particular edge of the rotor could "see" an edge of the stator. It was known that one of the conditions for stability was that each edge of the aluminium rotor (A and A¹ in Fig 3) should "split" the centre limb of its respective E-shaped stator block. In this position, it was argued, it was unlikely that the rotor edge A could "see" the edges B and C of the stator outer limb. The machine could therefore be made narrower without loss of performance by cutting the outer limbs away - and probably the sections DE could be cut away also, leaving the machine as shown in Fig 4.

At this point it is clear that the main flux paths become as shown in Fig 4, and these should not be affected if the return current conductors on the outside of the steel C-cores were moved down to the positions shown dotted on the diagram, immediately under the cores.

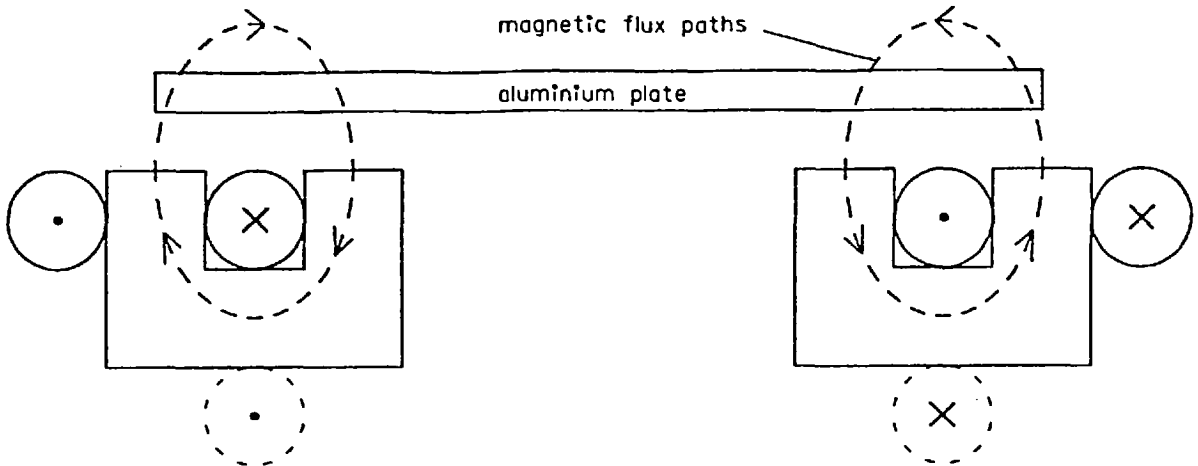


Fig 4. First modification to flat-plate floater.

The machine could then be reduced to a width of 20 cm. This then was the first of the new models to be built - and when tried it proved to be totally unstable.

1.2 The Birth of the Electromagnetic River

Now it happened that on the afternoon of the trial Professor Laithwaite was engaged with a visitor. In the middle of discussion the two men were interrupted by the sudden entry of the Professor's colleague, Dr. Eastham,* who after hurriedly apologising for the interruption, exclaimed "but it's stable!" and promptly disappeared back into the laboratory. Needless to say, the Professor finished with his guest as quickly as was politely possible, and hurried outside to see what his colleague had done. Dr. Eastham had, in fact, taken one of those "grasshopper jumps" of imagination, and for no good reason at all had reversed the current in one of the coils, to produce the system of Fig 5. Such a step seems even less logical when one considers

* Now Professor J.F. Eastham of Bath University.

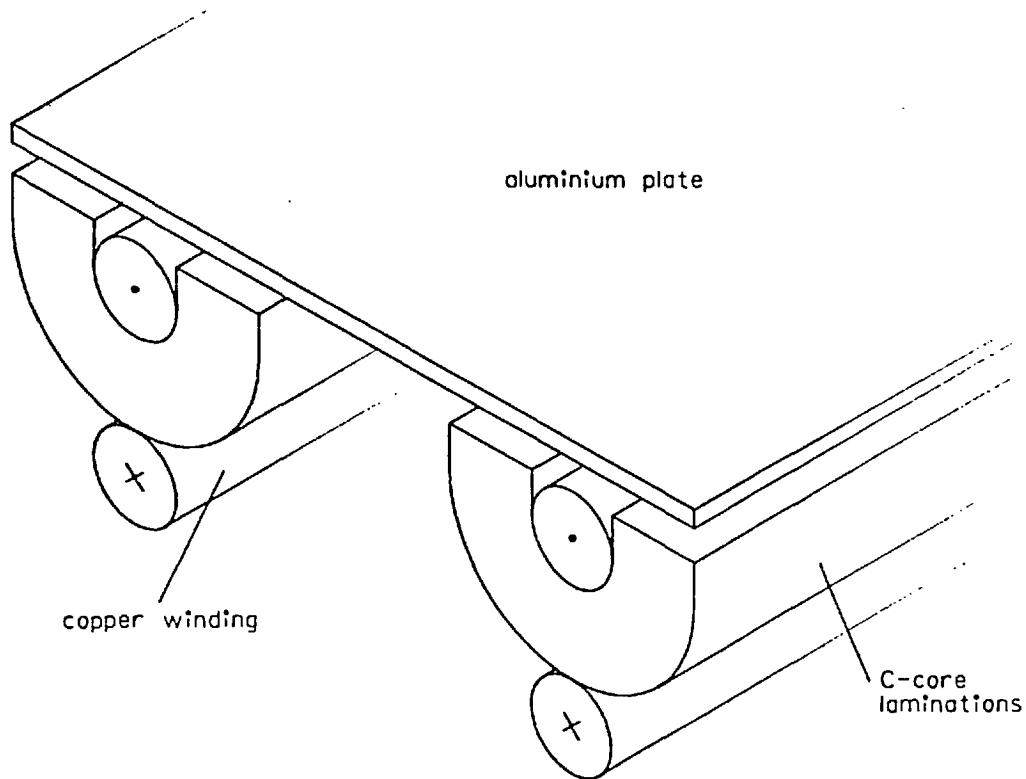


Fig 5. First successful modification to flat-plate floater.

that it was well-known in the laboratory that the same procedure applied to the original flat-plate levitator resulted in a complete loss of stability. (In fact so marked is the difference in behaviour between the two methods of connection that it has never been considered worth the trouble to label the correct polarity of the terminals to the flat-plate floater - it remains an even chance whether one happens to find the stable or the unstable mode when first connecting to the mains supply.)

Those working on the project immediately found themselves confronted with a new world of machines, about which nothing whatsoever was known. It took only a short time to discover that the configuration with the best lateral and roll stability was that illustrated in Fig 5, where the plate width was such that the edges now lay above the outer edges of the stacks of C-cores, and the gap

between the C-cores was still about 5 cm. The system was certainly the narrowest and most promising of those tried so far, so the next step was to consult an industrial organisation about the practicability of constructing ten metres of track to this design. It was soon pointed out that to construct in one unit such a length of narrow track, comprising tens of thousands of laminations and able to withstand shipment across the Atlantic Ocean, was a practical impossibility.

The idea of joining together a number of short sections of track was considered, and rejected on the grounds that each of the coils along the centre of the C-cores consisted of hundreds of turns, every one of which would have to be connected individually. However only a moment or two later Dr. Eastham made two suggestions. Not only could the coils be made in separate sections, but the sections could be short independent coils, fed from a three-phase supply. If the supply were connected in the normal sequence for a linear motor, i.e. R, -Y, B, -R, Y, -B, a travelling magnetic field would be obtained, thus providing the means for propulsion.

This was the birth of the electromagnetic river. Fig 6 is a plan of the first prototype.

It is worth digressing a little at this point to describe the "feel" of the electromagnetic river, from which it will become clear why it was so named. Some time ago an analogy was developed by Professor Laithwaite between the motion of an object floating in a real river, being dragged along by the flow, and the motion of a conducting sheet positioned within the travelling field created by the stator of a linear motor, being dragged along by its "flow".⁽¹⁾ The mathematical expressions for the input power, output power, loss power, slip and efficiency turn out to be identical for both systems.

The analogy is more than a mathematical one however, for if one takes hold of an aluminium plate and gently lowers it towards the surface of a linear motor, into the travelling magnetic field, the

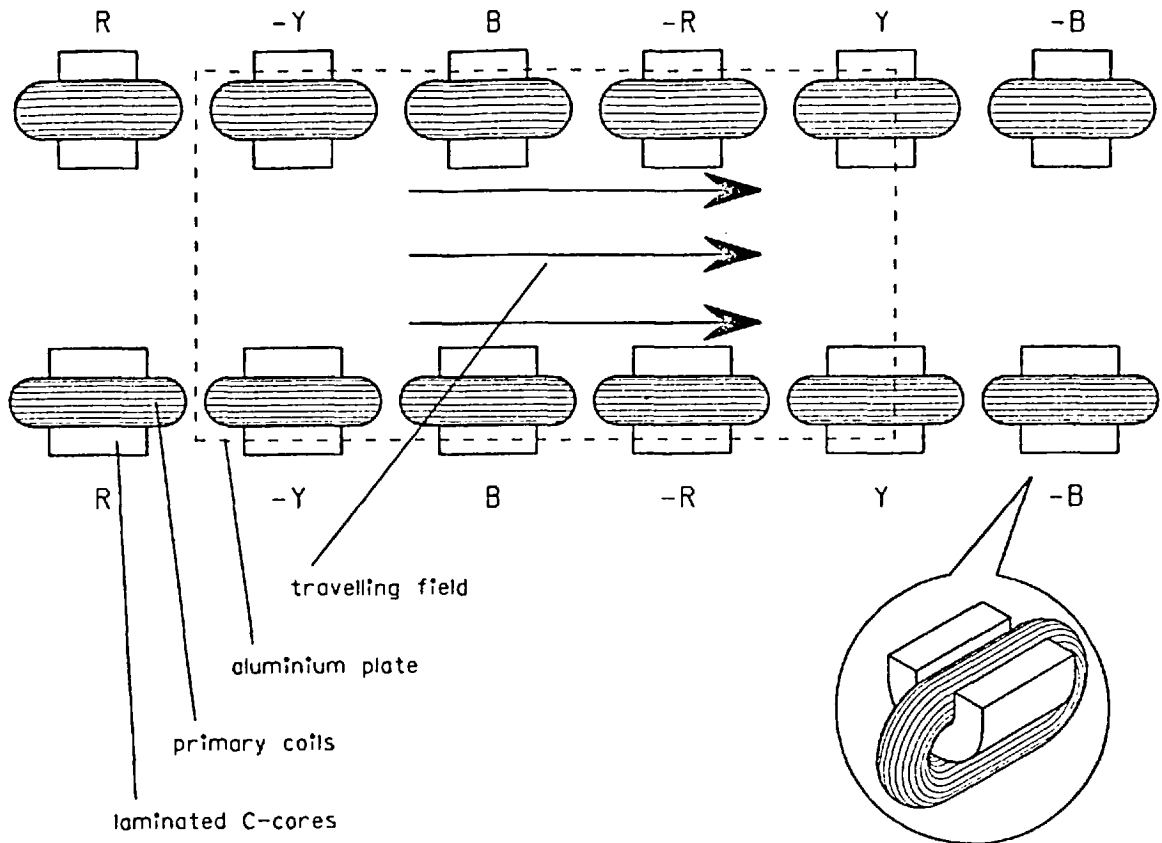


Fig 6. The first electromagnetic river.

feeling is just as though the plate is being dragged along by an invisible fluid flowing above the surface of the motor. One can even define, fairly accurately, the "depth" of the fluid over the stator by feeling for its "surface" (the point at which the pull first becomes significant) - and as might be expected this depth varies with the input voltage to the motor.

But when the same aluminium plate is lowered towards the surface of one of the new machines, the river-like feeling takes on a new dimension of reality. There is a feeling that river banks have come into existence. If an attempt is made to pull the sheet sideways, it is found to rise, up the sloping side of a bank. As the plate is pulled further the gradient begins to decrease, eventually becoming horizontal (thus defining the "height" of the bank), after which the

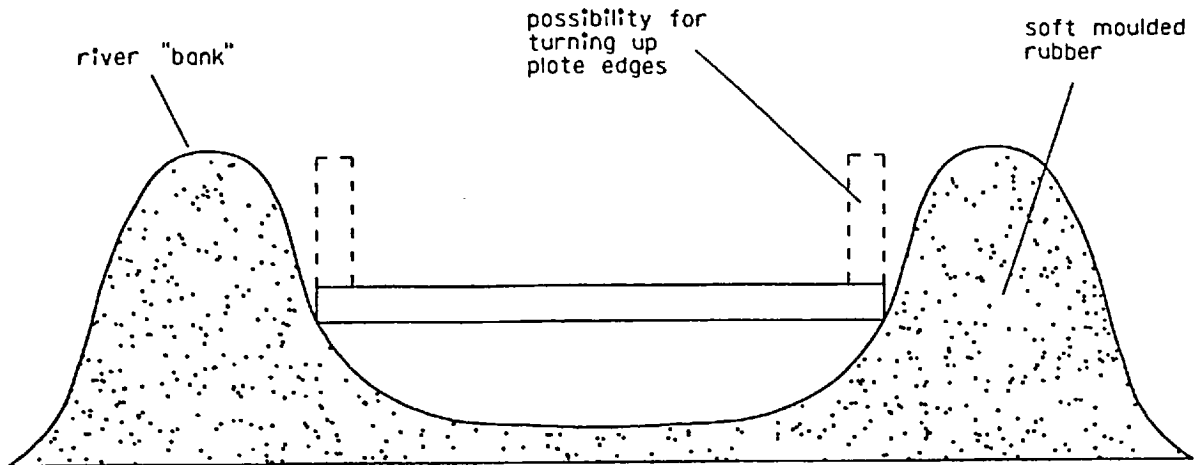


Fig 7. Plate suspended on rubber channel.

plate falls right out of the river. And now a variation of supply voltage affects not only the depth of the river, but the shape of its banks as well. (The nature of this variation will be described in a later chapter.) The whole effect feels much as though the plate were sitting in a trough of soft moulded rubber, of cross-section as shown in Fig 7.

1.3 The Washington Model

When the prototype of Fig 6 was built and tested, it performed sufficiently well for an order to be placed with a manufacturer to build the ten-metre length for the Dulles exhibition. But one aspect of the machine was still disappointing. In order to obtain the required lift (to give a clearance of about 12 mm), and to propel the plate with acceptable acceleration, the coils of the machine carried a current density so high that even with forced cooling a demonstration of two minutes duration could be given only about once an hour. The commercial machine had an air-duct incorporated within it, so that a continuous cooling blast could be forced between the two rows of coils, as shown in Fig 8. This system might have been

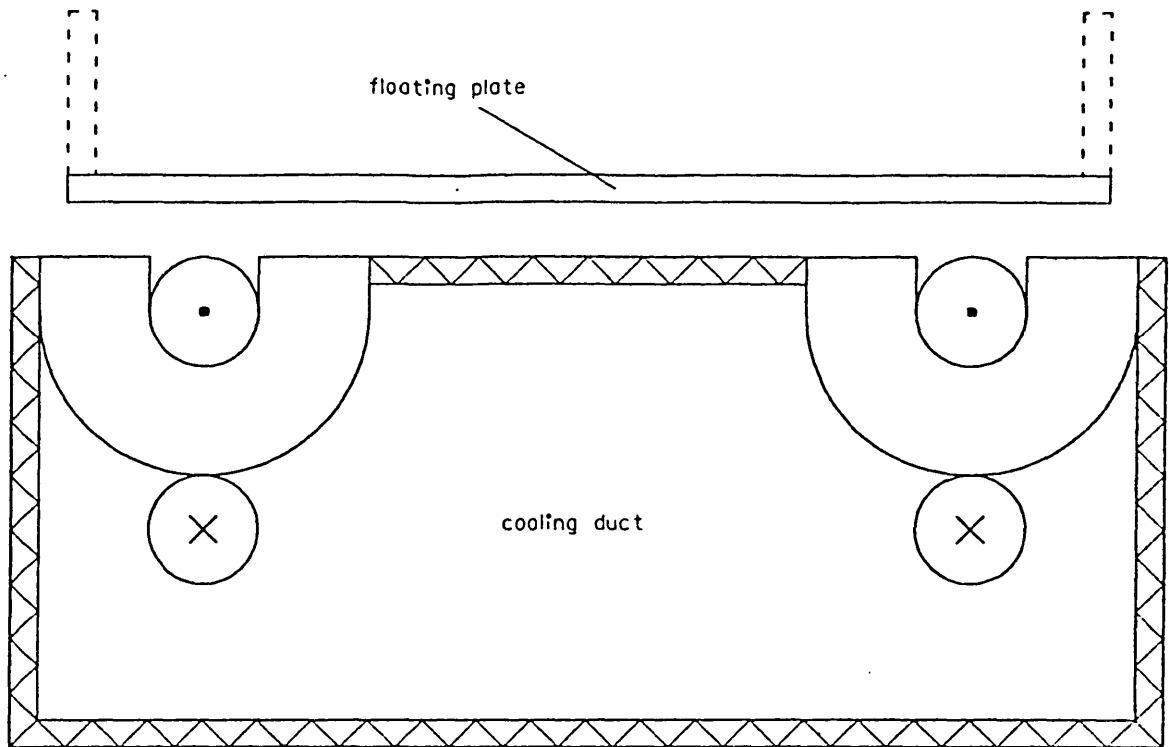


Fig 8. Electromagnetic river incorporating cooling duct.

just about practicable for the demonstration, but the unavoidable noise made by the cooling system was so great that direct use of the blast to provide an air-cushion lift would have been quieter!

Evidently the "goodness factor"* of the machine was still far too low to achieve the desired silent lift and propulsion of a model vehicle. It seemed that to try to design a continuously-rated levitator only 10 cm wide, with built-in guidance and propulsion, was to attempt the impossible. Yet at the same time there was a feeling that since the concept of the electromagnetic river was so new, the design of the prototype was most unlikely to have been the best possible shape at the first attempt. Perhaps an investigation into other shapes might lead to machines with a higher goodness factor.

* A mathematical term related to the performance of the machine - defined in Chapter 2 (page 39).

The propulsion, it was argued, was poor because the floating plate was narrow - necessarily so, to achieve stability. There was thus insufficient room at the edges for the "end-ring" currents to flow, resulting in an enormous Russell and Norsworthy factor^{*(2)} which all but destroyed the machine's performance as a propulsion unit. But it might be possible to bend up the edges of the plate to allow the end-ring currents to flow in a vertical plane, while retaining the horizontal dimensions and preserving the stability unchanged.

Accordingly a "trough" secondary was constructed, as shown by the dotted lines in Figs 7 and 8. The result of this modification was that the propulsive force increased by about three times, while the stability forces remained almost unchanged. The lift was also slightly increased. It was later realised that this was the first of a series of truly three-dimensional machines, with secondary currents flowing along and across the horizontal section of the plate and up the vertical sections. Perhaps it is not surprising that a machine involving electromagnetic control in unconventional planes should have produced current flow patterns in equally unconventional dimensions.

The thought then occurred that since providing an easier path for the return currents in the plate edges had resulted in a three-fold improvement in propulsion, even further improvement might be obtainable by similarly helping the return currents in the centre of the plate. A secondary of the form shown in Fig 9 was constructed. But this time the result was a disaster - the compound plate was totally unstable in roll. At the time the reason for this was obscure; later work however has gone some way towards providing an explanation.

* The Russell and Norsworthy factor is a mathematical correction factor developed to enable appropriate allowance to be made for the effects of end-ring current paths along the edges of a secondary. See reference 2.

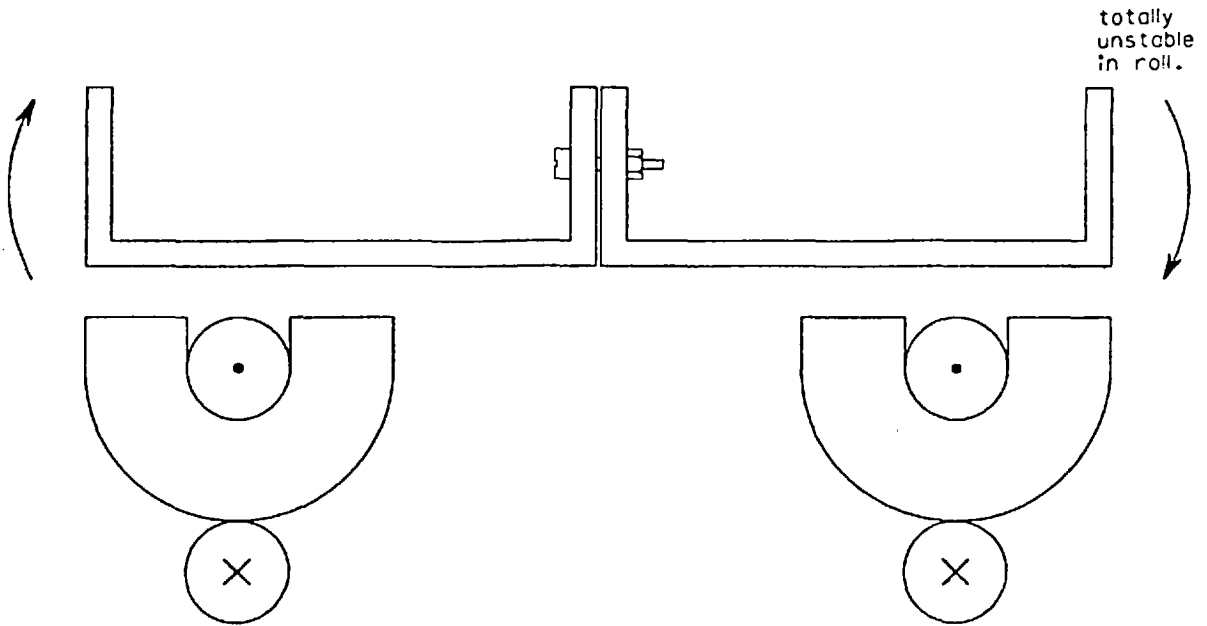


Fig 9. Double-trough rotor in an effort (unsuccessful) to improve propulsion.

The next stage of development was another of those unpredictable "grasshopper jumps", and is probably best explained by relating events as they occurred. Late in the evening of the day when the unsuccessful double trough was tested, Professor Laithwaite and Dr. Eastham were ready to depart for home. Dr. Eastham first put the idea into words - "I suppose it would be silly to try just one half of the secondary over a single row of coils". Certainly the suggestion did not sound promising. All the laboratory staff working on levitators knew that stable levitation had always required at least two coils in the primary. Every single coil system ever tested had actively thrown off all conducting secondaries.

But it was a simple matter to unbolt the two halves of the double plate and try one alone, above one of the rows of primary coils. When this was done the single trough floated, stable but slightly tilted. A moment later both men simultaneously reached

the same conclusion about the reasons for the tilt - "that's only because of the other half". While floating over one set of coils the plate was being tilted by the currents in the other set.

By this time the laboratory workshop was closed and no more could be done. The first prototype had been constructed with the two parallel sets of coils mounted on a wooden base, so the following morning the machine was literally cut into halves by a single run of a band-saw along the centre of the machine. The two halves were re-mounted end-to-end, and the machine tried again - with complete success. The trough now floated stable and level, and experienced a strong propulsion force - and the whole machine was now only 5 cm wide. Expectations were high indeed in the laboratory during the day of building the bigger version, 10 cm wide, since to double every dimension is to increase the goodness factor by four times.*

The model itself came to be known as the "Washington model" since although only a one metre length, comprising six cores and coils, was constructed for laboratory use, it was ten metres of this design that was finally built and sent to the Dulles exhibition. While it is true that the first electromagnetic river was that shown in Fig 6, it is with the Washington model of Fig 10 that we reach what the literary or musical expert would call the "definitive version" of the work. This is the simplest version of the electromagnetic river - it is the basic machine upon which all later developments have been founded. Many times it has been said that the best ideas are the simplest; at the same time, the best machines to be built on those simple ideas are the ones upon which a great deal of detailed development and design work has been done - eventually producing a highly sophisticated and complex piece of engineering operating on a simple principle. The major part of this thesis is concerned with developments in a number of directions from the Washington model.

* See explanation of goodness factor given in Chapter 2 (page 39).

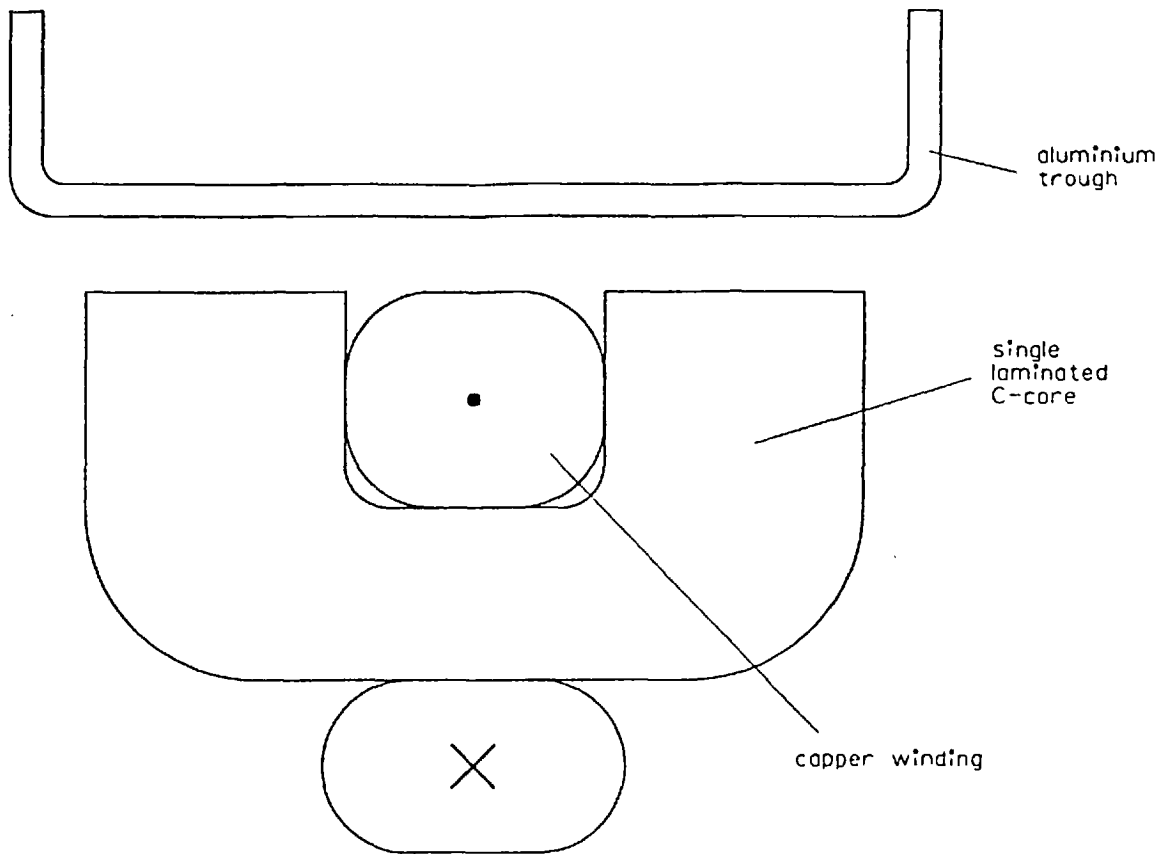


Fig 10. "Definitive version" of the electromagnetic river.

The stator itself behaved admirably. It was found to levitate flat plates stably at a height of several centimetres, damping out oscillations in the five axes of roll, pitch, yaw, vertical bounce and lateral shift, and in the sixth axis (longitudinal) the plate was propelled. And all this with a stator current density no greater than is found in many a commercial continuously-rated rotating machine.

In only one aspect was its performance lacking. While the damping in four of the five stable axes was generally good, damping in roll motion was not adequate - if the vehicle suffered a roll disturbance

as it started, it was still oscillating about this axis at the end of the ten-metre run. Several plates of different sizes were tested and it was found that no longer was there a single definite "best" size of plate for stability, as had been the case with the earlier models. Instead there was now the possibility of exchange between the two parameters height and stability. As the secondary was made progressively wider, for the same stator current, it became steadily less well damped to lateral displacements, while becoming better damped in roll. At the same time it floated at a greater height above the stator, and experienced a greater propulsive force. Thus the optimum width was a compromise between on the one hand obtaining maximum lift, thrust and roll stability, whilst on the other hand retaining sufficient lateral stability. The situation was even further complicated when plates with turned-up edges were included in the investigation. This complex subject of stability will be discussed further in later chapters.

1.4 An Expanding Geometry

There was yet one further unexpected feature of the Washington model. Earlier forms of electromagnetic levitating machines had invariably comprised two primary coils, carrying currents differing in phase (sometimes exactly in anti-phase). Investigations had shown that there was always a region above these coils within which small pieces of conductor (not large enough significantly to affect the magnetic field) were attracted towards the primary. Outside this region similar pieces were repelled. When attempting to levitate larger pieces of conductor, one of the conditions for stability was that the centre of gravity of the secondary should lie within this region of attraction. If the primary current were increased in an attempt to raise the floating object, a maximum height would always be found above which the secondary ceased to cut the region, and stability was lost.

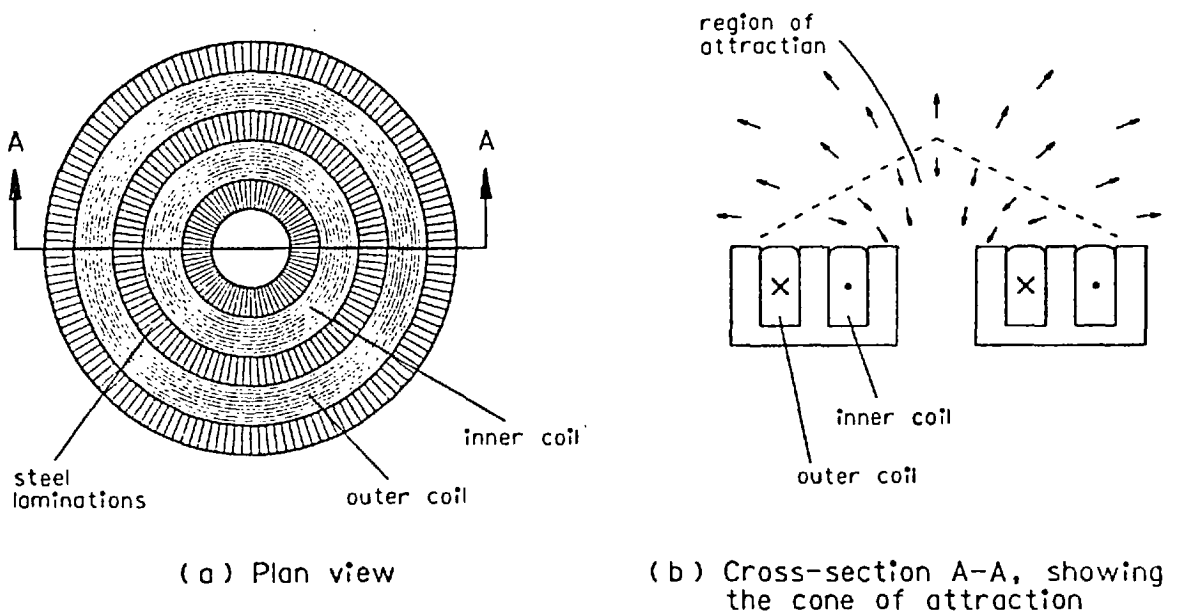


Fig 11. Circular disc-floater.

For a primary comprising two concentric circular coils, as in the disc-floater of Fig 11, the region of attraction was found to be a conical shape (see Fig 11(b)). Similarly, for a rectangular machine such as the original flat-plate floater of Fig 2, the region of attraction is a triangular prism with its parallel edges lying along the length of the machine.

It may be shown analytically that the cone or prism is always "shallow", i.e. the maximum levitated height for any plate, circular or rectangular, is small compared with its width. To use the words of Professor Laithwaite, "It was therefore assumed that there was some ultimate limit placed on the height at which a piece of metal could be floated clear of a primary coil system for a given supply frequency. Such a limitation, if it existed, would not have been unique in the subject of electromagnetism. Rather it would have been added to the list of analogous phenomena such as:

- (a) There is a minimum size of single-phase induction motor which can run, for a given supply frequency.
- (b) There is a minimum size of shunt generator which can self-excite for a given rotor speed."

Accordingly it was assumed that if the primary current of the Washington model were increased, the corresponding increase in rotor height would eventually lead to total instability. A wide sheet was chosen to demonstrate this effect, since its extra height of levitation put it already nearer the limit of lateral stability. When the stator current was raised, the plate not only lifted to a still greater height, but to everybody's surprise, it became significantly more stable laterally. When the current was then kept constant at its new value, it was discovered that a second plate, wider than the first, could be floated with the same degree of lateral stability as had the first plate at the lower current level. Again the height and stability of this second plate could be increased by raising the primary current still further.

Here was a new phenomenon indeed. Far from there being a triangular prismatic region of attraction as expected, there appeared instead to be an inverted prism of indefinite eventual height and width - an expanding geometry that had no limit. Fig 12 shows three possible configurations, each with its appropriate stator current. Any plate wider than the stator core can be "wedged" into the boundaries indicated by the dotted lines, and can be floated stably in that position provided that the stator current is sufficient to support it at that height. It was the realisation that there was no longer any theoretical limit to the height of levitation that led to two further ideas. Firstly it should be possible to design a much wider stator, to lift wide plates without the need for excessive height or current densities. Secondly large masses could be supported on these wide plates, and propelled at high speed. Indeed there seemed no reason why a full-scale vehicle of perhaps 50 tonnes weight should not be lifted, guided and propelled at say 400 kph by a purely electromagnetic system.

A few observations might not be out of place about the Dulles exhibition itself. The ten-metre track was fabricated in eight

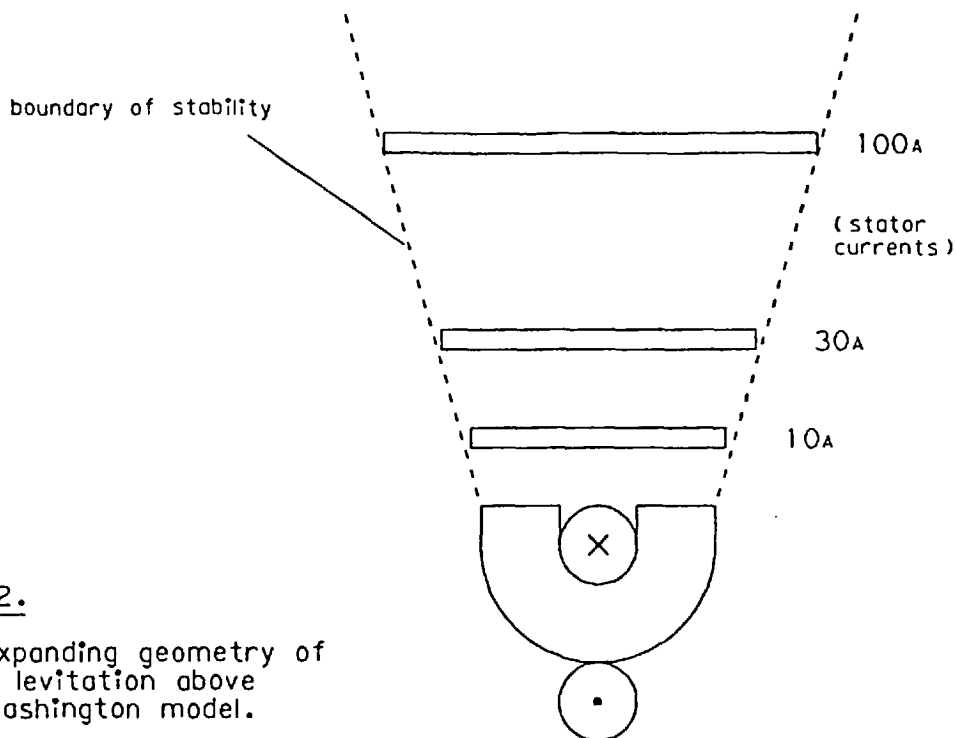


Fig 12.

The expanding geometry of stable levitation above the Washington model.

sections, each with its laminations and coils enclosed in a solid block of epoxy resin. The stator was thereby made absolutely silent, there being no portion of the windings or laminations free to vibrate to create the usual mains buzz. However at the same time the current rating of the machine was seriously reduced as a result of the poor heat-conducting qualities of the resin. The manufacturers attempted to overcome this problem by constructing a system of photo-detectors and switches to activate successively the individual coils as the vehicle approached. Even then, the demonstrations had to be limited to only one run every two minutes.

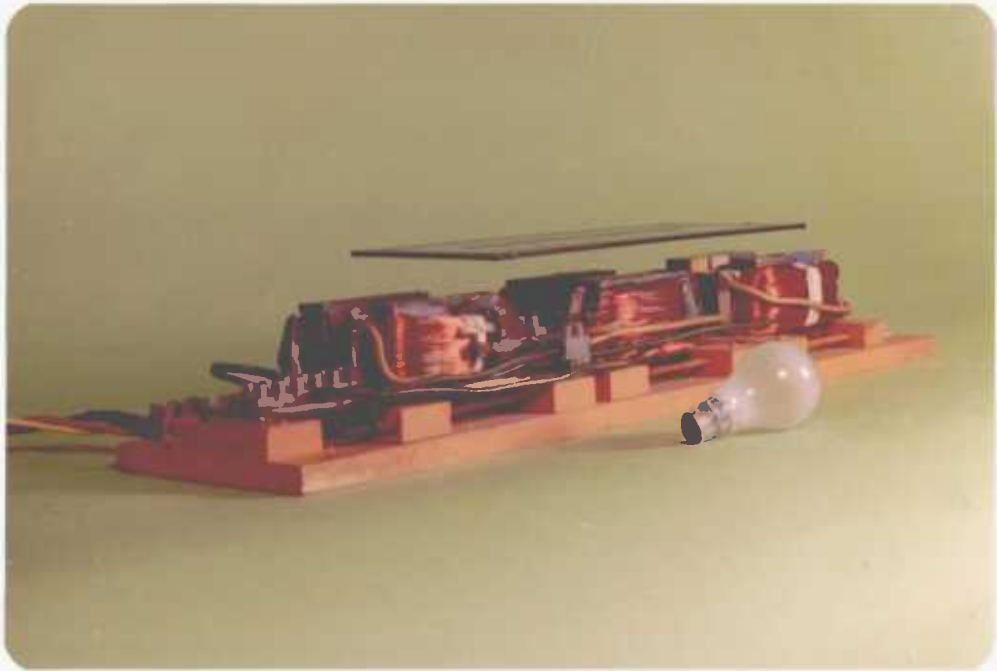
In the event, this restriction was turned into an asset for exhibition purposes. The track had, of course, been appropriately decorated and set against a futuristic-looking painted background. The majority of the track was supported on a viaduct across a model countryside, while a metre or so was hidden in a tunnel at one end and in a cutting at the other. The secondary, in the form of a

colourful streamlined model vehicle, consisted of a light fibreglass body constructed around a wide aluminium plate as its base. The time taken for the vehicle to travel along the track and back was only about five seconds so for most of the time nothing was happening at all, which itself tended to provide an air of expectancy for the people around the stand. Then once every two minutes, without warning, the system switched itself on and the vehicle appeared out of the tunnel floating a centimetre or two above the track. It glided swiftly into the cutting, paused for a second or two, then sped equally rapidly back along the track into the tunnel - all with no more than a slight swishing sound to mark its progress.

To the general public, the track looked like an oddly-proportioned proverbial black box (ten metres long and ten centimetres square in cross section). There was no clue that the box concealed anything active inside it so the spectators might be excused for thinking that the vehicle contained some amazing system of electronics or electromagnetics - presumably with its own internal energy source as well. This illusion was deliberately shattered by Tracked Hovercraft about once every half an hour, when the vehicle was replaced by an ordinary plate of aluminium that was allowed one return trip only!

CHAPTER 2

STABILITY IN ALL AXES



The "magic carpet" machine (p 30).
The plate being floated is 40 cm long by 15 cm wide.

CHAPTER 2. STABILITY IN ALL AXES

When Michael Faraday spent many years of his life investigating the mysteries of electromagnetic induction, he did so not because he was interested in the possible uses towards which his discoveries were leading, or out of a desire to give to the world a new method of energy conversion. He carried on his work simply out of sheer curiosity and fascination with the extraordinary effects he could produce, and with a desire to explain the new phenomena. When Henry Ford laboriously put together his first motor car in a little garage in the back-streets of Detroit, his ideals were not to provide humanity with the cheapest, most convenient form of personal transport ever known; he was merely pursuing his own hobby, trying to achieve with his own hands what he knew had been done in Europe - to mount an internal combustion engine to propel itself on four wheels, with a seat on top.

In similar fashion, with the return of the Washington model after the success of the Dulles exhibition, the laboratory staff set to work to pursue some of the many ideas and lines of thought that they had been unable to develop during the desperate inventive rush before the exhibition. No specific objective was held up as an ideal towards which to work, though many uses and applications suggested themselves in the course of investigations.

2.1 Longitudinal stabilisation

For many years researchers in electromagnetics had been building machines in an attempt to provide stable levitation of conducting objects on a magnetic field without the use of excessive electric power. Perhaps the most successful of these attempts had been that first performed in 1966 as part of the Royal Institution Christmas Lectures to children, when Professor Laithwaite succeeded in floating a hollow aluminium sphere, 1 metre in diameter, at a clearance of 20 cm above two concentric circular coils.⁽³⁾ The sheer size of

this system gave it the advantage of a high goodness factor, but still the necessity for the sphere to cut the "cone of attraction" over the coils severely limited the clearance attainable, and the stability was never great.

But the electromagnetic river was different. It was already known to be free from the limitations of cones or prisms of attraction, and the Washington model was stable in five axes. It seemed but a small step to create stability in the sixth axis, and thus achieve completely stable levitation. Initial experiments were performed by activating just two adjacent coils in the Washington model, but the conclusion was quickly reached that at least three cores would be needed to produce longitudinal stabilisation. Some doubt was expressed about whether the iron in the three remaining coils (electrically unconnected) would affect the fields produced by the three in use, so the Washington model was dismantled to allow separate assembly of the cores.

Fig 13 shows the resulting machine, the first of the "expanding-geometry" machines to create stability in all axes. The intention was to leave the five stable axes of the Washington model undisturbed, and to provide stabilising forces in the sixth axis by the use of two inwardly travelling magnetic fields, produced by connecting the individual coils to different phases of the three-phase supply. The actual phase connections (taken from the output of a variac, to permit overall voltage control) were +RED, -YELLOW, +RED. Thus the alternating current in the centre coil lagged the currents in the outer two coils by 60 degrees, and thereby created a pair of inwards-travelling fields. At least, the phase relationships were thought to be so, until it was noticed that the neutral lead of the supply to the variac had inadvertently been left disconnected. Re-connection of this lead, however, almost-completely destroyed the longitudinal stability, so it was thought better to retain the original connection.

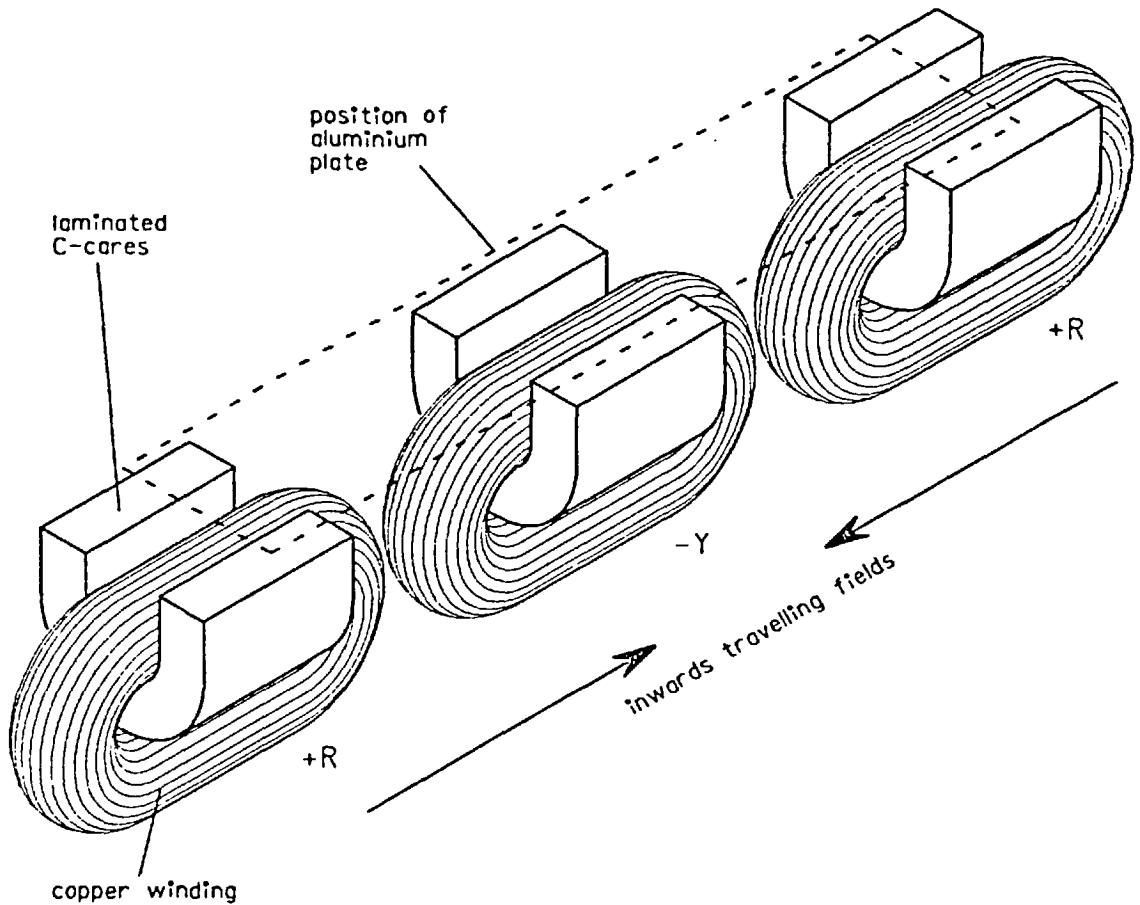


Fig 13. Machine stable in all axes.

In addition, a further slight improvement in stability was made by connecting the two outer coils in series instead of in parallel, resulting in a complete circuit as shown in Fig 14. It will be appreciated that the relative phases of the currents were by now somewhat obscure!

2.2 The Magic Carpet

It happened that the Washington model was required for operation in its complete form, so it was decided to construct a new machine, allowing research to proceed on both models. At the same time a new idea was incorporated - that it made no difference where the coil

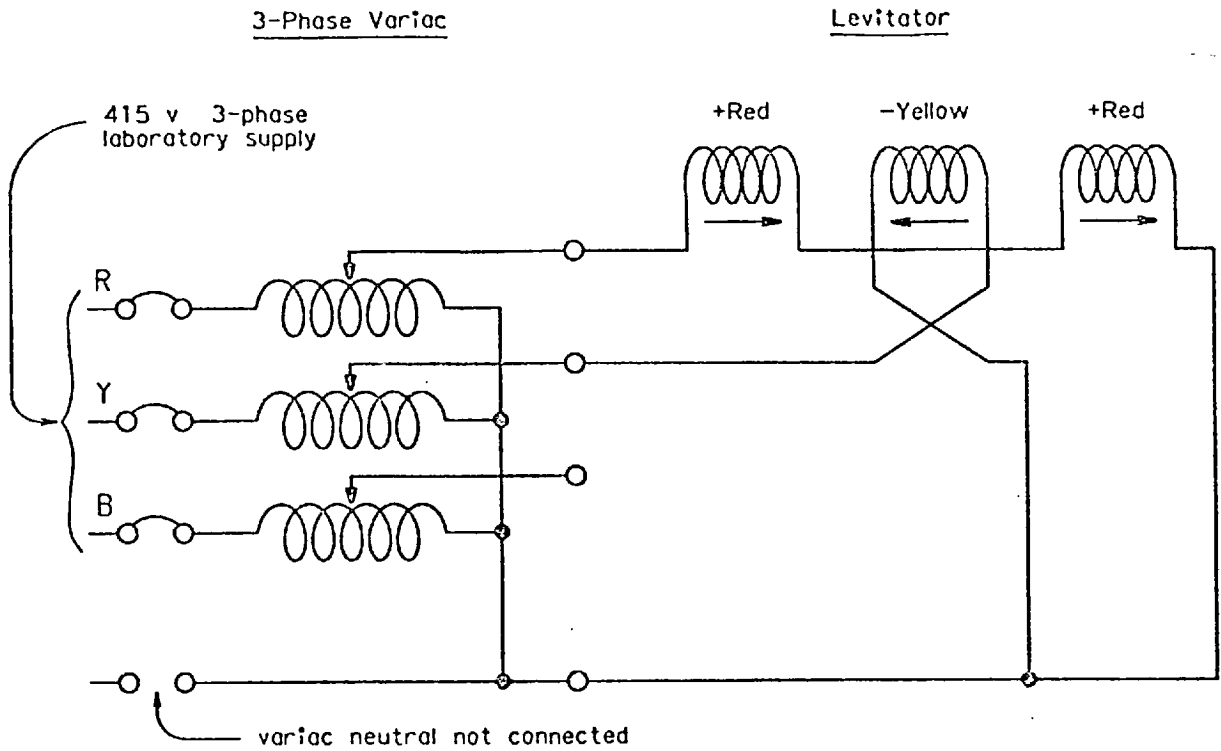


Fig 14. Connections to stable levitator.

current returned around the C-core of steel once it had passed along the centre. Thus one could split the coil into two smaller coils, as in Fig 15. Each component coil returns half the current around a side of the core instead of all the current returning underneath. The resulting machine was then wider than the Washington model, but less deep, and much easier to assemble. A complete engineering description is given in Appendix A.

It was soon discovered when trying various plates over the new machine that the length of the floating plate was a critical factor affecting longitudinal stability. A set of aluminium plates was prepared, each of the same thickness (6.3 mm) and width (10 cm), and increasing in length from 10 cm to 60 cm in 2.5 cm steps. These proved invaluable in tests both on the present model and on many later machines; in particular they enabled the optimum length of plate for the machine in question to be determined in a matter of

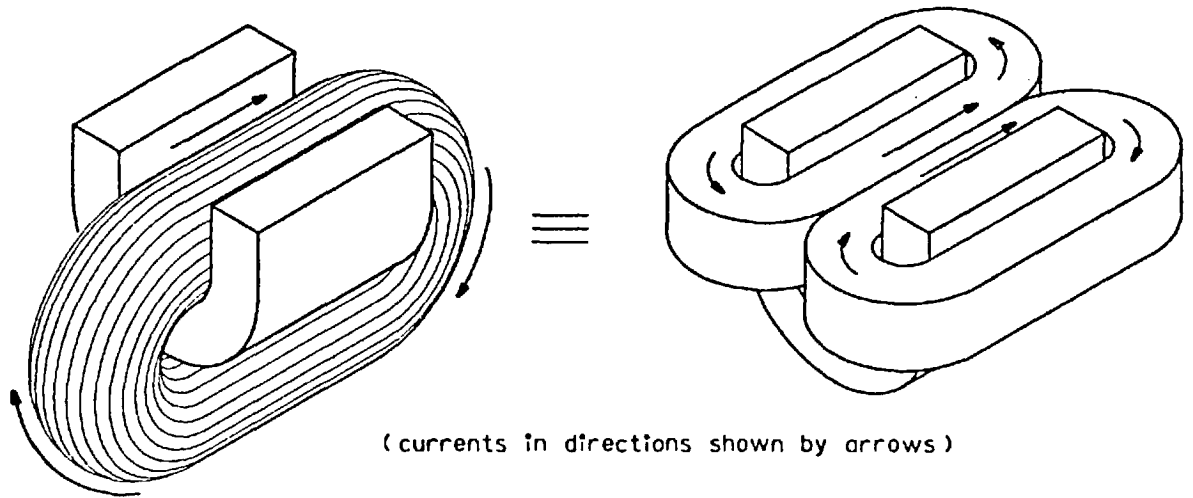
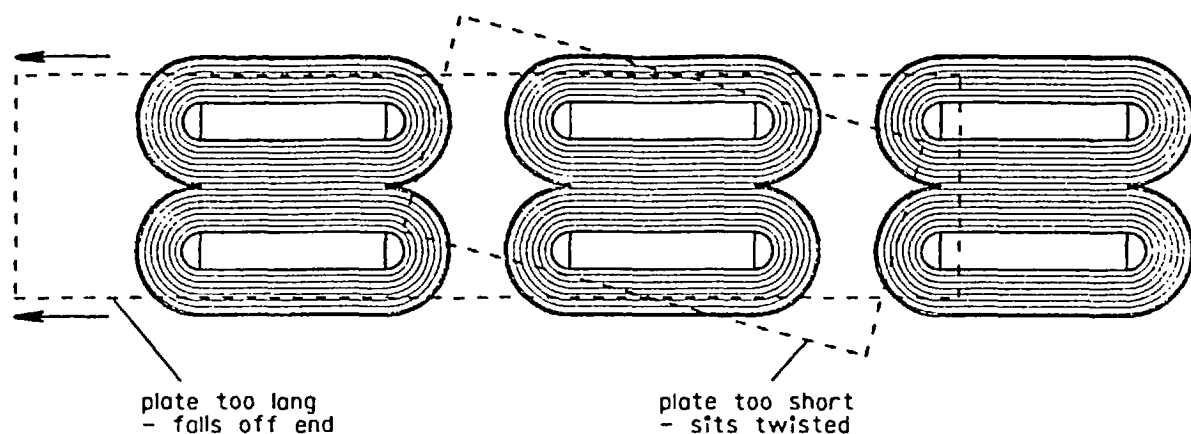


Fig 15. Single gramme-ring wound coil equivalent to two horizontal coils on same laminated iron core.

a few minutes. Plates longer than the optimum appeared to need stabilising forces stronger than the travelling fields could supply, for they tended to drift slowly but surely off one end or the other of the stator, while plates shorter than the optimum tended to stabilise in a horizontal but twisted position, apparently trying to align their longest dimension with the longitudinal axis of the machine. Both these modes of instability are shown superimposed on the plan view of the stator, Fig 16. Once the optimum length had been determined (about 40 cm for this machine) a new set of plates was made, all of the same thickness and length but of different widths.

It is difficult to convey in a work such as this the excitement of the moment when one first achieves what was previously thought to be impossible. The plates now floated stable and level, well clear of the stator, and their lateral stability, both static and dynamic, could be observed at leisure. Observations on the earlier machines, of course, could be made only during the short time taken for plates to travel the length of the Washington model, or under conditions of restricted freedom with the plates held back against



Plan view of new stable levitator, showing instability modes for plates of incorrect length.

Fig 16. "Magic carpet" machine.

the longitudinal field. The "expanding-geometry" effect could now be demonstrated more clearly than before. As successively wider plates were placed over the machine (with the stator current unchanged) each was seen to float higher than the previous plate, but to be more "floppy" laterally. And now an instant adjustment of the variac control could raise the stator current while a plate was floating, to show the immediate extra lift and increased stability thus obtained.

With a stator current density chosen to allow about five minutes running time before overheating, the limiting width of plate (at which all stability was lost) was found to be 19 cm. This plate was the one whose behaviour gave the machine its name. Since the plate was chosen to be almost on the verge of instability its damping to lateral oscillations was low, so that when given a slight disturbance the swaying motion continued for several minutes. To any observer not familiar with the mysteries of electromagnetic levitation, the sight (particularly if the visitor bent down to bring the machine to eye-level) of the plate levitated on seven or eight centimetres of nothingness, gently rocking and twisting from side to side on its

invisible support, looked for all the world like a magic carpet straight out of the Tales of the Arabian Nights!⁽⁴⁾

The plate also proved a most valuable aid in convincing knowledgeable but sceptical visitors of the reversal of the old "cone of attraction" theory. On seeing a plate supported high upon a magnetic field in a condition quite evidently on the limit of stability, common sense suggests that in order to make the plate more stable it is necessary to reduce the stator current, thus lowering the plate further into the magnetic "river banks". Demonstration of the converse (reducing the stator current causes the plate to drop a little, then fall right out) leaves no alternative but to accept what one sees in spite of common sense. Perhaps the easiest way to think of it is that the banks shrink even more quickly than the plate drops when the stator current is reduced.

2.3 Height, stability and efficiency of levitation

It will be recognised that all the work up to this point has been of a "try it and see" approach, with little organised experimental procedure. However by now it was beginning to be felt desirable to put the research onto a more formal experimental footing. Accordingly an investigation was made into the nature of the variation of levitated height and of lateral restoring force with stator current, for various sizes of plate. Measurements of height were made directly, those of restoring force were obtained by attaching a spring balance to the plate and using this to pull the plate steadily to one side, noting the maximum reading before stability was lost. In both cases the measured current was that in the centre coil. The corresponding current in each of the outer coils was approximately half that in the centre, but measurements of these were not taken. Results are shown as the graphs of Figs 17 and 18.

A glance at the first graph, showing variation of levitated height with stator current, confirms again what was already well

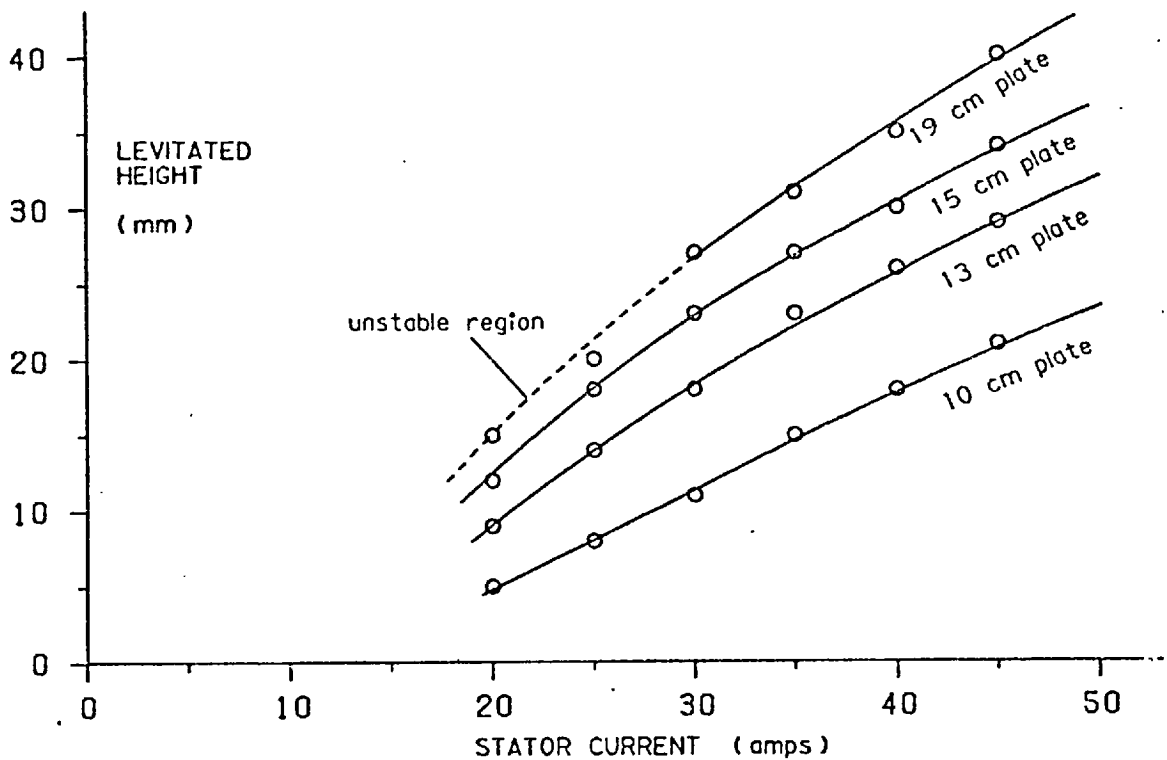


Fig 17. Variation of levitated height with stator current.

known from the "feel" of the plate - namely that with increasing stator current the height of a plate may be raised without limit, and that wider plates sit higher for the same current. The second graph, showing how the maximum lateral restoring force depends upon current, is more interesting in that it reveals a fact not previously suspected - that the restoring force does not increase without limit, but instead appears only to rise asymptotically to a maximum value (of 200 gmf for this particular machine). The width of plate determines the rate of rise of the stability force, narrower plates reaching the maximum more quickly than wider ones (the 10 cm plate reaches the maximum 200 gmf of restoring force with a stator current of only 30 amps, while the 19 cm plate has only just reached half that value at 50 amps). The implication of this is that the maximum possible stabilising force is determined by the design of the stator of the machine, not by the shape of the secondary - a feature not appreciated in earlier work.

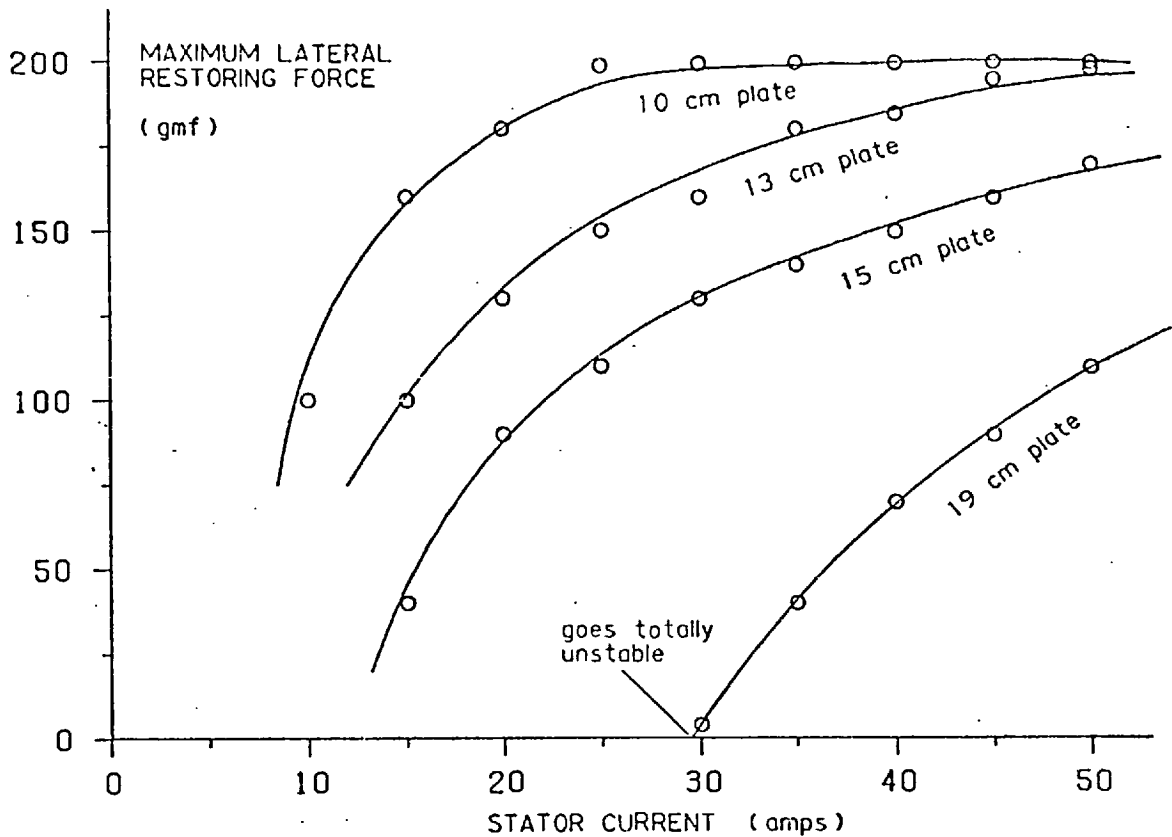


Fig. 18. Variation of lateral restoring force with current.

An attempt was made also to evaluate the "efficiency" of the machine as a levitator, where efficiency is here defined as the ratio of the power dissipated in the floating sheet to that delivered as electrical input to the stator. As is well-known, the accurate measurement of secondary power in induction devices is never an easy matter. For the present purpose, it was therefore taken to be sufficient to employ the admittedly approximate method of assuming that primary power losses are unchanged when a conducting secondary is introduced into the field. This makes determination of secondary power simply a subtraction sum of the input power with no plate present from the corresponding power with the plate in place. Again, all power measurements were taken for the centre stator coil alone, since it appeared that almost all lift and lateral stabilisation was obtained from this coil, the others providing longitudinal restraining forces only.

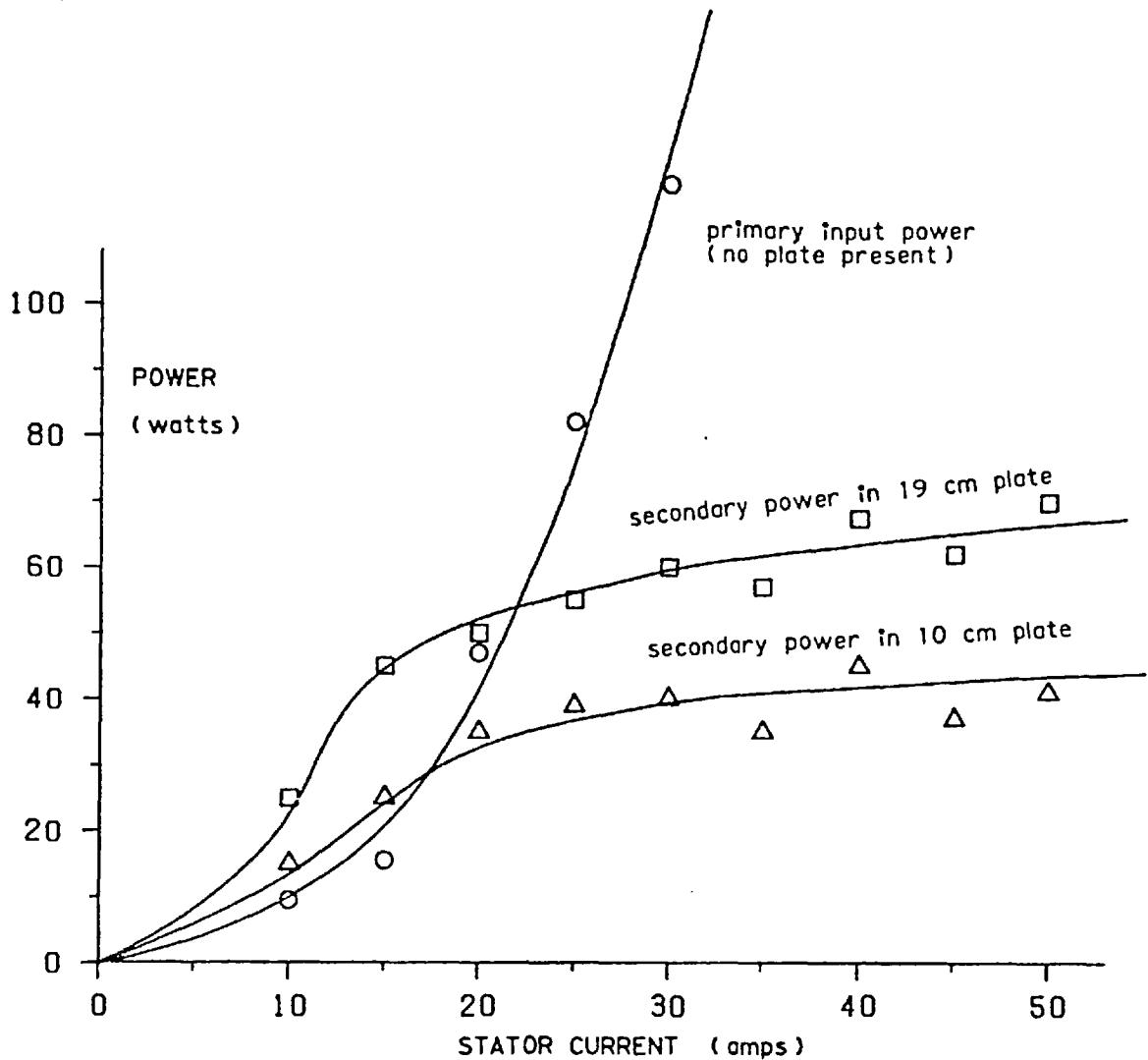


Fig 19. Power dissipated in plates.

Fig 19 shows the graph of power dissipated in the secondary for the two extreme widths of plate. It will be noticed in each case that once the plate has lifted clear of the stator (at about 25 amps of stator current) the power dissipated in it remains nearly constant, which suggests that the shape as well as the magnitude of the current flow paths within the plate does not change with varying height. This phenomenon is familiar to those working with conventional single-sided linear induction motors, where it is known that a change in height of a free rotor* caused by a new value of stator current results in no change either in the power

* - see footnote on terminology on the next page.

transferred to the rotor or in the thrust developed by it.⁽⁵⁾ Indeed it was an encouraging surprise to the laboratory staff to have found a mode of behaviour of the electromagnetic river which corresponded with that of a conventional machine!

2.4 Sustained oscillations

Experiments were also carried out using a set of plates all of identical length (the optimum) and width (13 cm) but of varying thickness. All tests hitherto had used aluminium plates 3 mm thick; the following tests investigated the behaviour of plates double and treble this thickness. With the stator current again set to allow about five minutes of running time the thinnest of these plates (3 mm thick and 13 cm wide - the second of the original variable-width set) floated at about 2 cm clearance, and remained stable, level and well damped to lateral oscillations.

Replacement by a plate twice as thick at first sight left conditions unchanged, but giving the plate a slight lateral disturbance revealed that the lateral damping was much lower than before. Substitution of a plate three times the thickness of the

Footnote on the terminology of "stator" and "rotor".

In the terminology applying to standard rotary machines the words "stator" and "rotor" carry the obvious meanings "that which remains stationary" and "that which rotates". In the case of a rotary induction motor the stator invariably carries the primary currents, i.e. those derived directly from the mains supply, and the rotor has the secondary currents induced within it.

By extension, a linear induction motor "stator" is the part carrying the primary currents, and is usually stationary, while the "rotor", whether comprising wound coils or a continuously conducting sheet, carries the secondary currents. The rotor is generally the part that moves, albeit no longer with rotary motion. The situation becomes more confusing, however, when the system is inverted, to form for instance a stationary "rotor" of aluminium track upon which is propelled a "stator" carrying primary currents. Perhaps the best approach is to regard "stator" as "that which carries primary current" regardless of whether or not it remains stationary, and likewise the rotor as synonymous with "the secondary".

original led to even more interesting behaviour - a small displacement sideways resulted in initially gentle oscillations which gradually built up, over a period of several minutes, into violent rolling and twisting motions threatening to throw the plate off the machine. In fact these oscillations were usually limited only by the plate clashing against the stator pole-faces.

For an explanation of these last phenomena it is necessary to consider the concept of "goodness factor", particularly as applied to back-to-back oscillating machines. Goodness factor is an attempt to quantify, in one mathematical term, all the advantageous features of any electromagnetic machine. For a full mathematical derivation see reference 6; it is sufficient here to state the final result, which is that a machine comprising an electric circuit of length ℓ_e and cross-sectional area A_e linking a magnetic circuit of length ℓ_m and area A_m has a dimensionless numerical value of goodness factor given by

$$G = \omega \sigma \mu \left\{ \frac{A_e A_m}{\ell_e \ell_m} \right\}$$

where G = goodness factor,

ω = supply frequency to machine,

σ = conductivity of electric circuit,

μ = permeability of free space (or of iron
if the magnetic circuit has no air-gap).

The goodness factor is seen to depend on a number of parameters. For example, as might be expected an increase in conductivity of the electric circuit results in a proportional increase in goodness factor. Less obvious until seen in this form is the effect of changes in linear dimensions. The right-hand part of the expression, enclosed in brackets, consists of the product of two areas divided by the product of two lengths, from which it follows that doubling every dimension of any given electromagnetic machine increases its goodness factor by four times. In general terms an increase in goodness factor represents an improvement in the performance of the

machine - this can be made to appear in the form of greater efficiency, a better ratio of power to weight, increased thrust, or in many other forms, the important point being that the machine is made in some way inherently better.

In the particular case of an electromagnetic machine designed to induce oscillation in a free rotor (for instance by mounting two linear motors end-to-end, each with its travelling field moving towards the centre of the combination - the "back-to-back" configuration), the numerical value of the goodness factor determines the subsequent behaviour of the rotor after suffering a disturbance.⁽⁷⁾ A value of less than unity predicts that the rotor will execute damped oscillations, finally coming to rest in its equilibrium position. If the amplitude of the oscillations is not to decrease then it is necessary for the goodness factor to have a value at least equal to unity. Above this value the higher the goodness factor the greater the self-oscillatory capabilities of the machine will be.

Now if the lateral stabilising forces on the static levitator are thought of as being caused by two inwardly travelling fields (created by a mechanism not yet understood, but possibly a form of shaded-pole action), then the requirement for a well-damped system is that the goodness factor should be low. But doubling the original plate thickness halves the electrical resistance of the secondary circuit by doubling its effective cross-sectional area, and thereby raises the goodness factor towards unity. This causes the inferior damping that accounts for the observed "floppy" behaviour. Trebling the thickness evidently increases the goodness factor so far that it exceeds unity, thereby producing continuous oscillations.

There is a conflict of requirements here. Maximum lift and propulsion require a goodness factor as high as possible, while a high degree of stability requires a low goodness factor. However it has already been noted that it is possible to achieve at least

some degree of independence between requirements involving different axes. For example the addition of upright edges to create a trough rotor improves propulsion without seriously affecting stability. Later work will show how this independence can be extended further.

The phenomenon of increasing oscillations (negative damping) was obtained again when experiments were performed using a copper plate in place of aluminium. The width of the plate was 13 cm (the same as for the set of variable thickness aluminium plates) and its thickness was 6 mm, i.e. double the thickness of the original aluminium sheets. The performance of the copper was similar to that of the treble-thickness aluminium sheet, the goodness factor again being fractionally greater than unity. However one facet of behaviour of the copper plate deserves special mention. On one occasion the plate was allowed to build up its oscillations until it began clashing against the pole pieces, and was then left for several minutes with the stator current unchanged to see whether the clashings would increase in violence sufficiently to throw the plate right off.

It is difficult to judge by eye the magnitude of the movements of a heavy plate undergoing violent oscillations about several axes of motion simultaneously (in fact it is a somewhat breathtaking sight to watch a 3 kg plate of copper being slung from side to side of a machine at a rate of about six oscillations per second), but it certainly did not appear that the movements were becoming any more violent. Indeed after some minutes there was the distinct impression that they were dying away. However by this time the stator coils (particularly the centre one) had heated up to the point where they were beginning to emit dense smoke, so the experiment was abruptly stopped.

The (painful!) discovery that the rotor also had become extremely hot suggested that the rotor temperature might in fact have been the reason why the plate did not behave in the expected way. This

suggestion was tested by allowing the machine to cool and then clamping the plate hard down to the stator pole pieces, so that when the stator was switched on the large induced rotor currents caused rapid heating of the copper. On releasing the clamps the plate floated perfectly stable and level, with lateral damping low but definitely positive. Suspicions were confirmed that it was indeed the temperature rise that caused the change in behaviour. The temperature change had affected the resistivity of the copper to the point where the reduced conductivity of the hot plate was sufficient to reduce the overall goodness factor to below unity, thus creating stability out of an initially unstable system.

Further investigation into the nature of the way in which rotor temperature affects the performance of the electromagnetic river was not pursued. The only account taken of its effects in the work to be described was to ensure that temperature changes in various parts of machines under test were never large enough to affect seriously the accuracy of measurements taken. (At times this involved waiting for an hour or more between consecutive readings in order that the machinery cooled always to room temperature before re-starting.) The subject might well, however, prove fitting for a research programme on another occasion.

CHAPTER 3

ELECTROMAGNETIC SPRINGS, WHIRLPOOLS AND OTHER THINGS



The "Catherine wheel" machine (p 50) - an attempt to obtain stability by providing an inwards component of travelling magnetic field in addition to the rotating component.

CHAPTER 3. ELECTROMAGNETIC SPRINGS, WHIRLPOOLS AND OTHER THINGS

3.1 The machine with long poles

No mention has been made so far of the pattern of current flow lines within the rotor, other than to note that in a free rotor their general shape remains unaltered by changes of stator current. The pattern of magnetic flux lines above the pole pieces, enveloping the rotor, has not been discussed at all. On the principle that a current-carrying conductor within a magnetic field can experience forces only at right angles to the direction of current flow, it seems reasonable to assume that the sideways stability forces are in some way produced only by those components of rotor current flowing longitudinally within the plate, lateral components contributing only to propulsion and lift. For this reason it was decided to construct a new machine, designed to simplify matters by confining lateral currents to the end regions only of a long sheet, leaving the centre section of the sheet free for investigation of the longitudinal currents.

Fig 20 shows the general form of the stator, consisting of a single pair of pole-pieces extending the whole length of the new machine (about 60 cm), embraced by a coil passing along the centre slot and returning around the sides of the poles. (Appendix 1 gives technical details of the machine.) First investigations of the machine were made using the set of aluminium plates all of the same width (10 cm) but varying in length from 10 to 60 cm. A number of the sheets were found to stabilise themselves longitudinally as well as laterally, without the need for externally produced inwards-travelling fields such as those in the levitator described in the previous chapter. Again, plates that were too long tended to drift slowly off one end or the other of the machine, while those too short tended to sit in a horizontal but twisted position. (The 10 cm square plate positioned itself always at an angle of 45° - with one of its diagonals aligned with the axis of the stator.)

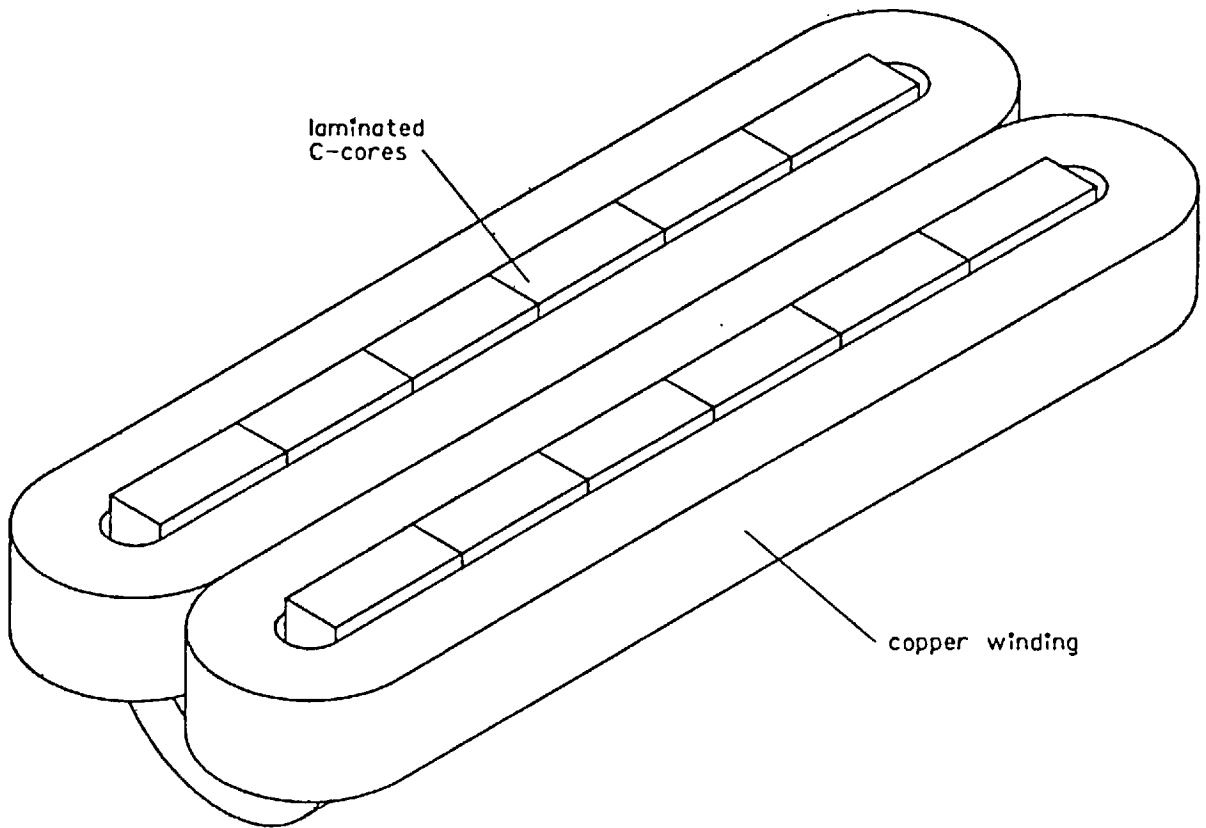


Fig 20. Single long pole-pair stator.

But instead of there being a single optimum length, there was now a range of plates all of which sat perfectly aligned and longitudinally stable.

Plates at the lower end of this range, being shorter than the stator itself, settled into a state of neutral equilibrium when near the centre of the machine (forming another "perfect spirit level"). When given a slight push along the length of the machine a small plate would glide gently, until upon approaching the end of the stator it appeared to experience a repelling force which brought it smoothly to rest and then accelerated it back towards the centre. The damping of the action induced by these "electromagnetic end springs" seemed to be very nearly zero, so

that a plate once set in motion could maintain its slow longitudinal oscillations for as long as half-an-hour. This behaviour is in direct contrast with that of the original "spirit level" machine, described in Chapter 1, where a plate approaching an end of the stator experienced an attractive force accelerating it towards the end, over it, and right off the machine. Explanations for these two contrasting end effects are not fully formulated, but both are related to the shaded-pole action of the ends of the plate. The subject will be returned to briefly in Chapter 9.

The new machine exhibited even more interesting behaviour when two of the smallest plates were placed simultaneously upon it. These would sit twisted, as explained earlier, and tended to space themselves well apart along the stator (but always contained within the boundaries set by the electromagnetic end springs). Indeed, if guided towards each other the plates showed a marked mutual dislike and pushed themselves strongly apart when released. But if the guidance was continued until one plate was forced to slip under the edge of the other, a point was reached when the repulsion suddenly changed into an attraction, resulting in the plates sliding rapidly on top of each other and locking together to form a combination exhibiting behaviour identical with that of a single plate twice the thickness.

Explanations here are rather more straightforward. When the plates are apart and independent the longitudinal currents, wherever they may flow, will be similar in both plates. The lateral currents that flow in the end regions of the plates to complete the rotor circuits must then be in opposing directions within the two plate ends facing each other, and the magnetic fields set up by two sets of currents flowing in opposite directions repel one another. When the plates are pushed close together so that an area of overlap is formed, the patterns of current in each plate within the overlapping regions are likely to be generally similar (since both are produced by the same magnetic field in the same position) - and like currents

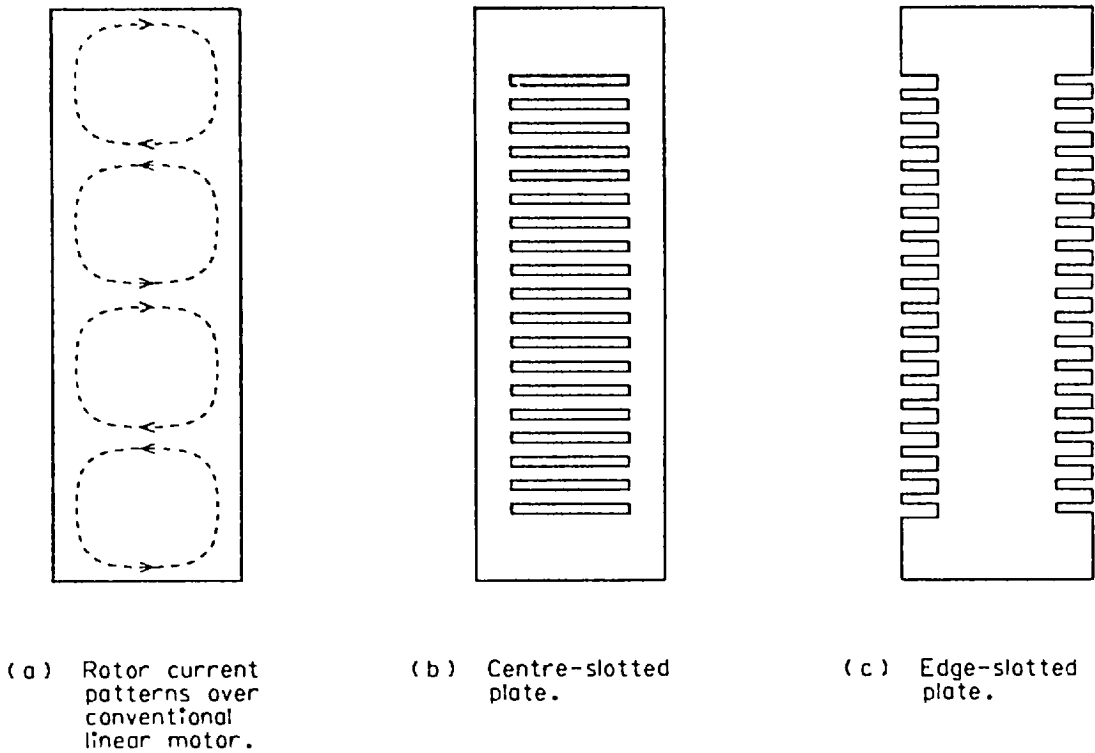


Fig 21. Test plates for conventional linear motor.

attract. The situation bears some resemblance to that produced when the North end of a bar magnet is made to approach the North end of a similar magnet which has had the area of its pole increased by the attachment of a piece of soft iron. Dimensions may be found for the soft iron such that the region of repulsion as the poles approach each other changes into a region of attraction once they come within a certain critical distance.⁽⁸⁾

3.2 The double-loop pattern

After the preliminary investigations described above, experiments were carried out to determine the shapes of the current flow patterns within the plates. First trials made use of plates that had had parallel slots cut within them, allowing current to flow only in directions aligned with the slots. For example Fig 21(a) shows the

well-known pattern of current flow in a sheet placed over a conventional linear motor. Replacement by a rotor having a series of transverse slots cut within it as shown in Fig 21(b) results in practically no change in the performance of the machine. The only noticeable effect is a slight loss of performance resulting from the effective added rotor resistance caused by the loss of material from the slots. Replacement, however, by a sheet of the shape shown in Fig 21(c), where short transverse slots have been made along each edge, almost totally destroys the action of the motor, the reason being of course that the edge slots prevent the flow of "end-ring" currents needed to complete the pattern of Fig 21(a).

When the same two patterns of slotted plate were tried on the new levitator, they both behaved equally disastrously - neither produced any lift whatsoever. Longitudinally slotted plates however, as shown in Figs 22(a) and (b), were more successful. The plate of Fig 22(a), with slots cut almost the whole length of the plate but stopping some way from each end, floated stable and level, nearly as high as an unslotted equivalent (again the slight difference can be readily accounted for by the increased resistance as a result of the missing aluminium). The plate of Fig 22(b), with a single slot cut some distance into the plate at each end, maintained considerable lift, but exhibited no stability at all. Cutting more slots to form the end-slotted plate of Fig 22(c) resulted in the loss of all lift as well as all stability.

These results led to the conclusion that the general current pattern in an intact floating sheet is of the form shown in Fig 22(d), where the induced current flows along the centre of the plate and divides to return along the two edges, forming the "double-loop" pattern shown. Perhaps the pattern should have been deduced immediately the first stable levitator had been built, since it is simply an image of the stator coil pattern beneath. Even the original Washington model could have been viewed as the

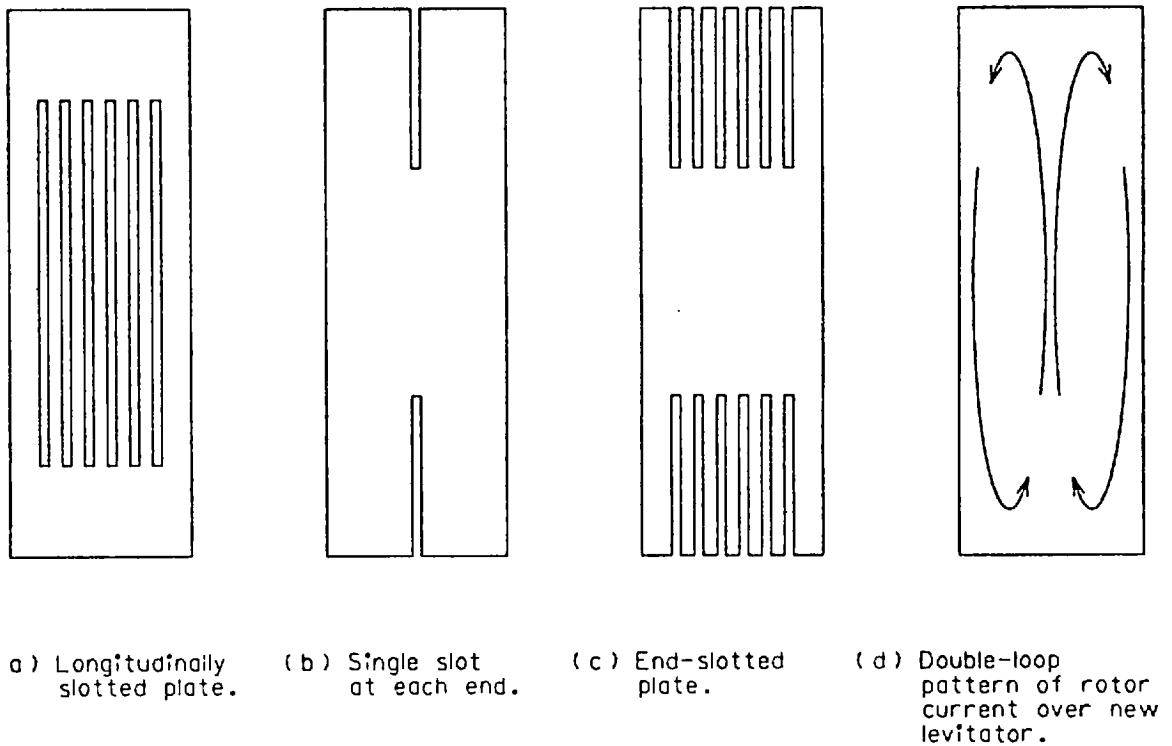


Fig 22. Test plates for new levitator.

electromagnetic inversion of a solenoid, with circular flux lines replacing helical current paths to produce a current along the centre in place of magnetic flux - see Fig 23. This centre current can then complete its circuit only by returning along the plate edges, forming the double-loop pattern of Fig 22(d) once again.

The behaviour of plates of different widths now becomes clear. A wider plate will provide a better return current path along each edge and will therefore lower the effective resistance, resulting in larger currents producing greater lift and propulsion. The situation is in some ways similar to the problem of the "end-ring" resistance of a conventional linear induction motor rotor, but analyses on the lines of the Russell and Norsworthy approach⁽²⁾ for conventional machines have not yet been attempted for double-looped systems. Any such attempt will be considerably more complex

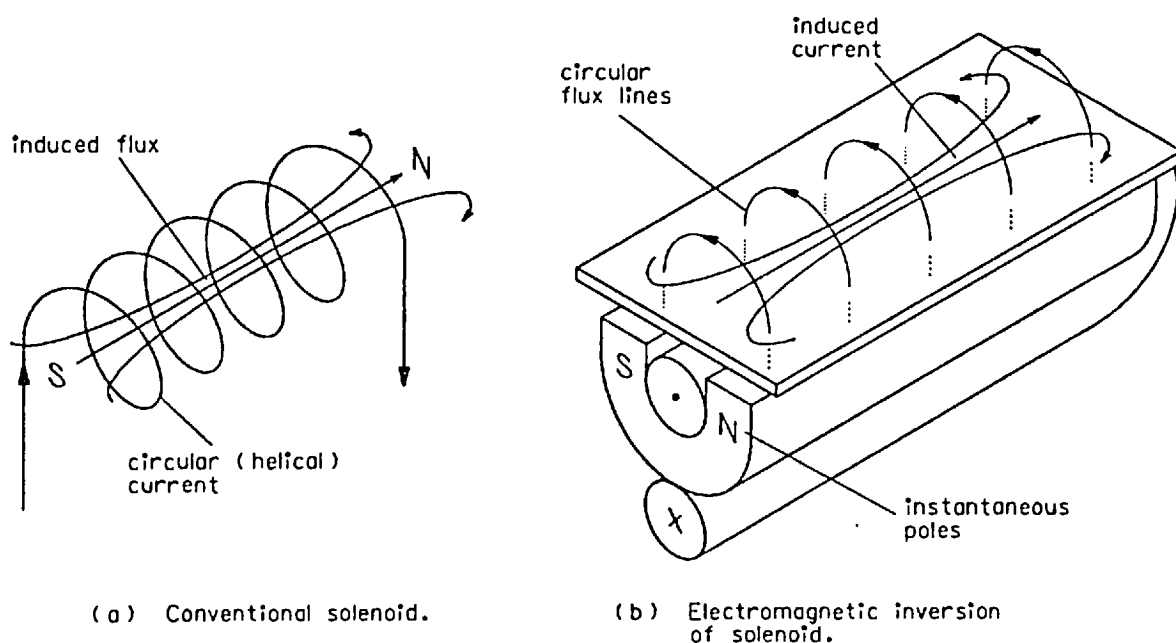


Fig 23. "A solenoid turned inside out".

because of the need to consider the effect of the current paths at the ends of the plate as well as the paths along the centre and back along both sides.

The behaviour of the plate with a single slot at each end seems to suggest that in addition to the requirement for a double-loop pattern there is a need for the end currents to have complete freedom within the end regions of the rotor. A single slot restricting this freedom was sufficient to destroy stability entirely. When the slot was extended throughout the length of the plate, thus cutting the plate into two halves which were then re-joined by a non-conducting material, the instability was even more marked, for the compound plate was now actively thrown off the machine whereas before it slid only gently off. The failure here is of exactly the same kind as that exhibited by the double U-channel rotor that formed one of the series of experiments leading to the development of the Washington model (see Chapter 1, Fig 9).

3.3 Circular levitators

Tests designed to carry out measurements on the rotor current patterns will be described in the following chapter, but before proceeding to this stage it may be worth commenting on other new designs of machine that followed directly from the Washington model. For a number of years before the invention of the electromagnetic river, attempts had been made to build a machine capable of floating a circular or annular plate while spinning it smoothly at constant speed, to create a frictionless bearing. It was a relatively simple matter to float stationary or slowly rotating plates, but problems always arose in maintaining stability as the plates accelerated towards the condition where their rotational speed became a significant fraction of the synchronous speed of the rotating magnetic field (usually 3000 rpm). In any case all the machines were limited in the clearances that could be achieved because of the necessity to stay within the bounds of the "cone of attraction".

Two of these early machines are particularly interesting. That of Fig 24(a) employed windings in spiral formation in order to produce a travelling field having an inwards (stabilising) component at the same time as the rotating (driving) component. Thus it was hoped to achieve stability of the same kind as that exhibited by the disc-floater of Fig 11, produced by inwards travelling fields. There seemed no reason why such stability should not be maintained at all rotational speeds since the radially travelling component of the field should be in no way affected by tangential velocity of the rotor. The machine was however a total failure - no stability whatsoever was achieved at any speed.

The second machine was built as a development of the primitive electromagnetic river described in Chapter 1 (see Fig 6). Imagine the original machine to be bent around itself in a horizontal plane until its ends meet to form a complete circle. The result is a circular levitator as shown in Fig 24(b). The rotor then takes the

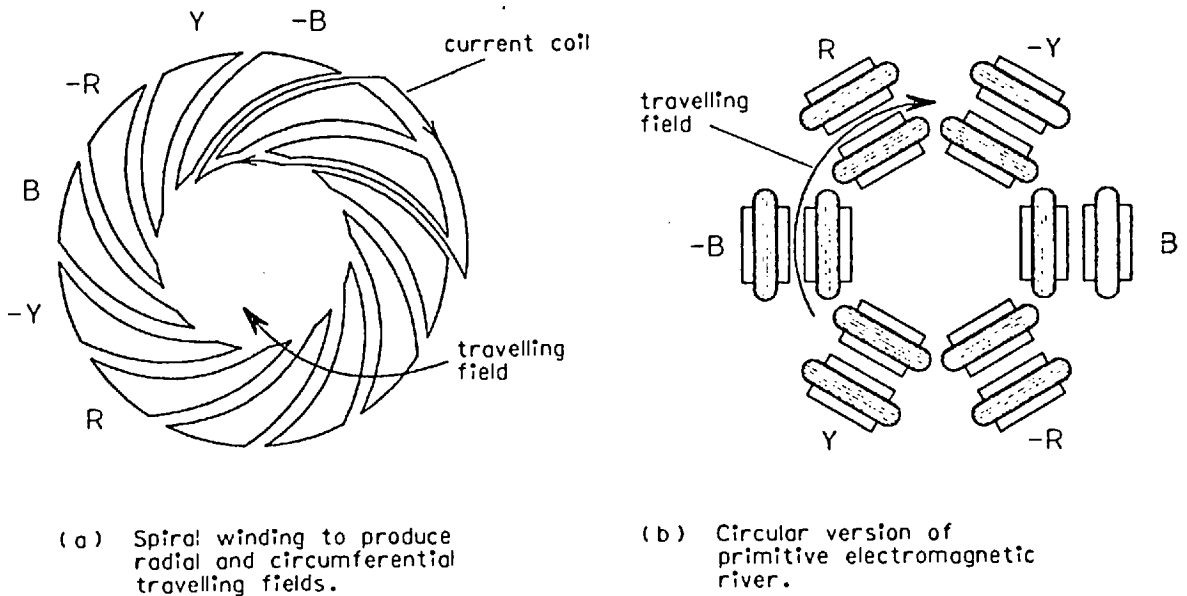


Fig 24. Circular levitators.

form of an annulus, or possibly a disc, of aluminium. This machine was more successful than the spiral version in that weak stability was obtained at least at low speeds, but at higher speeds the rotor soon became unstable. Moreover the stator was not of the "expanding-geometry" type so the height limit remained.

The same "circularising" process applied to the Washington model results in a configuration comprising just one half of Fig 24(b) - say the six outer coils. High expectations were held for this machine. It was thought that the superb stability and limitless height attainable by the system should produce a levitator far superior to any of its predecessors. But again the subject of electromagnetism provided some surprises, for the machine was totally unstable at all speeds and for all stator currents. This behaviour was the more puzzling because it was known that when only one of the six stator blocks was excited the annular rotor experienced strong stabilising forces over that block. It was found that two or three adjacent blocks could be excited without losing stability, but as more blocks were added the stability became steadily weaker until the addition of the sixth block destroyed it altogether.

The only significant topological difference between the circular and the original versions of the Washington model seemed to be that the latter possessed two ends while the former had none. Artificial ends were therefore made in the circular machine by cutting a radial slit through the rotor annulus (retaining mechanical rigidity by re-joining with non-conducting material). Stability was immediately restored. The final step towards construction of the first electromagnetic bearing was to cut a further two slits in the rotor, 120° either side of the first, to restore rotational symmetry to the system.

The machine now exhibited all the expanding-geometry properties of the Washington model and remained stable up to speeds far higher than those previously attainable. In fact, the ultimate limit of angular velocity became that imposed by the inability of the annulus to maintain lift as it approached synchronous speed; loss of lift occurs, as does loss of propulsion, as the frequency and hence the magnitude of the induced rotor currents both approach zero at synchronous speed. At the time, this effect was thought to place an unfortunate limitation on the performance of the machine; later work, however, has revealed methods by which the problem can be overcome (see Chapter 6, page 128), allowing lift and stability to be fully maintained up to speeds within a few per cent of synchronism.

The reason for the dependence of stability upon the presence of "ends" can be seen by considering the diagrams of Fig 25. The slitted annulus of Fig 25(b) has flowing within each segment the same double-loop pattern of induced current as does the original linear version of Fig 25(a). Replacement by a continuous sheet, however, allows current to flow around the annulus in a complete loop, and it is the absence of current along the inner and outer edges that destroys the mechanism of stability. Thus the double-loop pattern with its edge return currents is seen to be a requirement, rather than just a characteristic, of expanding-geometry self-stabilising systems.

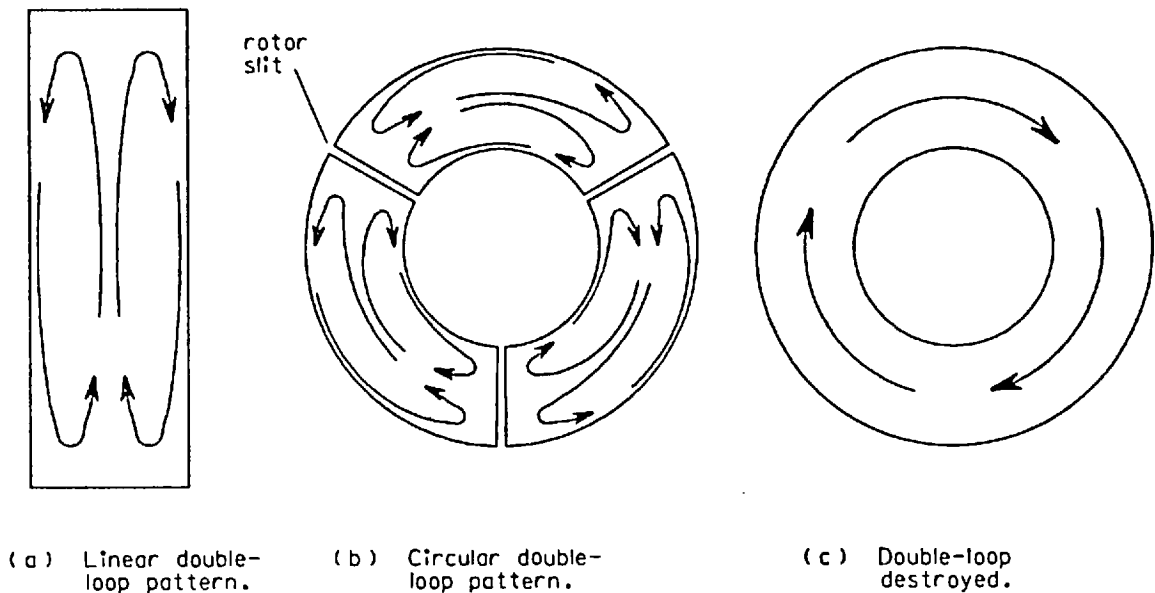


Fig 25. The double-loop pattern applied to annular rotors.

In the case of a machine designed to allow freedom of rotation for a floating annulus, but which is not required actually to drive the rotor, a second method of providing artificial "ends" can be employed. Instead of connecting the six stator blocks in continuous phase progression to produce a rotating field, as in Fig 26(a), they can be arranged in two sets of three, producing opposing fields each travelling around half the circumference, as in Fig 26(b). The net rotational force is of course zero, but artificial ends have now been introduced in the stator, allowing the rotor to be a continuous annulus carrying two current paths, one in each half-circumference but each of the double-loop pattern. The resulting behaviour is similar to that of a rotor provided with two slits (located in the positions of the dotted lines on the figure), but with the difference that the rotor has absolute freedom to rest in any angular position, with no tendency even, for instance, for slits to position themselves above the gaps between stator blocks.

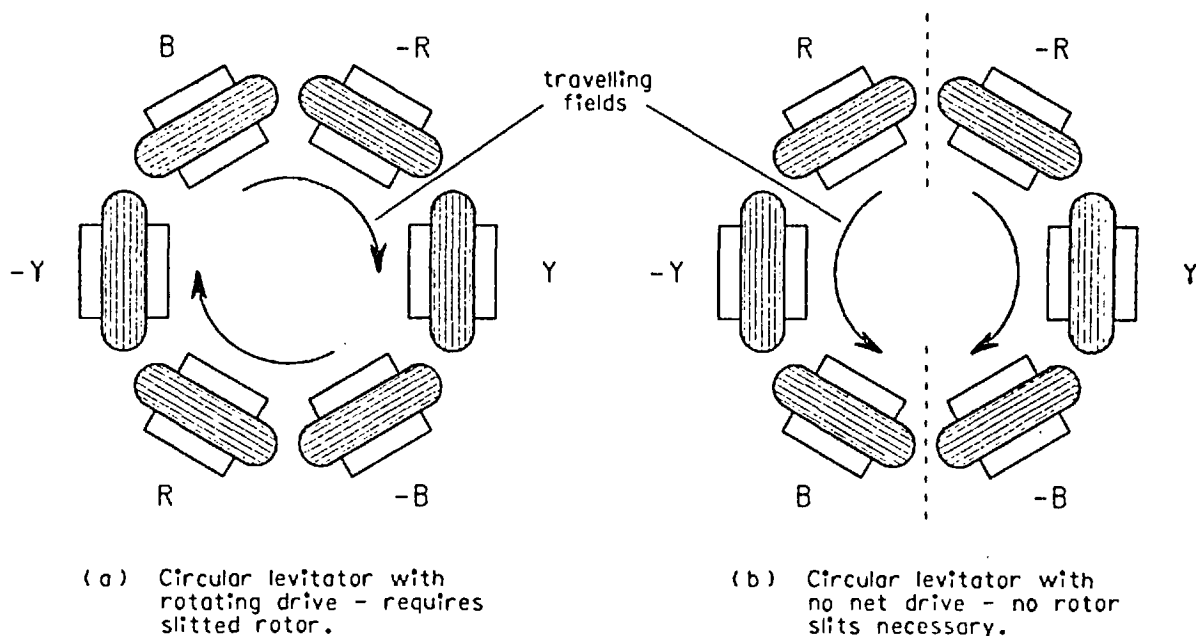


Fig 26. Circular levitators of the new design.

There is of course no reason why a separate propulsion device, even an induction machine using the same aluminium as its secondary, should not be used to rotate an annulus floating above a non-propulsive circular levitator. An obvious application for such a combination is to arrange that the propulsion unit dictates a rotational speed of $33\frac{1}{3}$ revolutions per minute, thus creating a perfectly rumble, wow and flutter-free record deck.

Such a machine was in fact constructed. It behaved eminently well from an engineering point of view, but it possessed two rather serious drawbacks from the point of view of the hi-fi enthusiast. Firstly the large currents induced in the rotor resulted in the aluminium heating up to the point where an ordinary vinyl record placed upon such a turntable would have a life of only a few seconds before melting. Secondly the enormous magnetic fields produced by the stator completely precluded the possibility of bringing a magnetic cartridge anywhere within yards of the system. Thus ended the first sortie of linear motors into the world of hi-fi!

3.4 The Electromagnetic Whirlpool

It is a lesson that has been taught many times during the course of investigations into electromagnetic levitation (and electromagnetism in general) that the world exists in at least three dimensions. Virtually all commercial machines have need to exploit only one of these (air-gap flux is assumed so far as possible to be purely radial, with no circumferential or axial components), so perhaps it is not surprising that it is an exploration into the second and third dimensions that frequently leads to new and exciting forms of machine. The circular levitators described above were obtained by "wrapping up" the Washington model in a horizontal plane, but there still remained two further ways by which a linear device could be wrapped up. Investigations were not pursued into the effects of bending the machine around an axis parallel to its own length, since the result would have been a tubular motor with transverse flux, better versions of which had already been invented some years before.⁽⁹⁾

However the third dimension seemed to offer more interesting possibilities. The mental process of forming such a machine is to imagine the ends of the Washington model to be bent upwards (instead of sideways as before) to form a complete circle, then to tip the whole device over onto its side, to form a horizontal circular ring. Forces normal to the pole-faces of the machine become radial centering forces, while any levitation is provided by forces tangential to the pole-faces, previously stabilising forces. The rotor becomes simply a cylinder, of axial length equal to the width of the C-cores. A cross-sectional view of the resulting machine is shown in Fig 27.

Once again the rule applies that stability (or in this case suspension) can be obtained only when the double-loop pattern is made to flow in the rotor. The same methods are available to achieve this condition - for a driven rotor the aluminium must have at least

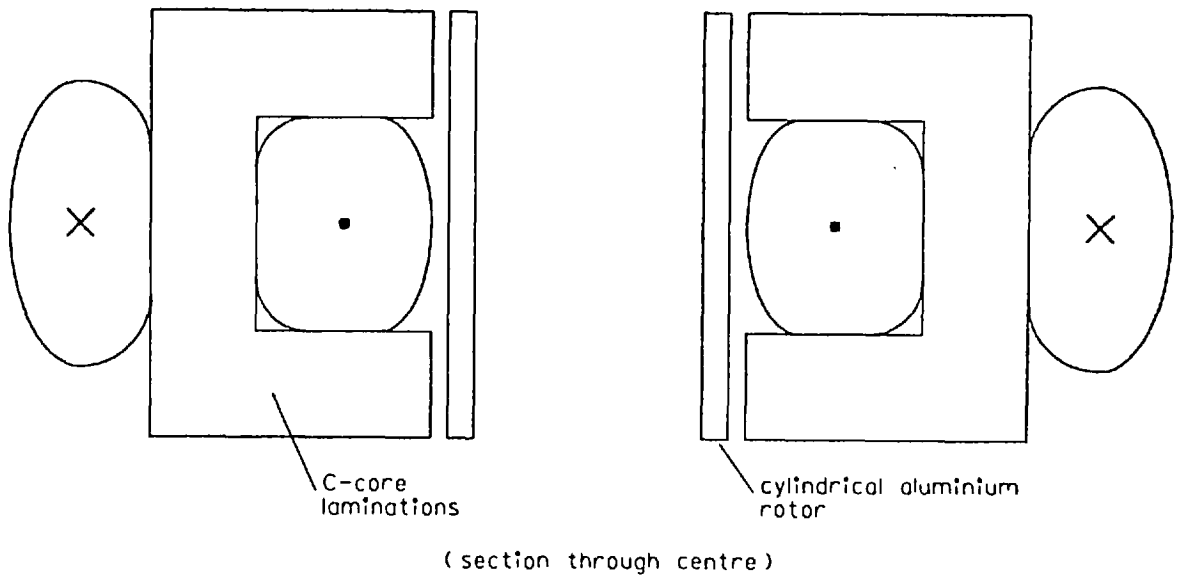


Fig 27. Washington model "wrapped up" in a vertical plane and tipped over to form a horizontal ring.

one axial slit (preferably three) to allow the six stator cores to be connected in phase-sequence, or for a non-driving system the six cores may be re-connected to produce two equal, opposing travelling fields allowing the rotor to remain in one continuous ring.

Three-dimensional thinking, however, can suggest a better way by which both the above modes of operation may be achieved. Instead of the six pole-pairs of the Washington model, imagine just one pole-pair (such as one pole of Fig 13 in Chapter 2) to be stretched in its longitudinal dimension, to form a stator of the same proportions as that shown in Fig 20, but with a single return current path below the C-core. The ends of this stator are then bent upwards to form a circle. Upon joining the sets of conductors, two independent coils are formed, one within the slot, producing useful flux, and the other around the back of the C-core, producing nothing. This second coil can be removed entirely, achieving a considerable saving in copper, and when tipped over onto its side as before the resulting machine is a non-driving levitator requiring, however, a slitted rotor. (since the stator has no "ends").

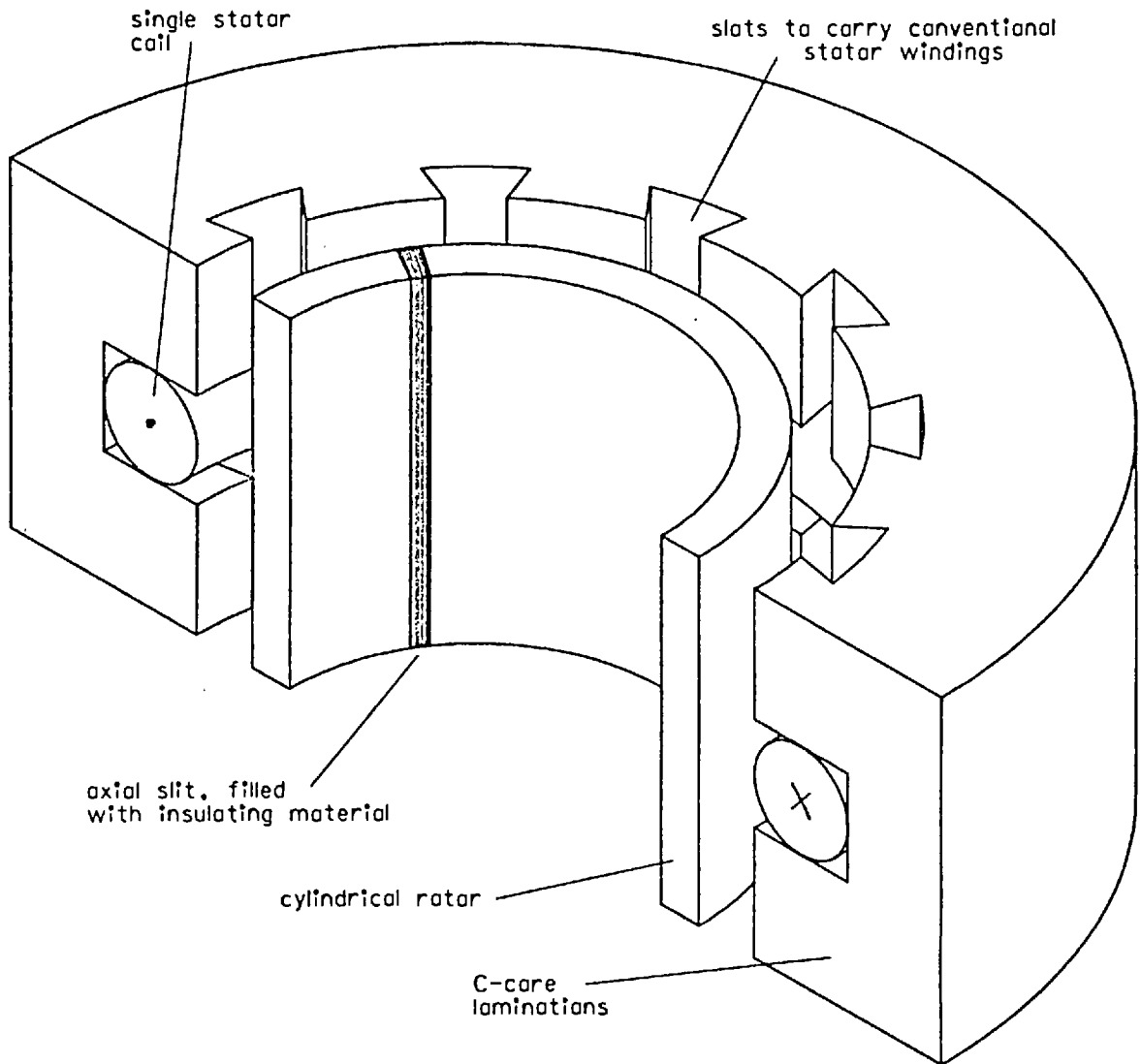


Fig 28. The Electromagnetic Whirlpool.

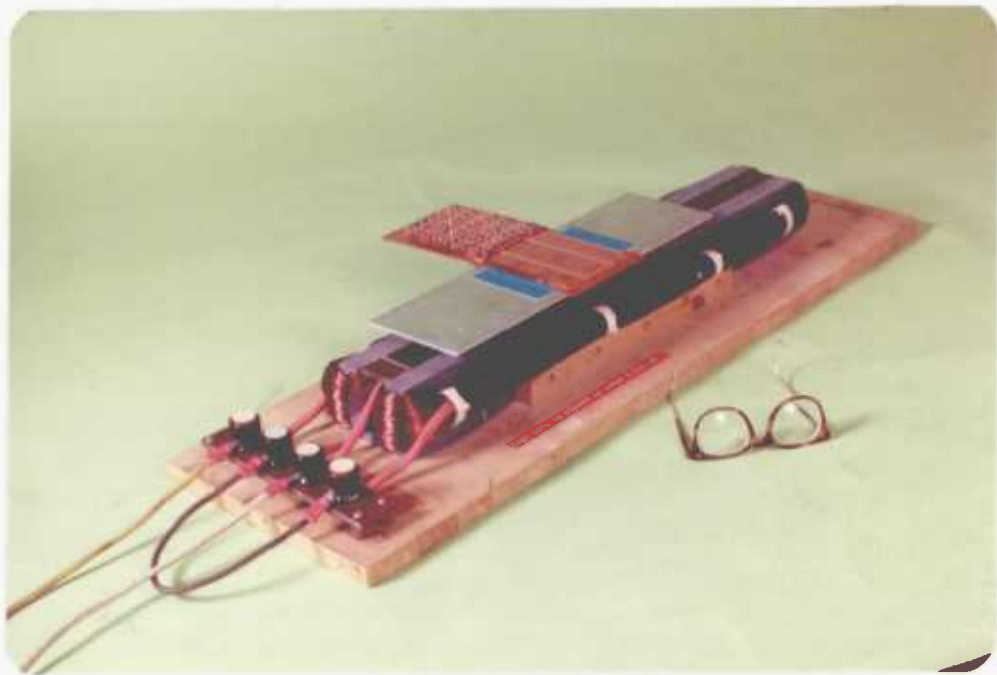
To achieve rotary drive, all that is necessary is to cut a set of axial slits in each limb of the C-core and mount within them the stator windings of a conventional induction motor. The resulting combination is shown in Fig 28. The torque required from the driving winding is not large, since the rotor is floating on a frictionless suspension. The induced rotor currents are therefore small compared with those induced by the main levitating coil, so they do not materially affect the behaviour of the suspension system. Suspension

can of course be maintained with the rotor spinning at any speed, including synchronous and beyond, since the suspension currents are entirely independent of the driving currents.

When the machine based upon these principles was built and tested its behaviour and performance were, for once, exactly as predicted. In fact it was the strong axial "suction" and spinning action experienced by any conducting cylinder of roughly appropriate size brought near to the opening of the machine that led to the christening of the device as the "electromagnetic whirlpool". Further investigations into these two rotary forms of the Washington model, the turntable and the whirlpool, have not yet been carried out, but clearly the subject remains open and could offer rewarding possibilities for future work.

CHAPTER 4

DISTRIBUTION OF FORCE ON FLOATING PLATES



The long pole-pair machine (p 43), with a rotor carrying a set of search coils to measure the distribution of normal flux (p 65).

CHAPTER 4. DISTRIBUTION OF FORCE ON FLOATING PLATES

4.1 Rotor surface voltage distributions

At the beginning of Chapter 3 a machine was described that had been designed to simplify the current and field patterns over a linear levitator by arranging that over a relatively long centre portion of the stator the current flow could be assumed to be purely longitudinal, and hence all fluxes to be purely in vertical transverse planes - see Fig 29. First investigations of this machine, using plates of varying lengths, have already been described (see Chapter 3, Figs 20, 21 and 22); further investigations, in more detail, form the subject matter of the present chapter.

Earlier experiments with slotted plates and rotary levitators had shown the need for the double-loop pattern of rotor currents. However nothing was yet known about the way in which this pattern changed, if at all, when the rotor was displaced sideways, or about how any resulting change in current distribution acted to produce the sideways restoring forces. Therefore it was decided to attempt to plot the current distributions, both with the plate in a central position and with it held in a displaced position (with the stator current unchanged). Direct measurement of the distribution of current within a continuous conducting sheet is not an easy task, but a good guide to the current flow lines can be obtained by determining the voltage equipotentials, knowing that current flow must be normal to these. This was the method initially adopted.

Fig 30 shows the construction of the voltage probe used, comprising two stainless steel pins mounted 1 cm apart in a paxolin holder provided with a handle. Connections from a co-axial cable passing through the handle were soldered close

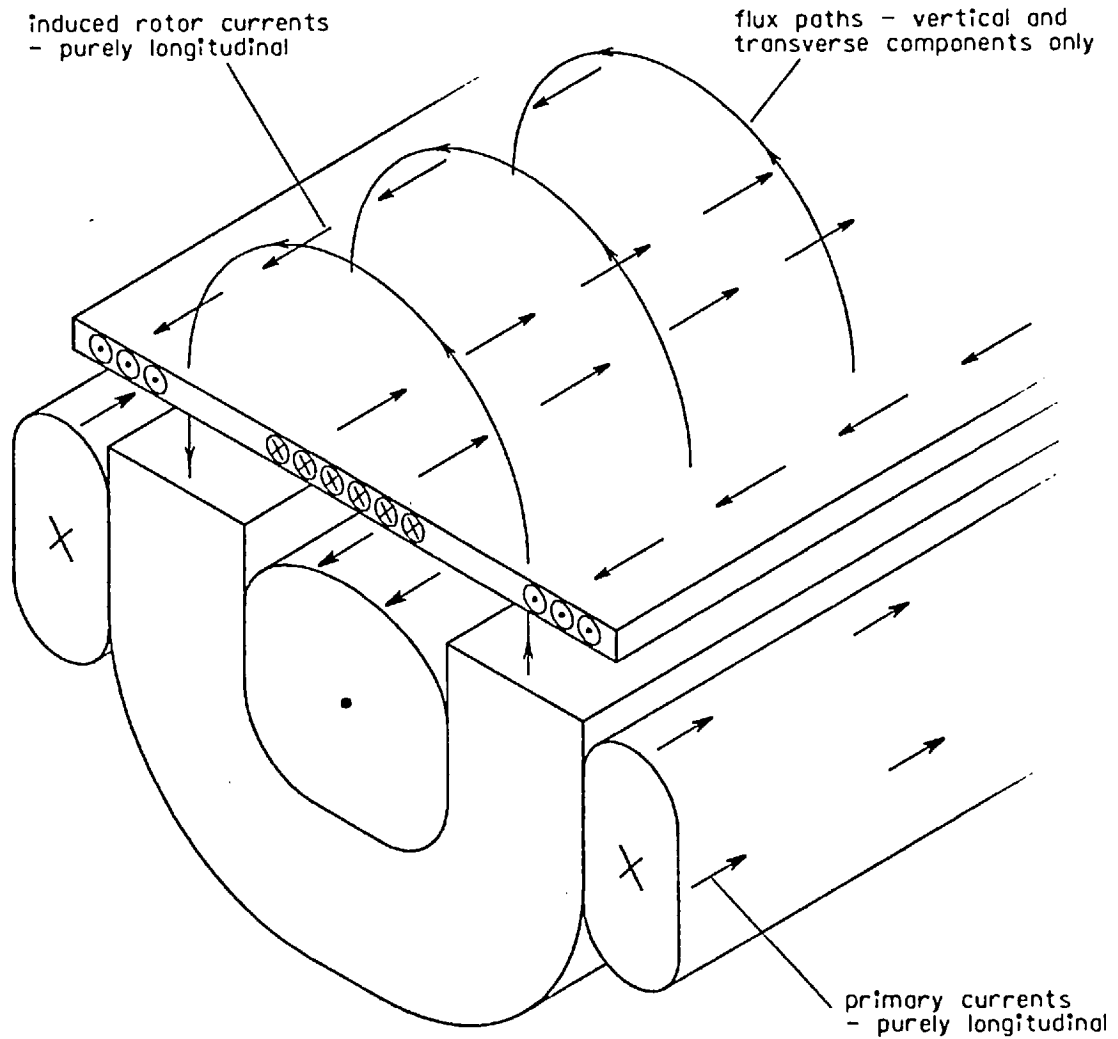


Fig 29. Section through long pole-pair machine.

to the tips of the pins, to minimise any loop area through which alternating flux could induce false voltages. For test purposes the rotor was supported at an appropriate height upon paxolin spacers, and strapped down firmly, thus allowing the voltage probe to be pressed hard into the aluminium surface to make reliable contacts. A rough plot of equipotentials near one end of the plate confirmed the general form of the double-loop pattern; it also suggested that instead of attempting to plot the complex equipotentials around the end-regions of a displaced

Fig 30.

Construction
of voltage probe.

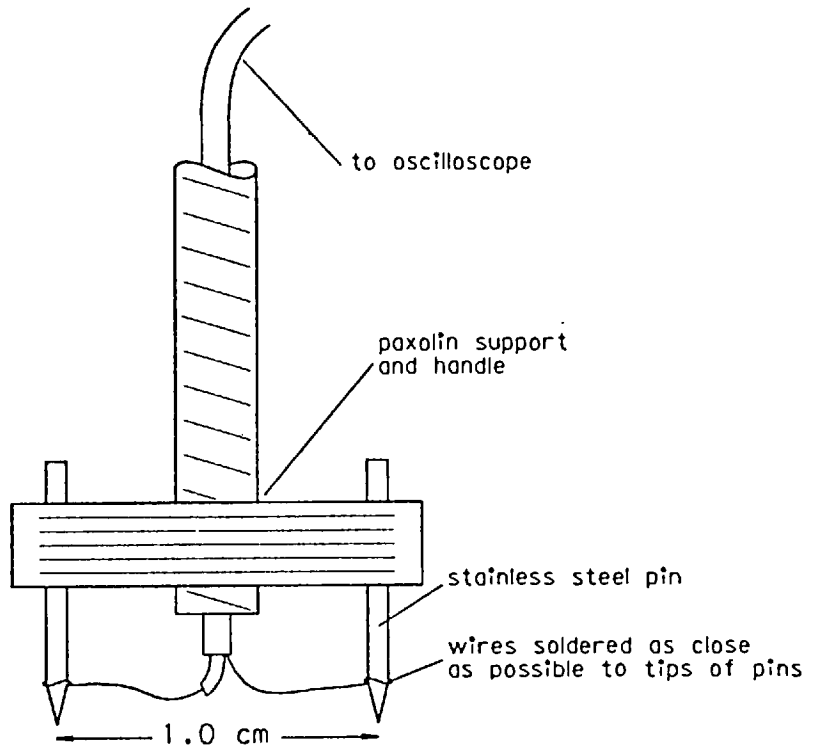


plate (which gives information on magnitude only of current, in a complicated area), it would be better to align the probe longitudinally and measure both the magnitude and the phase of the voltage potential between the pins. The current density could then be deduced for several positions across the width of the plate.

Fig 31 shows the resulting plot. The plate used, 3 mm thick and 7.5 cm wide, just covered the stator pole-pieces without overlap, and measurements were taken at thirty positions across its width. A sensitive digital voltmeter was used to measure the magnitude of the voltages (of the order a few hundred microvolts along 1 cm of the rotor), and a magslip (a variable-phase transformer) coupled to an oscilloscope was used to measure phase.

A striking feature of the graph is the high value of voltage at the edges of the plate, indicating that the maximum current density in the return current paths can be as much as double the maximum density in the centre path. The improved performance of a wider plate is clear. By offering a greater area for current flow in

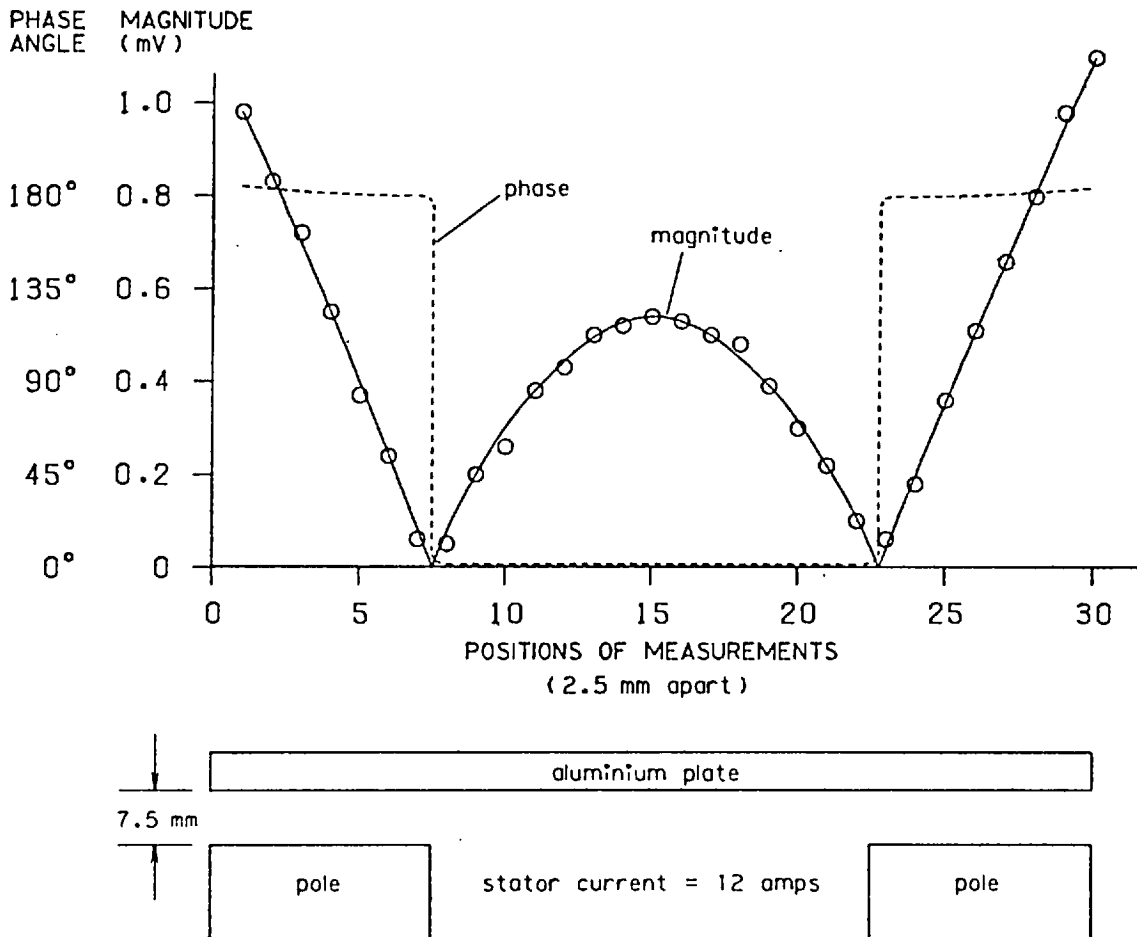


Fig 31. Distribution of probe voltages across plate.

regions of highest current density the resulting reduction in resistance occurs at the point where it is most useful. The abrupt phase-change between the centre and the return currents is also interesting as confirmation that the concept of the double-loop pattern is indeed an accurate representation of the situation.

The suggestion was made that if the current density across the thickness of the plate was assumed to be uniform, and the inductances of the current flow paths were assumed to be small compared with their resistances, then the voltage drop across the 1 cm length of current path could be used to calculate directly the distribution of current density across the plate width. The

appropriate formula is a slight modification of Ohms's Law thus:

$$J = \frac{v}{\rho \ell}$$

where J = current density,

v = probe voltage,

ρ = resistivity of aluminium,

ℓ = span of probe.

The magnitude of the current flowing longitudinally within a section from x_1 to x_2 across the plate is then given by:

$$I = h \int_{x_1}^{x_2} J dx$$

where I = current flowing within width
 x_1 to x_2 ,

h = thickness of plate,

or

$$I = \frac{h}{\rho \ell} \int_{x_1}^{x_2} v dx .$$

A quick check on this formula is to use it to confirm that the total current flow through the complete width of the plate must be zero - i.e. that the area under the centre arch of the graph of Fig 31 must equal that under the two triangular regions on either side. Upon measurement, the centre area = 13.6 units and the sum of the return areas = 21.0 units (where one unit of area = 1 mV-mm), showing that the assumptions upon which the method is based are not strictly valid. Measurements subsequently made on a piece of equipment to be described later in this chapter (the self-inductance probe of Fig 37) showed that it was not in fact the inductance of the current paths that could not be considered insignificant, rather it seemed that the difficulty arose from ignoring the effects of secondary leakage reactance between the rotor and stator current paths.

Nevertheless it is still interesting to pursue the calculation to the point of obtaining the value, albeit only to a first order

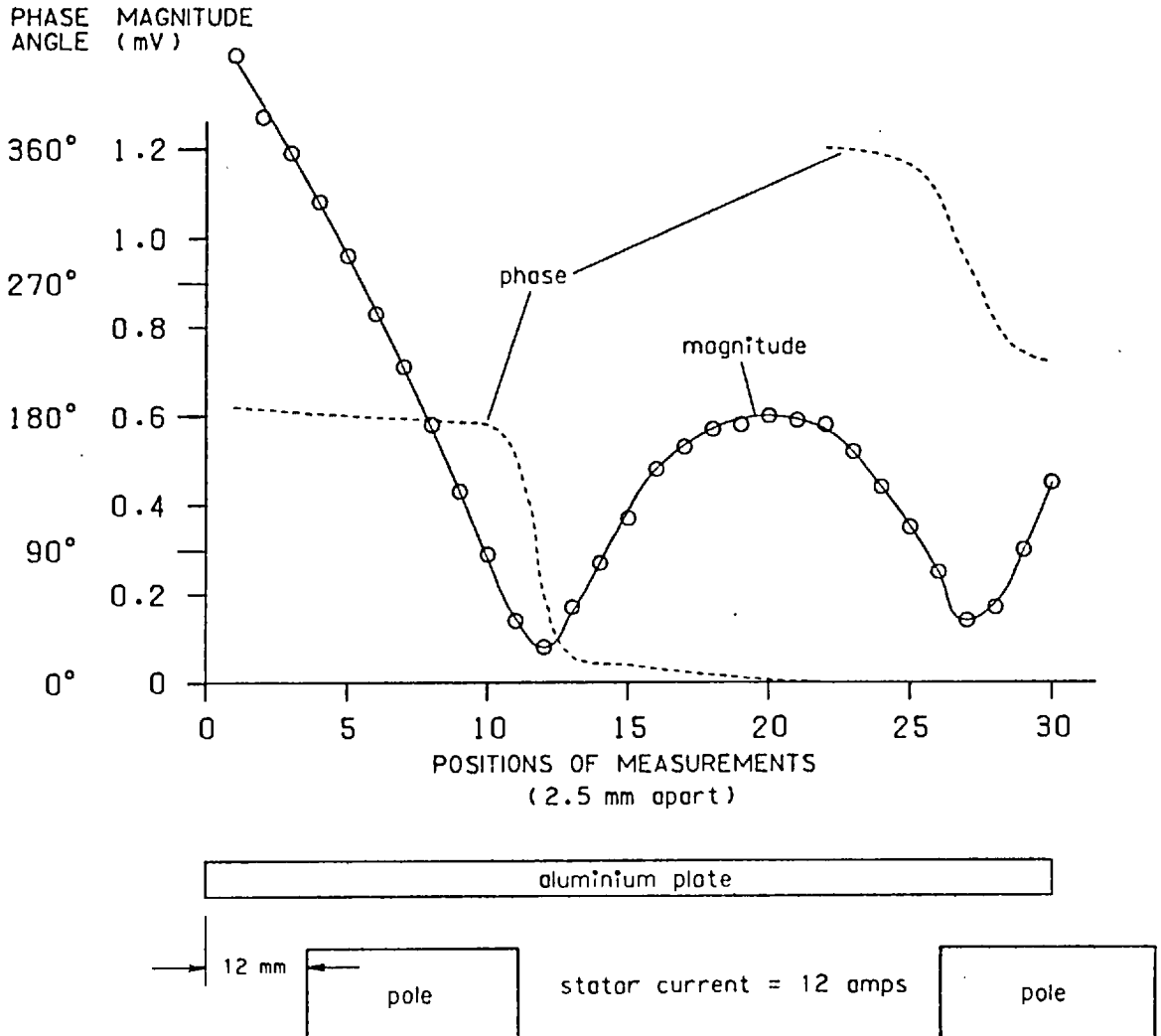


Fig 32. Distribution of probe voltages across displaced plate.

of approximation, of the current flowing within the rotor circuit when the plate is just supporting itself. The centre area is 13.6 mV-mm, whence the total centre current I_c is 150 amps. This applies for a stator current of 12 amps. But the stator current needed to just float the rotor plate is 42 amps, which scales up to $I_c = 530$ amps. Thus in this case around 500 amps flow along the centre and back around the edges of a plate only 3 mm thick simply for the plate to support its own weight. This figure is probably typical for a levitation machine of only some centimetres width; the situation improves progressively, however, for machines of larger size.

A second set of measurements of probe voltage magnitudes and phases across the width of a plate was taken, this time with the plate supported at the same height as before but displaced sideways by 12 mm from the centre position. The stator current was maintained constant at its former value. Completion of the graph - see Fig 32 - provided a new insight into the mechanism of stability. It was at once apparent that on displacing the plate the main induced current becomes shifted sideways within the plate so as to remain directly above the stator winding (symmetrically between the pole-pieces).

The return currents are then radically changed, since most of the centre current now returns along the side of the plate furthest from the centre of the machine. The reversal of phase between the main and the return currents is no longer sharply defined, there now being a smooth change of phase in the boundary region in place of an abrupt transition. A particular point to note is that the overall magnitude of the current appears to be little changed. This illustrates an important feature of the electromagnetic river - that the total upwards levitation force is not materially affected by small sideways displacements of the secondary.

4.2 Rotor surface flux

It seemed that the technique of measuring probe voltages could not usefully be extended beyond this point (without a knowledge of the inductances associated with the various rotor current patterns - extremely difficult quantities to measure or calculate), other than to continue to take sets of measurements with different shapes and sizes of plates, at different displacements, heights and orientations. However it was felt that perhaps an investigation into the distribution of the magnetic field around the rotor could lead to interesting results, particularly since established methods exist relating magnetic fields directly to the currents which produce them. It was decided that since only alternating quantities were involved it would be better to use small search coils to measure flux rather

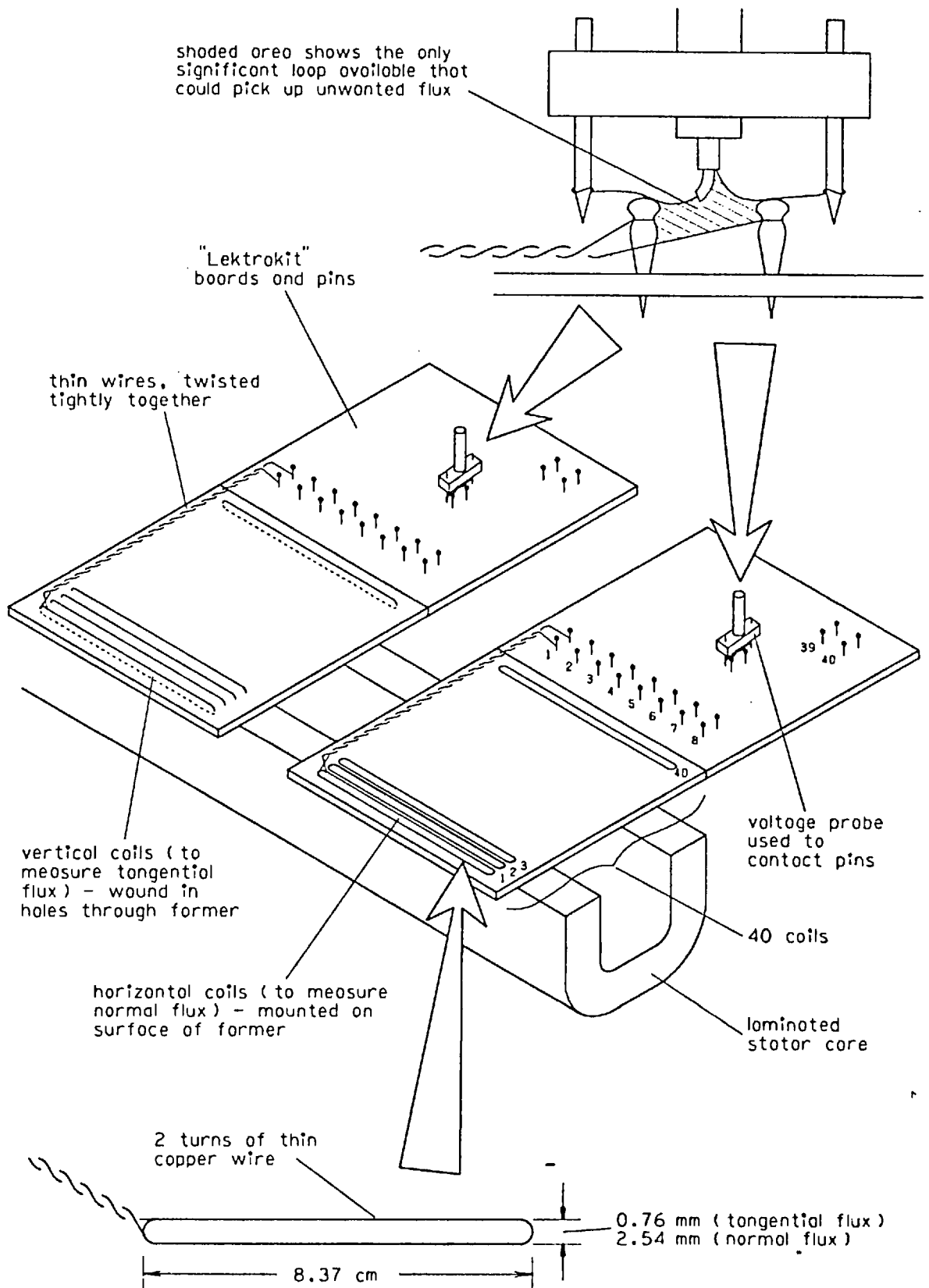


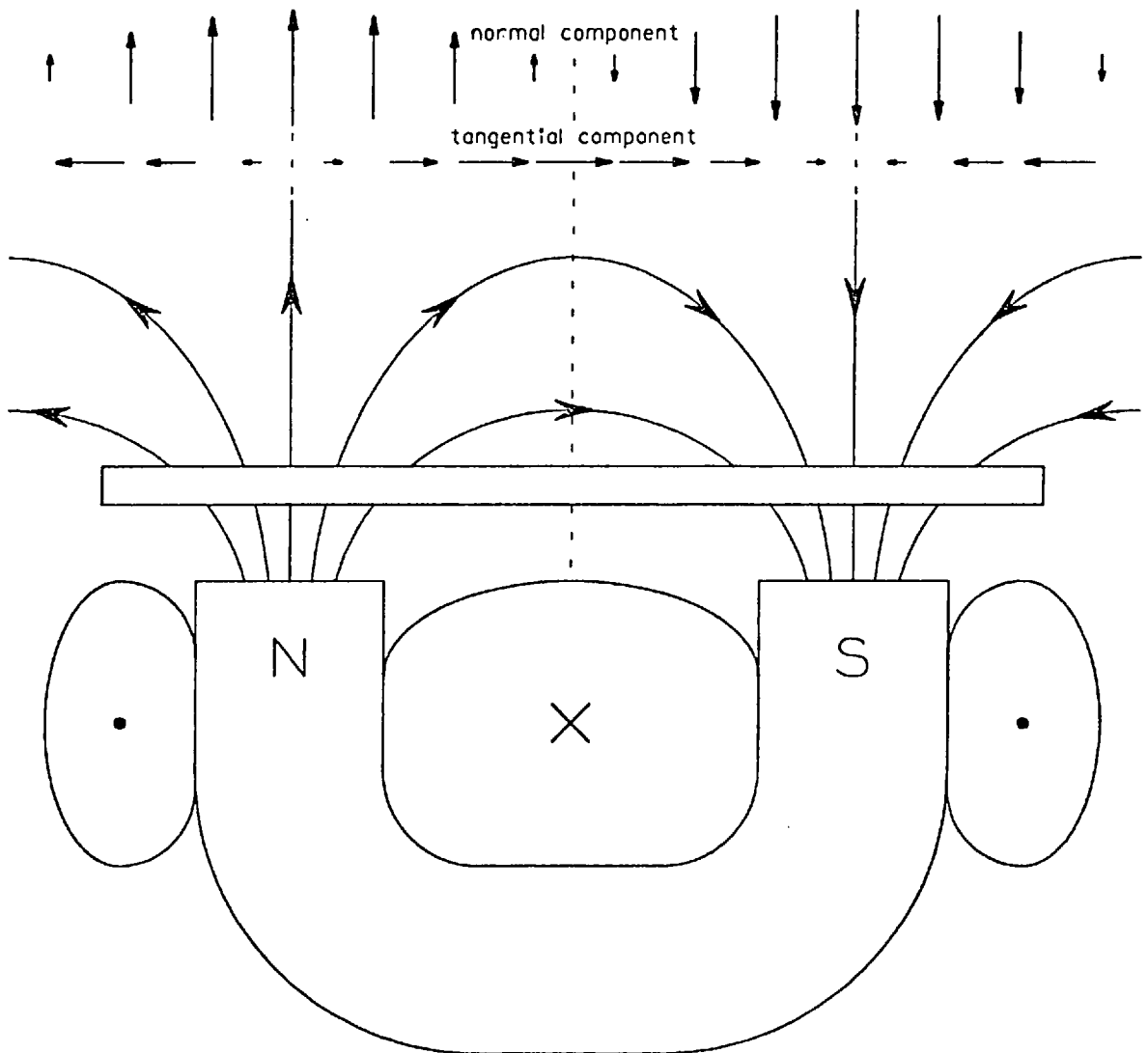
Fig 33. Search coils used to measure normal and tangential components of magnetic field above electromagnetic river.

than to employ Hall-effect probes in conjunction with commercial meters (personal experience of the latter has been that they are unreliable, less than straightforward to operate and constantly in need of re-calibration).

Two sets of search coils were constructed, one for measuring tangential (horizontal) flux near the surface of the plate, and one for normal (vertical) flux, both sets consisting of forty independent coils spaced equidistantly across a thin paxolin former 10 cm wide. Fig 33 shows the construction of the coils, making use of "Lektrokit" electronic circuit construction kit boards and pins. Connections from each coil were brought out to a separate pair of pins, positioned so that the voltage probe described earlier (see Fig 30) could be used to complete a circuit from any coil to an oscilloscope and digital voltmeter.

In view of the extremely small induced voltages to be measured (again of the order a few hundred microvolts), special care was taken to minimise the possible error introduced by pick-up of unwanted flux. Connections from the coils to the pins were of thin wires tightly twisted together, and the lead from the voltage probe onwards was co-axial cable, leaving available only the small area between the connection pins (shaded in the top insert of Fig 33) through which any unwanted flux could pass. And any such flux could be only that with a component in the longitudinal direction, itself extremely small within the centre region of the long machine.

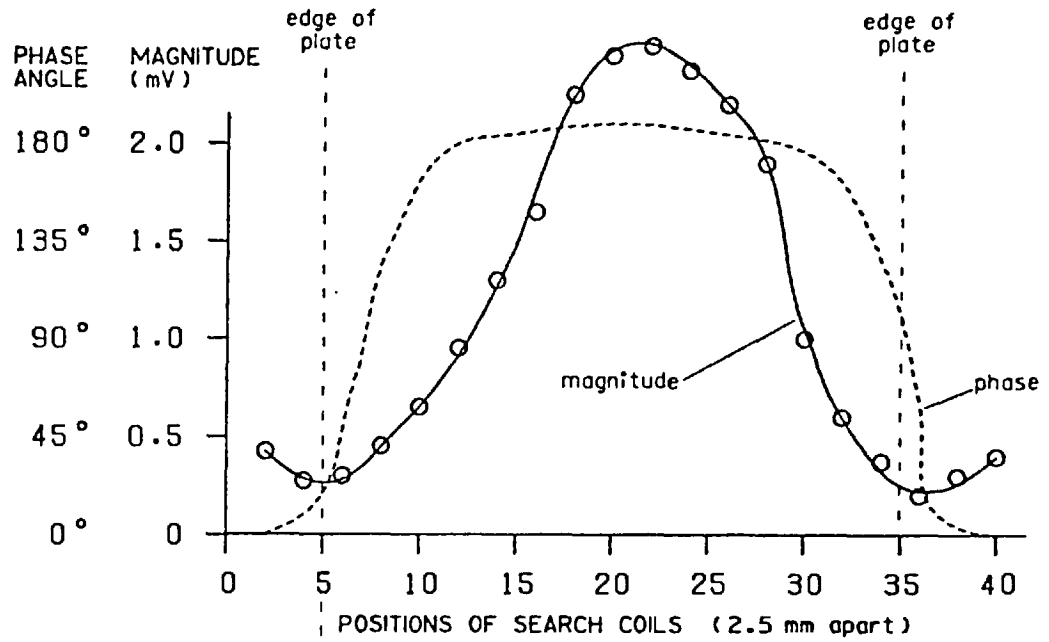
It seemed a reasonable assumption that the flux pattern above the stator poles was of the general form shown in Fig 34, at least to the extent that the tangential flux component within the region between the poles would be opposite in direction (i.e. in anti-phase) to that outside the poles, and that the normal flux component on one side of the system would be in anti-phase to that on the other. Complete plots were made of the magnitude and the phase of the normal and tangential components of the field, both across the upper and



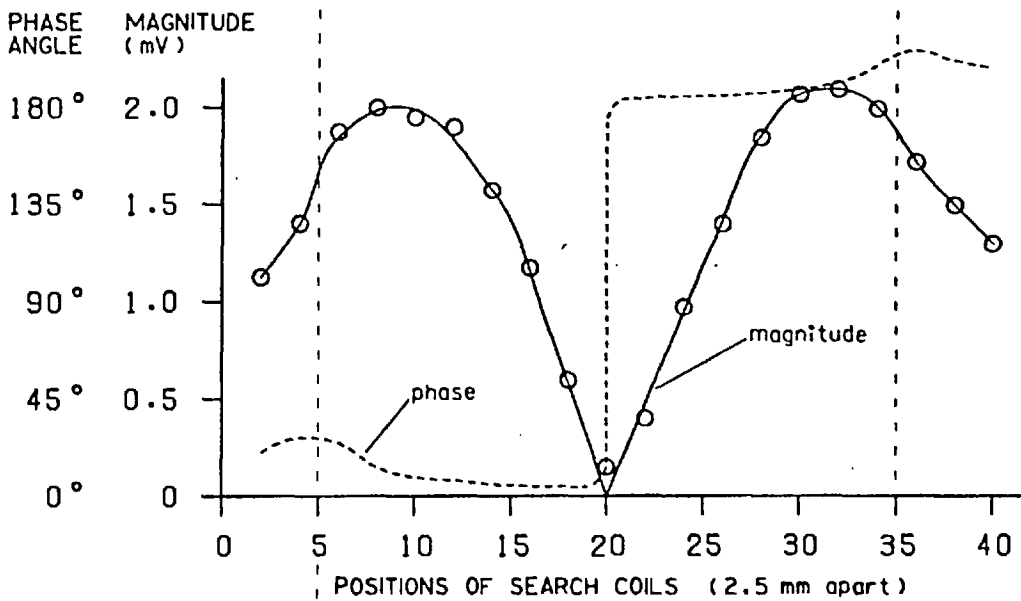
(instantaneous directions of currents and flux)

Fig 34. General pattern of flux lines around pole-pieces of electromagnetic river.

across the lower surfaces of the rotor plate. The plate used was that employed earlier to obtain directly the plots of voltage distribution - see Figs 31 and 32. The stator current was kept low throughout the series of measurements so that there was no significant rise of temperature during the considerable time necessary to take all the readings. A sample of the results is displayed in Fig 35.



(a) Tangential (horizontal) flux component.



(b) Normal (vertical) flux component.

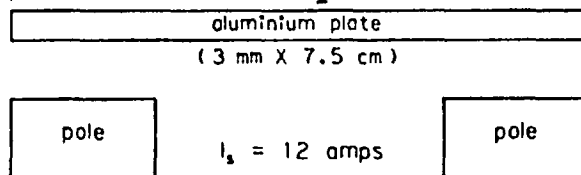


Fig 35. Plots of tangential and normal components of flux across the top surface of a floating plate.

As can be seen, the general shapes of the plots in Fig 35 are just as expected from Fig 34, with the tangential flux undergoing a change of phase above each stator pole and reaching its maximum magnitude at the centre, and the normal flux changing phase at the centre with maximum magnitude over each pole. The results displayed are those obtained along the upper surface of the rotor; those along the lower surface were similar in form but the flux was greater in magnitude. It will be noticed that the normal flux changes phase abruptly as its magnitude passes through zero, but the phase change for tangential flux is more gradual and the magnitude never reaches zero. The implication here is that there are regions where the phase angle between the two flux components is not exactly zero or 180° - i.e. there exist rotating components of magnetic field - and these regions are close to the edges of the floating plate. This result is interesting but not unexpected, since it is known that shaded-pole action caused by a plate edge within an alternating magnetic field frequently gives rise to rotating field components.

4.3 An analytical approach

Now the original intention was to use this detailed information about the magnetic field to deduce the actual currents flowing in the rotor, and then to calculate the forces between these and the main stator currents, thus giving the resultant force on the floating plate. This was to be done for several lateral positions of the rotor in order to gain some insight into the nature of the sideways guiding action. In fact it was thought that it might be possible to analyse the situation theoretically, by considering each independent search coil of the set to be associated with the current flowing within the corresponding width of aluminium below. Thus a 10 cm wide rotor plate could be considered to comprise forty independent "bars" of aluminium, electrically connected at each end of the plate, and each carrying its own individual current, as illustrated in Fig 36. Pairs of adjacent bars may then be considered to carry loops of current, $I_{R1}, I_{R2} \dots I_{RN}$ for a total of N loops, while the two stator loops

carry currents I_{S1} and I_{S2} . Since the total voltage around each rotor loop is zero, a series of vector equations can be written thus:

$$RI_{R1} + R(I_{R1} - I_{R2}) + j\omega L_1 I_{R1} + j\omega M_{12} I_{R2} + \dots + j\omega M_{1N} I_{RN} + j\omega M_{S11} I_{S1} + j\omega M_{S12} I_{S2} = 0$$

$$R(I_{R2} - I_{R1}) + R(I_{R2} - I_{R3}) + j\omega L_2 I_{R2} + j\omega M_{21} I_{R1} + j\omega M_{23} I_{R3} + \dots + j\omega M_{2N} I_{RN} + j\omega M_{S21} I_{S1} + j\omega M_{S22} I_{S2} = 0$$

⋮

⋮

$$R(I_{RN} - I_{R(N-1)}) + RI_{RN} + j\omega L_N I_{RN} + j\omega M_{N1} I_{R1} + \dots + j\omega M_{N(N-1)} I_{R(N-1)} + j\omega M_{SN1} I_{S1} + j\omega M_{SN2} I_{S2} = 0$$

where R = resistance of one rotor "bar",
 L_x = self-inductance of the x^{th} rotor loop,
 $M_{xy} = M_{yx}$ = mutual inductance between rotor loop x and rotor loop y ,
 M_{Sxz} = mutual inductance between rotor loop x and stator loop z ,
 $\omega = 2\pi \times \text{frequency}$,
 $j = \sqrt{-1}$, representing a phase lag of 90 degrees.

A pair of equations for the two stator loops can be similarly derived:

$$R_S I_{S1} + j\omega L_{S1} I_{S1} + j\omega M_{S11} I_{R1} + \dots + j\omega M_{SN1} I_{RN} + j\omega M_{SS} I_{S2} = V_1$$

$$R_S I_{S2} + j\omega L_{S2} I_{S2} + j\omega M_{S12} I_{R1} + \dots + j\omega M_{SN2} I_{RN} + j\omega M_{SS} I_{S1} = V_2$$

where R_S = resistance of one stator coil,
 L_{S1} and L_{S2} = self-inductances of the stator coils (equal when the rotor is central),
 M_{SS} = mutual inductance between the two stator coils,
 M_{Sxz} = mutual inductance between rotor loop x and stator loop z (as before),
 V_1 and V_2 = voltages applied to stator coils.

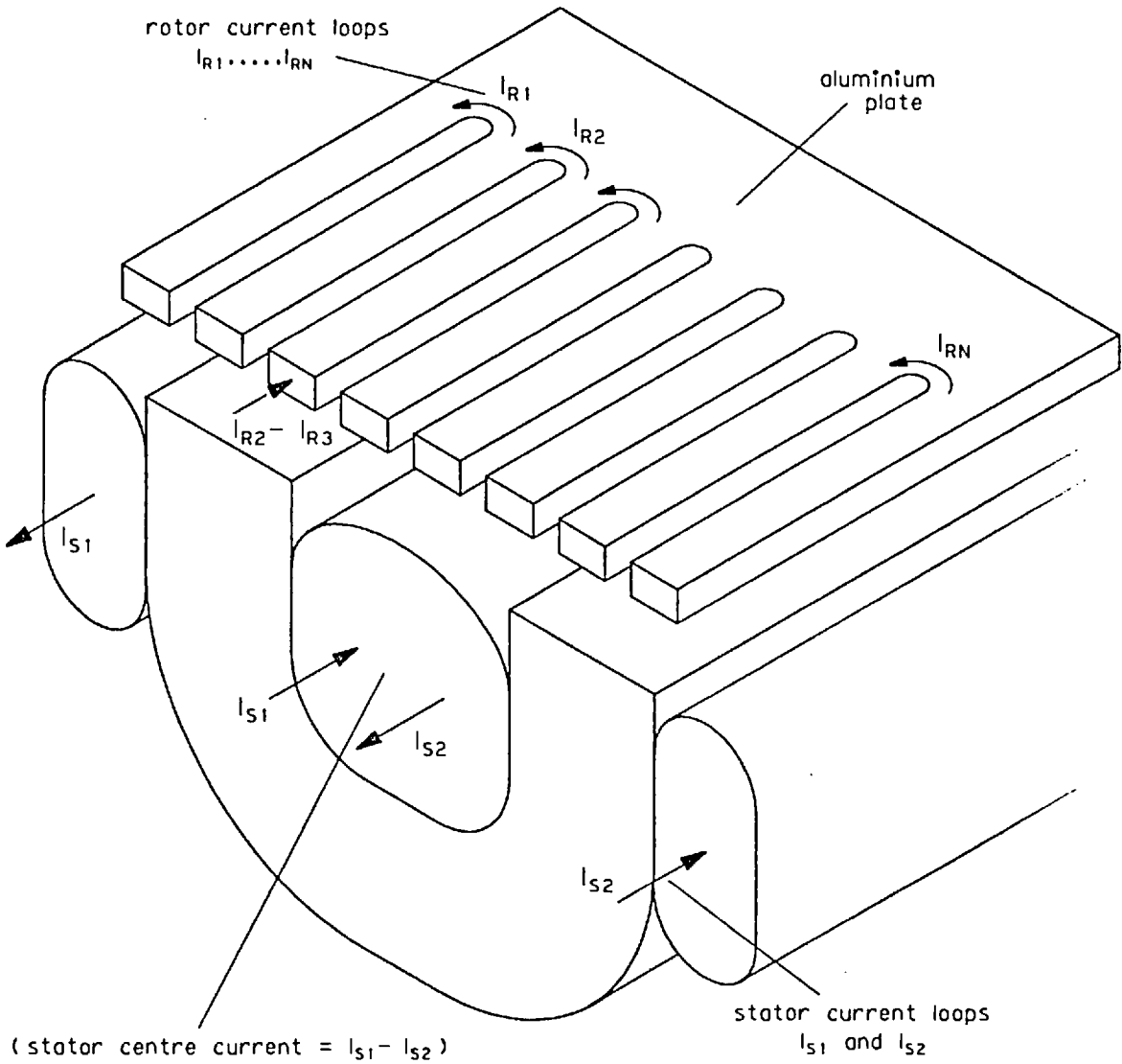


Fig 36. Rotor current distribution considered as a series of discrete "bars" carrying independent currents.

A final pair of equations may be formulated depending upon the connection of the two stator coils. For coils in series, $V_1 + V_2 = V_m$ where V_m is the applied mains voltage, and $I_{S1} = -I_{S2}$; for coils in parallel $V_1 = V_2 = V_m$.

The complete set of equations may be solved by using a standard matrix inversion procedure on a computer, to obtain the rotor currents in terms of the applied mains voltage and of

the constants, i.e. the resistances, inductances and mutual inductances. Of these constants, the resistances R and R_S may readily be measured directly. $M_{S11} \dots M_{SN1}$ and $M_{S12} \dots M_{SN2}$, the mutual inductances between the rotor and stator coils, may be easily obtained by passing a known current through the appropriate stator coil and measuring the resulting induced voltage in each of the respective search coils. A similar procedure gives the value of the mutual inductance M_{SS} between the two stator coils.

But it is with the remaining constants - the self-inductances of, and the mutual inductances between, the rotor coils - that difficulties arise. Methods of direct calculation or of numerical approximation were ruled out because of the complexities introduced by the presence of stator iron and the expanse of conducting material forming the rotor. Suggestions were made that the self-inductances of the individual coils might be obtainable by resolving the in-phase and the quadrature components of voltage needed to cause a small alternating current to flow within the search coils themselves. However calculation of the resistance and approximate inductance of a similar coil in free space revealed that its reactance at 50 Hz would be approximately ten thousand times smaller than its resistance, which would render any such measurement entirely impracticable. It seemed that the only method of measuring these constants was to employ a separate piece of apparatus, built especially for the purpose.

Fig 37 illustrates the apparatus proposed. A pair of copper bars are bent into the shapes shown in the figure and used to pass a heavy current up and back along paths equivalent to one "coil" in the rotor. Between the bars is sandwiched a search coil of dimensions identical with those used in the set for measuring normal flux. With the device in position at a selected point across the plate the voltage picked up in the search coil per unit current passed through the copper gives the self-inductance of the appropriate rotor "coil". Voltages picked up in each of the original set of search coils across the plate also enable the appropriate mutual inductances to be calculated.

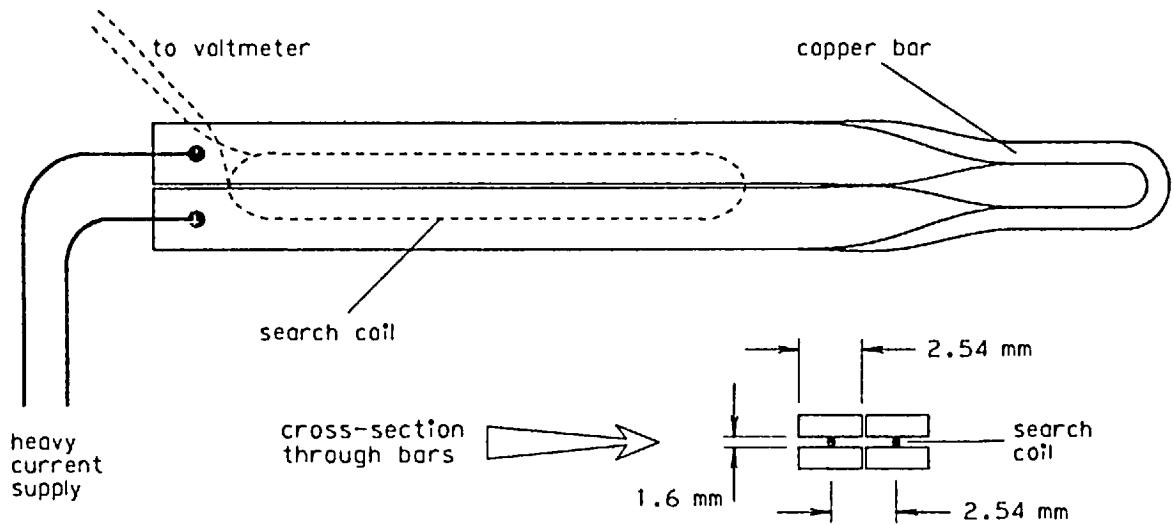


Fig 37. Suggested apparatus for measuring self-inductances of rotor "coils".

Each of these forty search coil voltage readings must be repeated for each of the forty positions of the inducing device across the plate, and any movement of the plate to a new position necessitates taking this entire set of readings again. For a set of constants of values roughly three orders of magnitude below other elements in the overall matrix the effort required seemed scarcely worthwhile.

Even if all these values are assumed to be negligible, there still remains a large amount of practical work in the "theoretical" approach. Measurements of the resistances, stator self-inductances, and mutual inductances between rotor and stator coils are made an easy matter by the existence of a laboratory machine, but the aim of the method should be to predict the performance of machines before they are built. The problem then becomes one of large-scale three-dimensional field solving by numerical approximation on a computer, and again each movement in position of the rotor entails a complete re-working of all the quantities involved. While development of such a computer program would undoubtedly prove an interesting project in itself, it was not considered suitable to take over from the practical work already begun.* The "theoretical" approach was therefore abandoned.

* See, however, Volume II (page 272) for details of some later work carried out along these lines.

4.4 Forces by Maxwell Second Stress

At this point the direction of thought took a new turn. Perhaps it would be possible to relate directly the magnetic fields around each rotor "bar" to the forces upon it, using a form of the "Maxwell Second Stress" method. Maxwell showed that the electromagnetically produced force on any body or part of a body, including iron and current-carrying conductor if present, can be obtained from a knowledge only of the magnetic field distribution around that body. More specifically, if any closed surface is drawn enclosing the part in question and no other part, and the magnitude and direction (and phase if a.c.) of the magnetic flux can be found at every point on the surface so drawn, then a process of integration over the whole surface yields the required force.

The necessary equations, most easily expressed in terms of the normal and tangential components of the force and flux at each point on the surface, are:

$$F_n = \frac{\mu_o}{2} \{ H_n^2 - H_t^2 \}$$

$$F_t = \mu_o H_n H_t$$

where F_n, F_t = normal and tangential components
of force at a particular point,

H_n, H_t = normal and tangential components of
field intensity at the same point,

μ_o = permeability of free space.

Derivation of the above equations from the set of general Maxwell equations is a standard piece of analysis which may be found in many reference works (e.g. 10), and is therefore not reproduced here. The Second Stress is the name given to the equations taking account of electromagnetic fields only; a similar pair of equations, usually referred to as the First Stress equations, may be derived to determine forces arising from electrostatic fields.

A positive normal component of force, F_n , derived from the equations indicates an outward-acting force upon the body enclosed (regardless of the signs of H_n and H_t), while a positive tangential force, F_t , indicates that the force is in the direction of H_t when H_n is positive. It is important to realise that the theory allows a physical meaning to be attached only to the total force given by the surface integral of the equations over an entire closed surface. Forces calculated for one point alone, or over any isolated portion of a surface, are meaningless. Note that a closed surface may, however, be arranged if desired to include only a selected part of the system in question, in which case the forces derived will be the sum of the forces acting only on that part.

Now with the aid of the two sets of search coils of Fig 33 it is a straightforward matter to obtain the magnetic field distribution around the surface of a plate supported above the single-phase stator. Fig 35 gives this information for the top of the plate, and the distribution for the bottom surface may be equally readily found. The flux distribution at the edges of the plate can be determined by winding a separate pair of search coils, or by using one coil of each of the sets of forty, vertically mounted. The total vertical force and horizontal force upon the plate as a whole may then be derived.

However these results are of only limited interest, since the vertical force is in any case simply the weight of the plate (when the plate is floating) and the horizontal force may be measured directly by using a spring balance or a force transducer. Of far more interest would be an attempt to use Maxwell's theory to give the distribution of forces acting over the surface of the rotor, but this is apparently precisely the kind of application that has already been rejected as giving meaningless results. In making such an attempt the following procedure therefore extends rather beyond the normal scope of the Maxwell Stress Method, and requires justification.

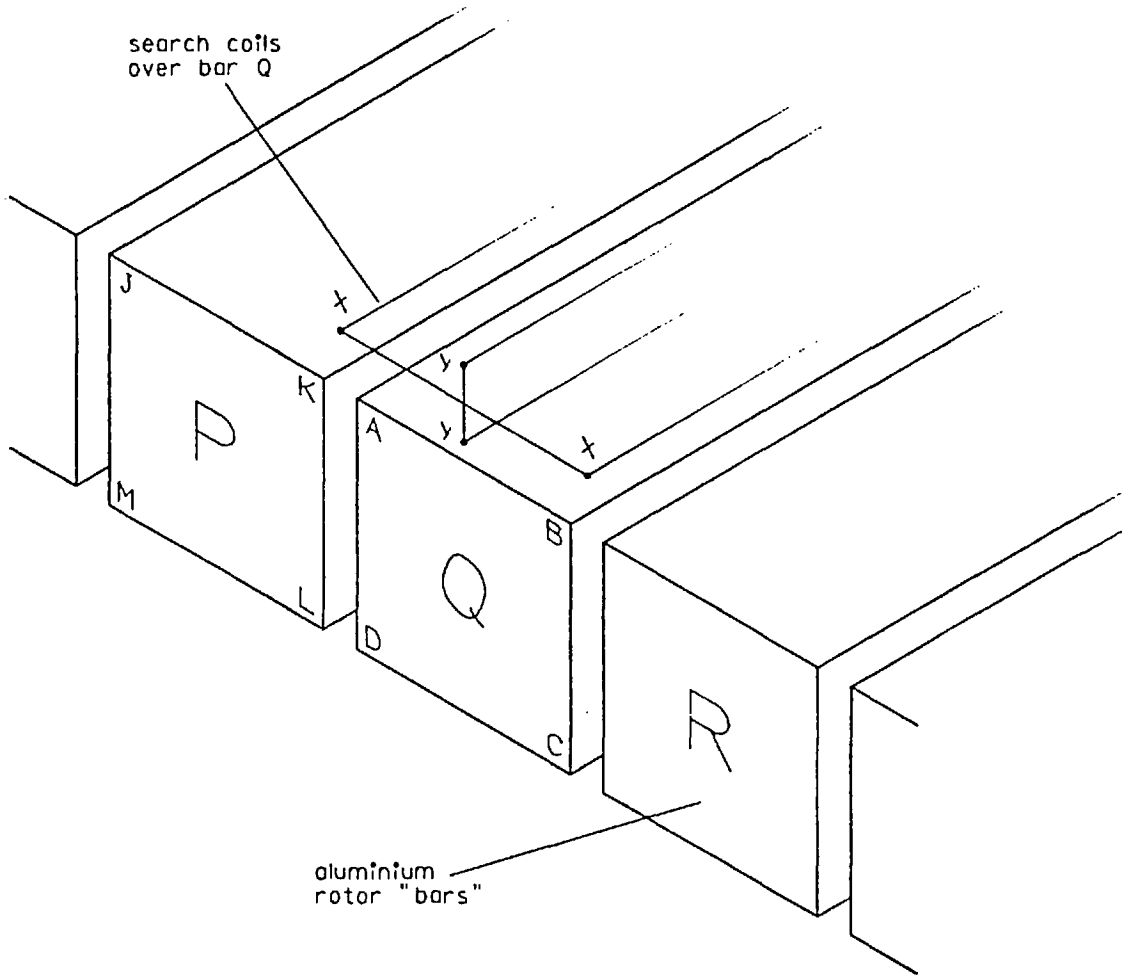


Fig 38. Section through rotor plate, considered as separate current-carrying "bars".

Consider the diagram of Fig 38, showing in particular three adjacent rotor "bars", P, Q and R. In order to obtain the force per metre length on bar Q let the Maxwell surface be chosen as the sum of the four surfaces of the bar, AB, BC, CD and DA, making it necessary to determine the normal and tangential flux components on each of the four sides of the bar. The search coil XX gives the normal flux component on side AB; coil YY gives the tangential component. The two components may similarly be found for side CD. But there is no similar easy way of determining the fluxes on the other two sides, because the gaps between adjacent bars exist, of

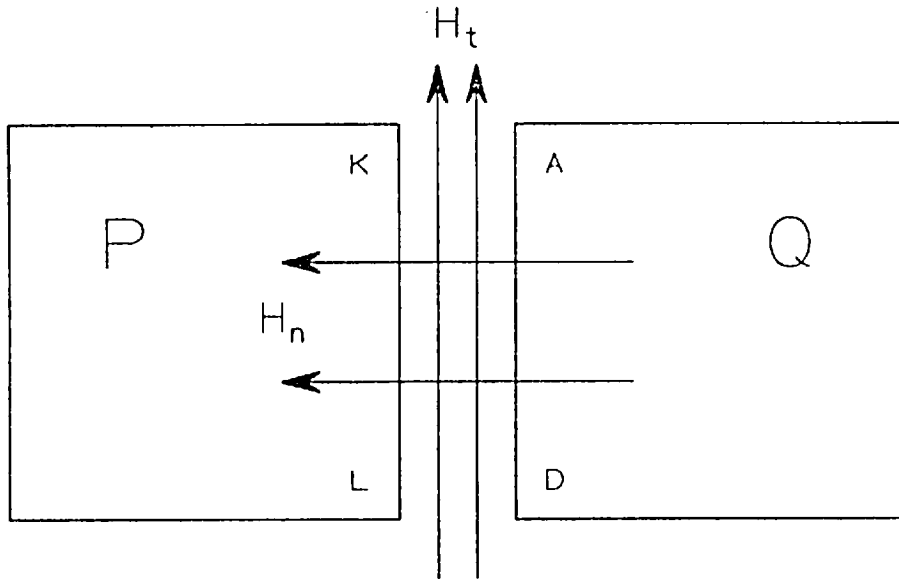


Fig 39. Normal and tangential flux components for faces AD and KL of bars P and Q.

course, only in the imagination. (It might be considered possible to wind a coil along the top of the rotor, passing over point A returning around the ends and back along the bottom, to measure the total flux normal to AD, but this would involve undesirable complications produced by the distorted fields near each end of the plate.

However if the face AD of bar Q and the opposing face KL of bar P are considered together as a pair, each forming part of their respective surfaces ABCD and JKLM enclosing bars Q and P (see Fig 39), then the values of H_n to be used in the force equation for the two respective surfaces must be of opposite sign since flux passing outwards normally through AD must pass inwards through KL. Likewise the respective values of H_t are the same sign - e.g. on the diagram, H_t is upward for both. The equation for normal force will therefore yield results identical in magnitude and in sign for both faces (the signs of H_n and H_t being irrelevant), showing that the normal forces on the two faces are equal and opposite (a positive normal force on

face AD being to the left on the diagram while that for KL is to the right). The equation for tangential force will yield results opposite in sign, again giving equal and opposite forces (since a positive result here means "in the direction of H_t ", and a negative "in the opposite direction").

Similar results will be obtained for face BC and its opposing member on bar R. It seems reasonable, therefore, to ignore the components of force evaluated for vertical faces such as AD and BC, on the grounds that for every unit of force in any direction calculated from one such face, there is an equal and opposite force calculated from the face opposite. Such forces can act only to produce stresses within the rotor (tensile or compressive stresses in the case of F_n ; shear stresses in the case of F_t) and can take no part either in the production of lift or in the mechanism of stability. The "useful" resultant force on bar Q, then, can be considered as the sum of the forces calculated from faces AB and CD only. Fortunately these are the faces for which flux measurements may readily be obtained from search coils.

If the useful resultant forces thus obtained are presented in some form relating each of the forces to the position at which it acts, then the resulting display can be taken as the real distribution of external forces acting upon the plate. Representation in this way of only the vertical force components gives the distribution of lift force, which should reveal for instance which parts of the plate experience the majority of lift and which parts, if any, experience a downwards force. Similar representation of the horizontal force components should indicate the regions of guidance force action.

It must be emphasised that the method does not invalidate itself by attempting to attach meaning to forces on one portion in isolation of the closed surface surrounding each "bar" - it merely displays those components of the total force which are not immediately cancelled out by equal and opposite components in adjacent bars. It

should also be noticed that the method can give no information relating to the internal stress distributions within the plate. Even if it were possible to measure the fluxes on the two vertical faces of each bar, to attempt to derive the resulting force on one such face would be to attempt to attach meaning to evaluations carried out over that one portion of the Maxwell surface in isolation from the other three portions. Such use is forbidden.

In order to apply the method directly to measurements taken from the search coils it is useful to develop the equations a little further. The original equations were:

$$F_n = \frac{\mu_o}{2} \{ H_n^2 - H_t^2 \} \quad \dots\dots (1a)$$

$$F_t = \mu_o H_n H_t \quad \dots\dots (1b)$$

Now the flux density B measured in each search coil is

$$B = \frac{V}{\omega N A} \quad \text{where } V = \text{voltage induced in coil,}$$

$$N = \text{number of turns in coil,}$$

$$A = \text{area of coil,}$$

$$\omega = 2\pi \times \text{frequency,}$$

The Maxwell surface is entirely within material of unit relative magnetic permeability (air or aluminium), hence the field strength H is:

$$H = \frac{V}{\omega N \mu_o A} \quad \text{where } \mu_o = \text{permeability of free space.}$$

Thus equation (1a) for normal force becomes:

$$F_n = \frac{\mu_o}{2} \left\{ \frac{1}{\omega N \mu_o} \right\}^2 \cdot \left\{ \left(\frac{V_n}{A_n} \right)^2 - \left(\frac{V_t}{A_t} \right)^2 \right\}$$

$$= \frac{1}{2 \omega^2 N^2 \mu_o} \left\{ \left(\frac{V_n}{A_n} \right)^2 - \left(\frac{V_t}{A_t} \right)^2 \right\} \quad \dots\dots (2a)$$

where V_n = induced voltage in coil measuring normal flux,

A_n = area of coil measuring normal flux,
and likewise for tangential subscripts "t".

Now the formulae as originally stated were derived for d.c. fields and steady state conditions. When dealing with alternating quantities, modifications may be needed to allow for the possibility of phase differences between the sinusoidally-varying quantities. It will be noticed that in the formula for tangential force, equation (1b), there is a direct product of the two components of magnetic field. This must be translated into a scalar product term when alternating quantities are involved.*

The tangential formula therefore becomes:

$$F_t = \frac{1}{\omega^2 N^2 \mu_0} \left\{ \frac{V_n V_t}{A_n A_t} \right\} \cdot \cos \psi \quad \dots (2b)$$

where ψ is the phase angle between V_n and V_t .

A corresponding modification to equation (2a) is not required since the scalar product of each voltage vector with itself is simply the square of its own magnitude. Equation (2a) can therefore be applied as written to alternating conditions.

Forces obtained from equations (2a) and (2b) then have to be evaluated for the top and for the bottom faces of each rotor bar, giving four forces whose vector sum is the "useful resultant force", given in both magnitude and direction, per metre length of the bar. This process must be repeated for all the bars across the rotor. A simple computer program was developed for the purpose. The output

* This is of course a specific case of the general rule that when equations involving the product of two sinusoidally-varying quantities are translated from instantaneous form (for which the Maxwell equations are valid as quoted) into time-averaged R.M.S. form, the direct product of two instantaneous values must be translated into the scalar product of two alternating quantities. For example the relationship $\text{Power} = V \times I$ is true instantaneously at all times under all conditions, but in the R.M.S. expression for alternating conditions it is necessary to write the scalar product: $\text{Power} = |V| \cdot |I| \cdot \cos \psi$, where ψ is the phase angle between the two quantities voltage and current.

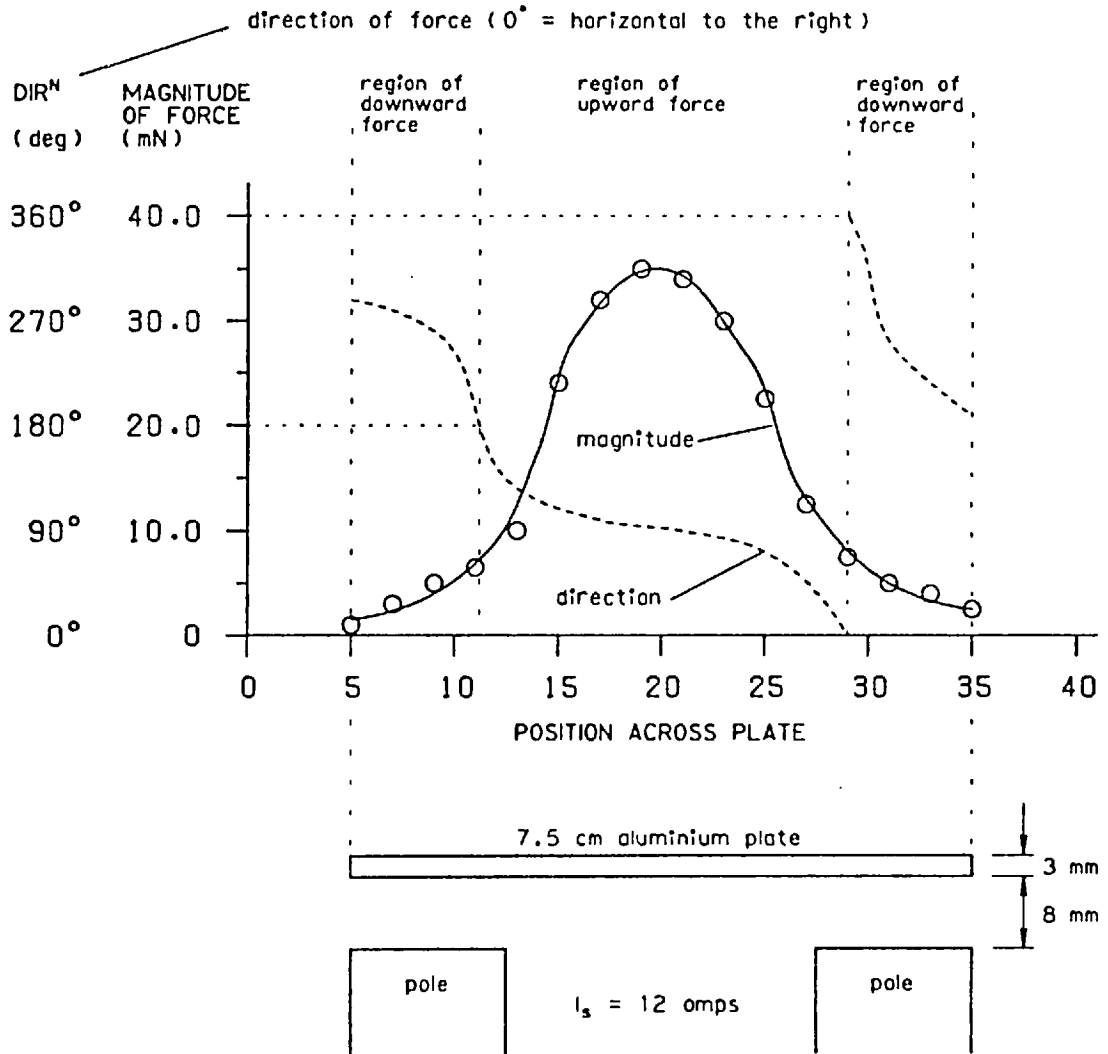


Fig 40. Graphical display of distribution of force across levitated rotor.

was arranged to give details of each of the four component forces, as well as the magnitude and direction of the resultant force, for every bar, and to sum the resultants to give the total force acting upon the plate.

Fig 40 shows a sample of the results, displayed in graphical form, taken for a plate 7.5 cm wide - these are the forces calculated from the magnetic field distribution displayed in Fig 35. It is immediately apparent that far from experiencing a roughly uniform

distribution of lift force across its width, as might have been expected, the plate experiences the great majority of upward force in its centre region. The angle of the resultant force (using the normal polar co-ordinate convention proceeding anti-clockwise from an initial direction horizontally to the right) actually exceeds 180° over considerable portions of the plate, indicating that the vertical component of force in these regions is downwards. The slight asymmetry of the display reflects an unevenness in the shape of the stator coils, probably as a consequence of employing a hand-built machine. This is encouraging in that it demonstrates the better ability of the method to show up irregularities of this kind, compared with procedures such as plotting measurements taken from the voltage probe (Fig 31) or with direct plots of flux distributions (Fig 35).

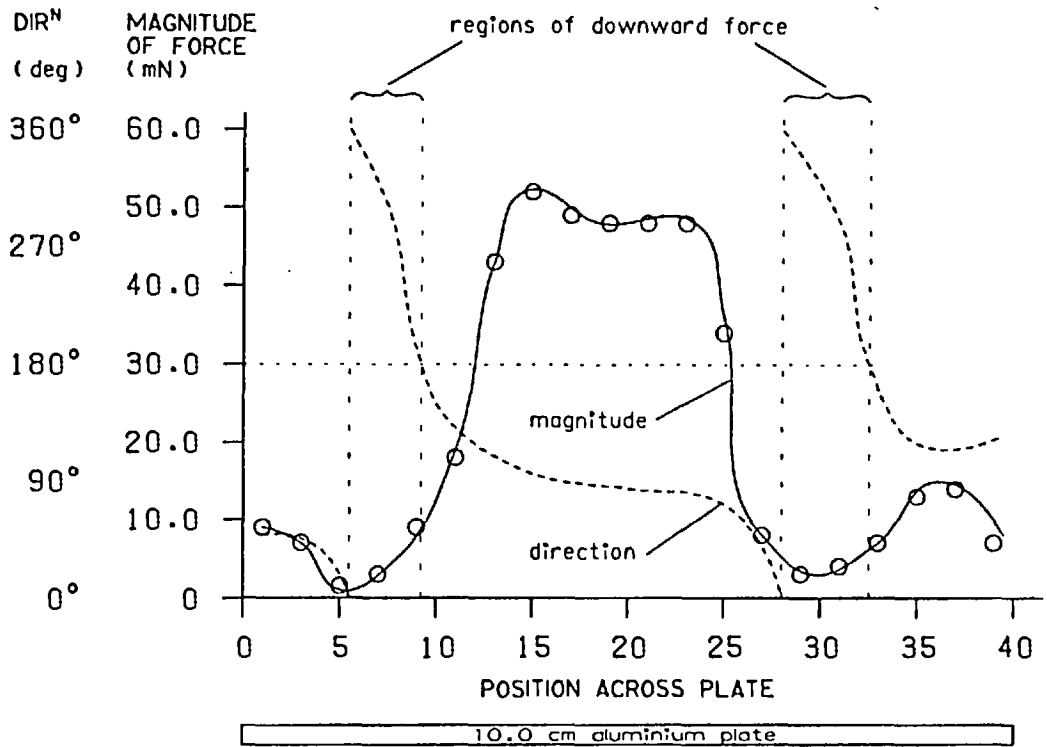
As a simple check upon the validity of the method, a comparison was made between the computer-evaluated magnitude of the vertical component of the total force acting on the rotor, and a direct measurement of the real force in operation. The computed resultant upwards force was 0.360 Newtons, or 36.7 gmf. An initial attempt to measure the upward force directly using a spring balance, by comparing the apparent weight of the plate with the stator current switched on with that for no current flowing, gave a result of about 40 gmf - with a likely margin of error of possibly 50%! (The total weight of the plate was 475 gm, the levitation force being so small because the stator current of 12 amps had been chosen to be sufficiently low that no significant heating of the rotor took place during the experiment.)

The more accurate method of raising the stator current until the plate just lifted clear of the supporting spacers gave the result that 41.9 amps were needed to float the plate. On the assumption that force is proportional to the square of current (in the absence of iron saturation), the lift force corresponding to the experimental current of 12 amps must therefore have been 38.9 gmf. This compares well with the computer-evaluated upwards force of 36.7 gmf. The

horizontal component of force acting upon the plate was given by the computer as 0.0204 Newtons, or 2.08 gmf - an order of magnitude lower than the vertical component. In fact a computed stabilising force of only 2 gmf acting on a plate of 475 gm mass probably merely confirms lucky centering of the plate on the spacer blocks when the experiment was prepared. Both these results lend confidence to the method as a whole.

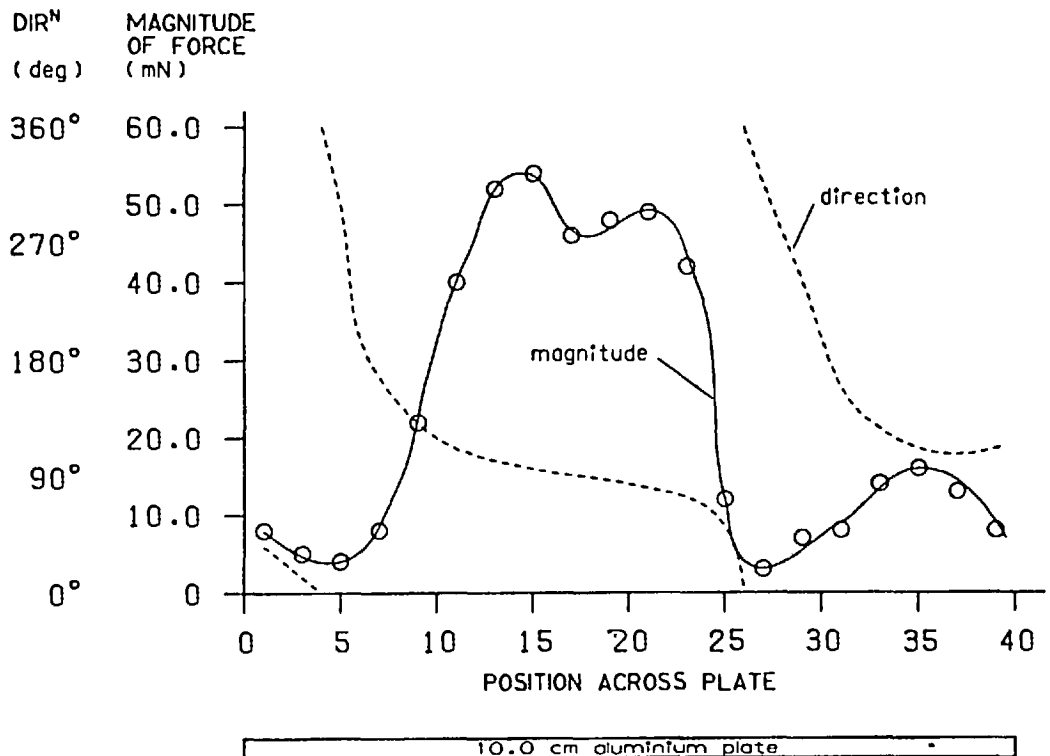
Now it will be recalled that one of the earliest discoveries concerning the electromagnetic river was that a wide plate tends to float at a greater clearance from the stator than a narrower plate, for the same stator current. Alternatively the wider plate experiences a greater levitating force if constrained to remain at the height of the narrower plate. It was decided to find out how well this established fact showed up on the Maxwell¹ force distribution. A complete set of flux measurements was therefore taken around a plate 10 cm wide, supported on the same spacer blocks as was the original 7.5 cm plate, and with the same value of stator current below (12 amps).

Fig 41(a) shows the resulting force distribution. The increased lift compared with the narrower plate of Fig 40 is immediately apparent, particularly in the centre region, where the lifting force is rather more extensively distributed than before. In the side regions significant lifting forces have appeared which were not present at all in the narrower plate. The regions experiencing downward forces are now confined to two small strips, positioned where the magnitude of the force is in any case at a minimum. Fig 41(b) shows the results obtained with the larger plate in a slightly displaced position. While it is clear that the movement has had a significant effect on the force distribution (particularly in the centre region, which has become markedly asymmetric), it is not easy to interpret at a glance the physical meaning of the changes. The following pictorial representation makes interpretation rather easier.



(a) Plate central.

pole $I_s = 12$ amps pole



(b) Plate displaced.

pole $I_s = 12$ amps pole

Fig 41. Force distribution across wide plate.

4.5 Pictorial representation of force distribution

The representation consists simply of drawing each of the computed values of force as a true vector (i.e. with length representing magnitude, and pointing in the direction of the force), whose origin is at the position of the search coil from whose voltages the force was computed. Each vector is thus positioned at the centre of the particular rotor "bar" on which its force acts. The effect is analogous to being given a photograph of a complex piece of equipment in place of a set of engineering drawings - the detailed information is perhaps less easily accessible, but the overall essential features of the system are brought to immediate attention in a way impossible within the confines of graphical representation.

Fig 42 presents three displays, corresponding to the graph of Fig 40 and the two graphs of Fig 41. Display (a), showing the distribution of force over the 7.5 cm plate (equal in width to the stator C-cores), reveals that the concentration of lift force towards the centre of the plate is perhaps not quite as pronounced as the graph of Fig 40 might tend to suggest, and that while it is true that there are extensive regions of the plate experiencing a downward pull, the magnitude of this pull is small compared with the central lift.

Fig 42(b) shows the forces acting upon the wider plate. The slight asymmetry apparent on the upper graph of Fig 41 shows up rather more clearly here, particularly at the edges of the plate. The central uplift forces are seen to extend over a larger area than before, and as predicted by the graphs the edge regions also experience upwards lift forces, though of considerably smaller magnitude than those near the centre. The forces on the edges themselves can now also be included, as shown, and these appear to accentuate the asymmetry caused by the hand-built stator coils.

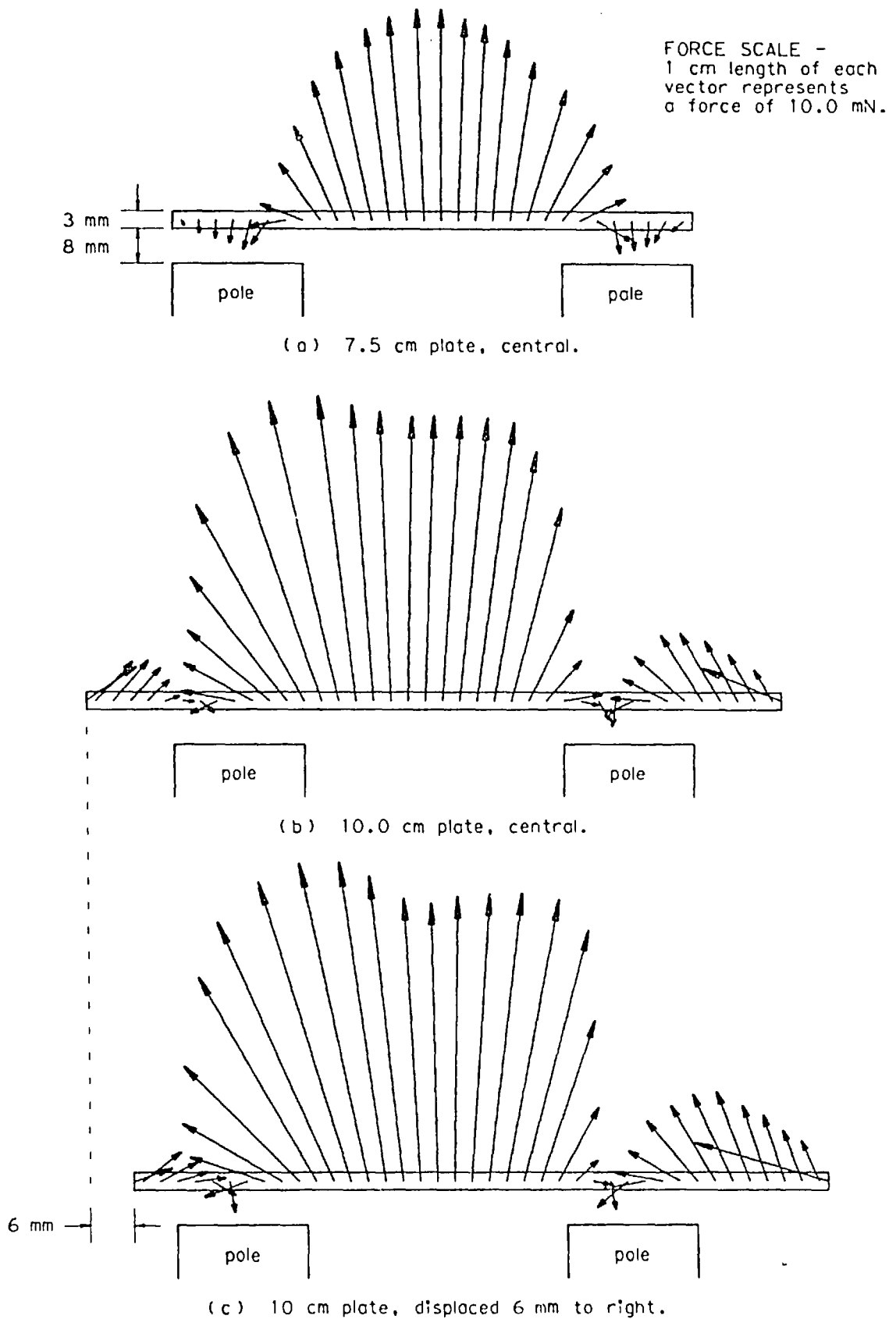


Fig 42. Pictorial display of rator force distribution.

Most interesting of all is the third display, showing the result of giving the rotor a small sideways displacement. The area of main uplift force is seen to move within the plate in order to remain above the centre of the stator, and there is a tendency for the large forces to the left of centre to become greater than those to the right, creating a component of tangential force in the direction tending to re-centre the plate. But a far greater stabilising effect is taking place at the plate sides. The upwards and inwards forces on the right-hand side have grown both in magnitude and in area of application, giving a strong re-centralising component, while those on the left, having the opposite effect, have shrunk almost to zero. The forces on the plate edges also contribute, the inwards force on the right-hand edge becoming almost doubled in magnitude.

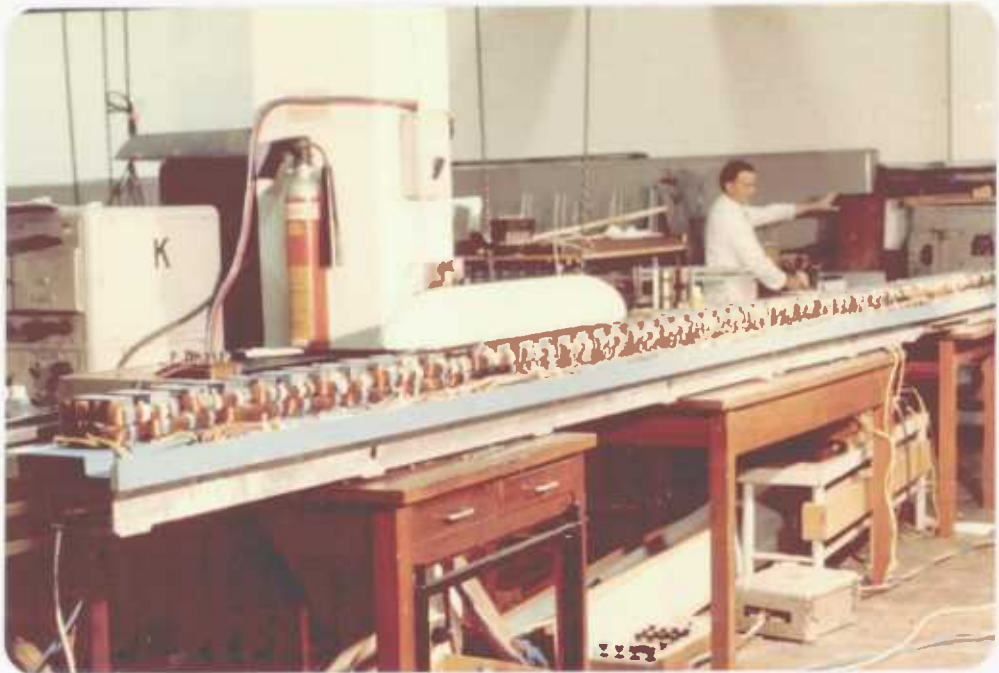
It should be pointed out that all these effects have taken place as a result of a sideways displacement of only 6 mm; the plate can in fact be displaced to ten times this distance before the maximum value of restoring force is reached. The computer summation of the tangential components gives the total restoring force as 10.6 gmf, by comparison with an upward force of 78.9 gmf. It is interesting to observe in passing that the uplift in the centralised position - Fig 42(b) - was slightly less, at 75.8 gmf. This tends to confirm the "feel" of the magnetic river banks as described in Chapter 1 (see Fig 7), where it will be recalled that the plate tends to "ride up" a bank as a result of a sideways displacement.

It is evident from the above work that this specialised use of the Maxwell Second Stress formulae provides a powerful research tool capable of extracting, from a specification only of the surrounding magnetic field, force patterns which could be obtained by direct experiment only with the greatest difficulty. At this point the decision had to be made whether to pursue the method further, by embarking upon a detailed series of experiments applying the technique to the many and various machines in the laboratory each with their set of possible shapes and sizes of rotor (there being sufficient work

here to form the basis for a complete thesis on its own), or whether to proceed to entirely new investigations, leaving this particular line of research open for others to explore. Since by this time a number of promising suggestions had been put forward for extensions to the Washington model, particularly for improvements to its performance as a propulsion unit, it was thought better to pursue these new ideas, thus maintaining the character of a research programme that was already tending to concentrate on opening up new paths, rather than on exploring in detail major routes already open.

CHAPTER 5

THE PHASE-MIXED ELECTROMAGNETIC RIVER



The seven-metre electromagnetic river (p 97).

CHAPTER 5. THE PHASE-MIXED ELECTROMAGNETIC RIVER

5.1 Improvements in propulsion

Although there is no doubt that the invention and building of the Washington model was a major breakthrough in the subject of electromagnetic levitation, those working on the machine held no illusions as to the value of the model itself other than as a prototype and a demonstration of what may be achieved when a machine is designed to make use of all three available dimensions instead of only one. As a propulsion unit the model could hardly be described as "efficient", since about ninety-five per cent of the input power was absorbed in lifting the rotor. The machine could indeed have been described merely as "a levitator, with a slight longitudinal thrust".

The reasons for this poor performance were largely the crude nature of the windings, the poor magnetic circuit and the small overall size of the structure. Firstly the coils were wound upon their C-cores in gramme-ring fashion, i.e. with all their conductors returning underneath the core - a design known to lead to high primary leakage flux. Secondly by using only one coil around each core, the winding configuration was equivalent to only one stator slot per pole per phase, and such windings have been shown to lead to large non-force-producing losses when the pole-pitch is greater than about 0.5 m.⁽¹¹⁾ (The Washington model had a pole-pitch of about 0.3 m, but this would be increased for motors on a larger scale. For example a working linear speed of 100 m/s from a supply frequency of 50 Hz would require a pole-pitch greater than 1.0 m.)

Thirdly the lack of magnetic material in the floating rotor led to an equivalent air gap of approximately 20 cm, resulting in a low value of goodness factor. Lastly the comparatively small overall size of the machine served only to accentuate the foregoing problems (though at the time of construction, of course, the size of the machine was deliberately limited to meet the requirements of the American exhibition).

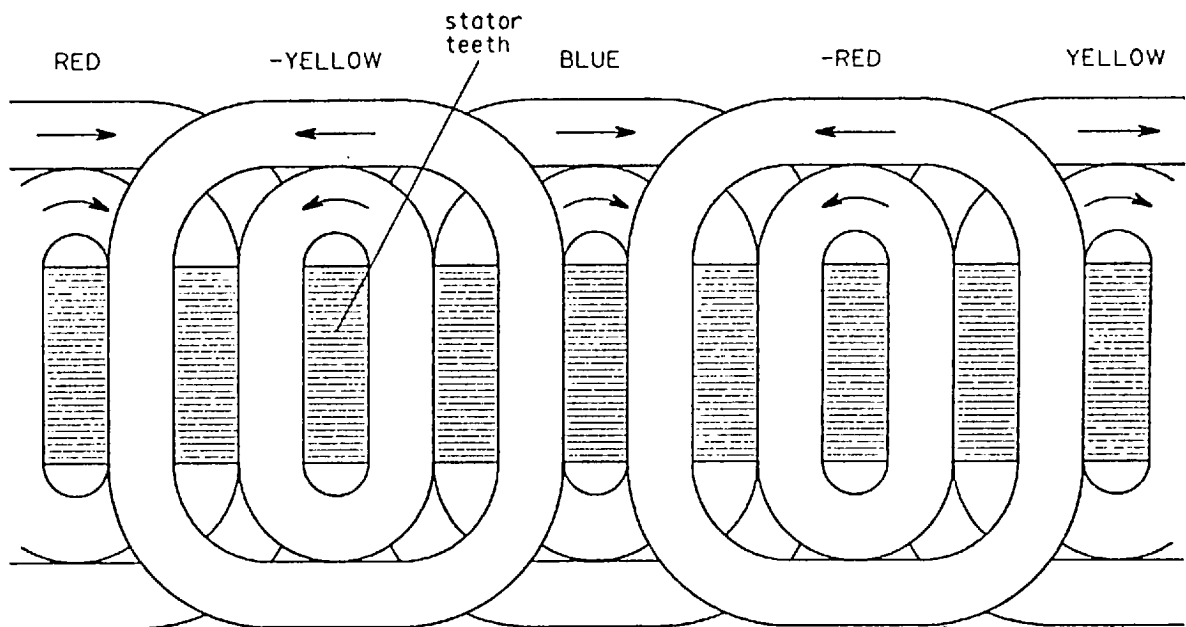


Fig 43. The two-layer concentric winding, as applied to a conventional longitudinal-flux motor.

The step forward from the gramme-ring wound coil to the double stator coil system, with the return currents flowing along the outer sides of the C-core, has already been explained at the beginning of Chapter 2 (see Fig 15). In order to improve the poor coil configuration it was decided to adopt a version of a two-layer concentric winding. This winding, invented in the laboratory a few years previously,⁽¹²⁾ was designed among other things to allow the maximum use to be made of the space available for the copper conductors between the limbs of each C-core. Fig 43 shows how the two-layer concentric winding may be applied to the stator of a conventional longitudinal-flux motor. The number of windings per concentric group can be made as high as desired, without theoretical limit, but it was decided initially to minimise the extra complexity by arranging each group in the form of a single coil.

The new machine was built to an overall size no larger than the original Washington model. Indeed the stator iron consisted of C-cores of identical cross-section, the reason for this being partly

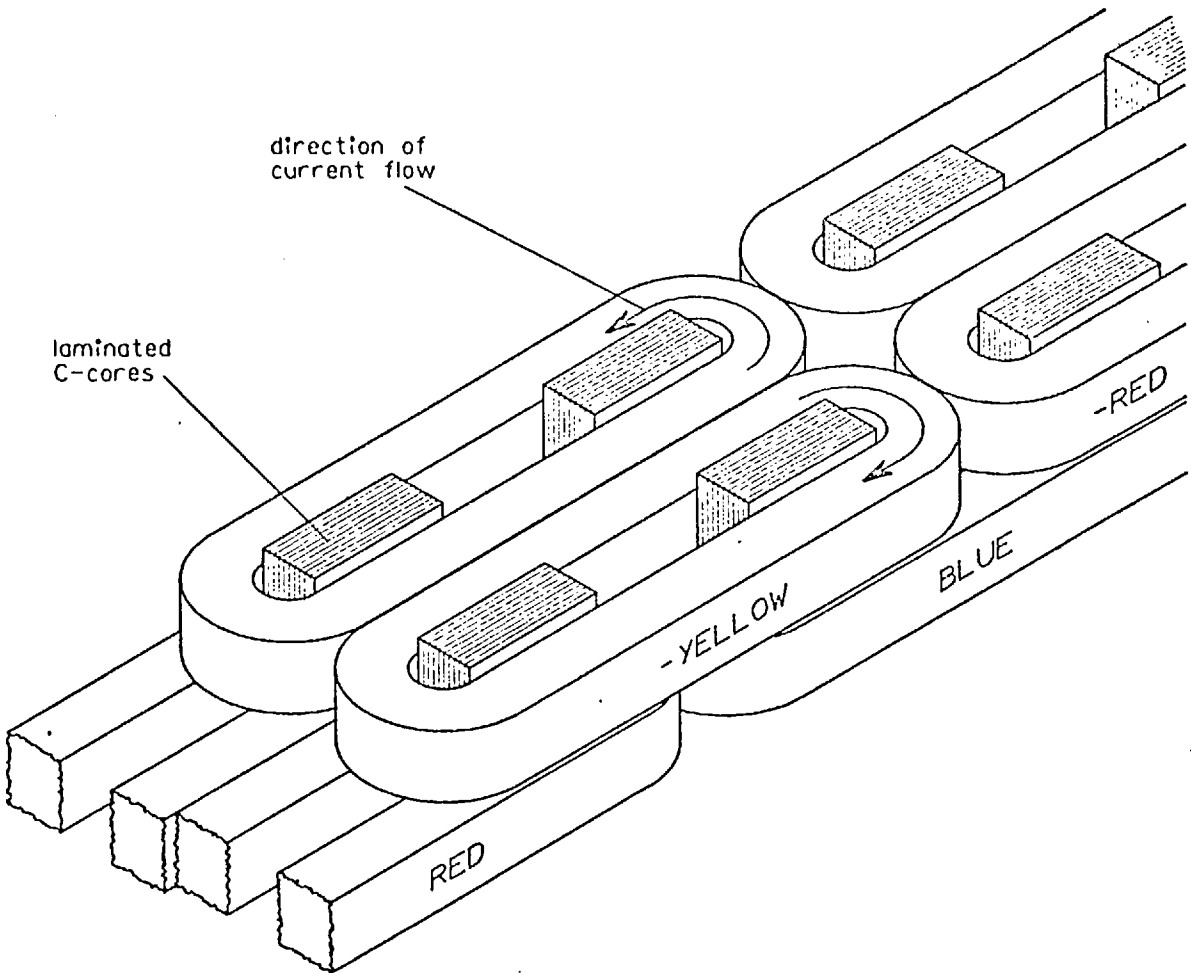


Fig 44. Final form of phase-mixed electromagnetic river.

to avoid introducing too many changes at the same time, and partly that those particular cores were the largest readily available on a commercial basis. Although the cross-section was not altered, the axial length of each C-core and the spacing between each pair were halved, giving a less coarse distribution of stator teeth along the machine. Combined with the phase mixing produced by placing in each slot coils carrying different phase currents, this resulted in a much smoother travelling field along the motor. The final version of the machine is shown in Fig 44 (see Appendix A for engineering details).

The most immediate impression on trying the new machine was one of a tremendous increase in longitudinal thrust. Measurement confirmed that the thrust was indeed an order of magnitude greater than had been achieved hitherto on an electromagnetic river. A more meaningful measurement, however, is the fraction of the input power that is converted to "synchronous driving power", defined by the expression:

$$S_p = \frac{fv_s}{P_{in}} \quad \text{where } S_p = \text{"synchronous rotor power fraction",}$$

f = standstill thrust on rotor,
 v_s = synchronous speed of field,
 P_{in} = stator input power.

The product fv_s , the synchronous driving power, represents the maximum power output theoretically available from the rotor (never actually attainable in practice).

The Washington model was capable of converting only five percent of its input power into synchronous driving power, the remainder being lost mainly in the heating effect produced by the large currents needed to support the rotor. But the new phase-mixed levitator increased this fraction to twenty-one percent, a most encouraging indication that further development combined with increases in size should allow the construction of an efficient propulsion system capable of providing simultaneously its own support and guidance forces.

5.2 Lift and guidance "for free"

There is an important point here. When electromagnetic systems are considered for the purpose of supporting heavy weights, an immediate impression is gained of large currents dissipating quantities of heat in the stator windings, resulting in a costly and wasteful system. Indeed all electromagnetic levitators built prior to, and including, the Washington model tend to strengthen impressions of this kind. But there is no inherent reason why

large amounts of energy need be expended in such systems. Theoretically, of course, it requires no energy whatsoever to maintain a force, provided the object upon which the force acts remains stationary or moves only at right angles to the direction of the force. But an electromagnetic machine designed to float and stabilise a heavy secondary must have flowing within the stator sufficient primary current to create a magnetic field powerful enough to induce large currents in the rotor. These react with the stator primary current in order to maintain the electromagnetic lift forces. The total power input to the machine is the sum of the heat losses in the stator and in the rotor, and must be written off as 100% total loss since the machine produces no power output.

Compare this with an electromagnetic machine in the form of a single-sided linear motor,* where it is well-known that an electrically-conducting non-ferrous rotor positioned within the field experiences a strong repulsion force from the stator, simultaneously

* Footnote on single-sided and double-sided motors.

A double-sided linear induction motor is one employing energised primary windings facing both surfaces of the rotor, so that the rotor moves in a slot between the two stator blocks. Such a system is highly efficient in propulsion, is unstable in a direction in the plane of the rotor but transverse to its motion (unless special stabilising grids are incorporated in the stator surfaces), and can be arranged to produce no force at all in the direction perpendicular to the plane of the rotor sheet. (Strictly the perpendicular force on the rotor is zero only when the rotor is placed exactly mid-way between the stator surfaces, but this is indeed the usual situation with a mechanically guided rotor.)

A single-sided motor employs an energised stator winding on one side only of the rotor, and is generally somewhat inferior to the double-sided motor in producing thrust. The rotor is again unstable in a transverse direction (with the exception of the electromagnetic river itself) but there can now be large forces, either attractive or repulsive, perpendicular to the plane of the rotor. Its particular advantage is the ease with which the rotor can be attached to a load or a support, since the whole of one face is available for mounting instead of only an edge. A more detailed comparison of the performances of the two designs, as high-speed propulsion units, is made at the end of Chapter 6.

with the forward propulsion. (For an aluminium plate placed above the surface of the stator this repulsion force becomes the force of levitation.) Consider a large single-sided motor designed to be as effective as possible a thrust device acting upon an aluminium rotor. The power output of the machine is the force upon the rotor multiplied by its velocity, and for a modern long pole-pitch transverse-flux linear motor this output may well comprise over eighty per cent of the input power. A detailed power balance can be evaluated to show that the sum of the mechanical output, the heat losses in the rotor and the stator, and the small iron losses, account for 100% of the input power. No power is being absorbed in the production of lift. Indeed a second motor can be built with a double-sided stator, in which a rotor placed mid-way between the stator surfaces experiences no force whatsoever perpendicular to its plane, yet the motor can require the same input power to produce the same thrust at the same speed as its single-sided levitating counterpart (though it is likely that it will have a better power factor and therefore require fewer volt-amperes from the supply).

On this basis, the I^2R and other losses must all be ascribed to the production of longitudinal thrust resulting in longitudinal motion, since such motion cannot be provided without them. It then appears that the electromagnetic lift of the single-sided motor has been achieved for zero extra power input. So what is the difference between the lifting capability of the single-sided linear motor, which costs nothing in terms of power, and that of the static levitator, which consumes large quantities? It is this: Whether the requirement is to levitate a conducting object, or whether it is to propel such an object horizontally, the basic operation of setting up stator currents to induce rotor currents inevitably involves severe heat losses, both in the stator and rotor. These must be supplied by the input power. But all such sets of currents carry inherent within them the characteristic of mutual repulsion, and once a current system has been set going and the losses are being supplied in order to provide thrust, this repulsion can then be utilised for lift purposes, thrown in as a free bonus. The losses do not have to be paid for twice.

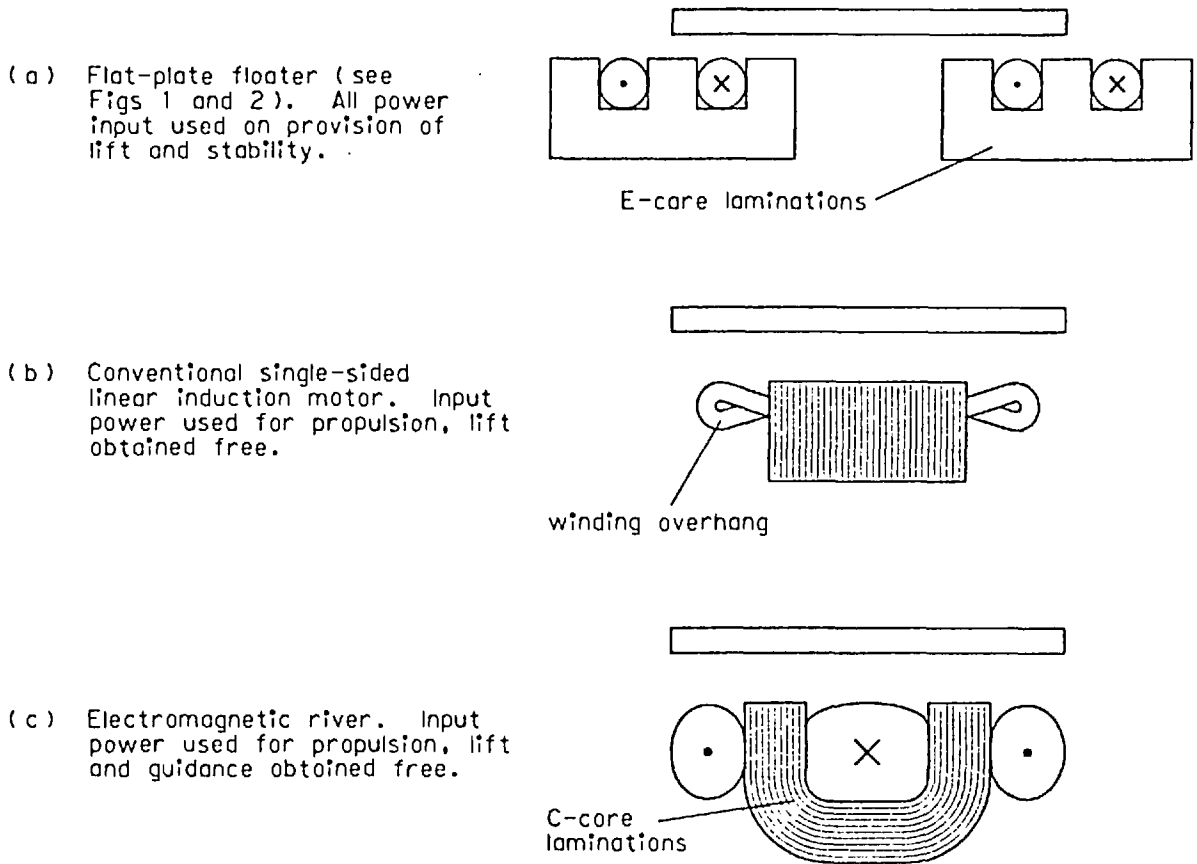


Fig 45. Lateral cross-sections of three machines.

The electromagnetic river takes this process one stage further, by utilising the free forces in the third dimension, the lateral guiding forces - see Fig 45. The same logic applies - that the propulsion currents set up by the special stator carry within them inherent properties of guidance as well as of lift, and utilisation of these costs nothing extra provided that there is no sideways motion of the rotor (i.e. no motion in the direction of the forces). In a practical situation involving a significant length of travel it is likely that there will be considerable sideways oscillation as the guidance system is continually called upon to perform its duties. It has not yet been established whether or not these sideways excursions are regenerative - whether they dissipate energy or - whether the energy is merely stored and returned as the displacement

reduces back to zero. The whole concept of free lift and guidance is an exciting one, the more so if it can be applied to scaled-up systems supporting several tonnes and travelling at high speed. The subject will be returned to in later chapters of this thesis.

It will now be appreciated that the improvement in the synchronous rotor power fraction (defined in section 5.1) from 5% in the Washington model to 21% in the new machine was encouragement indeed for those working on the concept of free lift and guidance. But nothing yet has been said about the lifting and guiding properties of the new motor. In fact about the only comment can be that in both these axes the behaviour was, as nearly as could be judged by "feel", identical with that of the Washington model. Certainly there was no suggestion that the improvement in propulsion had been made in any way at the expense of the other capabilities.

5.3 The seven-metre stator

The next development was one of those unpredictable events that tend to characterise researches in subjects as new as electromagnetic rivers. It will be remembered that the original research leading to the invention of the Washington model was initiated and supported by a commercial firm, Tracked Hovercraft Ltd, who wished to present an all-electric model system at the Transpo '72 exhibition. Although, as their name suggests, Tracked Hovercraft Ltd originally set out to investigate high-speed systems using air-cushions for support and guidance, they took great interest in the progress of the electromagnetic river and were even beginning to formulate plans for building a full-scale River for test purposes.

Then in February 1973, a series of political decisions resulted in the closure of the whole organisation. Some months later a Government Select Committee of Enquiry into the matter requested a visit to the laboratory at Imperial College in order to see for themselves what was behind the future plans of the company that had

been disbanded. In a kind of final effort to reverse the closure, and with only one week's notice of the date of the intended visit, the laboratory staff set out to make an electromagnetic river to outshine all other electromagnetic rivers - a machine built purely to impress non-scientific visitors with a display of "magic". The new phase-mixed levitator was by far the most promising machine built to date, so it was decided to extend this machine from its original length of just over half-a-metre to a total length of seven metres, and to use it to float one of the futuristic-looking fibre-glass vehicles that had been made for Transpo '72.

Thus it was that the laboratory came to be equipped with an electromagnetic river seven metres long, whereas for normal research purposes no more than one or two metres would have been built. In no sense, however, was any consideration given to optimisation of design features. The machine was simply a direct extension of the phase-mixed levitator, partly because the iron C-cores were readily available commercially in large quantities and the wooden formers for the coils had already been built, and partly because the machine was known in any case to work well, there being certainly no time in which to experiment with anything new.*

Quite apart from the greatly improved propulsion, the major difference between the finished long electromagnetic river (for details of which see Appendix A) and its ten-metre forerunner at the Dulles exhibition was that the new machine was almost continuously rated. This meant that none of the problems were involved of successive coil activation and photo-cell vehicle detection that were

* The whole seven-metre length was built and made operative within the seven days, and the resulting motor remains one of the most spectacular electromagnetic demonstrations built to date. Indeed when the machine was no longer required for research purposes it became so much in demand for exhibitions and lecture-demonstrations that it began to suffer considerable damage while in transit from one place to another. The motor has now been almost entirely re-built, to a more robust mechanical design, to become a permanent demonstration machine.

experienced in the earlier model. It was therefore possible to make full use of the exceptional length of the machine to observe the behaviour of rotors under dynamic conditions, by introducing for instance a disturbance in alignment half-way along the machine and noting the subsequent behaviour of plates during their high-velocity travel along the remaining half.

The acceleration given to each rotor varied, of course, with the dimensions and material properties of the rotor. A typical velocity achieved by a plate upon flying off the far end of the machine, having started from rest, was about 10 m/s (this particular figure measured on an aluminium plate 12 cm wide and 3 mm thick). Over a distance of seven metres this gives an average acceleration of 7 m/s^2 , which is just about three-quarters of the gravitational acceleration at the surface of the earth. (Even the dressed-up fibre-glass vehicle attained a velocity of 7.5 m/s, and it became a regular hazard of laboratory life to be asked to catch the model in mid-air as it leapt off the end of the machine after yet another demonstration run on behalf of one of the many interested visitors.)

In general, initial tests performed by sending various plates along the whole length of the machine revealed nothing that was not already known about electromagnetic rivers. However such tests were of value in providing visual confirmation of aspects of behaviour that hitherto had been little more than confident predictions, or deductions made rather from a "feel" of earlier machines than from real measurements. Examples of this are considerations of the roll, pitch and yaw modes of instability, whose actions are illustrated in Fig 46. (The figure also shows an impression of the fibre-glass vehicle built upon an aluminium base, regularly used for demonstration purposes.)

In Chapter 1, where reference was made to the effect upon roll-damping of varying the width of the secondary plate, it was

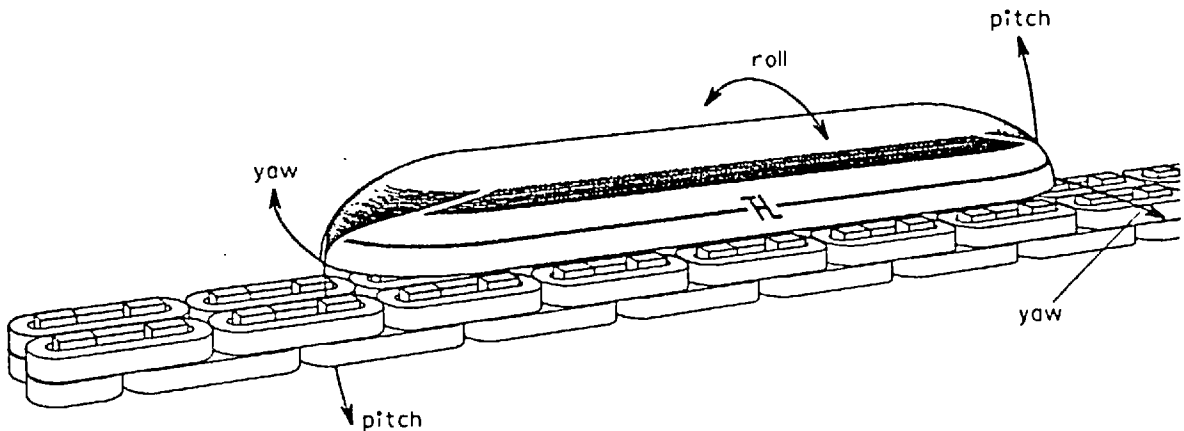


Fig 46. The Roll, Pitch and Yaw couples, as acting on a model vehicle over the electromagnetic river.

observed that wide plates tended to be better damped in roll than narrower ones, and that they also experienced greater lift and thrust but weaker guidance forces. Use of the seven-metre stator enabled observations upon roll-damping to be more easily made, simply by releasing a plate from a position initially slightly angled about the roll axis and watching its subsequent motion along the machine.

Investigations into pitch disturbances were helped by the fact that the machine had been constructed in two mechanically and electrically independent halves, each 3.5 m long. This enabled a controllable pitch disturbance to be introduced by raising one half of the machine a centimetre or so above the level of the other half, so that the leading edge of each rotor encountered a "step" of magnetism as it passed over the junction. Resulting observations showed immediately that the oscillations in pitch (and in overall bounce) were generally quickly damped out, almost critical damping being achieved on aluminium plates 3 mm thick. Thicker plates tended to be less well damped, and copper plates experienced the lowest damping of all. Variations of length and of width appeared to have little effect upon pitch-damping, the only exception being that plates shorter than about one and a half pole-pitches began to exhibit a distinct "dolphin motion"* as they passed over successive stator teeth.

* - see footnote on dolphin motion on next page.

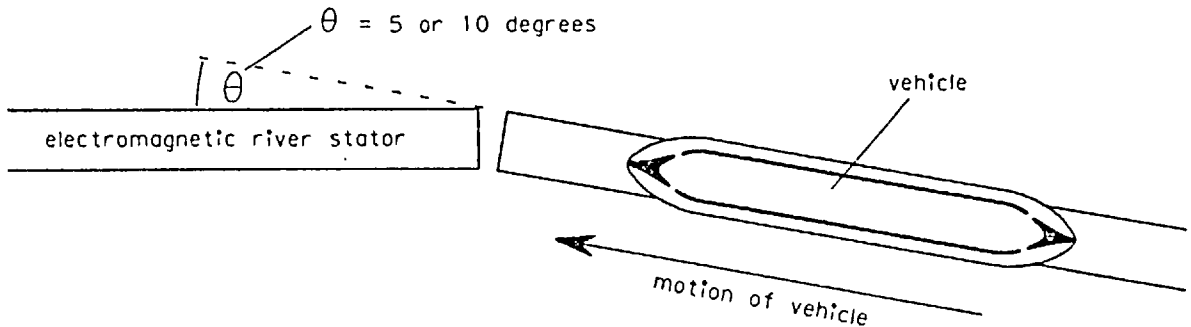


Fig 47. Artificial "corner" for demonstrating yaw displacements.

But perhaps the most useful (and certainly the most dramatic) of the instability mode investigations was that into instabilities of yaw. For this purpose the outer end of one of the halves of the machine was swung round through an angle of about 5° or 10° to form an artificial corner, as shown in Fig 47. It appeared immediately that aluminium plates of 3 mm thickness, regardless of length or width, experienced critical damping in yaw after passing the corner. Experiments performed to discover the greatest angle that the plates could tolerate gave the expected result that narrow plates could follow much sharper changes in direction, some as sharp as a 15° angle, than their wider counterparts, this being dependent mainly upon the magnitude of the sideways guiding forces, known to be greater for narrow plates.

Behaviour of the model vehicle, however, proved to be more instructive than observations of flat plates since its relatively high centre of gravity caused it to suffer considerable roll disturbance, simultaneously with yaw, upon encountering the corner. Oscillations

Footnote - dolphin motion: a continuous pitch oscillation of frequency directly proportional to longitudinal velocity, and of wavelength equal to the stator tooth pitch. The oscillation is caused by variations of lift force with longitudinal position, the regions of maximum force being concentrated in "humps" over the stator teeth.

in yaw were observed to be as near to critically damped as was possible to judge by observation alone. Roll-damping, however, was distinctly low, the vehicle continuing to rock from side to side throughout the remainder of its travel along the machine.

(The maximum angle that the vehicle could tolerate was limited to about 8° , but even at this small angle it was an impressive sight to watch the vehicle approach the sudden deviation at high speed and follow smoothly round it, with scarcely a trace of effort, on its invisible guidance and support. The whole demonstration, which became most popular with the many visitors to the laboratory, proved particularly valuable in providing the perfect answer for those sceptical guests who, having seen and even felt the rigid sideways stability of the vehicle over the stator, would then insist on asking "... but can it go round corners?".)

5.4 The Electromagnetic Shuttle

The extended length of the electromagnetic river enabled the above observations to be carried out more easily than was previously possible (and indeed allowed some that were hitherto impossible). However there still remained the limitation imposed by the short time taken for a rotor to travel the seven metre length. The real scope of the long machine was not revealed until the idea occurred to reverse the phase sequence of the supply to one half of its length, so that two travelling fields were created, each moving inwards from one end towards the centre, thereby creating a back-to-back oscillator. This process achieved for the electromagnetic river what the first longitudinally stable expanding-geometry machine (see Chapter 2) had done for the Washington model. Observations and measurements could now be taken over long periods of time. Effects of changes in various parameters could be studied under dynamic conditions, with the rotor shuttling to and fro undergoing alternate acceleration and deceleration, and achieving a usefully high velocity each time it passed the centre of the machine.

When the machine was first tried in this back-to-back mode, it was found that most rotors were unable to maintain the amplitude of their longitudinal oscillations. The plates tended instead to execute successively smaller oscillations, finally coming to rest at the centre of the machine. The degree of longitudinal damping, i.e. the rate at which this process took place, varied considerably between rotors, the model vehicle being the most strongly damped of all (it executed only five or six complete oscillations before coming to rest).

A summary of the behaviour of a number of rotors is presented in Table 1. Of the columns of the table the first five are self-explanatory, the sixth and the seventh (Static stability) refer to the presence or otherwise of forces tending to stabilise the rotors against lateral or roll displacements respectively, the eighth and ninth (Dynamic stability) refer respectively to the damping of oscillations caused by a lateral or a roll disturbance, and the tenth (End-to-end oscillations) describes the ability of each rotor to maintain a continuous shuttle motion up and down the machine.

The ideal rotor would have "excellent" in every column from 4 to 9, and possibly "poorly damped" or "self-oscillatory" in column 10 (depending on its purpose). None of the rotors included in the table achieves this ideal. Nor is it likely that one will be found to do so since, as first described in Chapter 1 and now confirmed by the table, high stability and damping laterally and high stability and damping in roll appear to be mutually exclusive attributes.

Table entries in capitals are those to which attention is drawn for the particular rotor concerned. In the second row, for example, all plates wider than 15 cm have excellent lift and propulsion, and are well stabilised and damped in roll, but their vital characteristic (in a negative sense) is that they are all laterally unstable and therefore totally useless. It should be noted that the entire table has been drawn up for the particular primary current of 30 amps in

TABLE 1. Comparison of rotor behaviour over long electromagnetic river.

(All results correspond to a stator current of 30 amps per coil, at a supply frequency of 50 Hz)

Rotor material	Thickness	Width	Lift	Propulsion	Static stability		Dynamic stability		End-to-end oscillations
					Lateral guidance	Roll restraint	Lateral damping	Roll damping	
aluminium	all tested thicknesses	< 7.5 cm	ZERO	- - -	excellent	- - -	very high	- - -	- - -
		≥ 15 cm	excellent	excellent	UNSTABLE	excellent	- - -	very high	- - -
	1.5 mm	15 cm	good	excellent	very poor	high	medium	high	SELF-OSCILLATORY
	3 mm	10 cm	fair	fair	very good	poor	high	low	high damping
		12.5 cm	good	good	fair	good	medium	medium	poor damping
		15 cm	very good	very good	poor	very good	low	high	SELF-OSCILLATORY
	6 mm	10 cm	fair	fair	very good	poor	medium	low	well damped
		15 cm	good	good	poor	good	very low	high	very low damping
	9 mm	15 cm	good	good	poor	good	SELF-OSCILLATORY	high	SELF-OSCILLATORY
copper	6 mm	10 cm	fair	fair	excellent	poor	SELF-OSCILLATORY	low	poor damping
brass dural	any dimensions		ZERO	ZERO	resistivity too great				
steel	any dimensions		NEGATIVE	ZERO	magnetic attraction to pole pieces				

each stator coil (approximately 200 amps line input to the whole machine). Many of the characteristics shown will change if a new value of current is chosen, but the general trends of differences in behaviour between various rotor sizes and materials will remain the same.

The most interesting rotors of those included in the table are those marked "self-oscillatory" in the last column. This means that after release from near one end of the machine these plates will shuttle back and forth with increasing longitudinal amplitude, unless careful active control of input stator current is exercised to maintain the amplitude constant.* One of these self-oscillatory rotors, the 15 cm aluminium plate 9 mm thick, was found to be almost equally self-oscillatory in lateral motion, with the result that once released it was apparently a matter of chance whether or not it fell off the machine sideways before its increasing amplitude caused it to fall off one end. (This particular plate was one that was carefully not shown to visitors!) But there are in the table two more longitudinally self-oscillatory plates that are stable and positively damped both laterally and in roll, and it is these plates that might prove to be the beginnings of useful industrial applications for the electromagnetic river.

The most obvious application in industry is suggested immediately by the sight of a plate supported in mid-air shuttling rapidly to and fro with an amplitude of seven metres and at a frequency of about one complete oscillation every two seconds. Such motion calls to mind the action of the shuttle of a weaving loom. The possibility that the violent and noisy mechanical system for sending a shuttle back and forth might be replaceable by a silent, efficient and maintenance-free electrical system seemed an attractive proposition indeed. There might even be further advantages to be gained - for example the maximum width of a conventional loom has always been limited by the

* For an explanation of the mechanism of self-oscillation in a back-to-back motor see references 13 and 14.

distance across which a loaded shuttle can be propelled and reliably caught on the other side (the actual limit being about 17 m). A linear motor system would be restricted by no such limit.

The proposal to use a back-to-back linear motor system for shuttle propulsion had in fact been first investigated in the 1950's⁽¹⁵⁾, but for several reasons the project never became capable of commercial exploitation. The principal problems emerged as being economic rather than technical, but other problems, mainly of an electrical nature, resulted from the less well-developed understanding of linear motors at that time. For example it was not known how to make a reasonably efficient machine capable of producing continuous acceleration on the rotor during the first half of its travel and continuous deceleration during the remaining half. For this and other reasons, thoughts of incorporating electromagnetic shuttle systems in weaving looms were postponed.

It might appear that one of the problems could have been the provision of a guidance system to counteract the strong tendencies to lateral instability of a rotor propelled by a conventional longitudinal-flux linear motor. This is not so. During its passage across the loom the shuttle is contained within a trapezoidal "shed" bounded above and below by the warp threads and to one side by the comb. The normal method employed to guide the shuttle along its path is to build the loom with a curved comb and to fire the shuttle against this so that centrifugal force keeps it against the comb throughout its travel.

Problems have, however, been experienced with guidance in mechanical looms at the start of this travel, where the shuttle has to enter the shed. On wide looms the frictional force experienced by the shuttle against the warp threads demands that the shuttle be dispatched with a very high initial velocity in order to guarantee safe arrival on the far side after its long travel. This velocity is achieved by imparting an impulse to the shuttle

with a heavy block. The slightest misalignment of the shuttle when receiving the impulse can cause the shuttle to break out of the shed through the warp threads, or even to miss it altogether. Quite apart from the danger of the lethal flying missile, such an occurrence constitutes a major interruption to the weaving process.

Here is where the long phase-mixed electromagnetic river operable in back-to-back mode could come into its own. The properties of lift and guidance inherent in this new breed of linear motor at once solve any mechanical problems of rotor guidance, and it is known that the rotor is capable of carrying the weight of a fully-wound shuttle. Indeed it is possible that some simplification of the mechanical design of the loom could result from the elimination of the need for a curved comb for shuttle guidance. Other advances largely overcome the electrical deficiencies of the early machines. In particular, the overall efficiency of the propulsion system can be greatly improved by the use of a graded pole-pitch stator. By this means a travelling field can be created itself increasing in velocity towards the centre of the machine, which can ensure that the rotor is accelerating always with a fairly low slip, and thus always near its peak of efficiency.

A further important feature of an electrical shuttle system could be the smoothness of its action. In the present mechanical system the shuttle acquires the whole of its acceleration within the first half-metre or so of its travel, and then has all of its remaining kinetic energy removed within a similar distance on the opposite side. There is a maximum acceleration that can be imparted at the beginning of this motion if the weft thread is not to break, and on wide looms the resulting velocity, and hence time taken per traverse, becomes the limiting factor on overall weaving speed. The same acceleration electrically applied continuously across half the width of the loom, followed by an equal deceleration, could greatly reduce the traverse time.

Continued discussion of these ideas is probably of little further value since no specifically relevant practical work has yet

been carried out. Electromagnetic shuttle propulsion is in any case just one of a range of possible applications for the electromagnetic river. The inherent properties of lift and guidance are particularly well-suited to those industrial situations where, maybe for reasons of chemical purity or perhaps to avoid the effects of friction, there is a need for support or motion in the total absence of physical contact. In cases where the material being processed consists of aluminium, copper or some other electrically-conducting but non-magnetic material, it might be possible to use a form of the electromagnetic river directly; in other cases means may have to be provided for mounting the required object upon a suitably conducting rotor. But even in already existing situations employing a linear motor drive merely for thrust production, the replacement of a conventional machine exhibiting its strong tendency to lateral instability by a new machine equally efficient in propulsion but tending always to align rotor with stator can only be to advantage.

The stator can, of course, be made totally silent and virtually invulnerable to damage within normal industrial environments simply by encasement of the coils and cores in solid blocks of epoxy resin. This is already done as standard practice on conventional machines, and the only extra precaution then necessary is to protect against overheating from within caused by excessive currents or periods of operation.

On looking back upon the work described in the whole of this chapter, it will doubtless be noticed that following the building of the long electromagnetic river the entire manner of research appears to have lapsed from its aura of "scientific respectability" as achieved in Chapter 4 back into the "try it and see" approach of Chapter 1. The reasons for this are simple. The new river, like the Washington model before it, confronted the laboratory staff with a machine so new, so completely outside the experience of anything before, that the immediate reaction was to explore everything about it, to experiment with rotors of all shapes, sizes and materials, without at first stopping to think out any logical, carefully

designed series of experiments and measurements. In any case it was desirable to obtain first-hand observations of the behaviour of the machine in as many conditions as possible, in order to be able to give at least partial answers to the many otherwise embarrassing questions posed by visitors to the laboratory.

The eventual return to more organised methods resulted in the series of experiments to be detailed in Chapter 7. These had as their ultimate objective the further possible application of electromagnetic rivers - high-speed ground transport. Such an application has been hinted at many times already, but all the relevant work described so far has been concerned with the development only of small-scale models. Extrapolation of such work to a scale appropriate to a full-size vehicle may seem a big step, involving much further time and effort. It may be helpful, however, to remember that the long phase-mixed electromagnetic river was built within eighteen months of the conception of the subject of expanding-geometry levitation machines; it is not unrealistic to suggest that a further few years might see in reality the support, guidance and propulsion at 400 km/h of a fifty-tonne passenger-carrying vehicle.

CHAPTER 6

LOW FLYING AIRCRAFT



The full-scale research test vehicle RTV 31 of Tracked Hovercraft Ltd. on its experimental track at Earith, Huntingdonshire (p 117).

CHAPTER 6. LOW FLYING AIRCRAFT

The development of aircraft since the beginning of the century has revolutionised long-distance travel and led to rapid world accessibility for all. By contrast there has been little corresponding progress in methods of transport from airports to city centres. The result is the situation, only too well-known to aircraft passengers, where it can take as long to reach Heathrow Airport from the City of London as to reach Glasgow Airport from Heathrow. There is, however, growing interest nowadays in the development of technology to replace the three-stage journey (centre-airport-airport-centre) by a single-stage ground transport system. Two further topics of today, if anything even more relevant to present times, are "stop pollution" and "prevent noise". It is hardly surprising then that many countries throughout the world are expressing interest in the development of silent, pollution-free high-speed ground transport systems from city-centre to city-centre.

All such research is directed towards tracked systems such as railways, rather than unguided systems such as cars on a motorway, simply because a succession of similar vehicles all moving at the same speed and guided on a rigid track can safely travel at higher speeds and in closer proximity than can a random collection of vehicles each with individual freedom both to wander sideways and to vary speed at will. At the same time, effort is being expended to devise transport systems capable of speeds considerably in excess even of today's high-speed railways. This is because such systems are seen as direct competitors to short-haul aircraft routes rather than as extensions to the present railway system. Thus it is hoped to offset the acknowledged inflexibility of a tracked transport system by gains in carrying capacity and cuts in travel time.

6.1 Steel wheel upon steel rail

In many countries attempts have already been made to improve city-to-city communication by upgrading and often electrifying existing railway routes. The Euston-Glasgow West Coast Main Line electrification is the major British example of this, and work has recently been completed on the first stage of electrification of the East Coast Line, from Kings Cross northwards. Simultaneously with electrification, a large amount of work has in each case been carried out on track re-alignment and station re-planning to increase the maximum allowable speed over difficult sections of route and through stations and junctions. While not undergoing electrification, the Great Western route from Paddington to Bristol and beyond has also been "treated" in this way for high speed, in preparation for the introduction of British Rail's "High Speed Diesel", which has achieved, for the first time in this country, regular scheduled services running at a top speed of 200 km/h.

However there is a limit to what may be achieved by localised track-straightening, since there exist far more permanent speed limits set by the twisting routes chosen by railway engineers of over a hundred years ago. In practice the values of the speed limits imposed by curvaceous trackwork are set not so much by the ability of trains to negotiate the curves in safety as by the frailness of passengers - their ability to tolerate the discomfort of centrifugal forces. In recognition of this, British Rail has supported an extensive research programme culminating in a new concept of railway vehicle, the "advanced passenger train". Among other new characteristics, the a.p.t. features the capability to tilt each vehicle as it enters a bend, in such a way as to balance the outwards centrifugal force acting upon the passengers - see Fig 48(a). By this means the speed limits imposed while negotiating curves can be increased by as much as fifty per cent.

The second major feature of the a.p.t. is that its suspension is specially designed to tolerate high-speed running on worn wheels. The

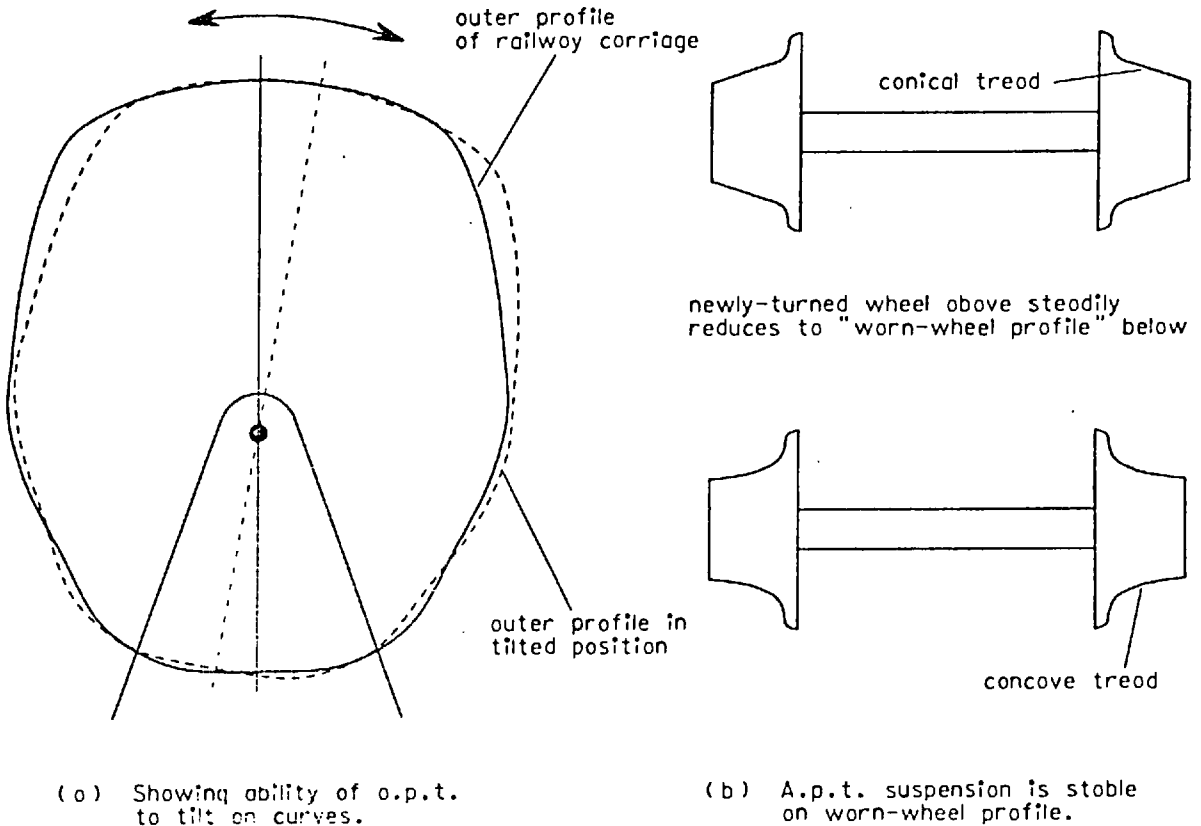


Fig 48. Features of the advanced passenger train.

"worn wheel profile" - see Fig 48(b) - is the shape into which an initially conical wheel profile gradually wears, and which is one of the causes of "hunting" instability at high speed on normal carriage suspensions. By designing a suspension which remains stable on this wheel profile it is hoped to increase considerably the length of time between routine overhauls and wheel re-turning.

Useful though these advances certainly are, they can at best extend only by a limited amount the maximum permissible speeds, and are likely to be profitable only on routes where high-speed high-quality track is already in existence. If it is required to go still faster even than safety on a curvaceous route will allow, or if it is wished to increase the service on a route where the tracks existing are already in use to their full capacity, then there is no alternative but to start afresh, building new tracks on a new route. The expense

involved in such construction is enormous, many times greater than the cost of designing and building a whole fleet of advanced passenger trains. However once such a decision has been taken, the opportunity is presented to eliminate the many archaic features, left over from the days of steam, that still plague the operation of modern railways. In particular, with high velocity in mind from the outset, the route can be chosen such as to maximise the length of straight track and to arrange that those curves that remain unavoidable (whether in a horizontal or a vertical plane) have radii appropriate to speeds of several hundred kilometres per hour.

The outstanding example to date of this "begin again from the beginning" approach is the Tokaido Line in Japan. Originally built as a single route connecting Tokyo with Osaka (a route served previously only by a twisting narrow-gauge railway, grossly overloaded), the system has proved so successful that it is now being extended to run eventually to all the major cities of Japan. Trains run at a maximum speed of 215 km/h, and cover the distance of 530 km in less than three hours. However again the system comes up against a speed limit barrier. The principal determining factors in this case are firstly the need for frequent track and rolling stock maintenance work to repair the wear and damage caused by such high-speed running, and secondly the excessive sparking and eroding at the pantographs where power is taken from overhead electrified lines.

It may at first sight appear coincidental that Japan's Tokaido Line, a brand new railway suffering no constraints of compatibility with older systems, and British Rail's advanced passenger train, designed to superimpose the speeds of today onto the curvaceous routes of the past, should both appear to be reaching an uppermost limit of speed at around the same value - somewhere about 250 km/h. But a more penetrating analysis of the subject of the transport of heavy masses at high velocities may reveal that there is a fundamental reason why this should be so, a reason perhaps as basic as that which dictates that "there is a maximum size of bird that can fly" because

as the bird grows larger its weight increases as the cube of its linear dimensions while its wing area increases only as the square.

There are indeed two major factors, either of which on its own would be sufficient to place an upper limit on the allowable speed of a system dependent on a steel wheel running upon a steel rail. It is well-known that the force of air-resistance acting upon a moving body increases as the square of the velocity of that body, and that the power requirement to keep the body in motion therefore increases as the cube. At speeds of 100 km/h and upwards, air-resistance becomes the dominant feature determining the total power input requirements of any vehicle. In the case of a vehicle depending on drive through its own wheels for propulsion, the transmission of this power is totally dependent upon the frictional forces acting between the wheels and the stationary surface upon which they run. This in turn places a limit on the maximum speed attainable, set by the maximum traction force that can be developed before the wheels begin to slip.

In the days of steam one of the means used to push this limit higher was simply to build heavier locomotives, thereby increasing the force required to slip the wheels. In more modern times suggestions have been made to employ high-temperature electric arcs or gas torches playing on the rails immediately in front of the leading pair of wheels, in order to burn off any dirt or grease deposits which lower the coefficient of friction.

The problem can of course be tackled in many other ways, one of the more obvious of which is to streamline the vehicle. While it is true that even many steam locomotives (notably the record-breaking "Mallard") employed some degree of streamlining, the advanced passenger train will be the first British train to be designed from the outset using all available knowledge of the nature and effects of air-flow around objects. The London Underground and similar systems tackle the problem in a different way. Their problem is not so much

to drive against air-resistance (though this can be significant in the tube tunnels) as to develop adequate acceleration on a packed train moving away from a station. The wheel-grip is not helped by the fact that the carriages, particularly those of the modern aluminium-bodied trains, are of much lighter construction than their main-line counterparts. The solution employed in their case is to replace the single powered vehicle at the front by a succession of powered axles beneath the carriages throughout the length of the train. The number of powered axles can be as high a percentage of the total as is necessary to transmit the desired accelerating force without slipping - in practice modern Underground trains have about fifty per cent of their axles powered.

However solutions such as these are capable only of pushing the maximum driving force a little higher, and each gain costs progressively more in terms of money and engineering complexity. Such processes cannot be continued indefinitely. British Rail now set the eventual speed limit on friction drive at about 250 km/h, and they are at present carrying out tests on the use of conventional linear motors for propulsion above this speed.

The inability to maintain sufficient frictional contact is the first of the barriers to ever-increasing speed. The second is if anything even more fundamental. It is the inability of engineering materials to withstand for long periods the vertical shocks and stresses caused by high-speed travel. The major vertical forces acting on a railway track arise at places of track irregularities, particularly at joints, points and crossings. The dynamic forces caused by the passage of a high-speed train can be exceedingly large, as much as four times the corresponding static forces, and these lead to high maintenance costs both of the track and of the rolling stock. Already this factor has been the cause of a reduction in the operating speed of the Tokaido Line from its projected value of 250 km/h to its present value of 215 km/h.

The magnitudes of such dynamic forces can be shown⁽¹⁶⁾ to be proportional to the velocity of each vehicle and to the square-root of its unsprung mass (to a first approximation the sum of the masses of all parts of the bogie between the track and the main suspension springs). For this reason the construction of modern high-speed locomotives and trains is aimed at minimising unsprung (and overall) mass, and in the a.p.t. an unsprung mass per bogie of 1.5 tonnes has been achieved, compared with 2-4 tonnes for a conventional modern locomotive. The effect of this reduction is that the a.p.t. is expected to run at speeds twenty per cent greater than conventional locomotives while exerting about the same vertical forces on the track.

Nevertheless once again it is thought unlikely that even the a.p.t. will be able to run much faster than 250 km/h unless new progress is made either in the further design of vehicle suspension or in improving the resistance of the track to wear and damage by vertical forces. It is coincidence that the value of this limit - 250 km/h - is about the same as that imposed by loss of sufficient frictional contact. Having once realised the significance of these limits, however, it will be appreciated that it is no coincidence that both the Tokaido Line and the a.p.t. experience difficulties as their speed approaches this value. The fallacy may now be understood in the suggestion that there need be no practical limit set even on today's requirements for frictional force transmission since one can always employ larger driving wheels to give greater area of contact, and run heavier locomotives upon them. Clearly such a suggestion is in direct conflict with the requirement to minimise damage by reducing weight, and indeed the tendency nowadays is to reduce the unsprung mass by making wheels as small as their mechanical resistance to centrifugal stresses will allow.

Here is not the place to become involved in justifications for man's incessant desire to travel ever faster. Suffice it to say that the railways have long recognised the commercial desirability of speed,

and that where they decide to step to one side there are several other concerns only too willing to press ahead. Since the present technology of the steel wheel upon steel rail seems unlikely to be able either to propel or to support vehicles at speeds much in excess of 250 km/h, there seems no alternative but to abandon altogether the principle of physical contact between the moving vehicle and its track, and find some other means for support and propulsion. (In the same way, to return to the earlier analogy, if a bird were to evolve to the size of a jet aircraft and still retain the capability of flight, then it would have to abandon flapping wings altogether and replace them with a new system, such as the shaping of air-flow across a fixed wing surface.)

6.2 Contact-free systems

Much research is in progress in many countries on the development of systems for high-speed land transport that eliminate physical contact with the ground. A comprehensive review of the world situation in 1974 is presented in reference 17 (which also includes over two hundred references to articles on modern transport in all its forms); it is sufficient here to give only a brief description of the four major systems at present under investigation.

The first of these systems is support by air-cushion suspension, the hovercraft principle. This was the method employed by the only major British effort on high-speed contact-free transport - the Hovertrain developed by Tracked Hovercraft Ltd. Air-cushions provided both support and guidance, the latter by means of air-pads mounted on the inward-facing surfaces of the sides of the vehicle, which extended downwards to embrace the two sides of the track - see Fig 49. Propulsion was by means of a conventional single-sided linear motor on board the vehicle, acting upon an aluminium reaction sheet mounted within a groove at the top of the track, and towards the end of 1972 the resulting full-scale test vehicle RTV 31 achieved a speed of over 160 km/h within the 1.6 km length of track available at that time.

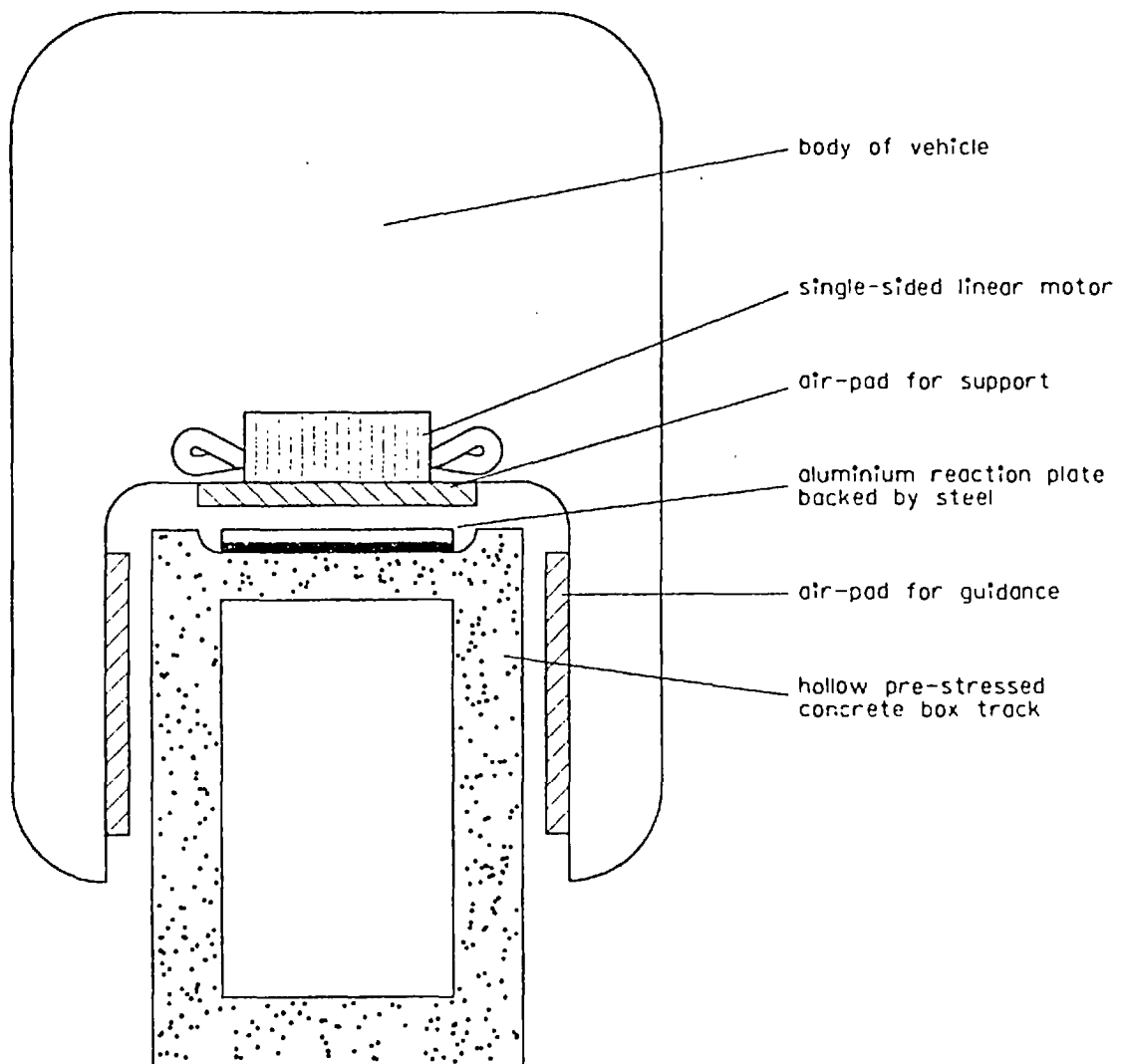


Fig 49. Cross-section through British Hovertrain, showing mechanism for support and guidance.

Much work on air-cushion suspension has also been carried out in France, notably in the development of the Aerotrain (by Bertin, with French government support). Experience there goes back to the time before linear induction motors were established for propulsion at high speed, and experimental runs were made using air-screws, jet engines and even rocket boosters. In the main, however, these served only to confirm the non-acceptability of such machines on account of noise and pollution, and the linear motor is now the only

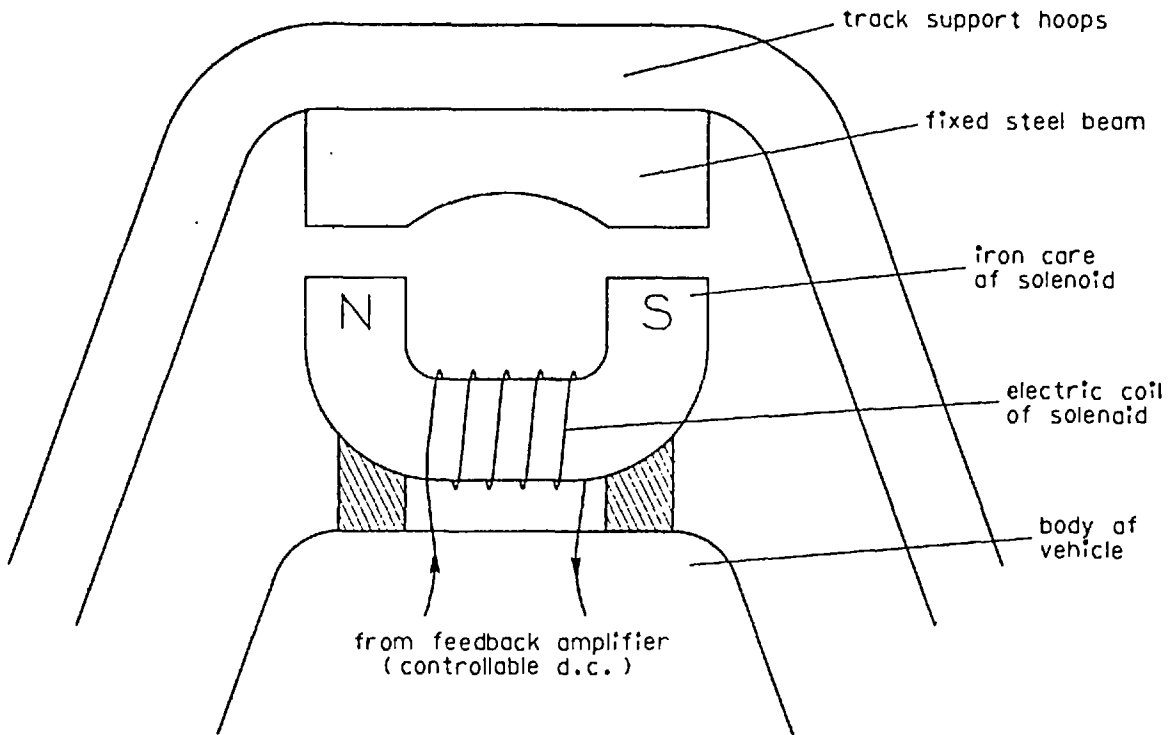


Fig 50. Magnetic attraction system for vehicle support.

means of contact-free propulsion under consideration in any part of the world. These same grounds, particularly that of noise, have also been the main cause for dwindling interest in the air-cushions themselves for means of primary support. While there is still some work in progress in France and in the U.S.A., it is now thought unlikely that further trains operating on the hovercraft principle will be built.

The second major system, upon which considerable effort has been expended in Germany, is the "magnetic attraction" system, which , utilises the forces attracting objects of steel towards the poles of an energised solenoid. Fig 50 shows one configuration for vehicle support by such a system but many others are possible. Uncontrolled, the solenoid cannot of course stabilise itself at a constant distance from the steel since any movement tending to increase or decrease the gap results respectively in a decrease or an increase in the

attractive force - the opposite to what is required for stability. The mechanism is therefore provided with a distance sensor which, coupled to an amplifier supplying current to the solenoid, detects changes in the air-gap and adjusts the current accordingly. By its attractive nature the system is clearly capable of producing strong guidance forces as well as support, leaving only propulsion to be supplied. The German researchers have experimented with both single and double-sided linear motors for this purpose.

Simple in concept, the whole system nevertheless presents the designer with a number of problems. Firstly the highly reactive nature of a solenoid wound upon a steel core makes current control not at all an easy matter. The long natural time-constant associated with changes in current renders simple voltage control useless. The rapid current changes necessary if stability is to be maintained can be achieved only by transiently raising the voltage to many times its required steady-state value in order forcibly to drive more current through the reactance, and conversely a short-duration high negative voltage is needed to reduce current. This process, applied to a solenoid large enough to support the weight of a full-scale vehicle, requires a feedback amplifier of enormous proportions. A particular penalty, even using the most modern techniques of transistor and thyristor technology, is the resulting weight of the amplifier, estimated in the region of several tonnes.

A second problem is that the action of a d.c. magnetic field in a solid steel beam is to produce drag forces when the energising coil is made to move along the beam. These forces are dependent upon velocity, and could necessitate a considerably greater propulsive effort at speed, though it might be possible to laminate the whole of the steel supporting structure to reduce the effect.

Neither of the above difficulties, however, is insuperable. Models employing the magnetic attraction system have been built and successfully run at high scale-velocities. But there is a third objection to the system, of a nature more fundamental than

those so far stated, and which could have far-reaching consequences for this and other magnetic systems.

In Chapter 2 (page 39) a brief explanation was given of the meaning of "goodness factor" as applied to electromagnetic machines. It is necessary to make a distinction here between two fundamentally different types of machine.⁽¹⁸⁾ For want of better distinguishing expressions, specialised meanings have been evolved by those working in electromagnetism for the words "electromagnetic" and "magnetic". In this specialised use (which is employed consistently throughout this thesis) an "electromagnetic" machine is one in which electric currents flow in the secondary (whether induced, as in an induction motor, or separately excited, as in an alternator), and a "magnetic" machine is one which employs no currents in the secondary (as for example a reluctance motor, a solenoid, or any motor employing a field supplied by a permanent magnet). The one exception to this rule is the synchronous machine with permanent magnet excitation on the rotor, which comes within the "electromagnetic" heading. A magnetic machine depends either on the action of the primary current on the magnetic field, or upon direct action of the magnetic flux itself (for instance on its tendency always to minimise the length of air-path), while an electromagnetic machine uses the magnetic flux only as the medium by which two sets of electric currents are made to react with one-another.

Now in the derivation of goodness factor⁽⁶⁾ the assumption from the outset is that the machine concerned is of the electromagnetic type. It has not been possible as yet to derive a corresponding mathematical expression for a magnetic machine, but practical experience can predict in any case what some of its results would be. In particular, whereas an increase in linear dimensions improves the goodness factor of an electromagnetic device, a corresponding increase is certain to have the opposite effect on a magnetic machine. (This result can in fact be theoretically derived from considerations of the way in which a magnetic circuit changes with increasing dimensions - see reference 19.) In short, for electromagnetic devices "the bigger the better", and for magnetic "the smaller the better". (As an

example of this consider the tiny permanent-magnet motors that work superbly inside a model railway locomotive. No induction device could operate on so small a scale. But never is seen a permanent-magnet motor the size of a full-scale railway locomotive, and even if one were to be built it would be a poor machine indeed at so large a scale.)

So here lies the difficulty with the magnetic-attraction system. It is a magnetic machine. It is certain, therefore, that as it is made larger the engineering problems will increase, and there will be found an ultimate limit of a nature identical to that which dictates that the ostrich will never fly - because it is too big. The value of this limit, of course, is yet to be determined. The system has been shown to work well on a model scale, but so far full-scale performances at high speed have been investigated only by simulation. It remains to be seen whether a 50 tonne vehicle travelling at speeds of say 400 km/h is or is not within the limit on size.

The third method of support, again simple in concept, is to use the repelling properties of similar poles of a pair of permanent magnets. Recent advances in materials, particularly the development of ceramic ferrites of coercivity many times superior even to modern steel magnets, have made the reliable support of several tonnes-weight a practicable possibility. Fig 51 shows in cross-section one configuration of such a system; again many others are possible. Clearly such a system needs rigid sideways support, for the position of maximum repelling force is also a position of unstable equilibrium, any sideways motion resulting in a tendency for the whole vehicle to slip sideways a distance of one "pole-pitch" and lock into a region of powerful attraction.

At first sight it would appear feasible to obtain guidance from a similar magnetic effect by repelling the sides of the vehicle from the inside surfaces of a U-shaped track. However there is a well-known proof⁽²⁰⁾ that it is impossible to stabilise one set of permanent magnets by means only of the action of another set of

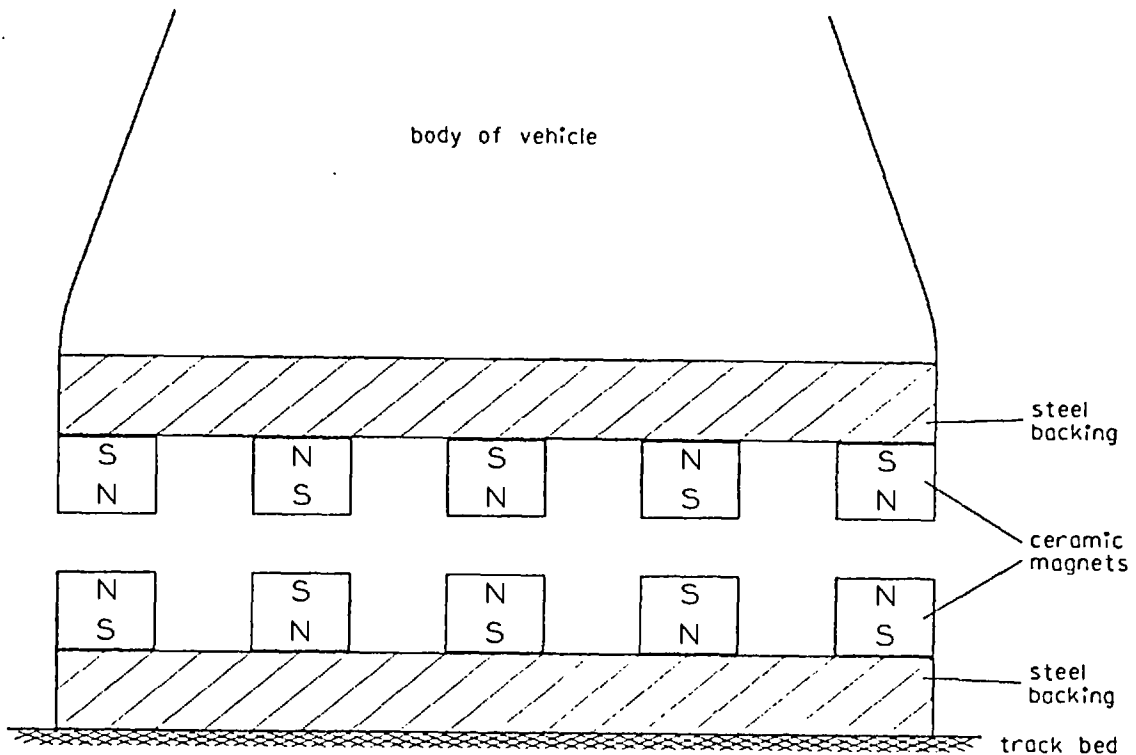


Fig 51. Mechanism of permanent magnet suspension.

permanent magnets. This is in fact a particular case of Earnshaw's Theorem, which in one of its forms states that such stabilisation is impossible by the use of any force-production mechanism dependent on an inverse-square law relationship between force and distance. (For example it is similarly impossible to suspend one electric charge stable in space by the use only of other electric charges surrounding it.) The only exception, not applicable here, is in the case of materials that are diamagnetic, i.e. have a relative magnetic permeability of less than unity; this case will be considered as part of the fourth suspension system.

Mechanisms proposed to provide sideways stability for permanent magnet suspension include rollers acting upon the two surfaces of the vertical secondary of a double-sided linear motor or acting on the concrete box sides of the track itself, or control of currents in solenoids reacting with vertical ferromagnetic members in the

track. But whatever mechanism is eventually employed, it must be capable of overcoming the instability tendencies of the main support as well as of controlling the normal lateral movements of the vehicle.

As a means for support the permanent magnet levitation system has a number of promising features. The lift mechanism itself clearly consumes no energy whatsoever, even when there is vertical movement of the vehicle, and the resulting independence of the support on any primary power supply is seen as an important safety feature (though this is strictly valid only if the guidance mechanism is similarly independent of supplies). In addition the electrical insulating properties of the ceramic magnets prevent the flow of eddy currents that would otherwise cause drag forces at speed⁽¹⁷⁾. Set against these, however, are once again the fundamental properties of a magnetic system, predicting that as the overall size is increased towards full scale, the engineering difficulties can but increase.

The fourth major system, on which a large amount of research has been in progress in Japan and the U.S.A., is that using cryogenics - the technique of cooling a conductor to below the critical temperature at which it loses all resistance to electric current. The mechanism of lift-production is rather less obvious here. As is well known, a magnetic pole travelling close to the surface of an electrically conducting sheet causes currents to flow within the sheet, and the pattern of flow of these currents is such that the resulting force between them and the moving pole is in a direction such as to oppose the motion of the magnet. It can be shown that there is in addition a force of repulsion between the pole and the sheet, which increases with velocity. With ordinary magnets or solenoids the repulsion force is not large enough to be of practical use, even at high velocities. However the use of cryogenics, creating superconductors through which currents thousands of times greater than is possible in normally resistive material can be passed, allows the production of

magnetic fields of such magnitude that the critical velocity at which a full-scale vehicle can just support its own weight can be less than 100 km/h.

The system can also achieve stability by the same mechanism, repelling from the inside walls of a U-shaped track. That this is possible notwithstanding Earnshaw's Theorem is a result of a particular feature of superconductors. The theorem, as stated earlier, precludes the possibility of obtaining stability by steady-state magnetic forces, except in the case where the materials involved are diamagnetic. A number of commonplace materials are very slightly diamagnetic - water, glass, copper for example - but each of these has a relative permeability differing from unity by less than one part in ten thousand so any magnetic stability obtainable is far too small to be of any consequence.

Now a superconducting coil, by virtue of its zero resistance, has an infinite time constant to changes in its current or to the magnetic field passing through it. An attempt from outside to influence the magnetic flux passing through the coil (e.g. by means of a current in a second coil, or a moving permanent magnet) would therefore require infinite time to take effect, and the coil can thus be regarded as possessing zero permeability to changes in magnetic flux. (The coil is energised and its own magnetic field first set up by inserting external resistance into the circuit, to reduce the time constant to as low a value as desired. The resistance is then short-circuited from within the cryostat to leave the current circulating indefinitely.)

The superconducting coil thus behaves in the manner of a highly diamagnetic material, and stable levitation is possible. The only remaining requirement is a propulsion unit, which can conveniently consist of a single-sided linear motor using as a secondary the same aluminium sheet that reacts with the superconducting coils to provide

lift. (An alternative design, under investigation in Japan, is to employ discrete short-circuited copper coils in the track in place of the conducting sheet.)

Two difficulties arising with the system are immediately apparent. Firstly the action of a powerful d.c. field moving along the surface of a conducting sheet is precisely that of an eddy-current brake, resulting in drag forces requiring large increases in the thrust and hence the power consumption of the propulsion unit. Secondly the essential requirement that the superconducting coils be kept always at a temperature within a few degrees of absolute zero can be met only by carrying quantities of liquid helium on board every vehicle - a severe penalty in terms of weight as well as cost. However at the same time the whole system is the only one of the four major types to behave according to the laws of electromagnetic machines - the larger the linear dimensions, the better the system will become. The limit now is how small it can be made before it ceases to be practicable, and once again it is yet to be determined whether an acceptable size of vehicle falls above or below this limit.

6.3 The Electromagnetic River for high-speed transport

Section 6.2 has given a brief outline of some of the technical aspects of the four major support and guidance systems for high-speed ground transport. A few of the more important features, both in a positive and in a negative sense, have been pointed out, mainly to serve as a background to the comparison which follows. All four systems need a propulsion unit, capable of working against the powerful air-resistance to a vehicle the size of a railway train travelling at perhaps 400 km/h, and the only propulsion machine acceptable in the present-day climate of concern about noise and pollution is the linear motor. This choice is not without its difficulties, the most severe of which is probably that of transferring adequate power from the trackside into the vehicle moving at high speed. Discussion of this, however, lies outside the scope of this thesis.

But having once made the decision to use a linear motor, and in the light of the discoveries concerning expanding-geometry stable levitating machines, the next proposal is obvious. In the electromagnetic river there exists a linear motor capable of providing simultaneously the triple functions of lift, guidance and propulsion and if, as is perfectly fair in a situation where 95% of the input power is used in "pushing the air out of the way", all the capital expense and the running costs of the linear motor are ascribed to the production of thrust, then the lift and the guidance are obtained free.

Investigations carried out in the laboratory as to the feasibility of such a proposal form the subject of the next chapter. Before proceeding thus far, however, it may be helpful to present in slightly more detail some of the predicted capabilities of, and problems resulting from, a purely electromagnetic transport system. Having discovered a machine capable of performing three separate functions in three differing dimensions, all from one set only of electromagnetic coils, the next concern is to devise means by which these functions can be independently controlled.

For example in use as a transport system there is a need for control of propulsion such that the vehicle can be accelerated, cruised at constant velocity, and decelerated (and even made to go backwards), while the lift and guidance ideally remain constant throughout. In Chapter 2 it was shown how exchanges between properties can be carried out by the substitution of rotors of differing geometries. Wide plates can support a greater weight and experience a greater thrust than narrower ones at the same height, but at the same time they are less stable; use of a U-shaped trough increases thrust without affecting stability or lift, etc. But all these are important considerations only in the original design of the vehicle and its track; they are of course not applicable to control of a moving vehicle once it has been built.

More relevant is to discover the way in which the force normal to the surface of the electromagnetic river, i.e. the levitating force, varies as the rotor accelerates within the travelling field. However in researches of the kind described in this thesis there inevitably occur certain subjects for the investigation of which there is insufficient time. This was the case with investigations into the nature of the variation of normal force with speed. In the absence of any concrete measurements, therefore, predictions of such behaviour can be made only on the basis of likening the normal force characteristics of the electromagnetic river to those of the conventional linear induction motor, about which much is known. There is in fact considerable justification for doing this, since similar investigations (described in Chapter 7) into the way in which normal force varies with changing frequency of supply gave results following a pattern very close to that of the corresponding behaviour of a conventional linear motor. In any case the mechanisms of lift and thrust production in the two types of machine are identical, the differences between the motors being only in the topological arrangements of the magnetic and electric circuits, so it is likely that the variations of those quantities with speed will be similar.

A study of the behaviour of the normal force over a conventional longitudinal-flux linear motor under dynamic conditions has been made by Lowther.^(21,22) His work has produced both theoretical predictions and real measurements of the variations of lift under conditions of acceleration, deceleration and super-synchronous operation, at supply frequencies varying from 20 Hz to 90 Hz, and with the motor connected both as a 4-pole and as an 8-pole machine.

The main point to emerge is that with a suitable design of rotor and stator it is possible for the lift force to remain essentially constant over most of the forward speed range, beginning to drop significantly only when the rotor speed comes within a few per cent of the synchronous speed of the field. On the assumption then that

the same applies to the electromagnetic river, it appears that something very close to the ideal of constant maintenance of lift throughout the operable speed range is indeed achievable in practice. Since the guidance forces are also obtained from the same magnetic flux, it is likely that they also will vary in the manner of the forces of lift. (Lift and guidance under decelerating conditions, i.e. with the motor "plugging", are fully maintained. It is only when approaching the field speed in the forward direction that there is danger of loss.)

Even further independence between the various functions of the electromagnetic river might be thought desirable, particularly the provision of progressive control over the longitudinal thrust of the motor. Various schemes have been proposed for this purpose, but the problems involved are essentially the same as those of building a variable-speed rotary induction motor. This is a subject well covered elsewhere in technical literature,⁽²³⁾ and need not be gone into here.

(An interesting and novel suggestion was made that it might be possible to excite the three-phase linear stator with a deliberately unbalanced three-phase supply. In this way several harmonics of travelling field could be super-imposed on the fundamental component, allowing the possibility of latching the driving speed of a vehicle to, say, a harmonic travelling at half the synchronous speed of the supply, while maintaining lift and guidance from currents induced by the fundamental field itself. Differing degrees of unbalance could allow the choice of different harmonics for propulsion, while a return to balanced conditions would cause the vehicle to accelerate back towards synchronous linear speed.)

The cost and weight of any control system able to handle the full load power of the propulsion unit (probably several megawatts) would of course be major items for consideration, and it has been said that the same weight of machinery could be put to better use

as an alternator coupled to a synchronous motor to create a three-phase supply from a single-phase input, thus easing the problem of power pick-up. (But again, the major problems of pick-up arise with the loss of the wheel-on-rail return current path, and the resulting requirement for two contacts instead of one. The step then to three contacts from two is a relatively minor one.)

There can even be made a virtue of lack of speed control, on the grounds that a tracked transport network on which all vehicles run at precisely the same cruising speed and with the same characteristics of acceleration and deceleration is much easier to supervise than one in which each individual vehicle is driven at a speed determined solely by its own driver. Sophistication such as controllably unbalanced supplies may therefore prove in any case to be unnecessary, especially if lift can be maintained without difficulty over the entire operating speed range of an electromagnetic river in the same way as it can over a conventional linear motor.

6.4 Protection against loss of supply

A further topic that must be carefully considered for any contact-free high-speed transport system is the maintenance of lift and guidance in the event of loss of primary input power. It is essential that some provision be made for such an event, for no electricity supply can be guaranteed. It transpires that the linear motor itself can be used for this purpose, and that it is possible to turn the kinetic energy of the vehicle back into electric support and guidance currents flowing within the stator windings. Furthermore the process can be made instant and automatic, no switching of electric circuits, or any other action, being required (and the process is equally instantly and automatically reversible should power chance to be restored).⁽²⁴⁾

In order to understand the operation of the system it is necessary to appreciate the action of an induction motor in its

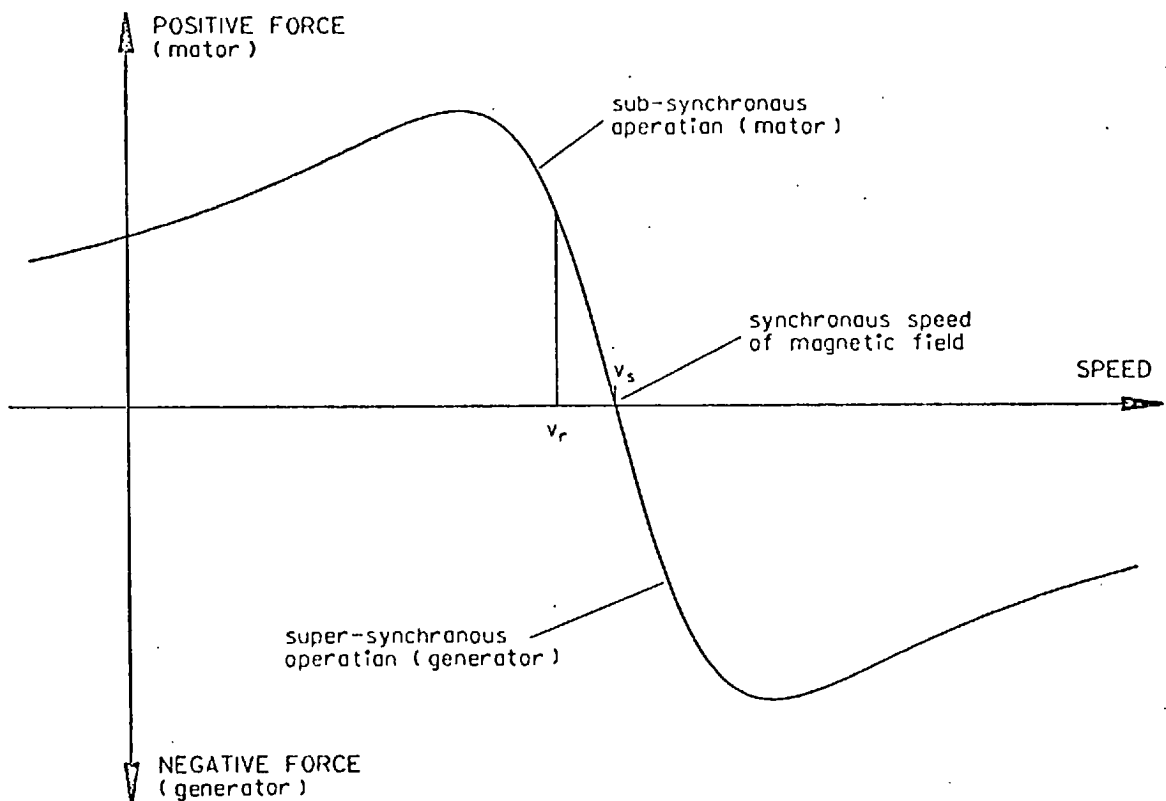


Fig 52. Super-synchronous operation of induction machine.

super-synchronous condition - i.e. when it becomes an induction generator. A detailed explanation of an induction generator can be found in many reference books on induction devices⁽²⁵⁾ but the essential result is that any induction motor, linear or rotary, becomes a generator as soon as its rotor is made to exceed the speed of the travelling field (see Fig 52), provided that stator magnetising current is supplied from an external source.

In effect, the stator of an induction machine requires its frequency of operation to be defined from outside; the speed of the rotor in relation to the synchronous speed so defined will then determine whether the machine acts as a motor or as a generator. On board a vehicle this external frequency source can take the form of a rotary synchronous alternator. The requirements of the alternator are to supply magnetising current and leakage flux to the induction stator, which in turn requires the rating of the

alternator to be of the order 30% of the full-load current of the main machine. Indeed the opportunity could be taken to employ a rather larger alternator operating with its field deliberately over-excited, to provide useful power factor compensation to the main motor. In either case the resulting combination of machines forms a system capable of becoming almost instantaneously a generator in the event of power failure.

The sequence of events is as follows. Under normal operating conditions the linear induction motor draws current from the main supply and propels the vehicle at a constant speed, say v_r , as shown on the diagram of Fig 52. The alternator spins at synchronous speed (v_s on the diagram) and absorbs no power other than to supply its own small internal losses. Upon loss of supply power the alternator, still connected in parallel with the motor, for a fraction of a second attempts to drive the motor by its own inertia, and in so doing rapidly decelerates until its speed is fractionally less than the frequency defined by the rotor speed v_r .

At this point the linear induction motor finds that its rotor speed (which has not changed in such a short interval) is slightly greater than the synchronous speed defined by the alternator, and the machine therefore begins to act as a generator, thereby preventing the alternator from decelerating further. The linear speed of the vehicle, the rotary speed of the alternator and the frequency of the generated current then slowly and steadily decrease, at a rate determined by the dissipation of the kinetic energy of the vehicle in the form of air-resistance and of heating in the current coils. The lift and guidance properties of the electromagnetic river are maintained by the currents flowing in the stator at all times except for the fraction of a second taken for the alternator to slow down after the loss of power.

The resulting deceleration of the vehicle can be improved from a passive coasting to an active braking action by the introduction of

a switching operation into the process. In this case, after loss of power one portion of the stator has the phase connections to any two of its supply leads interchanged, to reverse the direction of drive of that part - i.e. it is made to operate in plugging mode. The result is that the undisturbed portion of the motor generates in the same way as before, but now supplies output power to the plugging portion, which produces a braking force. In this mode most of the kinetic energy of the vehicle is being dissipated as heat in the aluminium track, and the deceleration is greatly improved. Such a combination of machines has been experimentally shown⁽²⁵⁾ to maintain generation and plugging down to a speed of a few percent of the original synchronous velocity, after which the point is reached when the whole electrical system suddenly collapses.

In this way the speed of a vehicle travelling, say, at 400 km/h can be brought down to perhaps 40 km/h before any secondary support system need be called into play. In practice it is unlikely that primary electromagnetic support would in any case be employed at speeds much below 100 km/h, since although the electromagnetic river is capable of accelerating from standstill, to attempt to maintain levitation of an entire vehicle at low speeds would involve severe problems of heat dissipation in the aluminium track.

6.5 Secondary support system and speed restrictions

The obvious choice for a secondary support system is to return to the steel wheel on steel rail since this remains by far the best tracked transport system for medium and low speeds. In fact the presence of steel rails on each side of the aluminium reaction sheet could be distinctly advantageous for a number of reasons. The normal running procedure could then consist of wheel-on-rail support and guidance while accelerating from standstill to about 100 km/h or thereabouts (propulsion provided either by wheel drive or by use of the main linear motor acting on the aluminium sheet), at which speed the primary support system could take over to lift the vehicle clear

of the track as acceleration continues to cruising speed. Deceleration to standstill simply follows the reverse procedure.

Continuation of the steel rails throughout the length of route can also form a back-up safety system, for in the event of a disaster such as total burn-out of the motor the vehicle could land on these rails even from full speed. A single such landing would be easily tolerable by the rails, even though they be known to be incapable of withstanding continuous high-speed heavy traffic. The steel rails could come into their own even more if it were arranged that their gauge was the same as that of a conventional railway, for it would then be possible to graft the high-speed routes onto those of a standard railway at the outskirts of a city and run into the centre on existing tracks, thus avoiding the need for new routes into the city itself. This and other simplifications make such "compatibility" with present-day operation an important consideration in the choice of systems for high-speed transport.

Most of the foregoing discussion has featured the support and guidance systems, but there remain a few points to be made of a more general nature. One of these concerns the possible speed ranges of the various ground transport systems mentioned. The lower speed limits are fairly clearly defined - the air-cushion and the two magnetic systems can maintain support from standstill, the cryogenic system requires a velocity of between 50 and 100 km/h before lift-off, and the electromagnetic river, while theoretically capable of lift at standstill, would in practice be restricted to a lower levitation limit of again somewhere in the region of 50 to 100 km/h to avoid problems of excessive track heating.

The upper speed limits are less clearly defined. Indeed once free of physical contact there seems no theoretical reason why such systems should not be capable of velocities approaching that of sound itself. However the power demanded by working against air-resistance sets a practical limit far below this, and while the exact value chosen is somewhat arbitrary, the deciding factor is

simply the point beyond which it is no longer considered worthwhile to pay the extra cost of the power required to go faster. To take for example the speed of 400 km/h which has been quoted a number of times already in this chapter, an increase of 12.5% to 450 km/h involves a corresponding power increase of 42% (on the assumption that all the output power is being dissipated as air-resistance, and therefore increases as the cube of speed), and a further increase to 500 km/h would all but double the original requirement.

The whole subject of high-speed ground transport can well be likened to that of low-flying aircraft - aircraft flying at an "altitude" of only some centimetres - and clearly there comes a point where high-flying craft must take over, for their ability to choose to travel where the air is thin and its resistance less inhibiting is the very reason for their existence. Ground transport systems are not regarded as competitors to machines such as these.

6.6 Choice of linear motor design

The last two points to be made before leaving this chapter of review, conjecture and discussion apply to the linear motor as a general machine for high-speed propulsion, and are therefore again relevant to all forms of lift and guidance. The first concerns the choice between a single-sided and a double-sided motor. As explained briefly in Chapter 5 the double-sided motor seems at first sight the obvious choice for a propulsion unit, simply because it makes better use of the space available by employing active windings on both sides of the rotor. Indeed until recently all the high-speed ground transport systems under investigation throughout the world were using or were planning to use a double-sided linear motor as the thrust unit, with the single exception of Tracked Hovercraft Ltd., who employed a single-sided motor from the beginning.

However when detailed design calculations for the motor are carried out, the resulting rotor shape assumes the proportions shown in Fig 53(a), where distance "x" is about 1 cm and distance "y" is 40 cm.

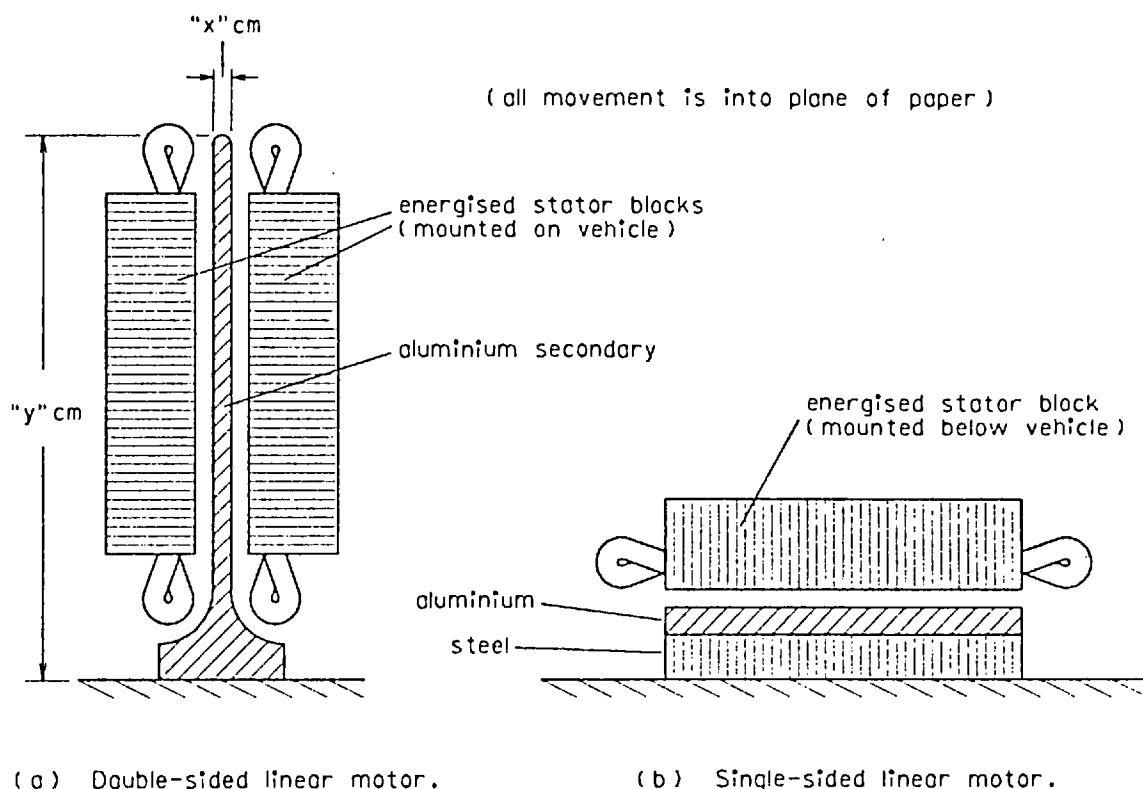


Fig 53. Two basic forms of linear motor.

It is necessary to minimise the rotor thickness in order to keep the total air-gap between the stator pole-faces as low as possible (the thickness of aluminium, of course, being included as part of the "air-gap"), and the need to develop thrust appropriate to a full-scale vehicle then results in the height of reaction plate shown.

Such a design presents severe mechanical problems. (Fabrication is not one of them, however - continuous lengths can be formed by extrusion.) Aside from difficulties of mounting and alignment, neither of which is troublesome in the rotor of a single-sided motor - see Fig 53(b) - one of the major troubles experienced to date has concerned track joints. The passing of a joint causes a serious transient in the magnitude of the propelling force and this, combined with the practical difficulty of maintaining accurate alignment across a joint free to move longitudinally to allow for

expansion and contraction, has led to attempts to eliminate joints entirely. These attempts have followed the standard practice employed by many railways, namely to overcome the need for expansion joints by laying the track under tension sufficient to ensure that the resulting longitudinal extension of the metal is greater than that producible by the highest temperature likely to be encountered. Under cold temperature conditions, of course, the metal is under high tensile stress, and it has transpired that aluminium, unlike steel, lacks the tensile strength to withstand these stresses. In fact an experimental track in the U.S.A. split in three places on one particularly cold day.

A second difficulty experienced with reaction rails of the shape shown in Fig 53(a) has been the formation of standing waves of lateral oscillations in the aluminium in advance of an approaching high-speed vehicle. The combination of these two problems has been the principal reason for a steady change-over on a worldwide scale from the use of double-sided to single-sided motors. A particularly worrying possibility is that the occurrence of a temperature almost as cold as that which split the tracks, together with the extra stresses of lateral oscillation experienced on the approach of a vehicle, could result in a fracture causing a catastrophe on the scale of a major aircraft disaster.

On the grounds of danger alone, therefore, double-sided motors are now being abandoned for high-speed use in all-weather conditions. A further consideration is that a recent patent⁽²⁷⁾, applicable only to single-sided motors, has been filed which discloses the construction of a track joint possessing almost none of the detrimental effects associated with a conventional joint. This is described in some detail in Section 6 of the following chapter. Lastly the single-sided motor requires less weight to be carried on board the vehicle since half the steel comprising its magnetic circuit is embedded within the track.

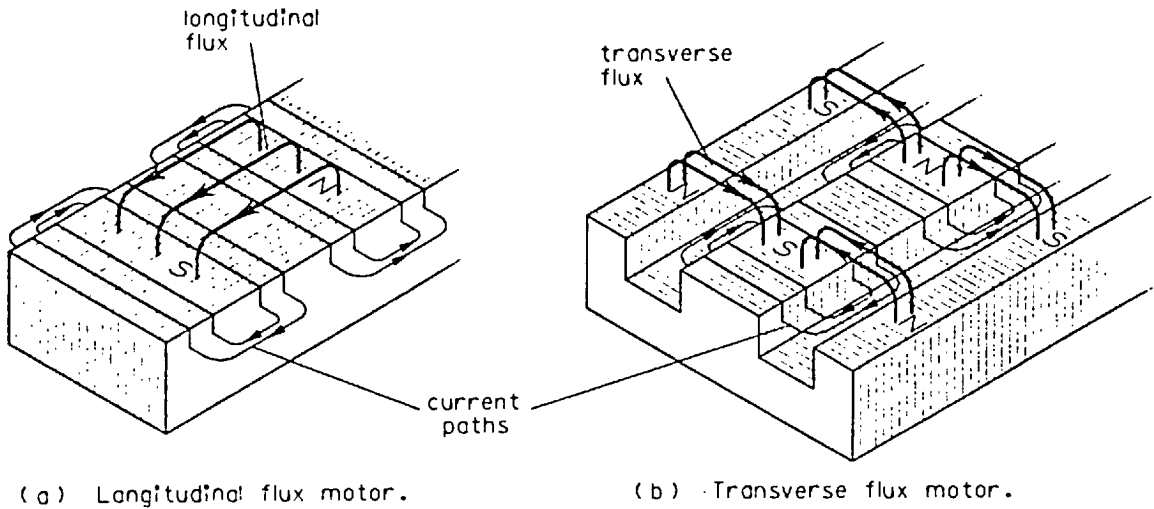


Fig 54. Longitudinal and transverse flux linear motors.

The second topic concerning the overall choice of motor design is the distinction between the properties of longitudinal-flux and transverse-flux linear motors. The basic difference between the two machines is exactly as their names imply. In the one case the magnetic flux paths between adjacent poles are aligned parallel to the length of the machine, as shown in Fig 54(a), and in the other case they pass across the machine, either from one side to the other as in the electromagnetic river (see, for instance, Fig 29 of Chapter 4) or from either side towards the centre as shown in Fig 54(b). (For a full treatment of the development and the properties of transverse-flux motors see reference 28.)

Now the velocity v_s of the travelling field set up by a longitudinal-flux linear motor of pole-pitch p and supply frequency f is given by $v_s = 2pf$. From this it can be seen that if the supply frequency is not to change then a high linear speed of travelling field requires a proportionally long pole-pitch. On this basis a motor capable of driving a vehicle at 400 km/h, requiring a synchronous field speed of perhaps 450 km/h, would need a pole-pitch of 1.25 m if it were to operate from the 50 Hz mains supply. But a pole-pitch of 1.25 m defines a length of magnetic circuit of over 2.5 m, a distance quite impracticable with present-day magnetically-

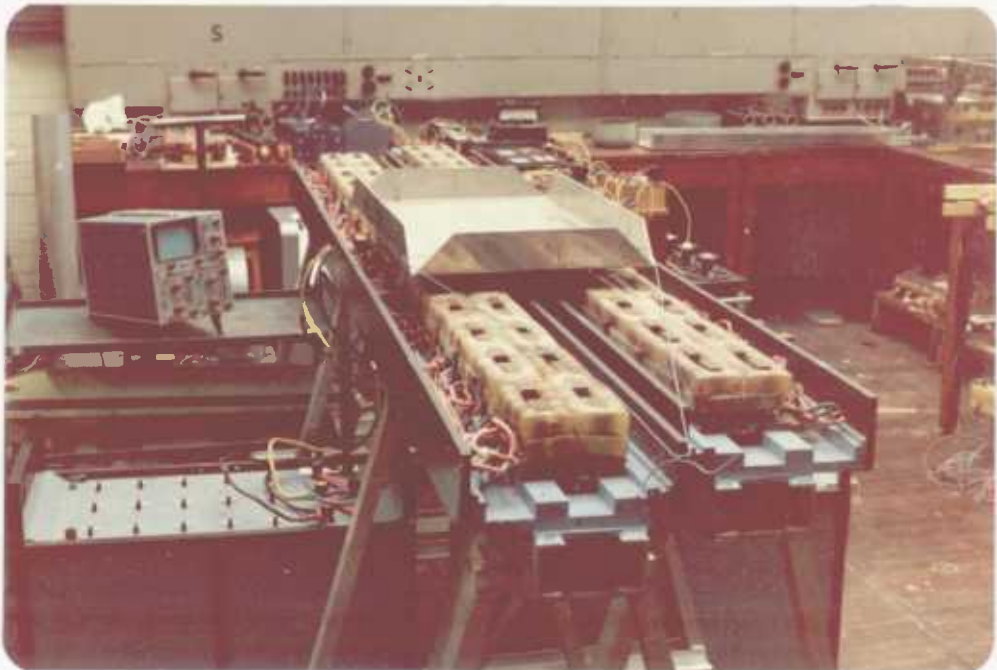
conducting materials. The only way out of the dilemma is to employ a higher frequency of supply, with all the expense, weight and complexity that a rectifier-inverter system entails.

The transverse-flux motor, on the other hand, has a magnetic field velocity and a magnetic path length that are mutually independent. There are now two pole-pitches, a "lateral pole-pitch" depending only on the dimensions of the stator laminations, which determines the magnetic path length, and a "longitudinal pole-pitch" measured from the centre of one set of current coils to the centre of the next set carrying anti-phase current. The velocity of the travelling field is determined only by the second of these parameters, and may consequently be increased without theoretical limit while operating at the same supply frequency. There is a practical limit imposed by the heavy chording of the electrical circuit necessary for very long pole-pitches, but this applies equally to longitudinal-flux motors as well. Certainly the transverse-flux machine is capable of driving a high-speed vehicle at any realistic speed desired while powered direct from the standard 50 Hz mains supply.

Taken together the two considerations concerning the nature of the propulsion unit lead to the conclusion that for any high-speed ground transport system, no matter what its form of support and guidance, the thrust will be provided by a single-sided linear motor, either synchronous or transverse-flux. It should be noted that the electromagnetic river is both single-sided and of transverse flux. This fact, combined with the built-in lift and guidance, has led to the electromagnetic river being regarded, by those who were responsible for its development, as a high-speed ground transport system eminently suitable to take over from that centuries-old means of transport - the wheel - and it is with experimental considerations of such a proposition that the following chapter is concerned.

CHAPTER 7

LABORATORY SIMULATION OF LARGE-SCALE ELECTROMAGNETIC RIVERS



The "catamaran" machine (p 140) - the two halves of the long electromagnetic river mounted side-by-side.

CHAPTER 7

LABORATORY SIMULATION OF LARGE-SCALE ELECTROMAGNETIC RIVERS

The first part of Chapter 6 mainly comprised a review of some technical aspects of systems for high-speed ground transport upon which experimental work is in progress throughout the world. The second part concentrated in particular on the use of the electromagnetic river in this field. Since no experimental work has yet been carried out on a full-scale electromagnetic river, much of the discussion in the latter half of the chapter was necessarily of a hypothetical nature.

However all such discussion is based at least on a foundation of fact, which is that there exists an electromagnetic machine capable of providing lift, guidance and propulsion upon a conducting secondary, yet with an effective width of only ten centimetres. Scaling up to full-size, for instance by multiplying every linear dimension by a factor of fifteen to bring the effective width to a metre and a half, results in a machine whose goodness factor has been multiplied by 225!

7.1 The "Catamaran" Machine

At the same time, experience with many types of electromagnetic machine has shown that proportionate scaling is seldom the best technique; improved though the system will become as it is made larger, it is likely that there will be better geometries still at the higher size. Two features in particular of the laboratory electromagnetic river led to an investigation of alternative geometries.

The first was consideration of the ratio of the lift force experienced by any secondary plate to the thrust acting on the same plate. This ratio, of course, determines the value of the longitudinal acceleration of the secondary after release from standstill. If F_n is the force normal to the surface of the stator, i.e. the lift force supporting the weight of the secondary, and F_ℓ is the longitudinal

driving force, then the acceleration is simply $\frac{F_l}{F_n} \cdot g$, where g is the gravitational acceleration at the surface of the earth.

To a first order of approximation these two forces acting on an aluminium plate over the electromagnetic river were equal, giving an initial acceleration of the order $1g$. (Once in motion plates tended to experience decreasing acceleration with increasing velocity, giving an average acceleration over the whole length of the machine of around $0.75g$, as quoted in Chapter 5.) However a full-scale passenger-carrying vehicle is likely to require to accelerate at no greater than about $0.1g$, this being generally regarded by transport authorities as the maximum value consistent with passenger comfort. (For comparison, $0.1g$ is about the value of acceleration with which modern London Underground trains begin to move away from a platform.) Thus one of the design criteria for an electromagnetic system is likely to be that it should prove capable of maintaining the normal force between rotor and stator at a value about ten times greater than that of the longitudinal accelerating force.

The second unsatisfactory feature of the electromagnetic river was its degree of stabilisation in roll. While most flat aluminium plates experienced reasonable or good roll-stabilisation and damping when supporting only their own weight, this was often no longer the case when the plates were made to carry some form of load. Indeed under some conditions of load certain aluminium plates proved to be totally unstable. The model vehicle, consisting of a fibreglass shell constructed over a base plate of aluminium, exhibited particularly low roll-damping (most easily demonstrated, as mentioned in Chapter 5, by causing it to follow a disturbance in alignment half-way along the electromagnetic river). These deficiencies were to a large extent the result of mounting the extra load above the aluminium plate, thus raising the overall centre of gravity of the supported system - a procedure well-known to lead to roll-instability. This form of mounting is, however, exactly that most likely to be used in practice, since the alternative of suspending the load at a level beneath the conducting

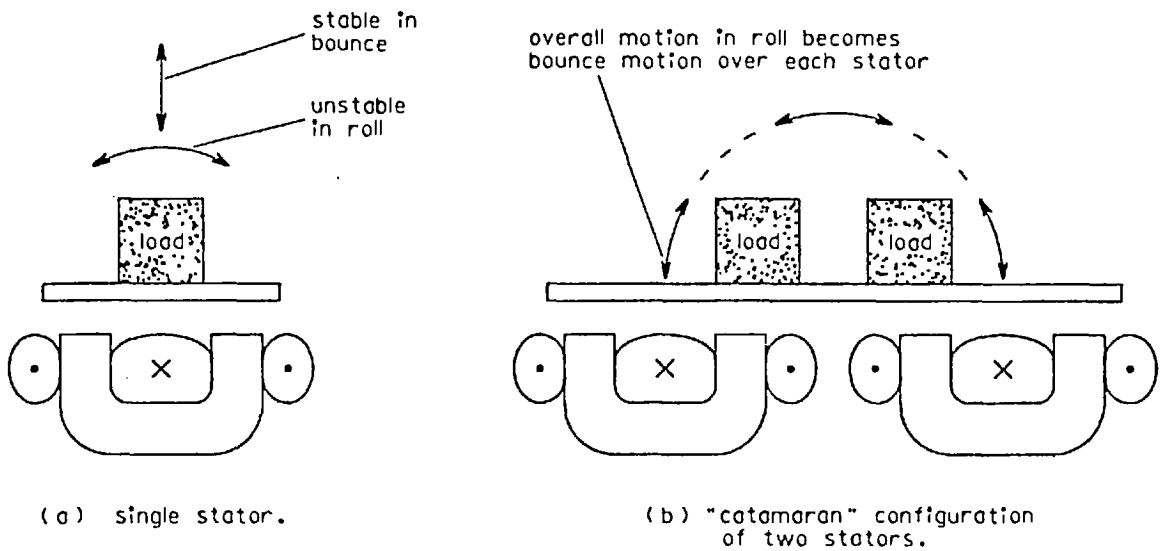


Fig 55. Use of two electromagnetic rivers to convert roll-instability into bounce motion.

plate, itself floating at a small clearance above the stator, involves considerable extra mechanical complexity.

These two shortcomings of the electromagnetic river, i.e. the low ratio of lift to thrust and the poor roll-damping under certain load conditions, led to investigations of a double-stator "catamaran" system comprising two electromagnetic rivers positioned side-by-side, as shown in Fig 55. The reasoning behind this development was that when supported on a composite system such as this, any overall roll movement of the rotor becomes mainly vertical movement over each of the individual stator units. In this way an instability of roll is converted into a motion of bounce, known to be stable and well-damped (see section 2 of Chapter 5 - pitch disturbances).

Realisation of a suitable system for laboratory experiments merely involved re-mounting the two halves of the electromagnetic river side-by-side a short distance apart, instead of end-to-end as before. Preliminary experiments using flat sheets of aluminium confirmed that the roll stability was indeed greatly improved. It was also quickly discovered that the conditions necessary for lateral stability were similar to those over a single-stator machine, in that an "expanding-

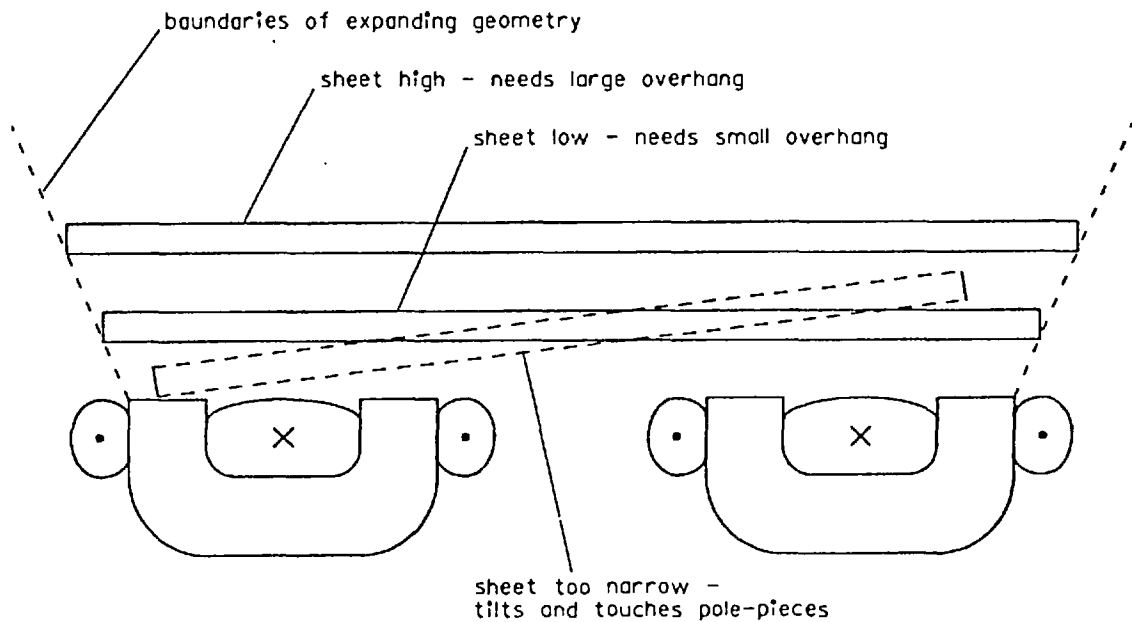


Fig 56. Expanding geometry of "catamaran" stator.

geometry" situation again existed relating the width of an aluminium sheet to the height at which it could float. Fig 56 illustrates this, and also shows the form of the resulting instability when the rotor sheet is too narrow. Too wide a sheet simply slips sideways off the whole machine.

The general "feel" of the lift and thrust capabilities of the machine were most encouraging. A sheet of the same thickness and length, and with a width chosen to give the same overhang, as one of the original test plates on the single electromagnetic river appeared to experience a longitudinal thrust three or four times greater than that acting on a plate over the original stator. As the sheet was pushed downwards towards the surface of the stator the force of vertical lift was found to be many times greater. Indeed it was a difficult matter for one person alone to force the sheet right down to touch the stator pole-pieces - the impression was that an average person needed to transfer something of the order of half his own weight to the plate in order to reduce the air-gap to zero.

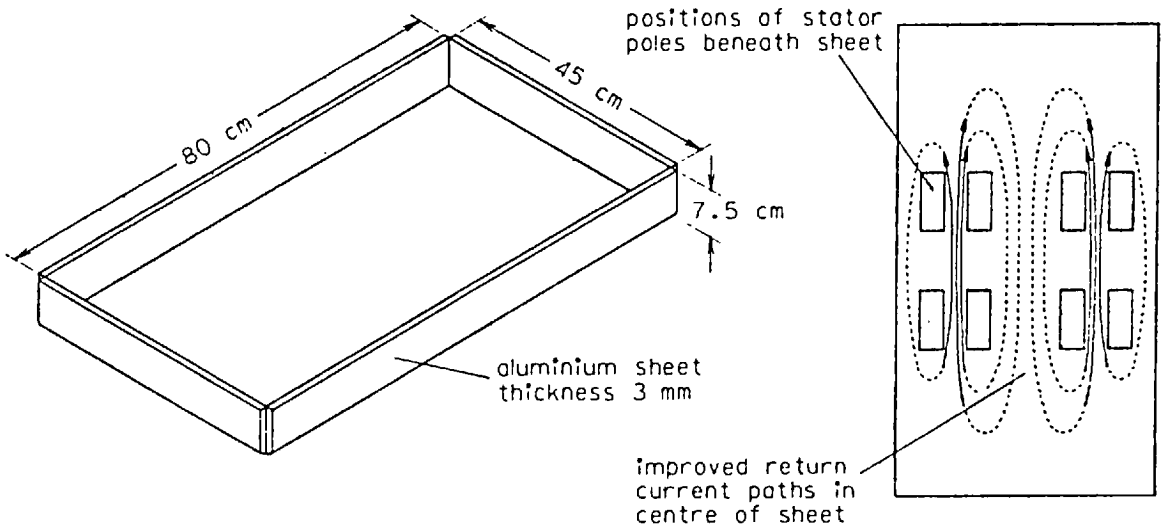


Fig 57. (a) Dimensions of aluminium tray.

(b) Improved return paths for currents induced in rotor.

These impressions were confirmed by measurements made on the machine. An experiment to investigate the relationship between thrust and lift was carried out using a large sheet of aluminium whose edges had been bent upwards to form a tray, into which quantities of sand were then poured to form a load. Fig 57(a) shows the dimensions of the tray. When unloaded, the tray was found to experience rather greater propulsion and lift than a flat plate of the same length and width, but the stability remained unchanged. The comparison here is of exactly the same kind as that between a U-channel trough and a flat plate acting as secondary over a single stator (see Chapter 1). The large increase of horizontal and vertical forces on both the tray and on the flat plate compared to the corresponding forces on plates over a single stator is probably the result of the improved current return paths along the centre of the sheet - see Fig 57(b).

The height at which the unloaded tray floated was about 5 cm, and as sand was slowly poured in this clearance was of course steadily reduced. The longitudinal thrust on the aluminium (measured by a spring balance) increased only slightly during this

process, showing the relative independence of thrust upon levitated height for any given size of plate. In order to maintain the same degree of stability while the clearance was being reduced it was found necessary to move the two stator units progressively further apart so as to adjust the degree of overlap of each plate edge to a value appropriate to the height reached (see Fig 56).

The loading was continued until the tray was floating at a clearance of only about 0.5 cm, at which point the total weight of the sand plus the aluminium was 35 kg while the thrust force was about 7 kgf at standstill. This already represented a lift to thrust ratio of 5:1, and the fact that such a simple modification to the topology of the system resulted in a five-fold increase of the ratio of lift to thrust was taken as a clear indication that with further sophistication the development of a machine capable of providing the required 10:1 ratio would not be a difficult matter.

Fig 58 shows one possible example of how such extra complexity might lead to a realistic system for a large-scale machine. The unit in the centre is a transverse-flux linear motor designed only to provide lift and propulsion, e.g. a waffle motor⁽²⁹⁾, while guidance and further lift are obtained from electromagnetic rivers positioned on either side of the central unit. It may or may not be advantageous in such a situation to insulate those portions of the secondary sheet acted upon by the electromagnetic rivers from that above the waffle motor. The number of other possible variations on this theme is of course enormous, and once again the subject must be left open for future investigation. The experiment succeeded in its original purpose however, which was to demonstrate the existence of different geometries of machine that could at the same time both improve the ratio of lift to thrust and also provide much greater roll stability than has been found possible on a single electromagnetic river.

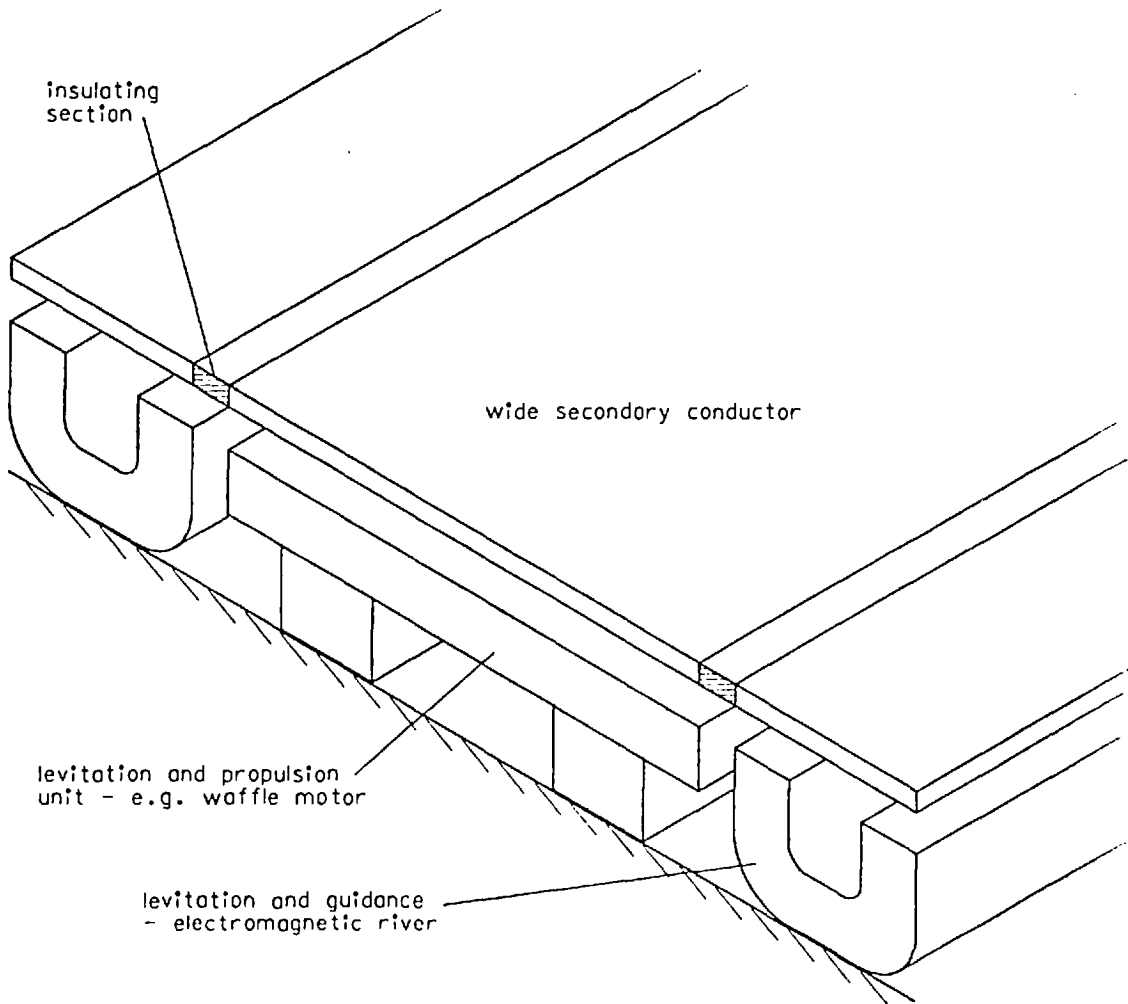


Fig 58. One example of a new geometry for a large scale machine.

7.2 Variable stator core dimensions - use of gramme-ring wound stator blocks

Following the catamaran machine a new series of experiments was begun, with the aim of discovering some of the effects of variations in the relationship between the transverse width of each individual pole-piece and the width of the slot carrying the main stator currents (i.e. the lateral distance between the pole-pieces). Fig 59 shows two extremes of variation, and also indicates the practical difficulties that arise as these extremes are approached. In the case of Fig 59(a), where the slot width is made small compared

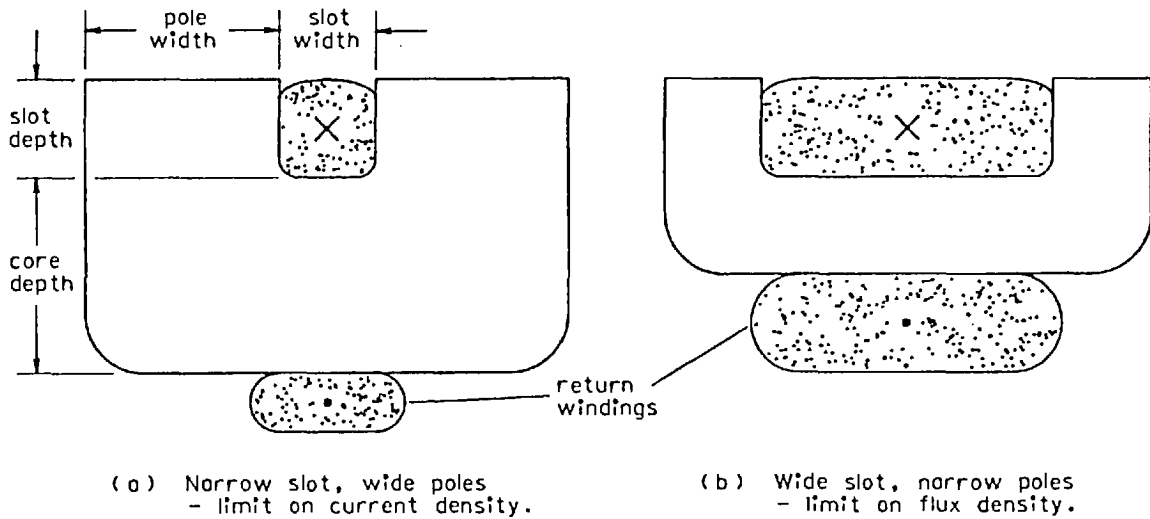


Fig 59. Examples of variations in the proportions of slot width and pole width of a single electromagnetic river.

with the pole width, the space available for the stator winding becomes restricted to the point where the current density needed to provide sufficient lift becomes too great (i.e. there is a limit on stator winding temperature).

In the other case, where the pole width is made small as in Fig 59(b), a limit is reached when saturation of the iron circuit prevents the passage of sufficient flux to support the rotor. The two further dimensions of the iron core, slot depth and core depth shown on Fig 59, have less flexibility of design, since once the slot width and the maximum sustained stator current are known then the slot depth is simply the minimum consistent with an acceptable value of current density, while the core depth would normally be the same as the width of each pole-piece, to maintain constant flux density throughout the iron circuit.

Now it would have been a laborious process to obtain or construct a series of iron cores of various cross-sections but of the same overall width, and then to wind an individual pair of coils to fit each one. Instead, a somewhat unusual use was made of a number of blocks of standard linear motor laminations which had had their stator

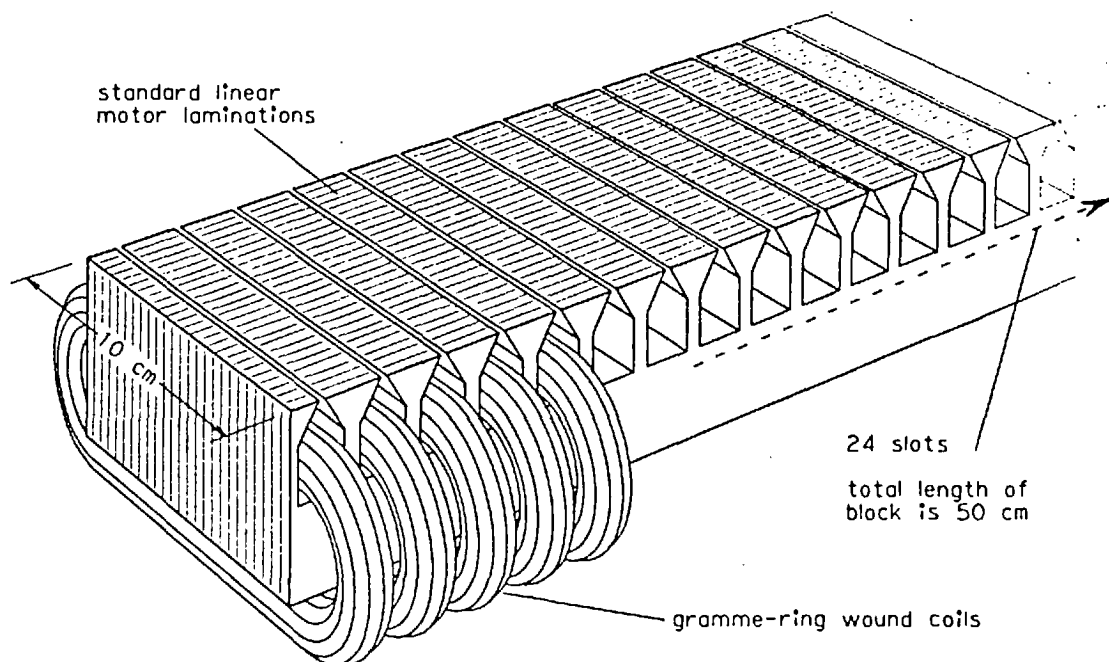


Fig 60. Gramme-ring wound linear motor stator block.

coils wound around them in gramme-ring fashion (instead of in the more normal form of a layer winding) - see Fig 60. The particular feature of such an arrangement in use as an electromagnetic river was that by suitable interconnection of the individual coils, simulation was possible of almost any configuration of slots and poles, of any overall width up to a value equal to the length of the linear motor block (about 50 cm).

Fig 61(a) shows an example of such a connection. Of the twenty-four individual coils, numbers 6 to 10 are connected in series and in the same sense, while numbers 15 to 19 are also in series but connected all in the opposite sense to the first set. Each of these sets simulates a single current-carrying coil filling a single slot of width equal to the distance embracing the five component coils. A further three sets of coils, numbers 3 to 5, 11 to 14 and 20 to 22, are left open-circuited, thus simulating three magnetic poles of corresponding respective widths. Finally the last two coils at each end of the stator are short-circuited

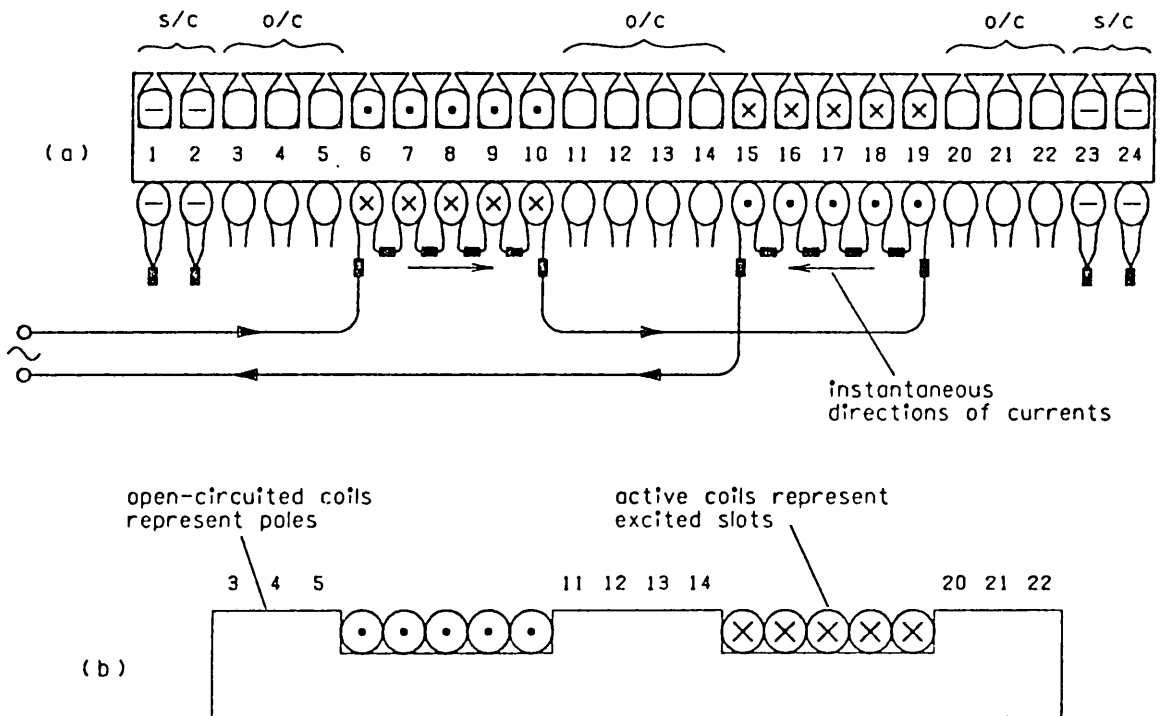


Fig 61. Simulation of E-core transverse flux motor.

upon themselves to present a high magnetic impedance to any flux attempting to pass through them. The effect of this is to reduce the apparent width of the simulated iron, since the flux is effectively contained within a region bounded by coils 3 and 22. The set of return currents below the stator has little or no effect on the flux passing through the top surface, and therefore need not be considered. The complete arrangement simulates an E-core transverse-flux motor such as that shown in Fig 61(b). It is then a simple matter to re-connect the coils to investigate the effect, for instance, of narrower slots and wider poles, or of changing the relative proportions of the width of the centre pole compared with those of the two outers.

Simulation of a C-core electromagnetic river is rather less complicated, since the required arrangement is simply a central block of coils all connected in series to simulate the single slot, bounded on each side by sets of coils left open-circuited to simulate

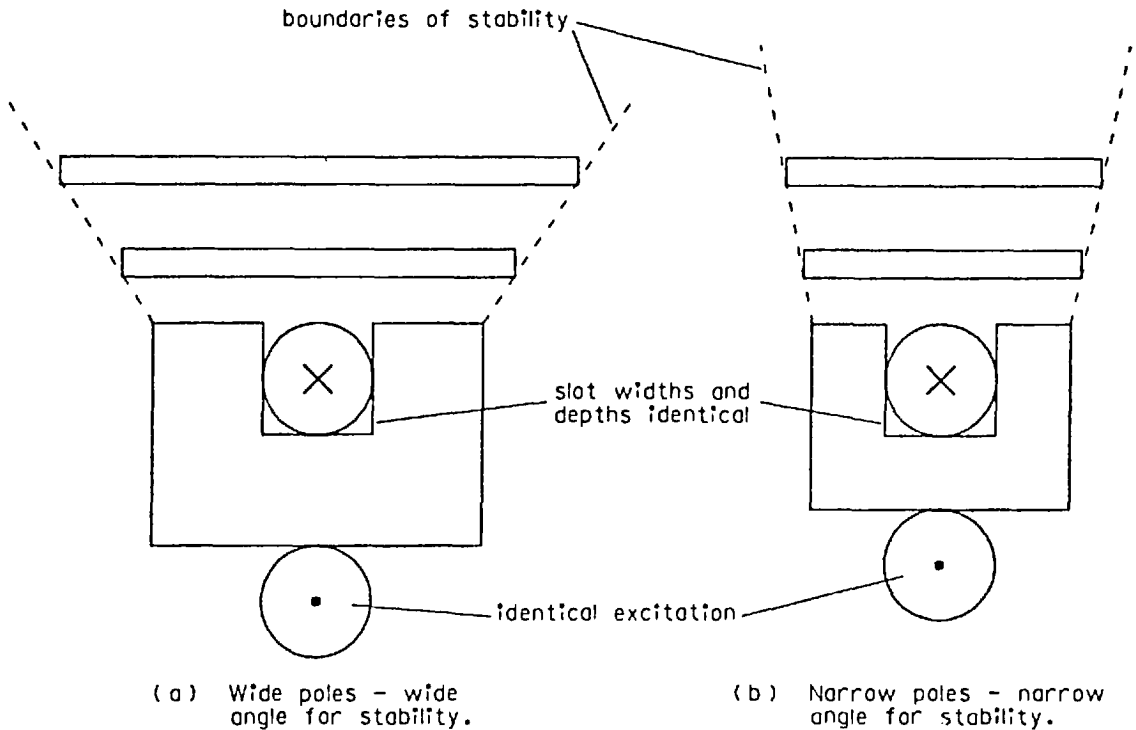


Fig 62. Effect of pole width upon boundaries of stability.

the poles (and possibly further coils short-circuited at the extreme ends to limit width). After many variations of this basic arrangement had been tested, the only significant conclusion to be drawn from the results was the somewhat negative observation that the relative widths of the slots and of the poles do not play a large part in the determination of rotor stability.

One point did emerge however, which was that the widths of the poles do appear to influence the rate at which the width of floating plates must increase with increasing height of flotation to maintain the same degree of stability. Fig 62 illustrates this - the stator on the left, with wide poles, has as its boundaries of stability an inverted prism of wide angle, while the narrow-poled machine on the right has a narrow-angled inverted prism for its boundaries.

A search for the configuration to give the maximum flux at the pole tips, and hence the maximum lift, led to the predictable result

that the width of each pole should be equal to the depth of the iron core below the stator slots, in order that all parts of the iron circuit should approach saturation at the same value of stator current. In the case of the particular stator blocks employed this requirement was met by leaving four coils open-circuited at each end. It was found that the best use was then made of the remaining sixteen coils by connecting them all in series as a wide central slot, to provide the maximum excitation for the poles. The resulting machine was a simulation of an electromagnetic river of 50 cm width.

7.3 Simulation of a wide electromagnetic river by gramme-ring wound blocks

At about this point the experiments tended to develop into an exercise simply to achieve the greatest possible height of levitation of an aluminium sheet, to see whether stability would be maintained at these sizes in the way that the expanding-geometry theories predicted that it should. It will be realised that one of the linear blocks of laminations on its own can simulate an electromagnetic river only 10 cm long (this being the width of the block itself). Extension to a more useful effective length was simulated by the use of several blocks positioned side-by-side, all electrically connected together in parallel, as shown in Fig 63. On the diagram, each individual block has sets of currents flowing instantaneously to the left over its top surface and returning underneath, forming a system having the same effect as one comprising a single set of currents flowing from right to left across all four top surfaces of the blocks, and returning below.

In practice it was found that each set of sixteen coils drew about 80 amps from a 415 volt supply, and since the main laboratory supply was fused at 200 amps only three blocks were connected in parallel at any one time. This combination, of three blocks in parallel each consisting of sixteen coils in series bounded on each side by four coils open-circuited, was found capable of supporting

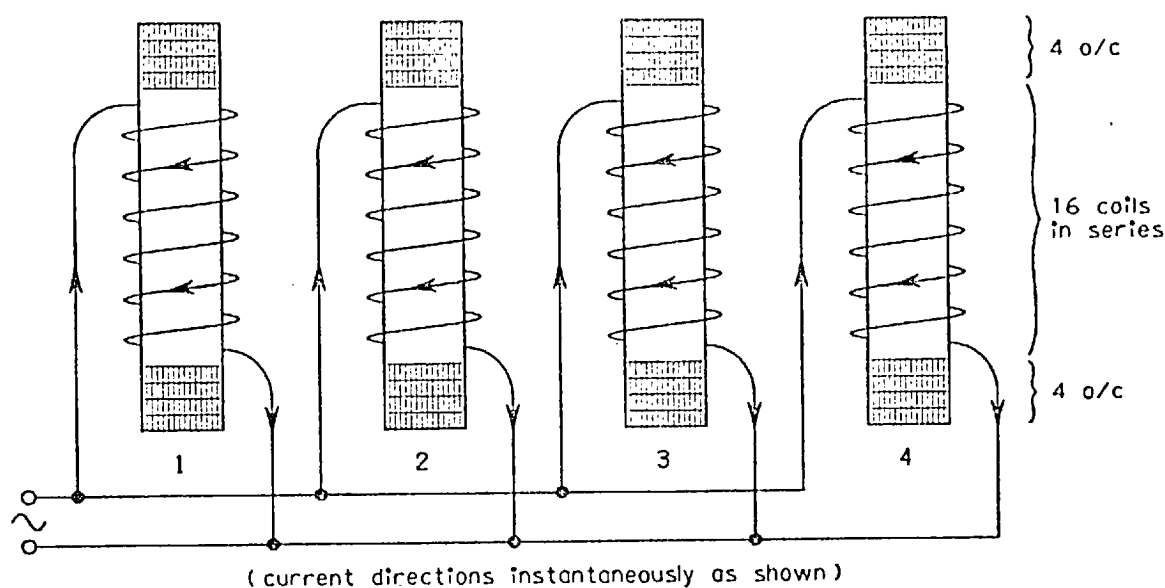


Fig 63. Parallel connection of several blocks to simulate a long single slot.

and stabilising a 3 mm aluminium sheet 60 cm wide at a height of nearly 25 cm. Furthermore the force then needed to push the sheet down to touch the stator poles exceeded 40 kgf - nearly half the weight of an average adult. That such a performance was possible from a machine that was, after all, no more than a rough "lash-up" of parts that happened to be available at the time is an indication of the advantages to be obtained from an increase in overall scale. A five-fold reduction in the dimensions of the blocks and their windings to bring the system back to the 10 cm width of the original Washington model and of the long electromagnetic river would carry with it a twenty-five-fold reduction in goodness factor, resulting in an utterly incapable machine.

The simulation can be extended. If, instead of a simple parallel connection, the individual stator blocks are connected to the mains supply in phase-sequence (block 1 to Red, block 2 to Yellow, etc.), then the longitudinal travelling field itself can be incorporated into the system. Note, incidentally, that the direction of travel of the field, while longitudinal with respect to the system

as a whole, is transverse to each individual stator block. This, of course, is a consequence of the blocks having been used in the construction of a transverse-flux machine.

Simple phase-sequencing of the coils in this manner proved of little value other than to demonstrate that the ideas conceived in theory did actually work in practice - the simulated electromagnetic river performed admirably, providing thrusts of up to 10 kgf while maintaining loaded plates stable and level. More interesting was an attempt to make use of poly-phase connections to create inwards travelling fields at each end of the system in order to provide longitudinal as well as lateral stability. Hence it was hoped to achieve levitation stable in all axes on a much larger scale than hitherto.

The method of phase connection was similar to that employed in the small stable levitator (the "magic carpet" machine) described in Chapter 2 - see Figs 13 and 14. The phases of the currents in the centre two stator blocks were made to lag sixty degrees behind those in the outer blocks, though in this case the phase difference was obtained by suitable interconnection between the 415 V live lines of the three-phase supply instead of by making use of the supply neutral as was done before.

It was found that longitudinal stability could be achieved only when the ends of the floating sheet were directly over the two end stator blocks. Provided this condition was met by suitable positioning of the blocks, almost any desired length of aluminium sheet could be stabilised. The width of the sheet was less flexible, since this had to be chosen to fit the boundaries of lateral stability for the particular height at which the sheet floated (itself dependent upon the mass of the sheet and the stator current). Under these conditions, it was realised, the major part of the lift force was being provided by the centre two blocks only. The support system could therefore be improved by spacing these two blocks well apart to give an effect nearer to that of a uniformly distributed

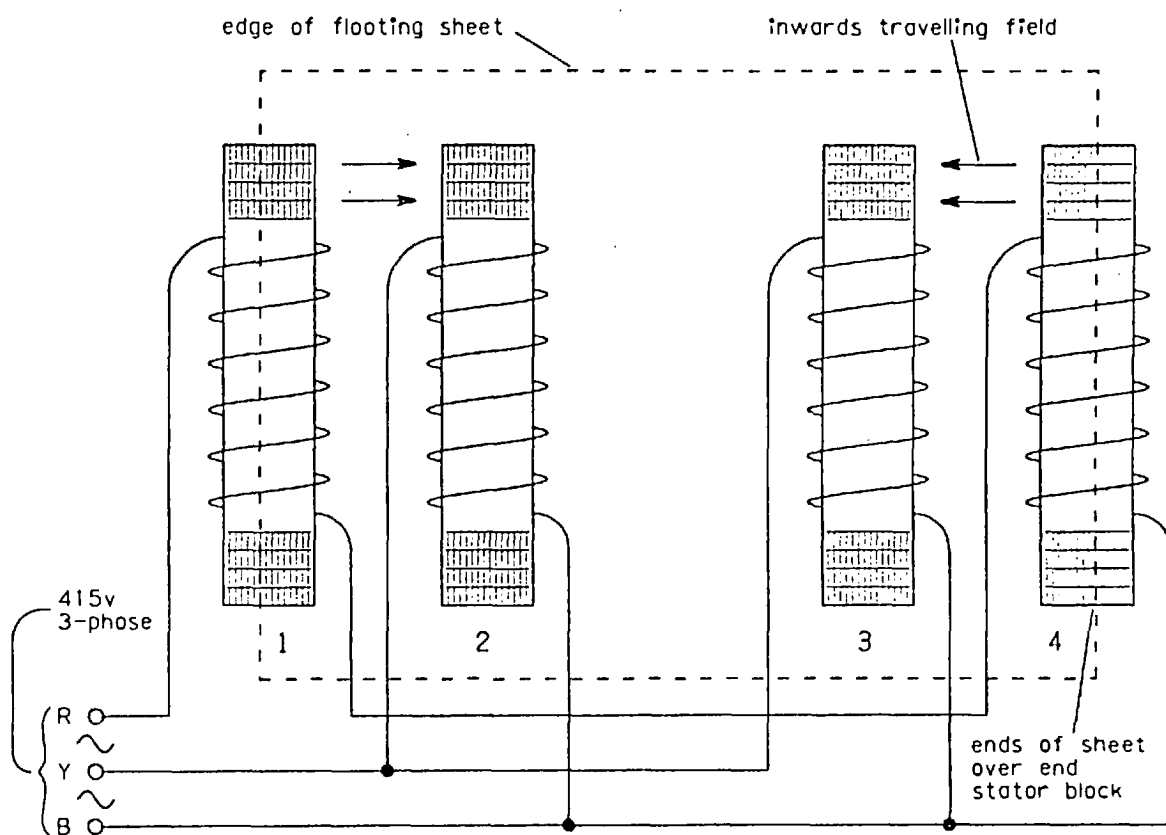


Fig 64. Connection of four blocks to provide inwards travelling fields from both ends.

lift force rather than to that of a single large force acting only in the centre region. Since the main effect of the two end blocks was then merely to provide longitudinal stability forces, it was found sufficient to connect these in series across the supply so that they each carried a current of magnitude half that of the two lift-producing blocks. The final physical spacings and the electrical connections between the blocks are illustrated in Fig 64.

Over this system the 60 cm wide sheet of aluminium was found to float stably at a height of about 20 cm. The stability was however very weak - in particular the sheet exhibited a strong tendency to slip round to a position in a horizontal plane but with one diagonal aligned parallel to the length of the stator. A better floating rotor was found in the aluminium tray used to test the side-by-side version of the electromagnetic river (see Fig 57). While

the floating height of this tray was not quite so great as that of the flat sheet (a consequence of the reduction in width from 60 cm to 45 cm), the stability, both longitudinal and lateral, was greatly improved. Indeed the tray could be released from a position as much as 15 cm displaced in any direction, and its resulting oscillation would be steadily damped to bring it once again to rest in its equilibrium position, about 16 cm above the stator surface.

The tray could of course also be weighted with sand, as before, to investigate the effect of additional loads. It was found that the stability at first increased as the extra load was applied, but a point was reached (at about 20 kg of load) beyond which roll stability began to deteriorate, and eventually failed altogether. The reason for this behaviour was simple. The extra load reduced the clearance between rotor and stator, and no account was being taken of the corresponding change in width of the rotor (or alternatively of the stator) necessary in order to maintain the edges of the tray on the boundaries of stability. Simulation of an increase in the stator dimensions was not attempted since the full width of the stator blocks was already being employed, and fabrication of extra hardware simply to provide further confirmation of an already established experimental fact seemed scarcely worthwhile.

It may have been noticed that there are a number of similarities between the machine under discussion and the original "magic carpet" machine of Figs 13 and 14. The use in both cases of currents of differing phase to create inwards longitudinal travelling fields has already been noted; in addition each machine had the same requirements for longitudinal stability regarding the positioning of the floating sheet with respect to the end stator blocks below. Furthermore in each case the main support was supplied from the centre blocks only, allowing an electrical connection such that the two end blocks carried only half as much current. These similarities are of course no coincidence since the two systems are in essence identical, the only fundamental difference being one of scale. Indeed the new machine could aptly be named a "child-scale magic carpet" since in the case of

the flat aluminium sheet the upwards levitation force (40 kgf) is sufficient to support the weight of a well-grown child.

7.4 Human levitation

Successful floating of the aluminium tray concluded the experiments carried out on variations of geometry of the electromagnetic river using the gramme-ring wound stator blocks, though the tray-floating machine itself remained in use for a considerable time as a demonstration model. Meanwhile the line of research took a new turn, into a direction originally intended as no more than an interesting sideline - to levitate an adult human on an electromagnetic field. In reality this merely involved the provision of a lift force sufficient to float a sheet of aluminium with the additional weight of a man sitting on top.

The machine employed for the purpose was a conventional longitudinal-flux linear motor, capable of providing only lift and thrust. The stator lamination block was 13 cm wide by 12 cm deep by 2.6 m long, and the winding overhang was such as to give the machine an overall width of 40 cm. The windings themselves had a continuous current rating of 80 amps, and the whole machine weighed 400 kg. The motor was in fact one half of an originally double-sided linear motor built by Associated Electrical Industries Ltd. (AEI) in 1957 for research at Manchester University. The double-sided machine had later had its two component stators unbolted one from the other; one of these had been left unmodified while the other had had its coils electrically re-connected to double the pole-pitch from the original length of 24 cm to 48 cm. This long pole-pitch motor was the one selected for the levitation experiments.

Over the stator a large sheet of aluminium, 2.5 m by 1.25 m by 6 mm thick, could be floated at a clearance of 15 cm with a stator current of 180 amps. It was found that the combined efforts of four people, one holding each corner of the sheet, were scarcely sufficient to force the aluminium down to touch the stator. The

task of holding the sheet down was made no easier by the enormous increase in longitudinal propulsion force (approximately an inverse fourth-power law with distance) experienced by the sheet as it was forced deeper into the magnetic field. Bearing in mind this powerful dependence of thrust upon clearance, the four people were asked to remain at the corners, providing no support but only restraining lateral and longitudinal movement, while a fifth person stepped onto the centre of the sheet and sat down. The sheet settled to a clearance of 7 cm, and the stator current increased to 210 amps.

Much encouraged by the large clearance still remaining even under the weight of one person, a second person was asked to step onto the aluminium and to sit down. (It was found unwise for the "passengers" to remain standing since the resulting high centre of gravity made the floating system highly unstable in roll. The responsibility for maintaining lateral stability and restraining longitudinal movement was already proving severely taxing to the four people at the corners of the sheet, without adding further to their task.) The clearance was now reduced to 2 cm, and the current increased to 240 amps. Not until the weight of a third person was added did the sheet touch the stator surface, bringing the current to 250 amps.

Now the whole attempt at human levitation may seem a somewhat flippant exercise, and indeed as such it was regarded by all concerned when it was begun. However as has often happened before, an original "try if out of curiosity to see whether it can be done" approach led to demonstrations and further researches of considerable value. Indeed demonstration of the support of two people itself became a valuable display of the magnitude of forces capable of production by an electromagnetic system. Large forces tangential to the interface between rotor and stator are commonplace, since it is upon these that almost every electric rotating machine depends, but large forces normal to the surfaces are a phenomenon unlikely to be encountered by most people. There are few better ways to be convinced of their reality than to be sitting on top of an aluminium sheet

supported entirely on an electromagnetic field (although possibly equally convincing is the violence with which the sheet hits the stator after dropping through the last 2 cm upon interruption of the electricity supply!).

7.5 Levitators turned "the right way up"

Of a more serious nature, however, were the ensuing experiments to find out how nearly the same linear motor could approach the objective of lifting its own weight. Behind these attempts was a desire to demonstrate a principle vital to the operation of an electromagnetic river in the form of a high-speed ground transport system. It will be recalled that all the levitation machines described so far have had as their stationary member the heavy stator, comprising quantities of copper and steel, and as their floating member a light sheet of aluminium, albeit sometimes with extra loads added. Such an arrangement on a full-scale transport system would be costly in the extreme, and would involve in addition severe problems of activation of successive sections of track on the approach of each vehicle - activation, moreover, capable of producing acceleration or deceleration of the vehicle according to conditions at the time.

The only realistic approach at full-scale is to invert the system. The secondary member then becomes an extensive length of aluminium sheet while the expensive primary windings are confined to the underside of the vehicle, and can be controlled directly from inside. Indeed it would be preferable to regard this arrangement as the "normal" configuration (as has been tacitly assumed in most of the discussion of Chapter 6, in particular the diagrams of Figs 49, 50 and 53). It follows that all the laboratory models have been built to operate "upside down".

There are good technical reasons why this inversion is necessary in a laboratory. A small electromagnetic machine, such as one the size of most of the laboratory models, is not capable of lifting its own weight, the fundamental reason for this being once again simply

a question of scale.⁽¹⁸⁾ Even the most sophisticated design techniques cannot alter the basic problem, which is that all the dimensions are too small. The only solution within the confines of a laboratory is to build the machine upside down, so that only a light rotor has to be lifted.

Once outside the laboratory, however, machines can be made bigger and therefore better. To double every dimension of a given machine is to increase its mass by eight times, but the normal force between the rotor and stator increases by a factor of sixteen times for the same stator current density. There is therefore a critical size at which the normal force becomes equal to the weight of the stator, and machines larger than this can be built the "right way up" to support themselves and a payload in addition. It remains only to determine the value of this critical size.

Now when the AEI machine was floating two people at a height of 2 cm, the total weight supported was that of two substantial adults plus the large sheet of aluminium, and a considerable portion of the weight of a third person was needed to reduce the clearance to zero. A reasonable estimate of the normal force at a small clearance might therefore be about 200 kgf - this at an input current of 250 amps. These figures suggested that it might be possible to pass sufficient current to increase this force to 400 kgf, equal to the weight of the stator, and thus to succeed in making the motor lift itself.

The necessary electricity supply was obtained by making use of a 200-amp voltage regulator connected back-to-front to create a supply voltage greater than the 415 V three-phase supply, and by connecting in parallel with the linear motor as many large capacitors as could be found within the laboratory in order to raise the overall power factor of the system. With this arrangement, shown in Fig 65, it was found possible to supply over 300 amps to the stator without exceeding the 200-amp limit of the laboratory supply and of the regulator.

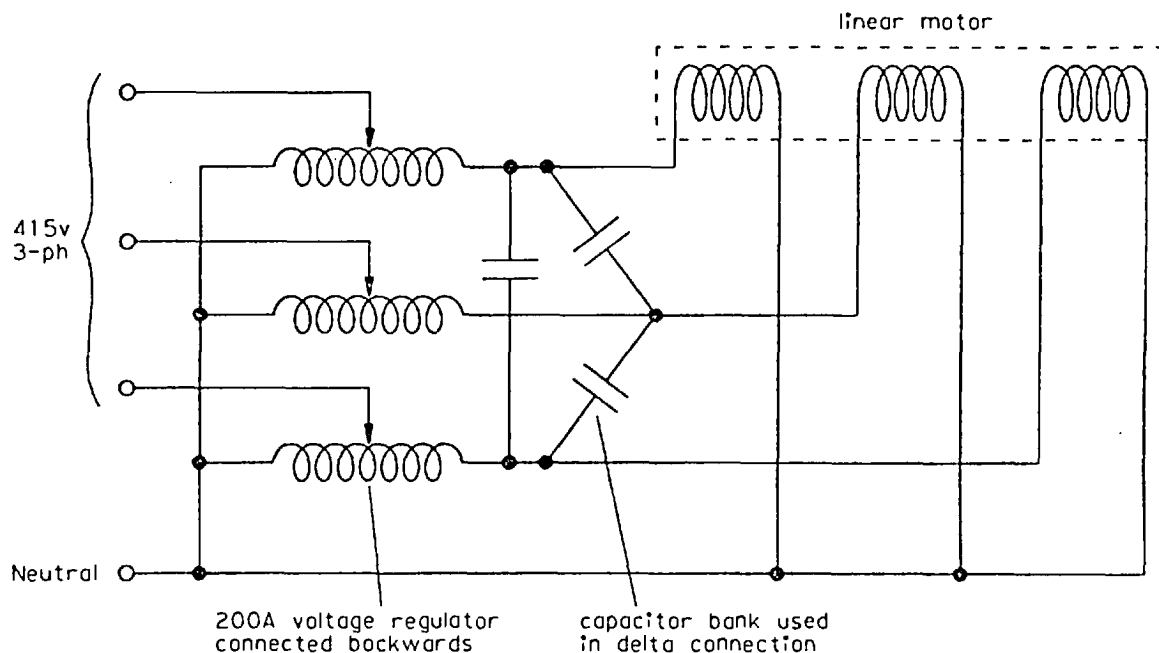


Fig 65. Supply to linear motor.

The mechanics of the experiment were simple. The motor was rolled over to direct its active surface downwards, then supported from an overhead crane. Several aluminium sheets were placed on top of one another to form a thick secondary member; these were stacked on the floor while the motor was hoisted to a position directly over but well above them. The current was switched on and the machine lowered towards the sheets, while several people restrained the motor against the effects of its own powerful longitudinal thrust. After several attempts at increasing currents (with long cooling periods between each attempt), the motor proved just able to support its own weight at an input current of 320 amps. Such a current could of course be sustained for only a few seconds by a winding with an 80 amp rating, but a single success was sufficient for the purpose. (It was thought wise to restrict the number of performances to only one!)

The critical size can now be calculated at which that particular design of motor could support itself indefinitely - i.e. at its continuous rating of current density. The continuously rated current

of 80 amps is one quarter of that needed for the motor to lift itself, and on the assumption that the normal force is proportional to the square of primary current, the force available at continuous rating is thus one sixteenth of that necessary. To double every dimension while keeping the current density constant is to double this ratio, as explained earlier in this section, from which it follows that in order to produce a continuously-rated machine all dimensions must be increased by 16 times. In practice to build such a motor would be idiotic, since the multiplication factor of sixteen would result in an iron core 2.1 m wide by 1.9 m deep, a pole-pitch of over 7.5 metres, and a total weight greater than 100 tonnes. Nevertheless it can confidently be predicted that were such a machine to be built it would be capable of supporting its own weight indefinitely without overheating, and would require a current input of about 20 kA to do so!

Further experiments of this kind, carried out on stators of transverse-flux design, have indicated that the critical size for a C-core electromagnetic river to lift itself is in the range 40 to 50 cm for the width of the iron core. Above this range such machines should be capable of supporting themselves and a payload in addition, providing both propulsion and stability over a track consisting of no more than a long sheet of aluminium, almost certainly backed by steel. (At this point, perhaps, the term "electromagnetic river" becomes something of a misnomer, unless the "river" is now presumed to be held into its inverted trough by a form of anti-gravity!)

7.6 The Electromagnetic Track Joint

Having established that a practical system would employ a track involving extensive lengths of aluminium, it might be worthwhile to mention one line of research upon which work is still in progress. This concerns the problem of track joints. Mention was made in Chapter 6 of the detrimental effect of a track joint - that a moving primary passing over a joint in the secondary aluminium experiences

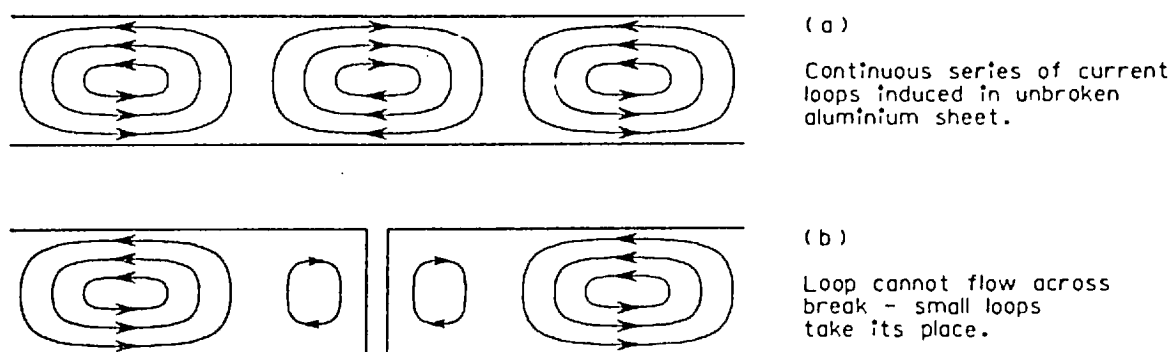


Fig 66. Effect of track joint upon secondary induced currents.

a serious transient loss of propulsion. The reason for this loss should be readily apparent upon reference to Fig 66, which shows the instantaneous current patterns induced by a conventional linear induction motor stator, (a) in a continuous sheet of secondary, and (b) across a secondary joint. In the latter case the usual large loop of secondary current is prevented from flowing, and all that remain are the two small loops shown. To the primary coils that happen to be over the joint at that instant it appears that their magnetic circuit has a much lower impedance than normal, and they therefore draw less current than their neighbouring coils. (A reduction of magnetic impedance implies an increase in the impedance of the corresponding primary electric circuit.)

At first sight it may appear that the reduction in current, and the consequent reduction in thrust, should be confined only to those coils in the immediate vicinity of the joint. However in practice linear motors nowadays invariably have their electrical connections such that within each phase all the coils along the whole length of the machine are in series. (There are good technical reasons why parallel-connected linear motors are undesirable⁽³⁰⁾.) Thus a high electrical impedance of one coil reduces the current in all the coils in that phase, and the performance of the whole motor suffers as a result. The drop in input current is so great that its effect has been used in the past as a convenient means for measuring the velocity

and acceleration of a moving stator over a regularly jointed track. A pen or ultra-violet recorder trace of the input current waveform shows an obvious transient whenever a joint is passed, from which it is a simple matter to measure the time interval between successive joints.

The effects of such a joint become even less desirable when an electromagnetic river stator replaces the conventional linear motor as the moving primary, for now each joint crossed involves the transient loss of lift and guidance as well as propulsion. It therefore becomes even more important that a way should be found to eliminate these effects before attempting a full-scale transport system.

It is not necessary to describe in detail the various suggestions and proposals that have been put forward in answer to the problem, since all are variations upon the same theme - to use flow paths in the third dimension to complete the truncated current loops on either side of the joint. In the end the simplest design emerged as the most effective. The invention as finally patented⁽²⁷⁾ is illustrated in Fig 67, and involves merely the bending of the whole width of the aluminium sheet through a right-angle to extend vertically downwards. Any backing steel below the aluminium is similarly bent and continued downwards, so that when this operation has been performed for both halves of the track the resulting vertical section comprises two sheets of aluminium facing each other, each backed by steel.

The current flow paths in the vertical aluminium sections are approximately as shown in the lower part of Fig 67, the essential feature to note being that the two vertical loops carry currents in opposing directions. The pattern shown is for a conventional longitudinal-flux linear motor; under an electromagnetic river stator the characteristic double-loop pattern would flow in both the horizontal and the vertical aluminium portions. The electromagnetic action, however, is the same. It will be realised that these components, two sets of currents flowing in opposing directions,

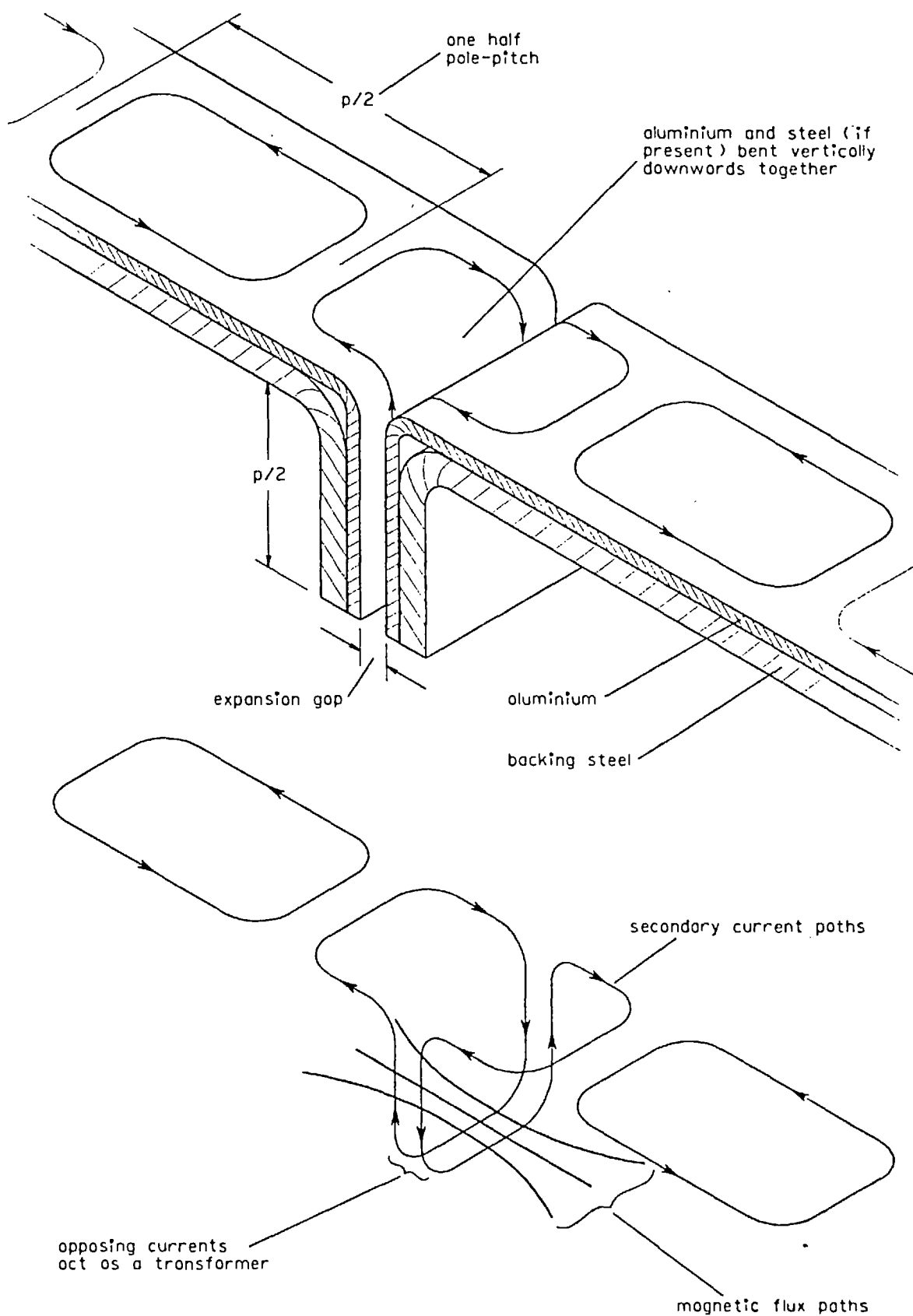


Fig 67. The electromagnetic joint.

surrounded by steel, are exactly those of which a transformer is composed. In fact the whole vertical portion of the electromagnetic joint is in essence a simple transformer of 1:1 turns ratio, and although the magnetic circuit has part of its route as paths in air, these paths are of large area and small length and consequently present only a small magnetic reluctance to the flux. The transformer can therefore possess a high goodness factor, and should be easily capable of obtaining an efficiency of well over ninety per cent. The joint, though mechanically discontinuous (with an air gap of possibly several centimetres) appears electrically almost continuous, presenting a secondary electrical impedance only fractionally greater than that of unbroken aluminium.

Laboratory tests undertaken to confirm these theoretical predictions have not yet been completed, so no numerical data can be presented as yet. However already the "feel" of the AEI linear motor stator suspended over an electromagnetic joint of appropriate dimensions (30 cm width of aluminium 6 mm thick, with a vertical portion 30 cm in depth, all backed by laminated steel) has given encouraging indications of the validity of the argument when compared to the "feel" of the same motor over an ordinary joint. In addition results obtained by British Rail from large scale dynamic tests have confirmed that the transient losses of input current that are so noticeable upon passage over simple joints become scarcely detectable when passing over a series of electromagnetic joints.

Little more can be said at this stage. The invention is here presented simply as another line of work in progress on the practical aspects of the use of full-scale electromagnetic rivers, and as yet another example of the way in which three-dimensional electromagnetism can achieve objectives impossible when the number of dimensions is restricted to only two.

7.7 Electromagnetic Scale Modelling

There is one further major line of research at present in progress regarding increases of scale. This involves the use of high frequency stator currents to simulate the behaviour of large machines, and is but one example of the application of a powerful research tool that, while not new in itself, has been applied only recently to linear motors. "Electromagnetic scale modelling" is the name normally given to the technique, which depends on the concept of the goodness factor for a machine in exactly the same way as scale modelling methods in the subjects of aerodynamics and fluid flow depend on the dimensionless quantity known as "Reynolds number". The basis of the approach is that any two electromagnetic machines of the same kind and having the same value of goodness factor are electromagnetically equivalent, even though they may be of radically different physical size.

It will be recalled from section 4 of Chapter 2 that the mathematical expression for goodness factor is:

$$G = \omega \sigma \mu \cdot \frac{A_e A_m}{l_e l_m}$$

where G = goodness factor,

ω = frequency of supply,

σ = conductivity of electric circuit,

μ = permeability of magnetic circuit,

A_e, A_m, l_e, l_m = areas and lengths of electric and magnetic circuits.

Now it is clear from the above expression that if two machines are constructed to be similar in every way except that one has all its dimensions a factor of N times smaller than those of the other, then the two machines will not be electromagnetically equivalent since the goodness factor of the smaller machine will have been reduced by a factor of N^2 with respect to the larger. However, equivalence can be restored by appropriate increases in one or more of the remaining quantities ω, σ or μ .

The technique of scale modelling by frequency control involves changes only in the first of these three parameters, the other two remaining constant, and as such the method represents only one of several aspects of electromagnetic scale modelling. It is, however, by far the simplest means of compensation, for materials of conductivity and permeability better than copper and steel are not readily available. (Effective increases in these quantities can be obtained by other means, however - see references 31 and 32 for a more detailed treatment of the whole subject of scale modelling.)

The use of frequency control involves an increase in frequency by a factor N^2 to compensate for a decrease in linear dimensions by a factor N .^{*} It is for this reason that scale modelling has not been used extensively in the world of rotating machines, for this frequency rise dictates a corresponding increase, also by a factor N^2 , in the rotational speed of the machine. In spite of the N -fold reduction in size this still leads to increased centrifugal stresses which rapidly become too great for normal engineering materials. In linear work, however, it is the linear synchronous velocity that rises, which need not present problems.

It has justifiably been assumed from the beginning that in any practical situation a scaled-down model operating at high frequency would be used to simulate the behaviour of a large machine at mains

* An alternative outlook on the whole method is to examine the variations with frequency of the "skin depth" of the rotor material, i.e. the depth of penetration of the magnetic field into a solid block of secondary material. An essential requirement for electromagnetic equivalence between two machines is that the skin depth should bear the same ratio to the total depth (or thickness) of the rotor in both cases. It too must therefore be made to decrease by the linear factor N .

Now the standard formula for the skin depth δ of a magnetic field of frequency ω in a medium of conductivity σ and permeability μ is:

$$\delta = \sqrt{\frac{2}{\omega \sigma \mu}}$$

and once again, if σ and μ are not to change, then ω must increase as N^2 in order that δ decreases as N .

frequency rather than the other way about. It happened that the only variable frequency supply with a useful current and power output available in the laboratory was a motor-generator set having an output frequency range of 25 Hz to 250 Hz. On the assumption that a large-scale machine would never be operated at a frequency of less than 50 Hz, this limited the scaling factor N to a value of about 2.2 (i.e. $\sqrt{250/50}$). Nevertheless such a small factor is by no means useless, and in fact most of the high-frequency testing was done at a frequency of 200 rather than 250 Hz, so that the simulation was of a machine exactly twice as big.

Work done by others in the laboratory has now taken this "times two" scaling factor one stage further, to give the method a firm practical foundation of experimental fact. For this work a machine was constructed to be as nearly as possible a direct scale-up of the phase-mixed electromagnetic river. The mechanical lengths, i.e. all the dimensions of the iron C-cores and the spacings between them, were doubled, to make a machine of core width 20 cm and pole-pitch 60 cm (but of overall length limited to only two pole-pitches, as was the original phase-mixed levitator described at the beginning of Chapter 5). The winding configuration was not scaled in so precise a manner, since to have done so would have resulted in a machine having inconvenient current and voltage ratings. Instead changes were made of a simple nature, such as varying the proportions of the number of individual strands of wire connected in parallel within each coil to the number of turns around the coil made by each set of strands - changes for which appropriate allowances could easily be made.

With such a machine set beside its half-scale model (the electromagnetic river of Fig 44) the test procedure becomes obvious. Theory predicts that the large machine operating at 50 Hz can be simulated by the small machine operating at 200 Hz, and this prediction can now be confirmed or otherwise by direct experiment. In fact equivalence of behaviour in the vertical and longitudinal directions (i.e. in lift and in thrust) has already been established by

corresponding experiments on conventional linear induction motors; the new part of the experiment is to determine whether the simulation extends into the third dimension, that of horizontal lateral stability.

On the assumption that validity in the third dimension is established (work is still in progress)*, the testing can then be continued on the large machine at 200 Hz, to predict the behaviour of a 40 cm wide machine of 1.2 m pole-pitch - predictions which can be made with a degree of confidence never achievable by methods based on theory alone. It will be appreciated that at a width of 40 cm the motor is approaching a size which might be appropriate to a small vehicle, and that only one further doubling, or a frequency source of 800 Hz, might be sufficient to achieve direct simulation of such a machine.

7.8 Tests at high frequency

To return to the 10 cm scale of the original electromagnetic river, one of the most revealing experiments to be carried out to date has been one making use of a supply neither at a constant 50 Hz nor at 200 Hz, but at a steadily increasing frequency. Now a low power factor machine such as an electromagnetic river stator has an input impedance that rises almost linearly with frequency. So also does the output voltage of a generator with a fixed field supply. The current drawn when these two machines are connected together is therefore almost frequency-independent. By the simple action of steadily increasing the speed of the driving motor coupled to the generator, the supply frequency to the electromagnetic river is made to rise while the stator current remains constant, and the behaviour is thus made to change in the same way as it would if it were possible to expand every dimension of the machine slowly and steadily while keeping the current density and frequency constant. Through the eyes of the electrical engineer the machine is observed to "grow".

* - recently completed, see reference 37.

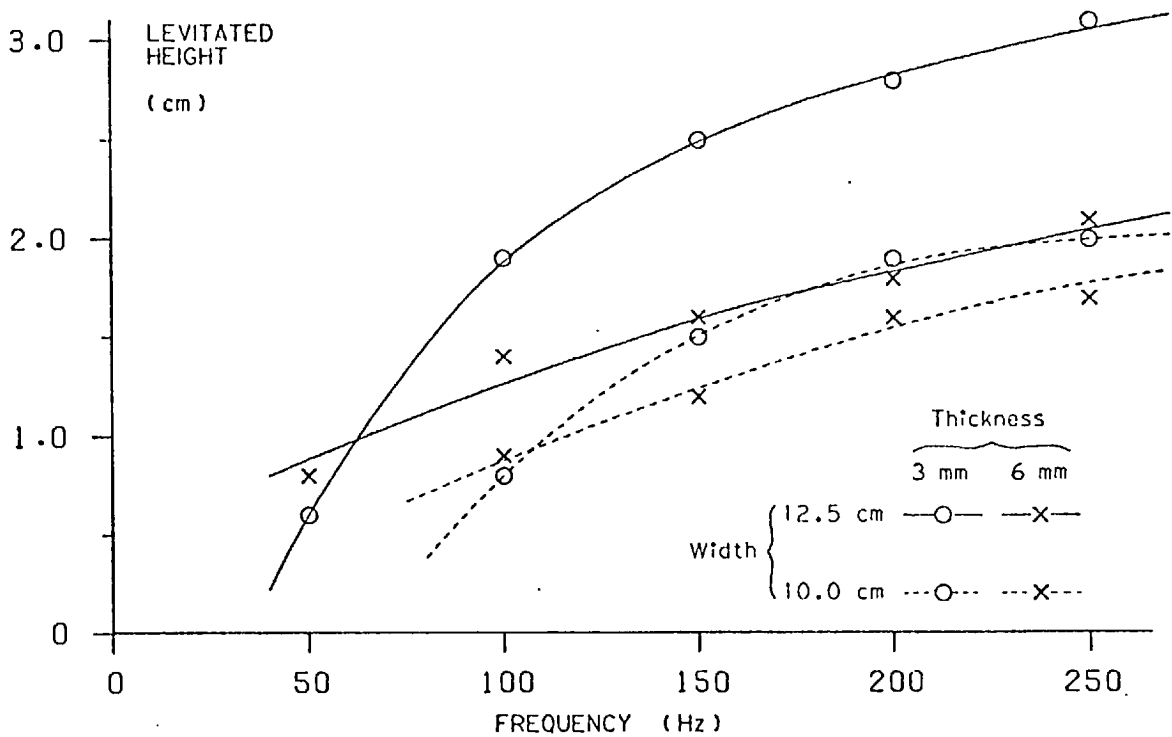


Fig 68. Variation of levitated height with supply frequency for four free plates over the electromagnetic river.

When this is done in practice the most obvious change in behaviour is the large increase in the levitated height of a free plate as the frequency rises. Fig 68 shows examples of this variation for four plates. It will be noticed that each curve appears to be tending towards an asymptotic value defining a maximum height obtainable at any frequency for each particular plate - in fact the two 3 mm plates almost reach their limiting values within the frequency range available.

This effect is related to the frequency dependence of the skin depth in the rotor. Initially as the frequency increases the overall goodness factor increases in proportion, so that the rotor finds that it can support itself at greater clearances from the stator. However at the same time the skin depth in the rotor material decreases (with the square-root of frequency) until eventually its value becomes equal to the thickness of the aluminium plate. Beyond this point the magnetic field can no longer penetrate throughout the thickness of

rotor so that as the frequency continues to rise the proportion of "active" rotor shrinks, while the remainder becomes a steadily growing "dead weight". The plate is thus prevented from rising further.

The technique becomes more useful when measurements are taken of the variations of thrust and of lift force with frequency while the rotor is constrained at a fixed clearance from the stator. Under these conditions the simulation is of a single machine increasing in size rather than of a series of machines of changing airgap. The experimental technique employed for measurements of this kind was to place the rotor upon paxolin spacer blocks at the required height, and then to raise the stator current slowly until the plate just floated clear of the blocks. At this point the lift force was of course exactly equal to the weight of the plate and the thrust could easily be measured with a spring balance. Both these quantities were then scaled up to a convenient reference value of stator current using the relation:

$$\text{Electromagnetic force} \propto \{\text{current}\}^2$$

- a relation long

established as valid, in the absence of iron saturation, for forces in any direction - longitudinal, lateral or vertical.

Fig 69 presents a sample of the results, taken for two sheets, each just lifting clear of the stator. The curves showing variations of lift are of the same basic shape as those of Fig 68, i.e. an initial rise in magnitude with frequency but soon tailing off to allow the curve to become asymptotic to a particular maximum value of lift, and the reasons for this are the same as before. The curves for thrust might at first sight appear contrary to expectations, since they fall with increasing frequency. However reflection upon the way in which the force / speed curve of an induction drive varies with increasing goodness factor reveals that the standstill thrust, i.e. that for which slip = 1, must fall as the position of peak thrust moves beyond standstill towards lower values of slip.

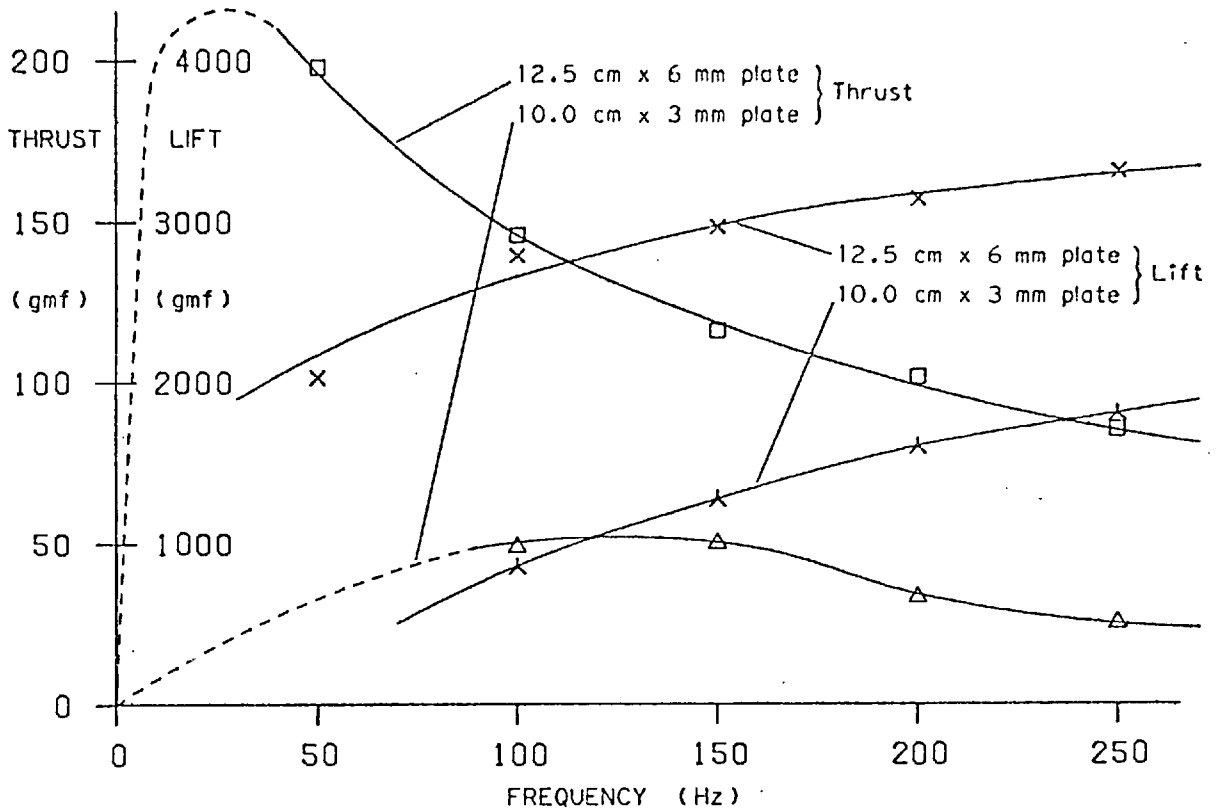


Fig 69. Variation of thrust and lift with frequency for rotors at constant height.

Some examples of this effect as they might apply to the electromagnetic river are shown in Fig 70. The back-to-back oscillating experiments described in Chapter 5 (section 4) suggested that at 50 Hz the machine had a goodness factor near to unity; thus it might possess a force / speed characteristic of the general form of the curve marked "G = 1" in Fig 70. At 100 Hz its goodness factor will have been doubled to form a curve such as that marked "G = 2", which has had its position of peak force shifted along the speed axis, resulting in a reduction in value of the standstill force. At 200 Hz, Goodness = 4, resulting in a curve with its peak further shifted and its standstill force further reduced.

But all this is standard theory which can be derived analytically from the force equations of a linear induction motor. (The mathematical formulae that result are that the peak value of force

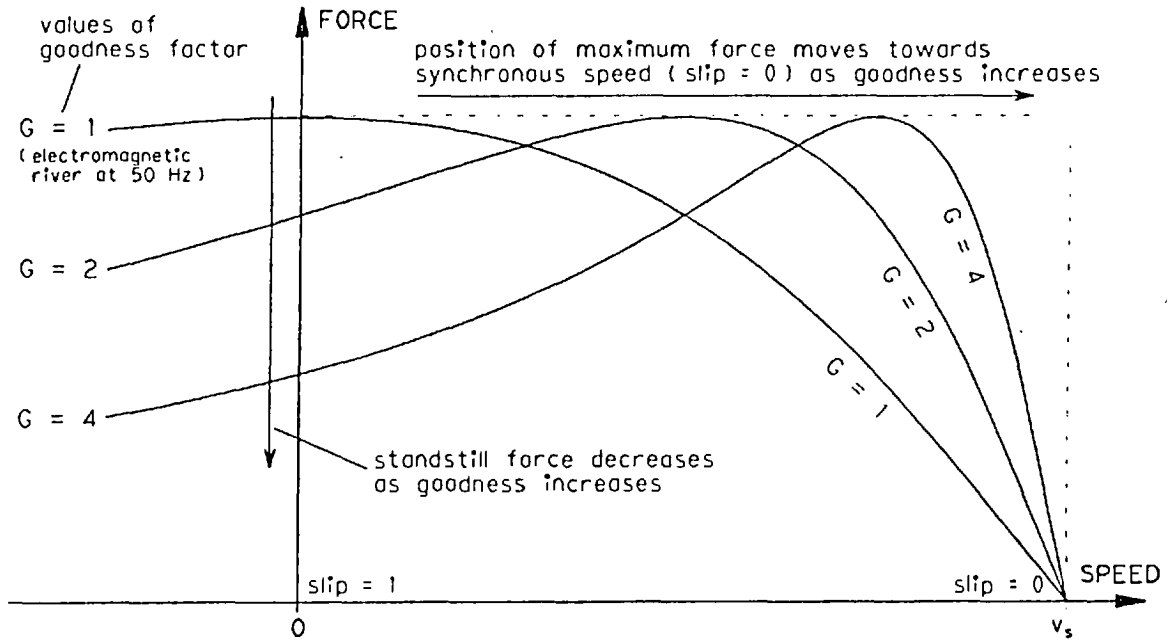


Fig 70. Effect of goodness factor upon shape of force/speed curves.

occurs at a speed v given by:

$$v = \left\{ 1 - \frac{1}{G} \right\} \cdot v_s \quad \text{where } G = \text{goodness factor,}$$

$$v_s = \text{synchronous speed,}$$

and that the standstill force f_0 is given by:

$$f_0 = \left\{ \frac{2G}{1 + G^2} \right\} \cdot f_p \quad \text{where } f_p = \text{peak force obtainable.})$$

The important point to note is that the behaviour of the lift and thrust forces of the electromagnetic river caused by changes in supply frequency are readily explainable by the theories established for conventional linear motors.

As further experimental evidence for the similarity between the lift and thrust mechanisms of the electromagnetic river and those of conventional linear induction motors, it is interesting to compare the curves of Fig 69 with those of Fig 71. The latter figure shows samples of results taken from tests on one of the large AEI conventional longitudinal-flux linear motors - this time the one of

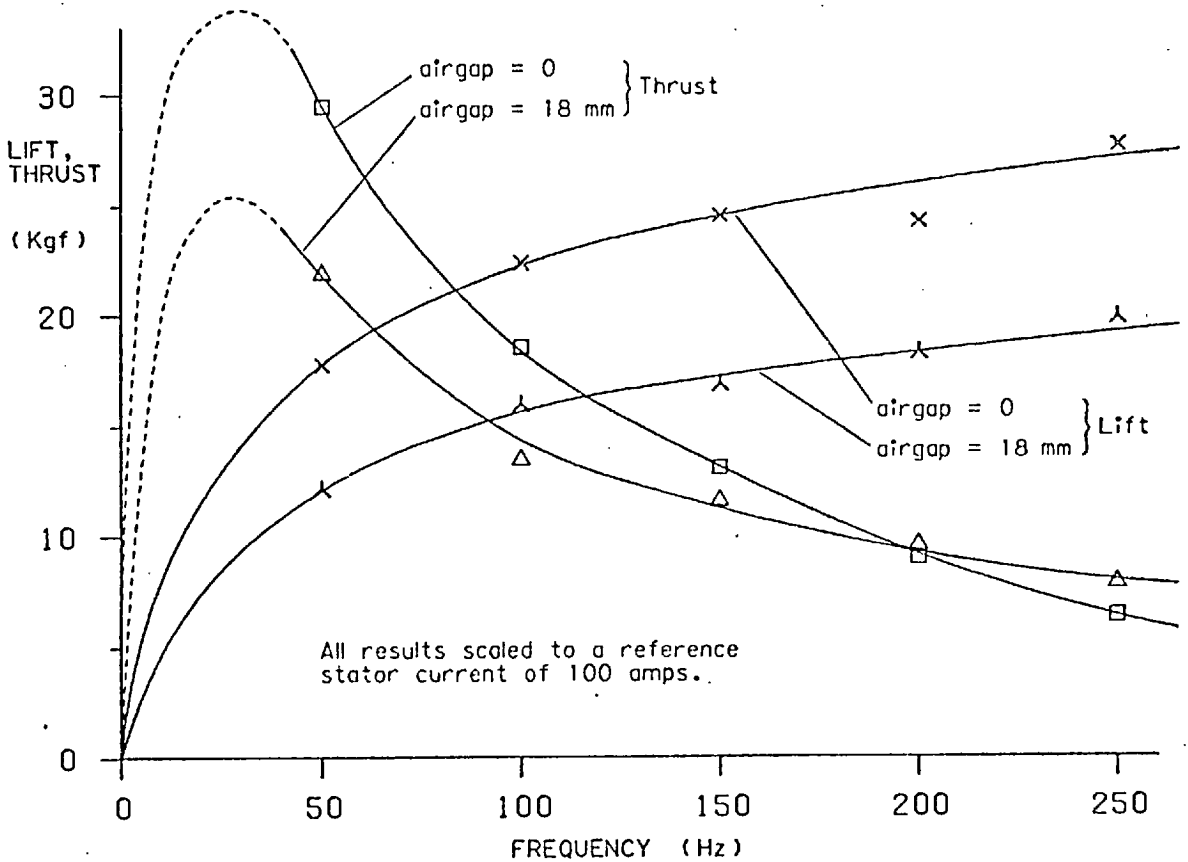


Fig 71. Dependence of lift and thrust upon frequency
- results taken for conventional linear motor.

smaller (24 cm) pole-pitch, the twin of that used for the human levitation experiments described earlier in this chapter. Again the lift and thrust measurements were obtained by adjusting the current just to lift the secondary sheet, and then scaling the results for a reference current of, in this case, 100 amps. The similarity between the sets of curves from the two machines is obvious, though the conventional machine has a goodness factor considerably greater than unity even at 50 Hz so that its thrust curves have not reached their peak at this point.

Upon this basis of similarity under conditions of variable frequency, then, was the assertion made in Chapter 6 (section 3) that the variations of rotor thrust and lift with changing rotor speed would follow the same pattern over an electromagnetic river

stator as they do over a conventional linear motor. From the viewpoint of the secondary any relative velocity between the rotor and the stator results in a change in frequency of the rotor currents which is in any case indistinguishable from a change caused by a variable input frequency. The assertion still needs experimental testing, but such tests can be treated merely as confirmations to be carried out at any convenient time when suitable equipment becomes available.

7.9 Tests on load-bearing rotors

The subject of frequency simulation of large machines will be returned to in Chapter 11, when similar tests carried out on a new machine will be described. Meanwhile two further short series of tests on the long electromagnetic river remain to be discussed. Both these sets of measurements were intended to give no more than a "feel" for the phenomena involved; neither was carried out with the care or detail appropriate to a complete investigation.

The first series was concerned with the effects upon the lift, thrust and guidance forces acting on a floating plate of the addition of extra static "dead weight" to be supported by the plate. In practice these extra weights took the form of a set of standard brass reference masses each of 200 gm weight, which were added one by one to the aluminium plate and secured by small blobs of plasticine.

Two plates were selected for testing that were known to maintain their stability over a considerable range of conditions. One of these was 10 cm wide and the other 12.5 cm; both were 50 cm long and 6 mm thick. During the experiments the whole length of the electromagnetic river was energised, thereby effectively ensuring constant current conditions without the need for continuous monitoring of input current (since the movements of half a metre of thin secondary are unlikely to have a great effect on a 7 m length of series-connected primary). The overall current was set at about half its normal maximum value in order to allow plenty of time for measurements to be carried out

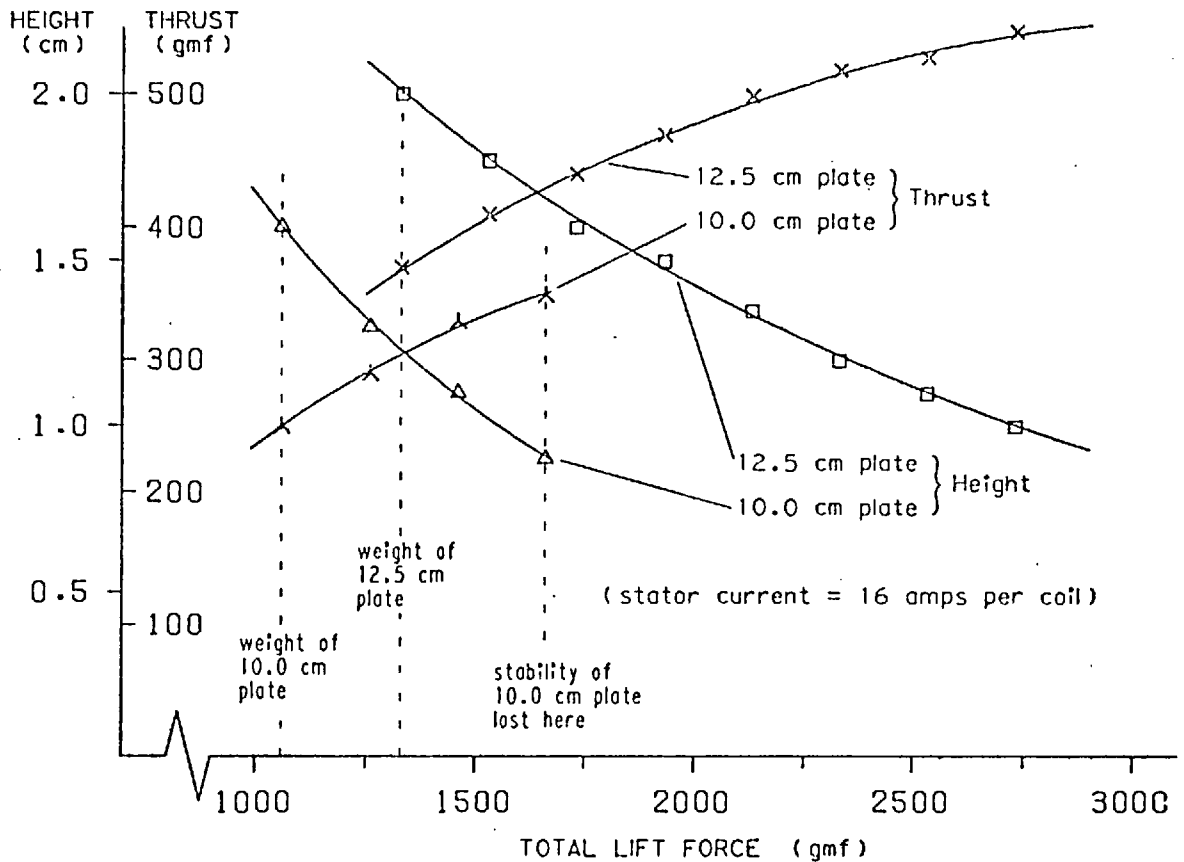


Fig 72. Effect of additional dead weight upon height and thrust of floating plate.

before the stator heated sufficiently for the effects of temperature to become significant. A series of measurements was taken of the free height of flotation of plates under various load conditions, and of the longitudinal thrust corresponding to each load.

The results are shown in Fig 72. The decrease in height with increase in load is entirely to be expected; it is interesting however that at this particular value of stator current the narrower plate can support only about one and a half times its own weight before losing stability, while the wider plate is capable of supporting more than double its own weight while remaining stable. An increase of primary current would of course increase the stability of both plates somewhat (as described in Chapter 2 - Fig 18). The steady increase in thrust with load is again to a large extent as would be expected, but is also interesting in that its rate of rise is

comparatively gentle. Here is experimental confirmation of the "feel" of the aluminium tray over the double-stator machine described earlier in this chapter (section 1), where it was noted that the longitudinal thrust did not appear to rise greatly as the tray was loaded. Corresponding measurements of thrust on a rotor that is steadily being forced down into the field of a conventional longitudinal-flux linear motor would show a much faster rate of rise.

An additional set of measurements was taken, this time concerning the lateral stabilising forces acting upon loaded plates. Under each condition of load, the plate was pulled slowly and steadily sideways by means of threads attached to a spring balance, so that readings could be taken of the variations of restoring force with lateral displacement. These readings were continued to the point of maximum restoring force. Beyond this point there exists a region of stability within which the restoring force decreases with increasing displacement; the nature of a spring balance prevents readings being taken in this region, but by replacing the spring balance with an inextensible thread the point could be found at which the restoring force once again reached zero - i.e. the displacement was measured for the condition in which the plate was just about to fall out of the machine.

Fig 73 displays the results of these tests, obtained from the same two plates and under similar load conditions as were the lift and thrust results of Fig 72. Once again the overall shapes of the graphs are roughly as could be predicted from earlier experiments. The narrower plate under all its load conditions experiences a greater initial rate of rise of restoring force with displacement, and achieves a higher maximum value of restoring force, than does the wider plate - this is further experimental confirmation of the "feel" mentioned in Chapters 1 and 2 that wide plates are generally "floppier" in their stability than narrow ones. The new point of interest to emerge from the graphs is that the lateral restoring forces show a significant increase as the plates are loaded - an

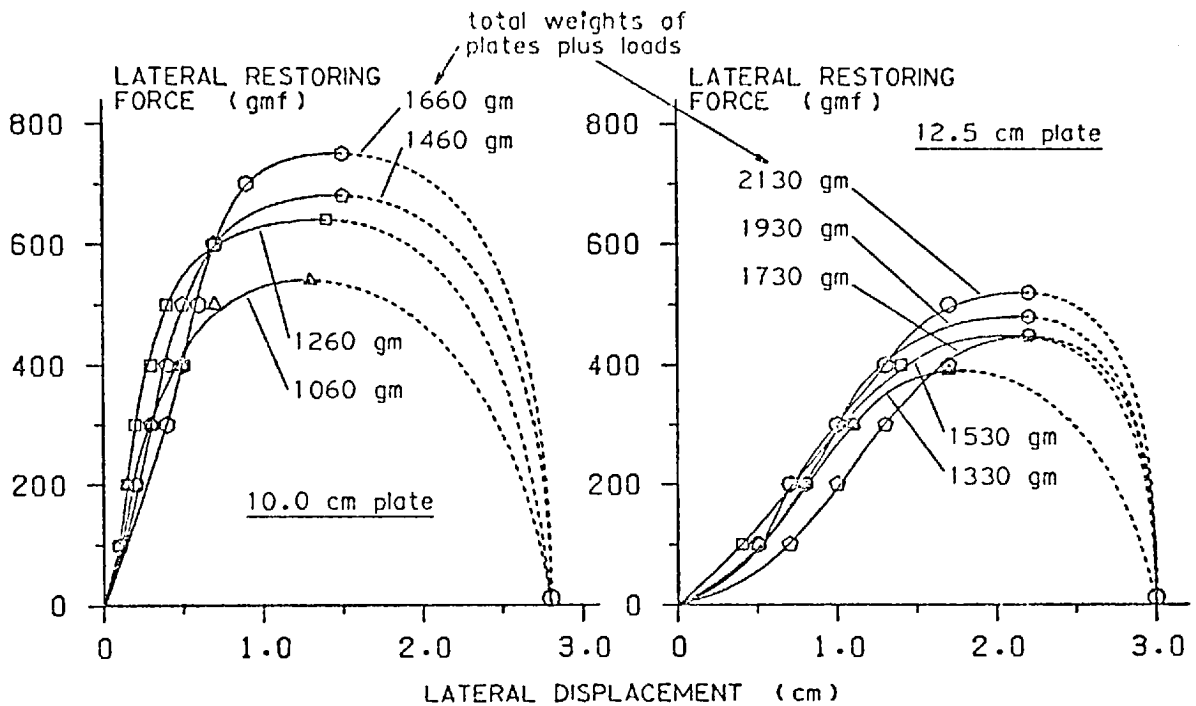


Fig 73. Variation of lateral restoring force with displacement for two plates, each carrying various loads in addition to their own weight, floating over an electromagnetic river.

encouraging aspect of behaviour from the point of view of the designer of a load-carrying vehicle. A second point, the significance of which has not yet been evaluated, is that the final maximum displacement before stability is lost appears to have the same value for all conditions of load.

7.10 Dynamic stability tests

The second short series of tests involving loaded plates upon the electromagnetic river was made in an effort to gain some idea of the behaviour of the stability forces under dynamic conditions. It will be appreciated that the provision of restoring forces under static conditions of displacement goes only part-way towards realisation of a system that will remain stable under conditions of real-life usage. Equally important is that any oscillations resulting from a transient disturbance of alignment must not be allowed to continue for much more than a couple of cycles but must be damped

down as rapidly as possible - ideally critically damped. Some simple observational experiments upon dynamic stability were described in section 2 of Chapter 5, where aluminium plates were sent along the whole length of the seven-metre electromagnetic river, which had had a deliberate misalignment introduced between the two parts of the river at their junction half-way along. The following experiments were an attempt to quantify these observations.

It was decided to treat separately the two modes of linear oscillation - vertical and lateral. Measurements of circular oscillations (movements in roll, pitch and yaw) were not attempted. After giving a loaded plate a disturbance in one of these linear dimensions two quantities were measured: firstly the frequency of the resulting oscillations (measured by timing ten or more complete cycles), and secondly the number of cycles completed before the oscillations reduced to the point of invisibility to the unaided human eye.

The results are displayed in Table 2. Tabular form was chosen for presentation because there did not seem sufficient regularity in the various measured quantities to construct a graphical presentation having much meaning. In fact it is difficult to see any significant pattern at all within the table, with the possible exception of the damping of vertical oscillations, where it appears that increased loads upon the aluminium plates tend to lead to better damping.

A couple of interesting aspects of the experiments do emerge however. One of the plates, the first in the table, was found to transform vertical oscillations rapidly into small horizontal movements which then took some time to decay. Violent horizontal oscillations also disappeared rapidly, leaving similar small-amplitude horizontal movements. By contrast neither of these effects was apparent with the second plate, only 2.5 cm wider than the first. The third plate, half the thickness of the first two, behaved differently again, having almost critical damping to

Plate	Load	Vertical oscillations		Lateral oscillations		Comments
		total weight (gm)	freq (Hz)	cycles to die out	freq (Hz)	
10 cm x 6 mm	1060	4.15	10	4.15	100 or more	Vertical motion quickly damped but transforms into horizontal. Violent horizontal motion quickly damped (2 or 3 only), leaving small amplitude, low damping movements.
	1260	4.1	10	4.0	50	
	1460	3.77	8	3.77	40	
	1660	3.22	2	3.22	undamped	
	>1660	unstable in roll				
12.5 cm x 6 mm	1330	3.8	40	1.96	10	No comparable separation of violent and small amplitudes.
	1730	3.8	30	1.92	undamped	
	2130	4.0	25	1.85	40	
	2530	4.16	20	1.67	20	
10 cm x 3 mm	540	4.5	3	4.5	1.0 (critical)	
	740	4.7	2	3.1	3	
	> 740	unstable in roll				

TABLE 2. Experiments in damping.

horizontal oscillations. Clearly here is a subject upon which much further work needs to be carried out, and it is evident that more sophisticated measuring techniques are necessary, possibly in the form of a test rig that can be used at least to impart closely controllable disturbances to the floating plate. The subject was pursued no further at the time.

7.11 Review of Chapter 7

Now this has been a long chapter covering many different aspects of experimental work relevant to the electromagnetic river. To summarise, the double-stator "catamaran" machine described in section 7.1 can be used to increase the ratio of lift force to thrust and to overcome the problems of poor stability in roll. It may be that an additional motor, possibly a conventional transverse-flux motor,

would then be mounted between the two electromagnetic rivers to form a complete support and propulsion system.

Two forms of simulation of large machines have been investigated - the first a mechanical system employing gramme-ring wound stator blocks whose coils could be connected in many combinations to simulate variations in the mechanical proportions of stator design (sections 7.2 and 7.3), and the second a method of simulation by scale modelling techniques using high-frequency power supplies to maintain electromagnetic equivalence (7.7 and 7.8). Static variable frequency tests have also been used to demonstrate the similarities between a conventional longitudinal-flux motor and an electromagnetic river with regard to their thrust-producing and lift-producing mechanisms. The tests provide support for the assumption that these similarities extend into conditions of relative velocity between rotor and stator. Work done by others has demonstrated that it is possible to maintain lift over a conventional linear motor at rotor velocities up to a few per cent of synchronism, and on the basis of extended similarity it is predicted that the same will apply to the electromagnetic river.

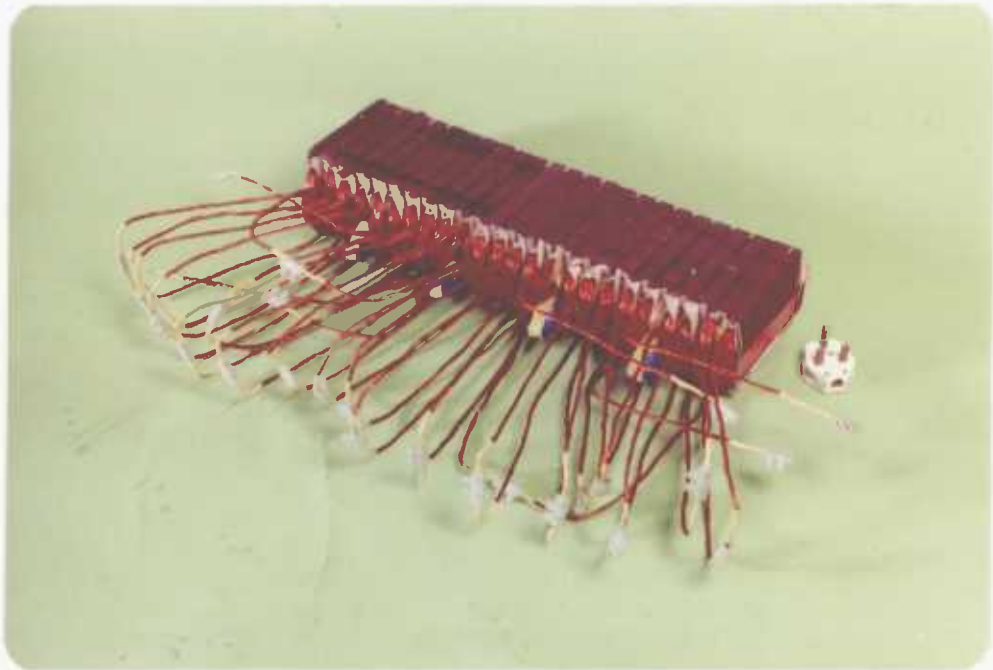
With a view to the "right way up" to build a system intended for transport, investigations have been carried out concerning the magnitude of the lift forces obtainable from various stators (7.4 and 7.5), the aim being to produce a machine capable of lifting its own weight in order that the primary itself can become the moving part. Following from this the stationary member must then comprise extensive lengths of conducting secondary, which immediately presents problems of track joints to allow for construction and expansion - hence the work being carried out on the "electromagnetic joint".

Finally a brief series of tests on loaded aluminium plates, measuring both their static and their dynamic behaviour, has been included (7.9 and 7.10). These proved to be of little value other

than to confirm the need for further work to be set in progress on the subject. This concludes the research work carried out upon the long electromagnetic river and the machines associated with it, except for one further new machine, which will form the subject of Chapter 11. Meanwhile the chapter immediately following is concerned with machines designed for a different and highly specialised purpose.

CHAPTER 8

THE LECTURE NOTE FLOATER



A gramme-ring wound linear motor block (pp 146 and 193).

CHAPTER 8. THE LECTURE NOTE FLOATER

In 1972 the desire of Tracked Hovercraft Ltd. to exhibit an all-electric levitated transport model at the Transpo '72 exhibition set in progress the work leading to the invention of the Washington model (see Chapter 1) and to the opening-up of the whole subject of electromagnetic rivers. In 1974 Professor Laithwaite similarly had in mind a new demonstration for one of his lectures. The work set in progress to design and build a machine to meet his requirements led to new ideas and discoveries going far beyond the original purpose. The lecture in question was due to be given at the Royal Institution, and it was given the deliberately provocative title "All Things are Possible". The main subject matter was concerned with experiments involving gyroscopes, but by way of introduction a couple of electromagnetic demonstrations were to be included - the first of these, to take place at the beginning of the lecture, being the one towards which the work described in this chapter was directed.

The lecture was planned to commence as follows. The Professor was to walk into the lecture theatre, carrying in his hand a wad of notes to which he was frequently to refer as he began. After a few sentences of introduction he was then forgetfully to release hold of the notes, continuing to speak apparently unaware that instead of falling to the lecture bench the notes were remaining hovering unsupported in mid-air! The mechanism of the demonstration was intended to be a straightforward adaptation of one of the laboratory levitators - within the bogus notes a hidden sheet of aluminium, later to be revealed to the audience, was to be levitated by an appropriate design of machine mounted directly under the bench surface. The whole concept may well appear to be an exercise in triviality, but once again a task originally thought to require little more than simple modifications to already existing machines (such as the "magic carpet" machine described in Chapter 2) instead developed into a research effort involving many different machines, and from which much valuable experience was gained.

8.1 An Annular Magic Carpet

Now the main requirements of the system were to levitate a suitably sized sheet of aluminium at as great a clearance as possible from the stator, horizontal, stable in all axes, and able to support a load of twenty or so sheets of notepaper as camouflage - all this to be achieved by a machine with stator windings of current rating sustainable for several minutes rather than only a few seconds. The principal problem quickly revealed itself as being again a question of scale. To levitate a large sheet of aluminium 20 cm above a series of modified gramme-ring wound linear motors was a relatively simple matter (see section 3 of Chapter 7), but to maintain similar clearances while scaling the floating sheet down to the size of an A4 sheet of notepaper proved altogether less easy.

The machine that seemed the most promising for development was in fact the original "magic carpet" machine of Chapter 2 (see Figs 13, 15 and 16). It will be recalled that in its final version each of the three sets of windings of this machine was formed of two coils side-by-side in a horizontal plane, mounted one upon each limb of a standard C-core pole piece, and electrically connected so that the current in each coil flowed in the same direction along the centre of the slot - see Fig 74(a). The three such sets of windings were aligned longitudinally in a straight line, forming a machine that was found capable of levitating and stabilising a 40 cm by 19 cm aluminium sheet at a height of 7 cm. However the lateral stability was very weak for this size of plate, narrower ones being better, and the longitudinal stability was never strong for any size of plate. It was decided therefore to investigate first of all a square shape of machine, in an attempt to produce two sets of "lateral" stabilising forces acting at right angles.

The magic carpet machine was accordingly dismantled and the cores re-arranged in the plan of Fig 74(b). Evidently the pattern as shown is not complete, but it was felt that the time and effort necessary to wind a fourth core was not really justified since an

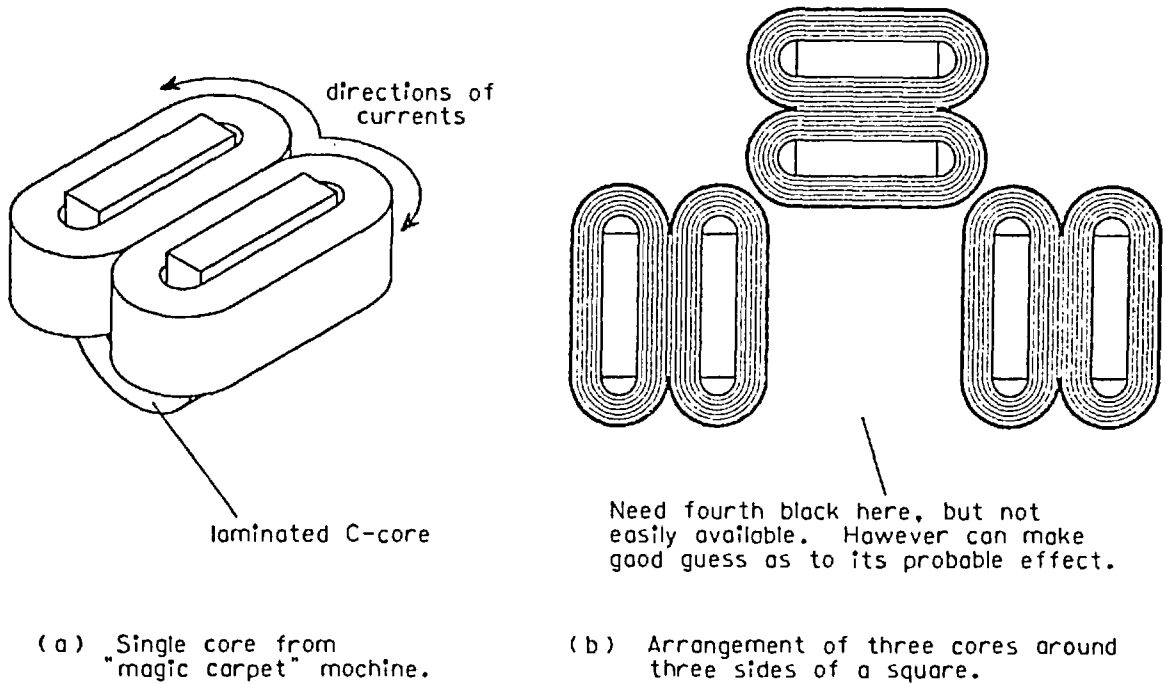


Fig 74. First attempt at lecture note floater.

experienced operator should be able to tell by the feel of a plate held over the machine what would be the effect of the missing core.

When tried the performance of the machine was disappointing. A square plate was able to float at only a small height, a maximum of 1 cm if the stator coils were not rapidly to overheat, and with only weak stability. However the impression was gained that the addition of the fourth coil would indeed provide stability in both axes.

A circular plate of diameter equal to the length of one side of the square plate behaved in almost exactly the same fashion. Since the absence of corners removed one degree of complication from the system, and also it would not matter for the demonstration if the lecture notes were gently to rotate in mid air rather than to keep to a definite alignment, the sequence of experiments was continued using circular plates - both annuli and solid discs.

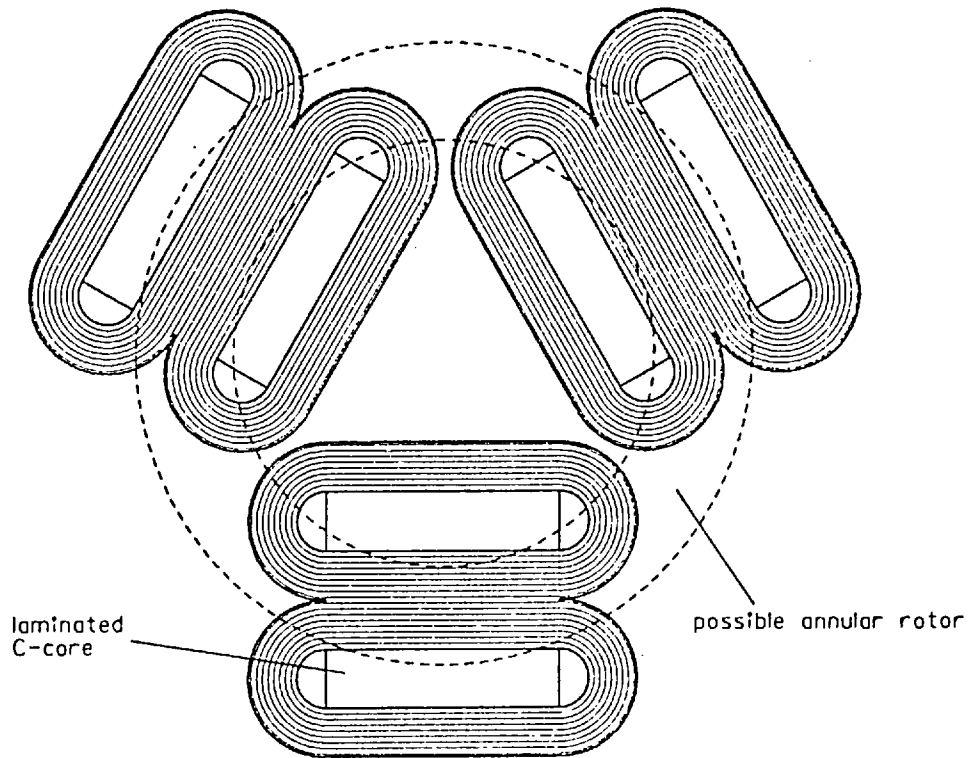


Fig 75. Triangular formation of stator blocks.

The next attempt was a triangular formation of the same stator blocks, as shown in Fig 75. It will be realised that such an arrangement is no more than a condensed version of one of the circular forms of the Washington model described in section 3 of Chapter 3 (see Fig 26). As such, therefore, it is necessary to arrange that either the rotor or the stator has "ends" introduced at some point so that the induced currents are not allowed to flow in a single circular path around the rotor but are forced instead to form the double-loop pattern necessary for stability.

It was soon discovered that to introduce these "ends" in the form of slits in an annular rotor, as was explained in Chapter 3, was to step backwards. A single slit represented gross asymmetry and caused severe loss of lift in the surrounding region, resulting in the plate sitting in a tilted position, while the symmetrical arrangement of three slits evenly spaced constricted the rotor current flow paths

to such an extent that the lift force was almost entirely destroyed. Provision of "ends" in the stator was scarcely any more successful, for now there is a fundamental problem of symmetry. If all three blocks are not to be connected sequentially in phase, and the use of currents obtained from different lines of a three-phase supply is also forbidden (to avoid rotational drive), then the only remaining possibility is to connect two of the coils in phase and the third in anti-phase to them both. Again the configuration forms an asymmetric system, and again the result is a plate that floats severely tilted, in practice receiving most of its lift on the side above the two in-phase coils. Nevertheless even in this unbalanced condition it could be clearly felt that stability forces in all dimensions were present.

8.2 A square levitator

At this point the main difficulty appeared to be to obtain sufficient lift whilst maintaining stability, and it was felt that perhaps a different design of iron core might lead to machines of greater lift capacity. There were at that time in the laboratory several laminated steel cores of "E-core" design, as shown in Fig 76(a), and it was decided to investigate the effect of their rather different geometrical proportions.

Two electric coils were wound per core, each with as many turns as could be fitted into the available slot, and each connected so that the directions of current flow were as shown in Fig 76(b). It will be realised that this pattern of currents induces two magnetic poles of opposite polarity on the outer two limbs of the E-core, while the centre limb is magnetically dead, i.e. the effective shape of the iron is a C-core. The intention was that if such an arrangement proved successful then further improvement could be effected by cutting away the centre limb altogether and increasing the number of turns on each coil to fill the extra space thus obtained.

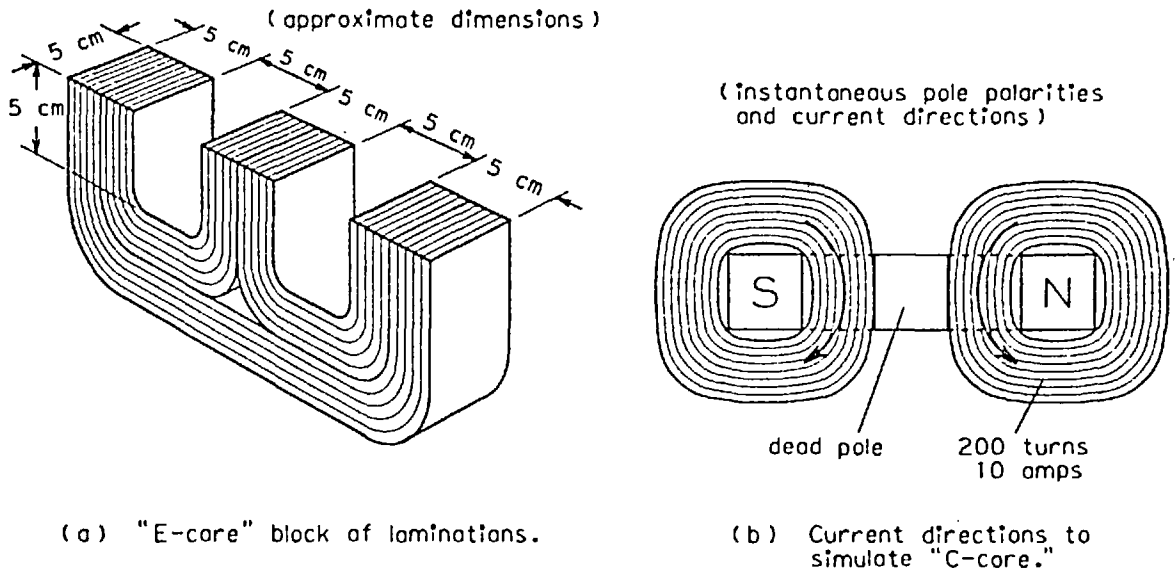


Fig 76. Use of "E-core" laminations to form wide "C-core".

Experiments were carried out first of all using one core only, over which was placed an annulus of aluminium, of mean diameter equal to the distance between the centres of the two outer limbs of the core. Naturally such a system could provide stabilising forces only in one direction - parallel to the straight line containing the centres of the three limbs - but once again the first priority was merely to obtain a "feel" for the stability of the system rather than to attempt a complete system all at once.

The first such annulus to be tried had an inner diameter of 18 cm and an outer diameter of 22 cm. The stability force experienced by this was found to be enormous. In fact with the rated ten amps of current flowing in the stator coils a lateral force of several kilograms was needed before the annulus could be entirely removed sideways from the machine. However when in its equilibrium position this rotor experienced a lift of almost zero, although the interesting point did emerge that upon displacement of the rotor the lift force increased dramatically, even only about 1 cm of lateral displacement being sufficient to raise the height of flotation to over 5 cm.

It seemed that the only reason for the lack of lift was that the "width" of the annulus, i.e. the difference between its inner and outer radii, was not sufficiently great. A larger annulus was therefore tried, of outer diameter 25 cm (and inner diameter 18 cm as before). With this was at last achieved some degree of success, for the plate floated at a height of about 5 cm, with strong lateral stabilising forces in the one direction (but no stability, of course, in the direction at right angles to the line of poles). This result gave much encouragement since it was felt that the addition of two more poles to create stability in all directions, plus the removal of the redundant central pole and the consequent increase in the quantity of copper in each coil, possibly combined with a further increase in the size of the floating annulus, might well increase the lift and clearance to that required for the lecture demonstration.

A slight digression was made at this point. When floating the wide annulus it was noticed that the aluminium became heated only in the two regions directly over the stator pole-pieces, the remainder staying cool - see Fig 77(a). The implication here is that only these two regions were carrying significant current. If this were the case then the behaviour of the system should not be altered if slots were cut in the positions of zero current, as shown on the diagram, and the two half-annuli re-joined by non-conducting material. Having done this, the topology of the system again should not be changed by straightening out each of the half-annuli into rectangles (e.g. of length equal to half the mean circumference and width equal to the difference between the radii of the original annulus), and extending the insulating joints into long bars to maintain rigidity, as shown in Fig 77(b). Such a composite rotor would certainly be a more suitable shape to conceal within a pad of lecture notes.

When tried, however, the system was a disaster, no stability whatsoever being achieved in any direction at all although the lift was not inconsiderable. It is not yet entirely clear why an apparently small topological change should have led to such a drastic change in behaviour, but the most likely explanation seems to be that although

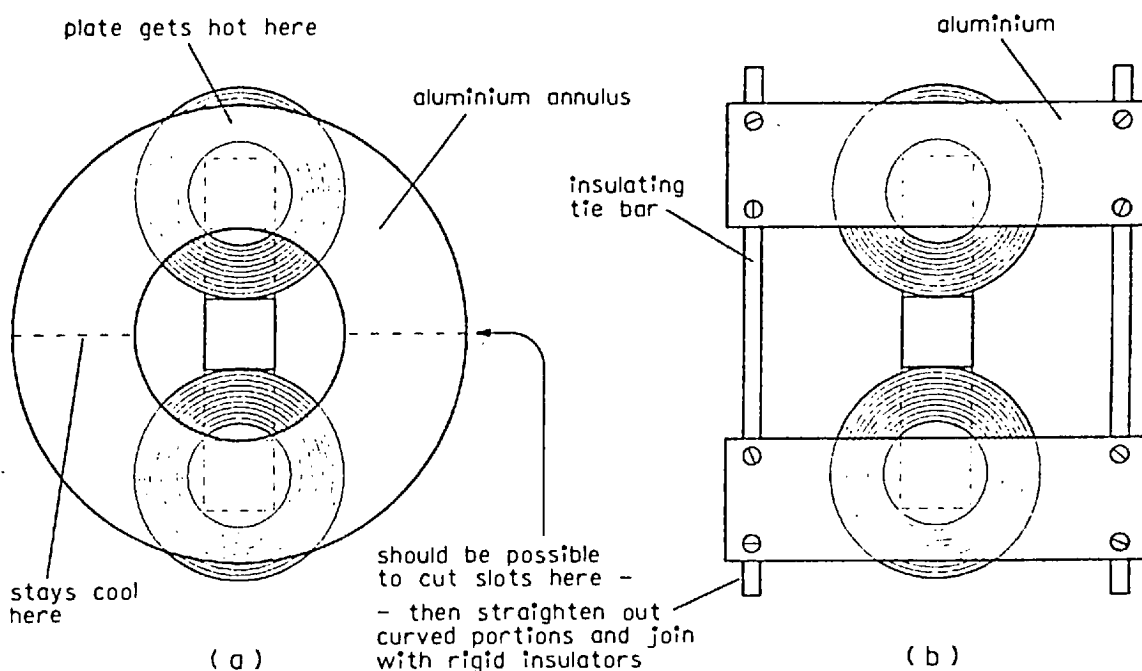


Fig 77. Development from single annular rotor to double rectangular rotor - unsuccessful.

the rotor currents confine themselves to the indicated regions when the rotor is in its equilibrium position, they must be allowed freedom to flow elsewhere as necessary in order to counteract the effects of a displacement.

To return to the circular annuli, the next stage was to attempt stabilisation in all directions. The method attempted was the obvious one - to use two sets of opposing pole pieces aligned mutually at right-angles, in the hope that each set would provide stability in a direction parallel to the line joining its own pole-pieces, without affecting the action of the other set. Clearly such an arrangement could not be constructed directly using the "E-core" stator blocks since their horizontal portions would have to pass through each other at the point of intersection below the centre of the system. It was thought undesirable to complicate matters by allowing magnetic flux to pass between the pole-pieces only in pairs and in only one of the two directions in which stability was sought, as would be the case were

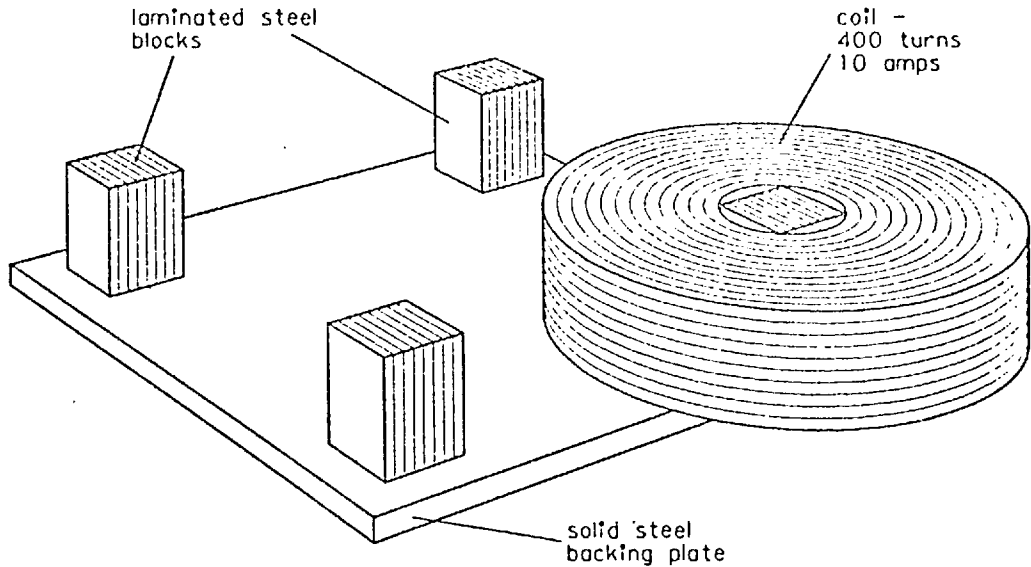


Fig 78. Use of four coils to create stability in all directions - unsuccessful.

two pairs of pole-pieces to be placed side-by-side a short distance apart to form a square of pole faces. Instead, therefore, the system shown in Fig 78 was set up, using four individual blocks of laminations of cross sections identical to those of the vertical portions of the E-cores, mounted upon a solid steel base allowing the magnetic flux freedom to pass between any pair of poles.

Now there are only two arrangements by which a system of four coils such as this may be connected together electrically in such a way that two of the poles are at every instant opposite in polarity to the other two. (To have three poles of one polarity facing a single opposite pole would not appear sensible, and only a single-phase current source is allowed since three-phase would induce rotary or linear drive.) The first such arrangement is the obvious one comprising alternate polarities in succession around the machine (i.e. one pair of diagonally opposite coils are electrically connected for their currents to flow in the same sense while the other pair are connected together in anti-phase to the first pair - see Fig 79(a)).

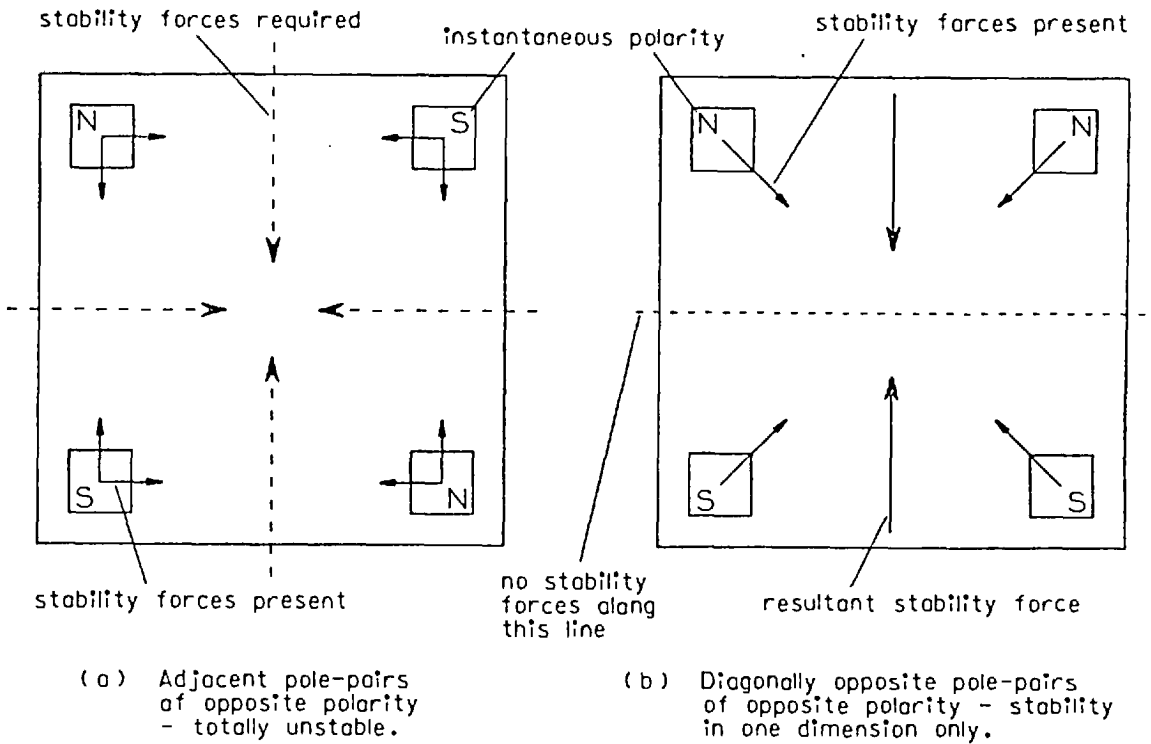


Fig 79. Alternative connections for four-pole stator.

It was hoped that when thus connected, each of the four pairs of adjacent coils would act as an individual "C-core" unit, providing stabilising forces such that an annulus placed over all four poles would be unable to move in any direction. In practice, however, the system achieved the opposite, for the annular plate was found totally unstable in all directions. Indeed all the rotors that were tried, whether annular or solid disc, and of whatever size, were unstable over this machine. It seemed that stability forces acting along lines joining adjacent pole-pairs, forming a square around the centre as shown in Fig 79(a), were not at all what was required (though these did serve to guide the rotor neatly between a pair of pole-pieces as it fell off!). Instead forces were needed at right angles to these, acting inwards towards the centre of the system along horizontal lines passing mid-way between each pair of adjacent poles.

The second alternative connection is as shown in Fig 79(b), in which the members of each pair of diagonally opposing poles are

connected with opposite polarity. Certainly each diagonal pair when excited on its own provided superb stability along a line joining the pole centres, but when all the coils were excited simultaneously the effect was to concentrate the stability along one axis between the poles and to eliminate it entirely along the other - see again Fig 79(b). This second result was in fact not entirely unexpected, for it was realised that each pair of adjacent poles similar in polarity could be regarded merely as a single extended pole - thus the machine is reduced to one extended pole facing another of opposite polarity, which is a single-phase version of an electromagnetic river, providing stability in one dimension and (in the absence of a longitudinal travelling field) neutral equilibrium in the other.

By this time there was among those working in the laboratory the general feeling that the series of failures was not so much a consequence of an inability on the part of the designers to achieve precisely the right dimensions of the rotor and stator of a given basic design, as of a fundamental inability of the entire class of machine to perform in the way that was needed. Though promising at its outset the whole concept of extending into two dimensions the one-dimensional stability of the simple C-core was beginning to look like a task impossible of achievement. Accordingly the experiments were turned to a different direction, to make use once again of the old gramme-ring wound linear motor blocks.

8.3 Return to gramme-ring wound stator blocks

It will be recalled that the previous chapter described the technique by which four standard blocks of linear motor laminations, on each of which had been wound in gramme-ring fashion twenty-four electric coils, could be used to simulate a variety of electromagnetic levitating machines (see Figs 60 to 64). In particular the diagram of Fig 64 showed the configuration of stator connections over which a large tray of aluminium was floated stably at a height of 16 cm. The new series of experiments had as their aim to discover whether different

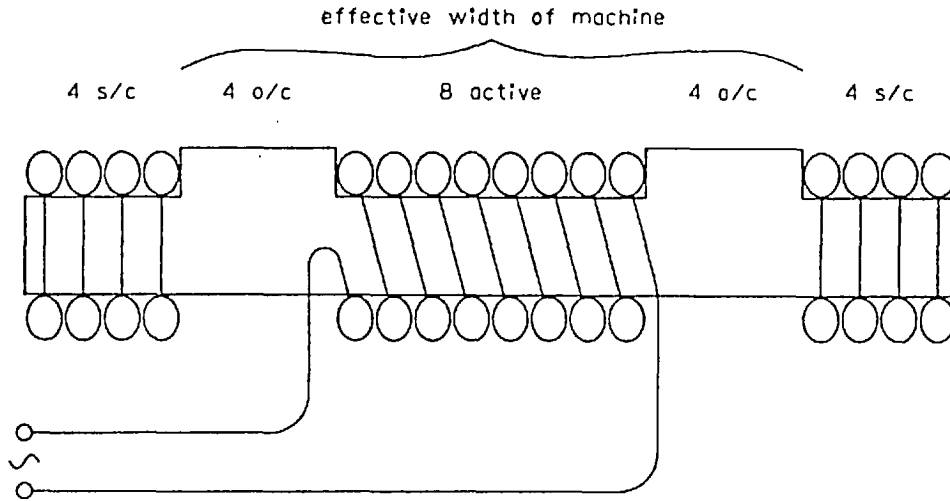


Fig 80. Gramme-ring block as narrow levitator.

connections of the same stator blocks could be used to float stably a much smaller rotor plate - the size of one (or two) sheets of A4 notepaper.

The size of stator appropriate to the floating of a large tray was clearly too large for the smaller aluminium plate, so the first step was to restrict the effective width of the stator. This was done by short-circuiting the first four coils at each end of every stator block upon themselves. The next four coils from each end were left open-circuited to form a pair of magnetic poles, and the remaining eight coils in the centre were connected electrically all in series and in the same sense to form a slot of excitation. (The specific numbers of coils to be left open and short-circuited were arrived at by experiment - the values quoted were found to be the best for the particular plate under investigation.) Fig 80 shows the complete set of connections.

The four stator blocks thus connected were placed side-by-side to form a complete machine (in the manner of the machines shown in Figs 63 and 64), and immediately the system achieved more than did any of the simple C-core systems. The plate could be floated at a

height of 8 cm, stable in all directions. However the stator currents required to achieve this were enormous, over 80 amps in each coil (obtained for all the blocks in parallel by means of capacitor banks, as with the old AEI large-scale linear motor described in the last chapter), which gave the machine a rating of only about ten seconds.

The idea then occurred that the outer four coils, short-circuited to limit the effective machine width, could be put to better use if they were made to carry currents in anti-phase to those flowing in the eight coils forming the centre slot. In this way the total flux passing through each pole would be increased, as shown in Fig 81(a). When tried this idea was indeed found to work, and the current required to float the plate at the same 8 cm height was reduced to about 60 amps per coil. However raising the current beyond this value in the hope of raising the height of flotation even further resulted instead in an instability of roll. The machine appeared to have a "wide-angled inverted prism of stability" such that even a small current increase was sufficient to remove the edges of the plate from the stability boundaries.

Now in such a situation one of two solutions would normally be employed to regain stability at a greater height. Either the plate itself would be replaced by a wider substitute so that the increased width at the greater height would restore the plate edges to the boundaries of stability, or in a case where there is flexibility of positioning of the stator poles, the poles would be brought closer together, bringing the stability boundaries inwards to meet the plate edges. Neither of these options would have been desirable in the present case, however. The size of the plate was restricted to that able to be hidden within the lecture notes, and to bring the poles together, though an easy matter with the gramme-ring wound blocks, would impose too great a restriction on the number of coils remaining to provide excitation in the central slot.

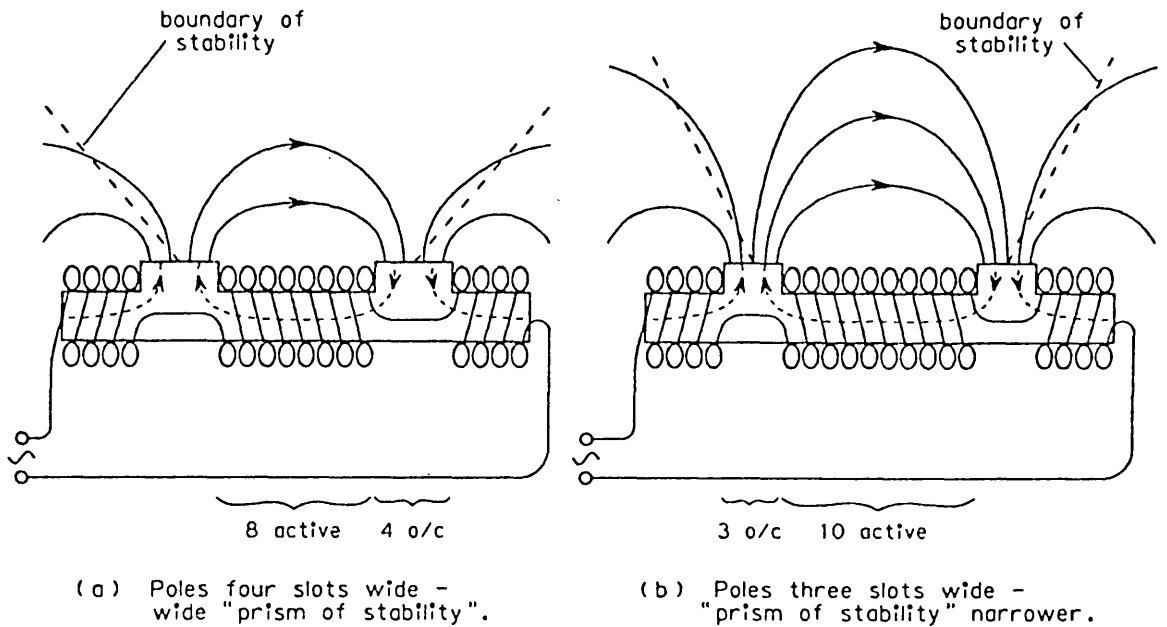


Fig 81. Use of negative excitation to increase working flux - effect of pole width upon boundaries of stability.

A third technique was therefore attempted, making use of observations made in earlier experiments using the gramme-ring blocks. The original aim of investigations involving these blocks was to discover whether variations in the relative proportions of the pole width and the central slot width had a significant effect upon the magnitude of the stability forces experienced by a floating rotor. While it was found that such variations had little or no direct effect, at the same time it was noticed that the "sharpness" of the inverted prism of stability was influenced by the width of the stator poles - wide poles defining a prism of wide angle and narrow poles one of narrow angle (this was shown in section 2 of Chapter 7, Fig 62).

Acting on this observation, the innermost coil of each pole, open-circuited in the diagram of Fig 81(a), was added into the series connection of the central excitation coils, thus narrowing the poles and at the same time introducing more current excitation to compensate for the consequent increased reluctance of the flux path. The

resulting connection is shown in Fig 81(b), and it was hoped that the boundaries of stability would thereby have been made "steeper" so that the plate could float stably at a greater height.

In essence the approach did indeed work, for after modifications to all four blocks had been completed the plate could be floated at a height of about 10 cm in its equilibrium position. Its equilibrium position however was no longer quite as had been intended, for the rotor now preferred to position itself with one or other of its diagonals aligned along the axis of the stator. In this position the plate tended to tilt somewhat, particularly if required to support any kind of load, and the stability was at the best of times weak, there being a considerable tendency after a slight disturbance for the plate to slip round from one diagonal position to the other and to continue to oscillate between the two. Again, attempts to raise the plate further to restore normal longitudinally-aligned stability resulted in excessive stator currents allowing only a few seconds working time of the machine.

Although the use of the gramme-ring wound linear motor stator blocks had achieved rather more than did the use of simple C-cores, these results were still disappointing in that the price of such achievements was one of large increases in the size and weight of the stator, in the excitation currents necessary, and most of all in the overall complexity of the whole system. Again it was felt that to ask a large system of stator coils to support and stabilise only a small size of plate was to request behaviour in conflict with the natural capabilities of such a machine.

8.4 Success at last

Further experiments were carried out on yet another system, this time a direct scale-up of the old circular disc-floater machine mentioned in Chapter 1 (see Fig 11). Details of the experiments need not be given here because this design of machine is not one of the "expanding-geometry" type and is therefore not relevant to the

subject matter of this thesis. In any case the attempts failed. Such a system is of course of the kind limited by the "cone of attraction" boundaries for stability, and the main reason for the failure was simply that the cone could not be made sufficiently high. It appeared that the note-floating demonstration called for an altogether unfortunate size of floating plate - too small for expanding-geometry systems such as the gramme-ring blocks, and too large for machines of the cone of attraction type.

Finally it was decided that with a little added "stage craft" the demonstration could still prove effective even with a floating height of only six or seven centimetres and with a machine of current rating only about fifteen seconds. Having been reduced to this level the requirements could then be met by use of the "magic carpet" machine of Chapter 2. In fact it was found convenient to use three of the coils of the original Washington model mounted in the mechanical arrangement depicted in Fig 13 of Chapter 2. The longitudinal spacing was adjusted so that the distance between the centres of the outermost coils was equal to the length of the floating plate (whose dimensions were 40 cm by 28 cm, being slightly less than two sheets of A4 note-paper side-by-side), and in this condition the shaded-pole action of the plate ends proved sufficiently strong to supply the necessary longitudinal stabilising forces without the need for poly-phase supplies creating inwards travelling fields. Thus the three coils could be connected directly in parallel across a single-phase supply (lateral stability of course being supplied by normal electromagnetic river action). All three coils and cores were encased in blocks of epoxy resin to reduce mechanical noise as far as possible, and finally the complete machine was built into a large lectern, the top surface of which was of thin material just covering the stator pole pieces.

In the event the demonstration was an unqualified success. Even after encasement of the cores in resin, the large currents flowing through the coils, combined with the sounding box effect of the lectern case, resulted in a machine that emitted a distinctive buzzing sound when switched on. Rather than to give the game away to the lecture

audience by suddenly allowing this noise to intrude a moment before the notes were to be released, it was thought better to cover up the sound by the introduction of suitable background music, emerging at first unobtrusively to build up rapidly to a climax as the machine was switched on. An eminently suitable such composition was the well-known opening to Richard Strauss's symphonic poem "Also Sprach Zarathustra". In fact the initial feeling of surprise as the first sound of the solo trumpet permeated through the lecture theatre a few minutes after the beginning of the lecture rapidly turned into one of total disbelief as the notes remained floating, unsupported, to the accompaniment of a crashing chord on full orchestra and organ. There resulted spontaneous applause of such enthusiasm that the orchestra was faded back into oblivion without any of the lecture audience noticing its disappearance. (It goes without saying that the bogus sheets of notes were then ripped away and the lid of the lectern raised to reveal to the audience the mechanism of the demonstration.)

From one point of view the "exercise in triviality" of which this chapter has been composed was no more than an extended waste of time, the more so because none of the machines investigated succeeded in their purpose, and the machine eventually employed was taken directly from research completed earlier. However in Chapter 1 a similar haphazard succession of trials and error was described, which culminated in the invention of the Washington model, the basis of all the work described in Chapters 2 to 7. While the haphazard researches of Chapter 8 have not culminated in a breakthrough of equivalent proportions, they have served to consolidate several ideas and concepts concerning electromagnetic levitation, and particularly to define some of the limitations of such systems. Some of these ideas will be returned to in Chapter 9, which is a review of the many theoretical descriptions and explanations which have been put forward in attempts to help the understanding of electromagnetic levitation and stability.

CHAPTER 9

THEORY



The Jumping Ring (p 201).

CHAPTER 9. THEORY

9.1 A Hypothesis

Consider the following: "Any system of electric coils wound upon magnetically-conducting cores produces a magnetic field through and around the cores when an electric current is passed through the coils. Any electrically-conducting material placed within the bounds of the magnetic field will have voltages induced within it if the field changes, and secondary induced currents will therefore flow. The direction of these currents can be predicted in simple cases by one of many "rules of thumb", but in all cases the general rule applies that the directions of flow of the secondary induced currents are such that their magnetic effects act to oppose the changes in the original magnetic field.

"If the changes are the result of an alternating current flowing in the primary, then the directions of the secondary currents will always be opposite to the primary currents (or equivalently in anti-phase) since one set of currents is producing the magnetic changes and the other is opposing them - and two currents flowing in opposite directions exert upon each other a force of repulsion. This is the mechanism by which a lifting force is produced on a conducting sheet placed in the field of a conventional single-sided linear motor.

"Now if the system of primary cores is such that the pole-faces of all the cores lie in a horizontal plane and form a pattern symmetrical (in position and polarity) about some line within that plane, then a secondary plate positioned symmetrically above such a stator will experience a repulsion force acting directly upwards through its centre - see Fig 82(a). If the plate is then displaced to one side, the repulsion force will change direction, to continue to act roughly in a line joining the centres of the rotor and stator, i.e. it will act upwards and outwards as shown in Fig 82(b). Such a system is unstable. Since no assumptions have been made regarding

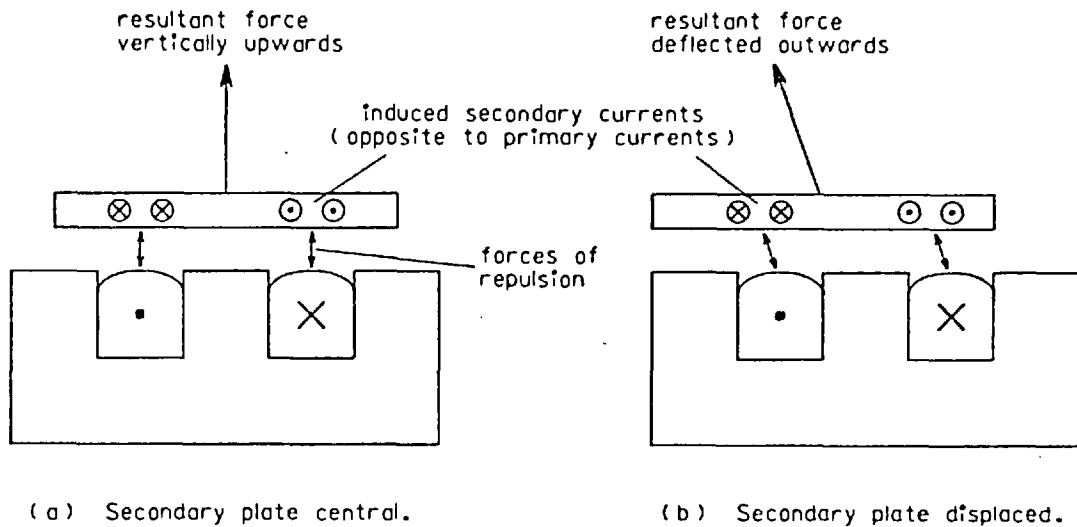


Fig 82. Forces on conducting plate over an electromagnetic coil system.

the arrangement of the stator coils or the nature or shape of the floating rotor, it follows that to achieve any form of lateral stability over such a system is impossible." End of hypothesis.

Evidently the above argument is fallacious, since the electromagnetic river possesses lateral stability as its key feature, and devices employing "cone of attraction" stability, such as the disc floater of Fig 11, have been known for many years. Indeed the argument contains two fallacies, one of which will be considered later in this chapter (p 219). The other fallacy, and the correct argument to take its place, may be most readily understood by reference to one of the simplest forms of electromagnetic levitator, the "jumping ring" machine shown in Fig 83. It is worthwhile to consider this machine in some detail, since many of the concepts involved are also relevant to the electromagnetic river.

9.2 The Jumping Ring

The stator of the jumping ring machine consists of a single coil, wound upon an iron core (usually comprising a bundle of thin iron rods to minimise eddy currents) which extends a distance of

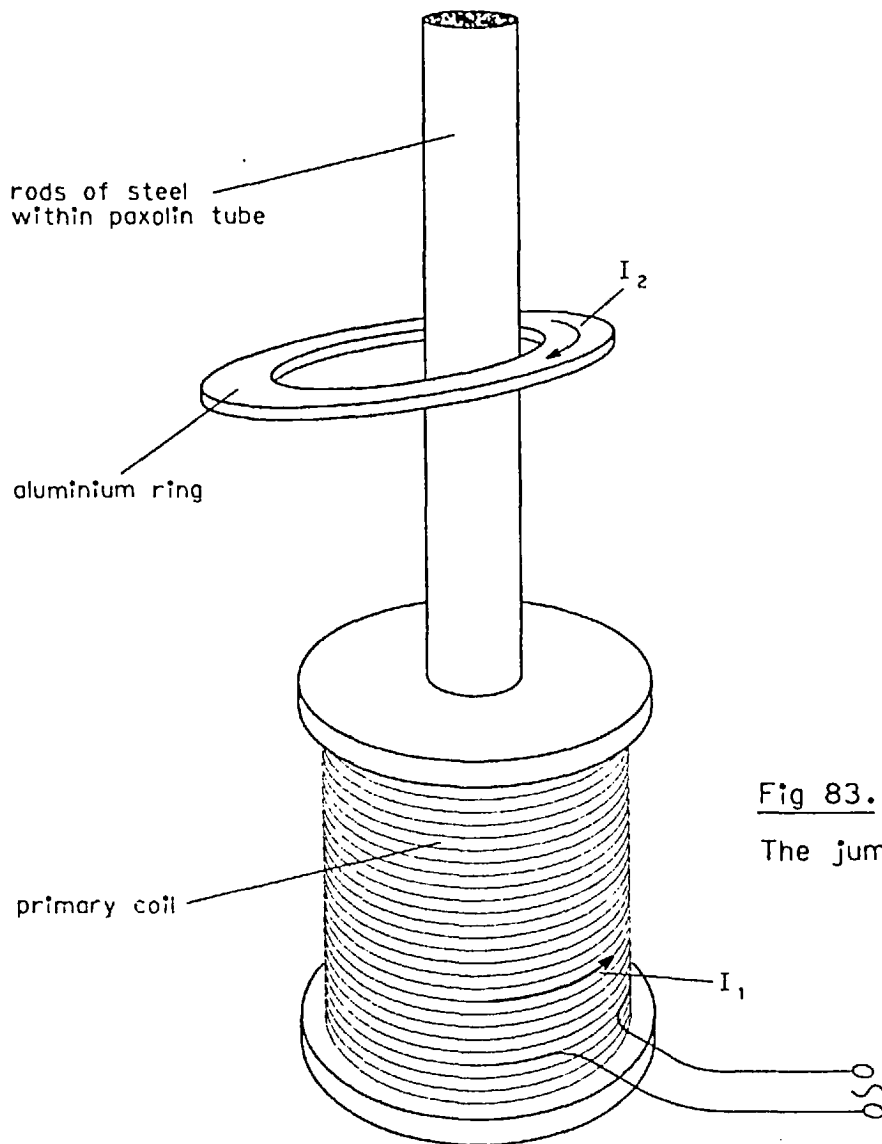


Fig 83.

The jumping ring.

half a metre or so beyond one end of the coil. The rotor is an aluminium ring, cut from solid plate. On activating the machine, a ring previously placed over the core on top of the primary coil is violently ejected into the air - hence the name of the machine. If the ring is then replaced over the core with the primary current still flowing, it floats, as shown in the diagram. This is, of course, an unstable position - only the central iron core keeps the ring in place.

According to elementary theory, the primary current I_1 sets up a magnetic flux along the core, which threads the floating ring and induces a secondary current I_2 , in opposition to I_1 . The force F between the two currents is then proportional to the magnitude of each and inversely proportional to the square of the distance d between them, i.e.-

$$F = k \cdot \frac{I_1 I_2}{d^2}$$

where k is a constant of proportionality.

As it stands the argument sounds convincing, and indeed it may be used to predict certain aspects of the behaviour of the machine. For example if asked to predict what would be the effect of substituting a second aluminium ring of identical horizontal plan dimensions to the first but of only half the vertical thickness, the answer would be obtained that the new ring would float at the same height for the same value of primary current.

The reasoning is simple. Assume that the new ring is first positioned at the equilibrium height of the old. Then in this position the same area of ring will be threaded by the same primary magnetic flux, and therefore the voltage induced in the second ring will be the same as that induced in the first. But the electrical resistance is twice as great (on account of the thickness having been halved, all other dimensions remaining unchanged), therefore the secondary current I_2 will be halved. This results in a halving of the repulsion force F - but the ring itself is only half the mass of its predecessor, and therefore the force does indeed just support the required weight. So the second ring remains floating at the same height as the first.

By extension of this argument all rings of the same plan dimensions will float at the same height, regardless of their thickness. In practice there is an upper limit of thickness, reached at the approach of the skin depth of aluminium at the frequency of supply (and in any case the argument breaks down as the thickness becomes a significant

proportion of the separation between the two circuits, since it is then no longer possible to assume that the same flux is enclosed by the ring). However there should be no lower limit - a ring of one hundredth the thickness of the original should have one hundredth the current flowing in it to support one hundredth the mass at the same height.

But such is not observed in practice, for a ring of one hundredth the thickness is scarcely able to float at all. In order to re-construct the argument to account for this departure from the expected behaviour it is necessary to return to the equation relating the repulsion force to the two currents. To state that the force is directly proportional to the product of the two currents is naive, for this applies only when both currents are unchanging. The jumping ring is an alternating current device. The required modification is the replacement of the direct product of two direct currents by the scalar product of two phasor (alternating) currents,* to give:

$$F = k \cdot \frac{|I_1| \cdot |I_2| \cdot \cos \psi}{d^2}$$

where $|I|$ = magnitude of current I ,

ψ = phase angle between I_1 and I_2 .

To be strictly accurate the force thus expressed, between two currents flowing in the same direction, is one of attraction. Only when ψ exceeds ninety degrees, to make $\cos \psi$ negative, does repulsion occur, and this then reaches its maximum value when $\psi = 180^\circ$, i.e. when the two currents are in anti-phase. Here lies one of the fallacies in the original argument stated at the very beginning of the chapter, for it was implicitly assumed that the angle ψ was 180° (i.e. that the rotor and stator currents were in exact opposition) - by no means always the case in practice.

* see footnote on similar modification needed to the Maxwell Second Stress equations, section 4 of Chapter 4 (page 81).

Modified to include $\cos\psi$, the argument as applied to the jumping ring now reads as follows:

"The primary current I_1 sets up a flux through the iron core which is in phase with I_1 . The flux induces a secondary voltage in the ring whose phase lags the flux by 90° ($E = \frac{d\phi}{dt}$), and this voltage sets up the secondary current I_2 which is itself in phase with the secondary voltage and hence 90° out of phase with I_1 . The cosine of ninety degrees is zero, therefore the lift force is zero for all rings!"

The fault now is that only half of the necessary modifications have been carried out, for implicit in the above argument are two statements of Ohm's Law, each of which is again true only for d.c. quantities. Firstly the relationship between secondary current I_2 and secondary induced voltage is dependent on two properties of the ring, its inductance as well as its resistance. The presence of inductance causes the current to lag the induced voltage, and therefore to differ in phase from the primary current by something other than 90° . Hence lift is obtained. This effect is however small, and in practice all aluminium rings of depths up to at least one centimetre are resistance-dominated (for which reason the observed behaviour is that lift height is independent of thickness for a large range of rings - to this extent the original simple theory ignoring inductance is sufficient).

The second implicit statement of Ohm's Law is less apparent since it involves the magnetic circuit rather than one of the electric circuits. Here is not the place to embark upon an explanation of magnetic equivalent circuits⁽³³⁾ - suffice it to say that in this machine the magnetic flux can conveniently be split into two component paths in parallel, one of which carries all the flux passing through the ring, and the other all that does not. Fig 84(a) is a representation of the flux paths around the jumping ring, and Fig 84(b) is the corresponding magnetic equivalent circuit.

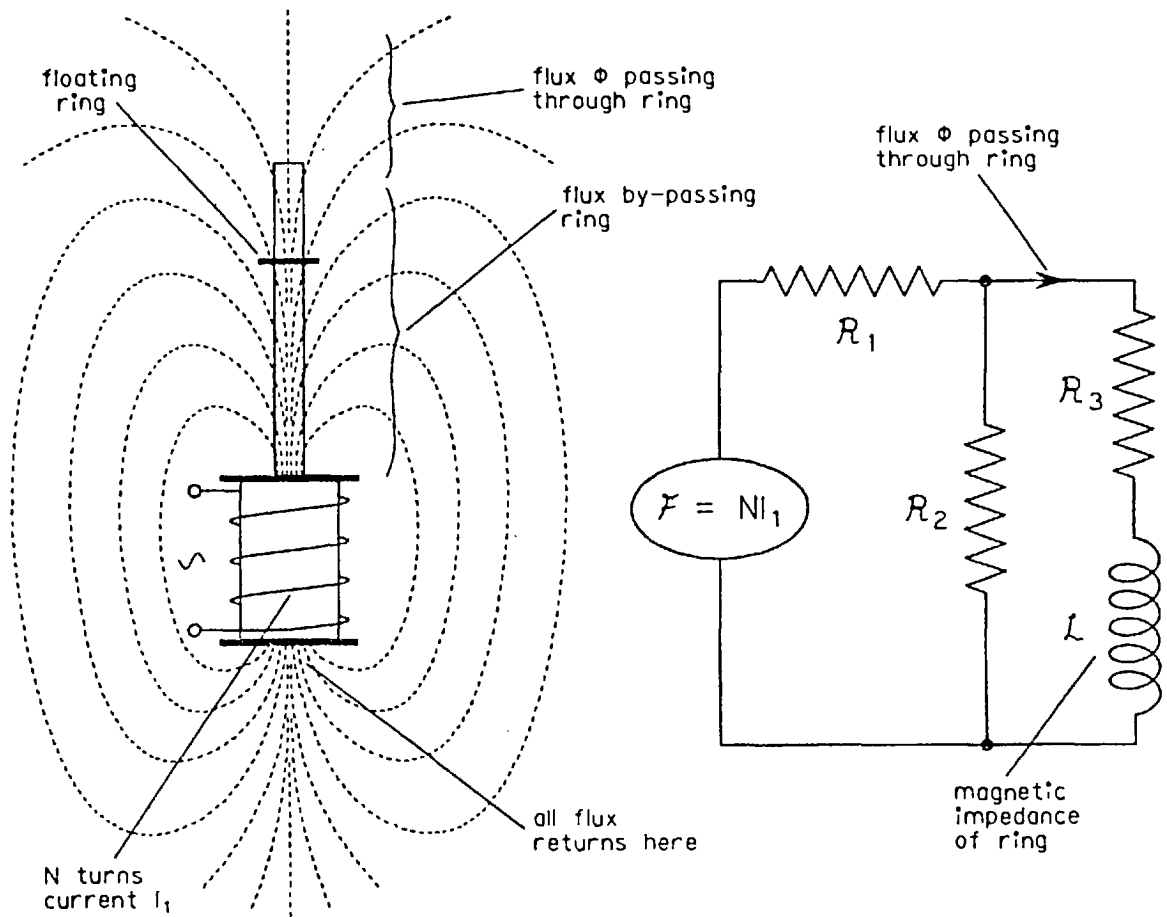


Fig 84. (a) Flux paths around jumping ring.

(b) Magnetic equivalent circuit.

In the equivalent circuit of Fig 84(b), the magneto-motive force \mathcal{F} (the magnetic equivalent of electro-motive force E) is given by $\mathcal{F} = NI_1$, where N is the number of turns on the primary coil and I_1 is the primary current. The three reluctances \mathcal{R}_1 , \mathcal{R}_2 and \mathcal{R}_3 represent respectively the magnetic resistances of the path through the primary coil (for all the flux), the path outside the primary coil for all the flux by-passing the ring, and the path outside the coil for all the flux passing through the ring - each reluctance given by the expression:

$$\mathcal{R} = \frac{\ell}{\mu A} \quad \text{where } \ell = \text{effective length of relevant portion of magnetic path,}$$

$$A = \text{effective area of path,}$$

$$\mu = \text{absolute permeability of medium.}$$

The presence of the aluminium ring shows itself as a magnetic inductance \mathcal{L} , whose value is inversely proportional to the electric resistance R of the ring. (For a full derivation of these quantities see reference 33.)

The magnetic inductance is the key to the operation of the jumping ring, for its effect is to cause the flux passing through the ring to lag the primary magneto-motive force, i.e. the flux ϕ lags the current I_1 . Thus the secondary current I_2 in the ring, while ninety degrees out of phase with the flux (for a resistance-dominated ring), is further out of phase with the primary current I_1 , and the cosine of the larger resultant phase angle is once again no longer zero. A very thin ring, of high electrical resistance, will constitute a low magnetic impedance so that the flux is caused to lag the m.m.f. scarcely at all - hence no lift is obtained. Rings of thicknesses greater than only about a millimetre, however, have an electric resistance so low that the resulting high magnetic reactance (or "transference") becomes the dominant term in the magnetic circuit. This causes the flux to lag the primary current by nearly ninety degrees, giving an overall phase difference between the two currents of almost 180° - which is the result that the first, naively simple theory assumed. It is seen that only the combination of a resistance-dominated secondary electrical circuit with a transference-dominated magnetic circuit acts in the way predicted by the simple theory.

This explanation has been presented in some detail because the jumping ring is an example of an electromagnetic machine the action of which is completely understood and explainable (at least in so far as any electromagnetic phenomenon can be completely understood; the basic fundamentals of the subject remaining one of the "mysteries of the universe"). In a more general form the same argument accounts for the lift forces observed in other shapes of levitator (such as the flat-plate floater of Chapter 1, Fig 1), in conventional single-sided linear motors, and in the electromagnetic river. In like manner the method of production of a travelling magnetic field (linear or rotary) from a polyphase alternating supply is considered to be fully

understood⁽³⁴⁾, as is the production of accelerating forces on conducting objects placed within such travelling fields - induction motor action^(1 and 34). Both these mechanisms operate for the electromagnetic river in precisely the same way as they do for conventional longitudinal or transverse-flux linear motors. The mechanism of stability for the electromagnetic river, however, is not understood, and consideration of some relevant theory comprises the major part of this chapter.

9.3 Arguments with limitations

Before proceeding to theories of stability it is useful to consider further the mechanism of lift-production in the jumping ring. The following two attempts at explaining the action of the ring, though both promising at their outset, ultimately provide less insight into the mechanism at work than does the explanation already presented. The reason for giving these attempted explanations here is that each of the approaches to be outlined can be applied also to the stability mechanism of the electromagnetic river. It is helpful to appreciate to what extent a method can be of use in explaining a phenomenon already understood before attempting its application to the unknown.

Firstly an argument can be formulated based on the well-known premise that when a current-carrying conductor experiences a force within a magnetic field, the directions of the force, the field and the current are mutually at right-angles. In the case of a floating ring the force is evidently vertically upwards, i.e. axial to the ring; the current is circumferential (as can be easily demonstrated by substituting a ring with a single radial slit, which does not float at all), and therefore the component of flux producing the upward force must be radial to the ring, i.e. in a horizontal plane.

Theoretical confirmation of the obvious fact that the force does indeed act upwards and not downwards may then readily be obtained by the use of one of the elementary "rules of thumb", as follows.

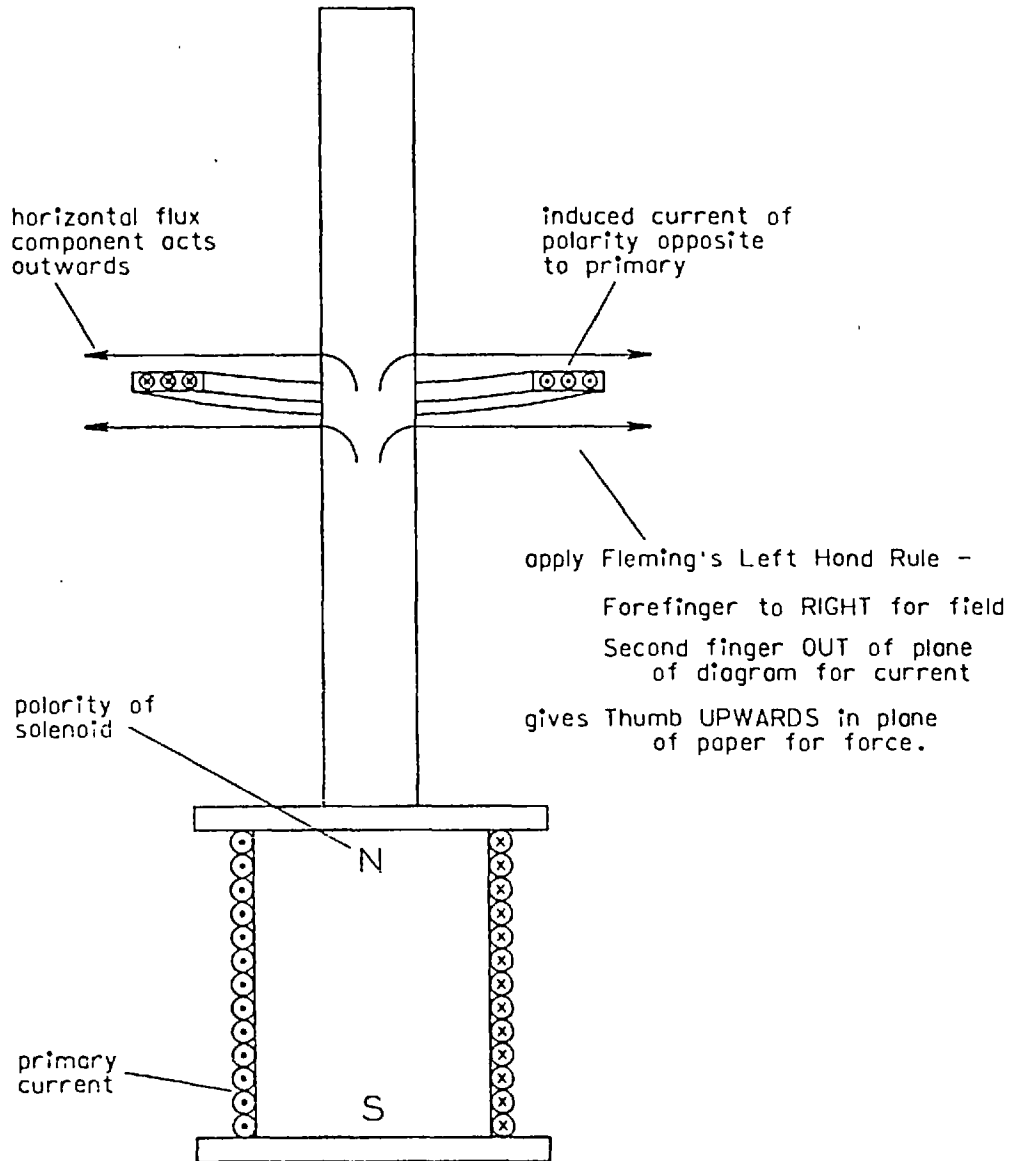


Fig 85. Instantaneous current and flux directions in jumping ring.

Taking the direction of the primary current to be instantaneously as shown in the first diagram of the jumping ring (see Fig 83), the polarities of the induced flux and of the secondary current become as shown in the cross-section of Fig 85. Considering the right-hand side of the ring, the direction of the horizontal component of flux is outwards to the right and the direction of the secondary current is out of the plane of the diagram, from which, using Fleming's left-hand rule, the resulting force on that part of the ring is upwards.

In a similar manner all other parts of the ring can be shown to experience an upwards levitating force. This, however, is as much information as can be obtained from the method without a detailed knowledge of the magnetic field distribution along the length of the extended iron core, and of the way in which this field itself varies with changing positions of the ring. Determination of such information is a laborious process, and once obtained it applies only to that one particular ring.

The second approach makes use of the concept of "shaded-pole action". The name derives from the frequent use of the principle for the purpose of starting machines such as single-phase induction motors, where one or more of the stator poles has part of its face area "shaded" by an encircling thick ring of copper - see Fig 86(a).

The effect of this ring may be understood by reference to the magnetic equivalent circuit of Fig 86(b). As in the jumping ring, the flux emanating from the pole is split into two parallel paths. The left-hand path on the diagram comprises a reluctance representing the air-gap, while the right-hand path comprises a transference (magnetic reactance) representing the shading ring, in series with the air-gap reluctance. The flux passing through the transference lags in phase behind that passing through only the reluctance - and any pair of alternating fluxes in close proximity but differing in phase by an angle other than zero or 180° constitutes a travelling magnetic field, the motion of which passes from the leading to the lagging flux. The top surface of the rotor in the diagram of Fig 86(a) is thus acted upon by a travelling field passing from left to right, which produces a torque acting clockwise on the rotor as a whole.

More generally, any electrically-conducting material placed within a magnetic field presents a transference to flux passing through itself, and if placed so that part of the flux from the same m.m.f. source is allowed to by-pass the conductor then a travelling field will be set up which moves in a direction from the by-passing flux

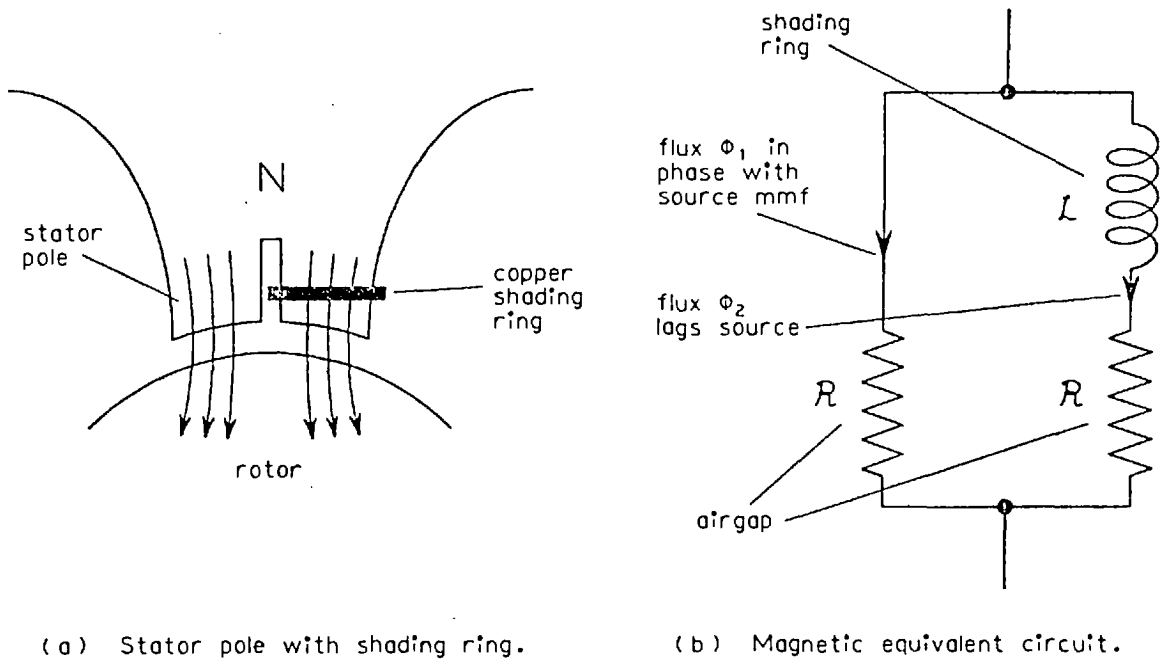


Fig 86. Shaded pole action.

towards the conductor itself. The secondary floating ring acts as a shading device over the jumping ring stator, causing the flux emerging above the ring (see Fig 84) to lag in phase behind that emerging below. The resulting travelling field is vertically upwards, and the ring will settle itself at the height for which the upward force produced from the travelling field equals the downwards force of gravity.

The concept of shaded-pole action is a perfectly valid approach to an explanation of the mechanism of the jumping ring, but again its useful application is limited. Prediction of the direction of the resultant force is about the extent of the information that may readily be obtained, the method lending itself only with the greatest difficulty to calculation of the magnitudes of the forces present, or of the effect on them of changes in the position of the ring. Further complication, for instance by the addition of a second ring to the system, takes the problem right outside the scope of theories such as

those based on shaded poles or on Fleming's left-hand rule. Only the approach based on the magnetic equivalent circuit can handle situations such as this (in this case by splitting the flux into three parallel paths; for flux passing through both rings, through only the lower ring, and through neither ring).

9.4 Stability by attracting and repelling currents

Having seen how several different methods of approach may be applied to an apparently simple phenomenon such as the jumping ring, it may now be appreciated that it is possible to consider a complex device such as an electromagnetic river in a number of different ways. In none of these ways however has a satisfactory explanation yet been forthcoming that can account for even the principal trends of stability and instability behaviour. All the explanations presented in the following pages are therefore incomplete. Some indeed are little more than mere ideas needing much work to develop them to the point where they can be of any practical use at all. They may nevertheless be worthy of some consideration, not so much for the purpose of providing an understanding of the phenomena involved, for that cannot be done as yet, but rather to stimulate further thought along some of the lines suggested.

The first approach to be considered, and one of the more useful of those developed to date, starts from simple ideas concerned with attracting and repelling forces produced by pairs of currents. In fact this approach is hardly more than the original naively simple theory stated at the beginning of this chapter. There is however the major difference that experience with the jumping ring has indicated some of the limitations of the method, so that appropriate allowances can be made in the new application.

The idea behind the method may be more readily appreciated by reference to the simplest design of electromagnetic river, the Washington model of Chapter 1 (see Fig 10). In this design the stator current returns along a single bunch of conductors below each

iron C-core. When a rotor plate is positioned above the pole-pieces of the machine, the active part of the stator current, i.e. that flowing along the slot, induces an image current in the centre of the plate. It may be said either that the direction of this current is opposite to that of the stator current in the slot (the "naïve" outlook), or that the phase difference between the two currents approaches 180° (the "comprehensive" approach). In the latter case the secondary electric circuit is assumed to be resistance-dominated in the same way as was an aluminium ring of similar thickness, and the dominant component of the magnetic circuit is taken to be the transference presented by the plate, known to be significant because the plate could not be floated if it were not. In either case the resulting force between the central induced current and the main primary current is one of repulsion. This constitutes the levitation force upon the plate, as shown in Fig 87(a).

The induced secondary current must then complete its circuit within the plate, which it does by splitting to return along the two plate edges, forming the characteristic "double-loop" pattern as discussed in section 2 of Chapter 3. At each plate edge a current is thus formed which is roughly in phase with the stator current, and hence a force of attraction exists between each of the edge currents and the primary current in the core centre. The complete system of electromagnetic forces acting upon a floating plate in equilibrium thus comprises a central region of repelling forces acting upwards and outwards from the primary slot, bounded on each side by attracting forces acting downwards and inwards. It will be recalled that such a system of forces is similar to that experimentally obtained by the use of the Maxwell Second Stress formulae from measurements of the magnetic field surrounding the plate - Chapter 4, Fig 42.

Having determined the force system acting upon a centrally placed rotor, the next stage in the prediction of stability effects is to determine how these forces change when the plate is displaced. Fig 87(b) shows the plate in a position of lateral displacement.

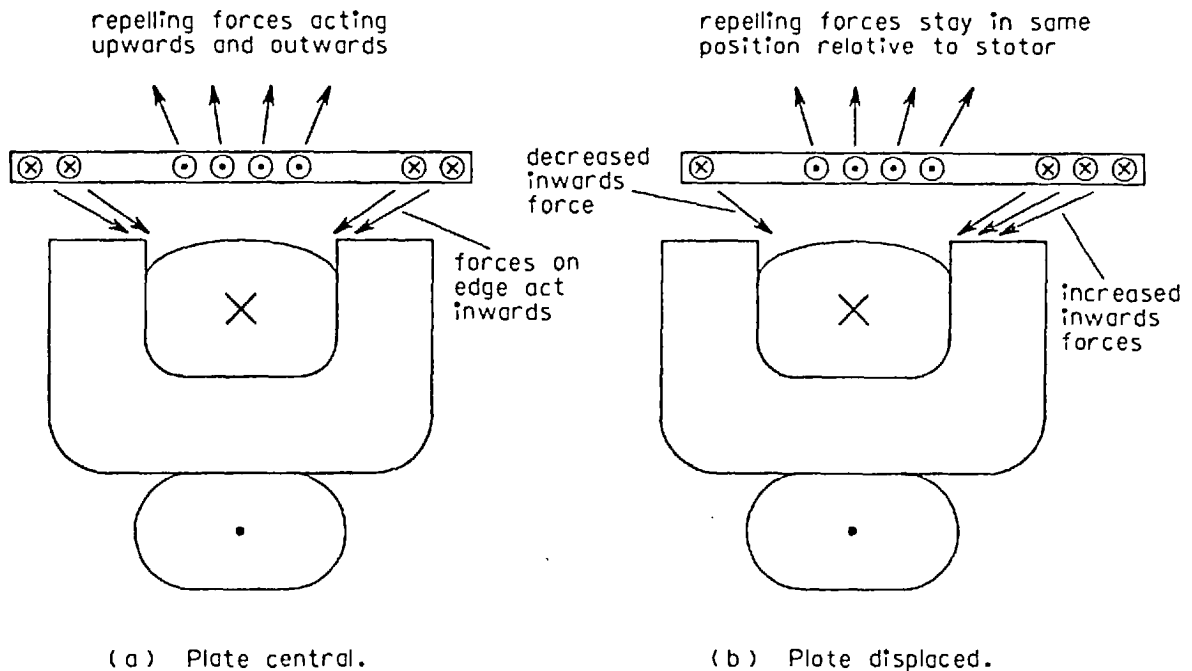


Fig 87. Theory of stability based on forces between pairs of currents.

In this position the main image currents are still induced in that part of the plate directly above the stator slot, so that they and the repulsion forces produced by them are no longer central with respect to the rotor. This causes a change in the pattern of the return currents, since now the greater part of the secondary induced current elects to return along the outer edge of the plate, i.e. the edge remote from the central slot. (The experimental confirmation of this revised flow pattern, it will be recalled, was presented in section 1 of Chapter 4 - see Fig 32.)

The resulting changes in the magnitude of the attracting forces at the plate edges are not so readily predictable. Considering, for example, the outer edge of the plate, the increased current flow strengthens the attractive force towards the stator slot, but the increased separation as a result of the displacement weakens the attraction. Similar considerations apply to the forces on the inner edge. The only criterion for the existence of lateral stabilisation (on the assumption for the moment that the central levitation forces

do not play a significant part) is that the net effect should be to leave the attractive force at the outer edge greater than that at the inner, the absolute increase or decrease of either force with respect to its original value being irrelevant here.

At this point the theory approaches the limit of its usefulness. Practical experience has shown that lateral stability is achieved only for certain widths of plate, in general the narrower the better, and that for any given plate width there is a minimum value of stator current below which stability can never be achieved. It would be of interest to investigate the way in which each of these variations affects the magnitudes of the edge currents, with the plate both central and in a variety of displaced positions. But such research would be essentially practical rather than theoretical, and it seems improbable that investigations of this kind would lead to development of the theory of attracting and repelling currents that could provide the means for predicting the lateral stability or otherwise of a new shape or size of rotor, untried in practice.

The method appears even less promising in its application to stability in roll, for here predictions can be distinctly misleading. For example if the plate in Fig 87(a) is made to suffer a disturbance in roll about its longitudinal axis, there is nothing to suggest that the induced current pattern should be significantly altered. If this is the case then whichever edge of the plate has moved downwards will experience an increased attractive force towards the stator slot (being closer to it than before), while the upper edge will experience a smaller force. These force changes act to increase the roll disturbance, and the system is therefore unstable. But in practice many plates are found to be well stabilised against roll disturbances, the general rule appearing to be "the wider the better". The attracting and repelling current theory sheds no light upon such behaviour.

Misleading results are also obtained from considerations of the roll torque resulting from a lateral displacement. Fig 88(a) shows

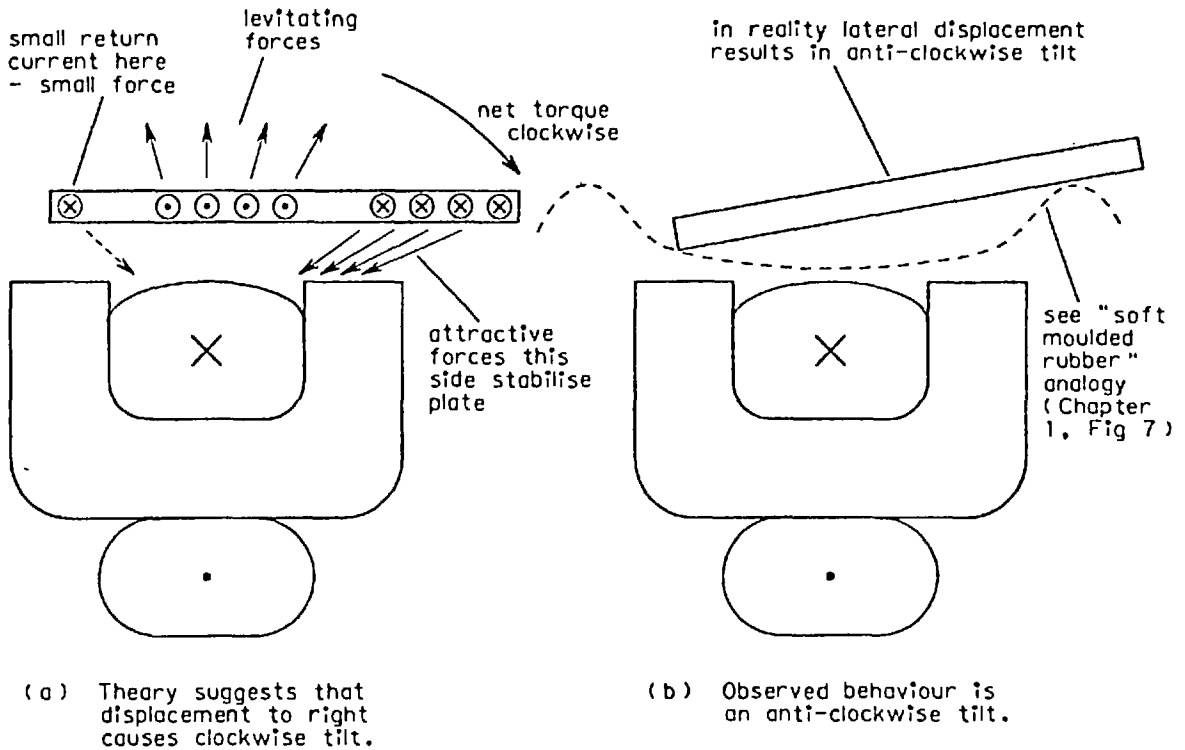


Fig 88. Displaced plate - behaviour about roll axis.

again the pattern of rotor currents caused by a small displacement to the right, from which it can be predicted that the resulting torque acts to tip the plate clockwise. The observed behaviour, however, is quite the opposite. It may be recalled that at the beginning of the thesis the "feel" of the support and stability forces was described as being somewhat akin to a plate sitting within a trough of soft moulded rubber (see Fig 7 of Chapter 1). Certainly it is an observed fact that the effect of a lateral displacement is to cause the outer edge to lift, giving the plate an anticlockwise tilt after a small movement to the right, as shown in Fig 88(b). Again the only conclusion to be drawn is that the theory is inadequate for predictions of effects in roll.

The uses of the method appear therefore to be restricted to considerations only of the horizontal effects of horizontal displacements. Even here predictions are confined to little more than

statements of the possibility, rather than the actuality, of lateral stability for a particular configuration of machine. One aspect that the theory does highlight, however, is the necessity for the rotor current paths to have complete freedom of flow. This necessity was deduced from experiments with slitted plates, described in section 2 of Chapter 3, but now a clearer understanding of the phenomenon is possible. As was discussed in Chapter 3, a single slit cut into the end of a plate (such as in Fig 22(b)) was sufficient to destroy all lateral stability. It can now be appreciated that the effect of the slit was to prevent the flow of end currents needed to complete the double-loop pattern shown in Fig 87(b), and in the absence of the shift of return current to the outer edge of the plate there could be no stability of any kind. (Similar considerations apply also to the failure mentioned in Chapter 1 of the double-trough rotor over one of the early stabilising machines - see Fig 9.)

9.5 Stability over a conventional linear motor

Before moving on to consider other theoretical explanations of the electromagnetic river, it is interesting to apply the ideas of attracting and repelling forces between currents to the conventional longitudinal or transverse-flux linear motor. Experimental experience is that such machines are laterally actively unstable - rotor plates do not merely fall off sideways but are violently thrown off by the electromagnetic forces. This behaviour can be deduced from considerations of the forces acting between currents as follows.

The single-loop pattern of stator current sets up a corresponding opposing loop in the rotor, as shown in Fig 89(a). These currents then react to produce two sets of repulsion forces, one on each side of the plate and both acting vertically upwards to provide lift, and two sets of cross-attraction forces whose resultant is a small downwards force. Upon lateral displacement of the plate the pattern of rotor currents can scarcely alter (apart from possible slight bunching of the current paths at the inner edge and spreading at the outer edge), but the physical movement of the plate causes the repulsion

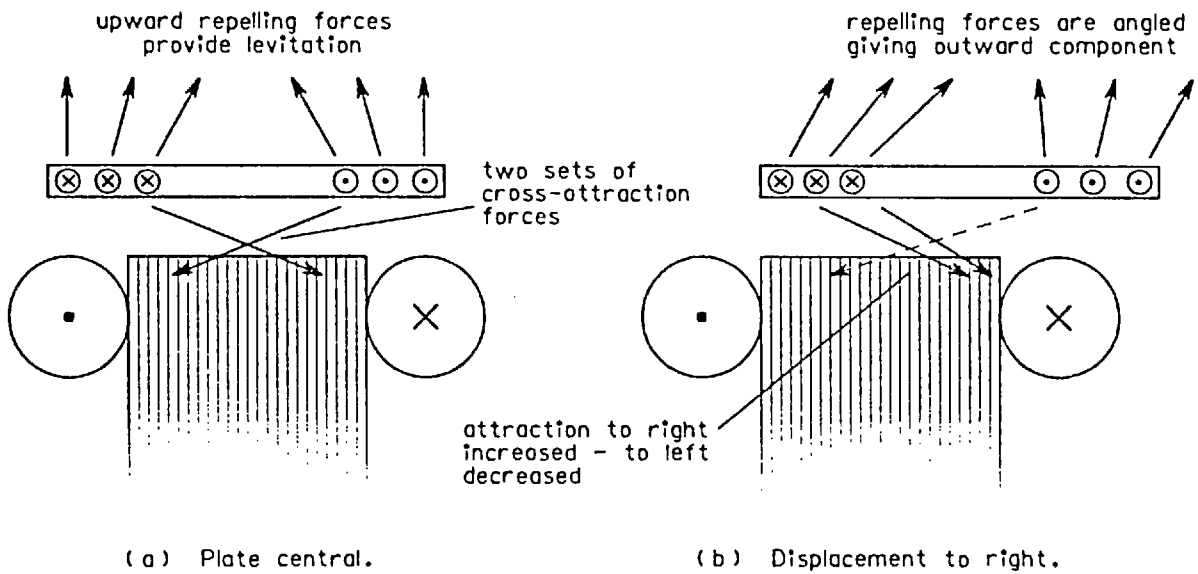


Fig 89. Instability of rotor above conventional linear motor.

forces to change direction, resulting in an outward component of force as shown in Fig 89(b). The cross-attraction forces are affected not so much in direction as in magnitude, one set finding its parent currents moving closer together, increasing the attraction between them, while the other pair of currents moves further apart.

It can be seen from the diagram that each of these changes acts to increase the original displacement, and the system is therefore actively unstable. Furthermore the argument will apply to any single-loop pattern, regardless of the shape or size of the rotor or stator or of the magnitude of the stator currents. Stability within only a single loop of rotor current is therefore impossible. (That is not to say, however, that stability cannot be created by other means, such as by cutting slots in the stator surface or even inserting conducting grids. Such devices can and have been used with great success, but their application is not relevant to the present discussion.)

Thus stated, the argument is of course a particular case - in this instance a valid case - of the general argument presented at

the very beginning of this chapter. Only now does the second of the fallacies in that original argument become clear. When the rotor current pattern is confined in such a way that its pattern is not changed by displacement of the plate, then it is true that the repulsion forces between the rotor and stator currents change direction in such a way as to increase any displacement. There are several ways by which such restraints on current patterns may be applied, for example by defining the current flow paths themselves as in a wound rotor, by restricting the freedom of the current patterns in a sheet rotor as in the plate with the slit at each end, or by setting up a current pattern so basic that there is no scope for it to change, as in a rotor over a conventional linear motor. But when the rotor current patterns are free to change, for instance by varying the sizes of individual loops in a double-loop pattern and altering the proportions of the current flowing in each loop, then the situation is no longer so simple. The electromagnetic river is an example of a machine where under some conditions the action of the force changes is reversed - i.e. the rotor is stabilised.

It might be hoped that an entirely different approach to the problem of stability could lead to an explanation with less serious inadequacies than those of the attracting and repelling currents method. Unfortunately such has not been the case so far. The theory as presented is, indeed, a typical example of all the ideas developed to date - grossly incomplete, for use only with care, and always with the knowledge in the background that satisfactory explanations for the phenomena as a whole have not yet been found.

9.6 Stability by Shaded-Pole Action

The next approach to be considered is one based on the concept of shaded-pole action. (It is tempting to write "the next approach to be eliminated ..." since the method is of little help in predicting the stability or otherwise of an unknown system.) Consider once again a conventional linear motor, with an aluminium rotor positioned centrally above it as shown in Fig 90(a). Flux passing upwards

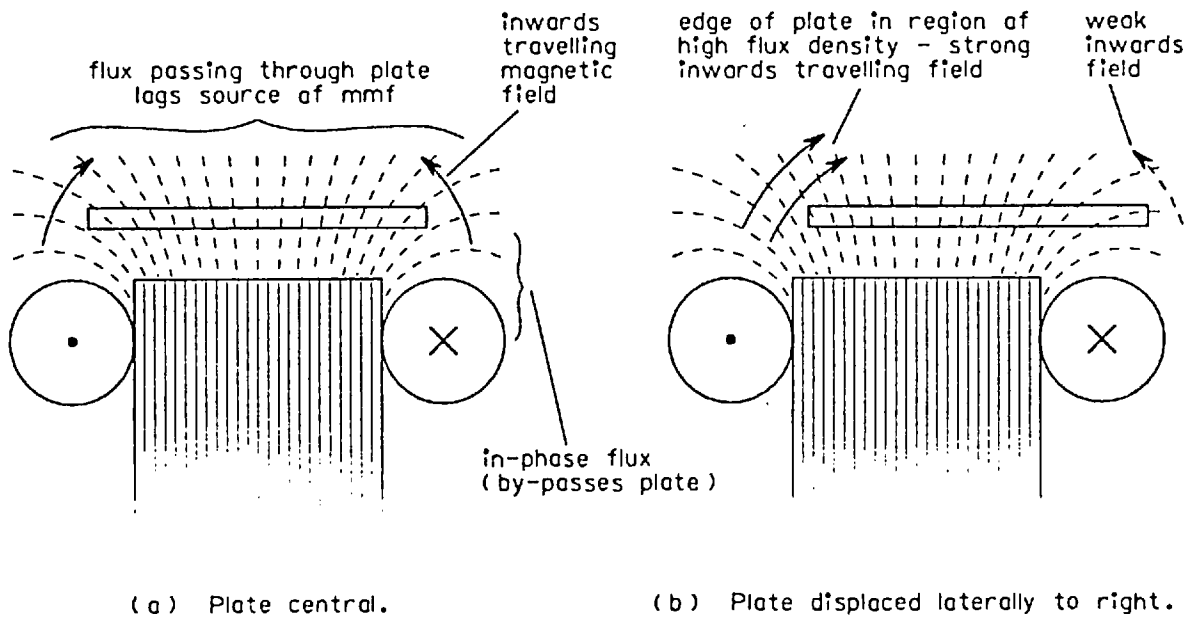


Fig 90. Shaded pole action at edges of plate over conventional linear motor.

through the plate experiences a transference (the magnetic reactance of the plate itself) in series with the reluctance of its air path, while flux "leaking" sideways without passing through the plate experiences only an air-path reluctance. The central flux therefore lags in phase behind that by-passing the plate, and at each plate edge an inwards-travelling magnetic field is created.

After lateral displacement the inner edge of the plate has moved into a region of increased flux density while the outer edge is in a region of lower flux density. The travelling field acting on the inner side therefore becomes stronger than that on the outer, with the result that the plate is thrown off, as shown in Fig 90(b). The theory is thus seen to predict correctly the unstable behaviour of a conventional linear motor.

At first sight it may appear that precisely the same argument should apply to a plate floating above an electromagnetic river, for instance as shown in Fig 91(a). Without doubt the inner edge of the plate finds itself after displacement within a stronger

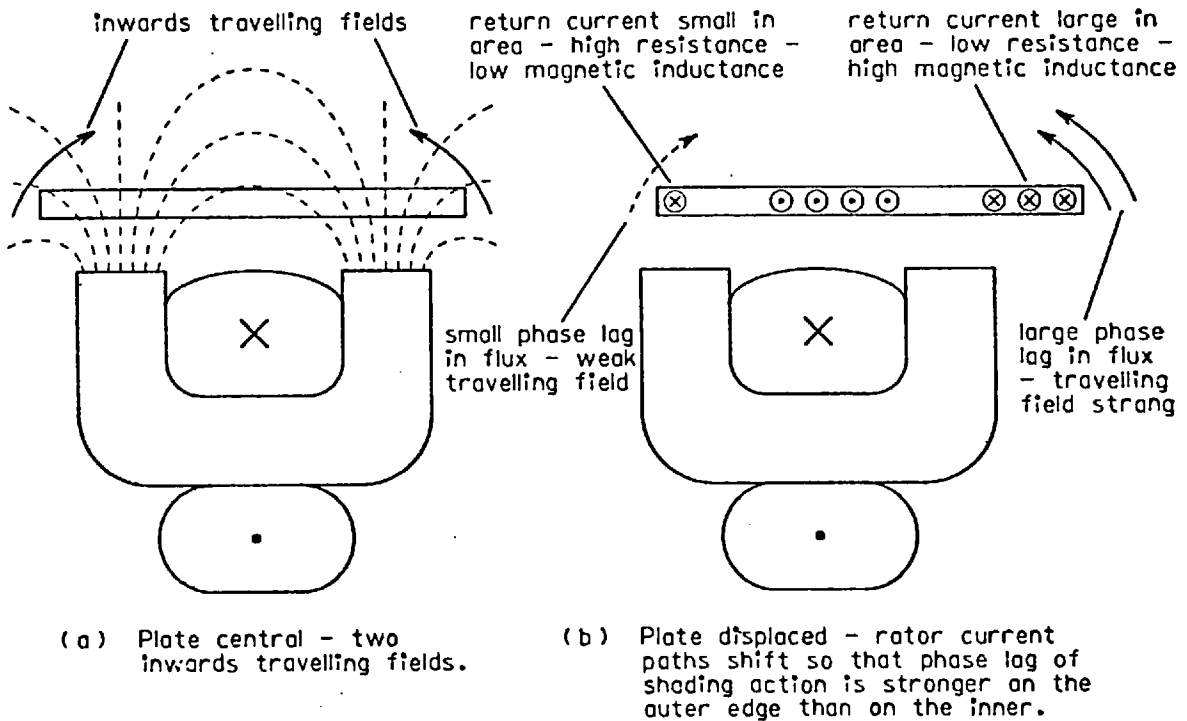


Fig 91. Shaded pole action of plate over electromagnetic river.

magnetic field than does the outer, and de-stabilising effects occur as a result. But now a second effect is present, which under some conditions can override the de-stabilising action. For the secondary current is now flowing in two loops, which in the displaced condition can be of entirely dissimilar characteristics; in particular the electrical resistances of the loops can be widely different.

Now the magnitude of the shaded-pole action produced by two adjacent magnetic fluxes differing in phase is dependent upon two factors - the magnitudes of the respective fluxes and the phase difference between them. Maximum effect is obtained for any given strengths of fields when the phase difference is ninety degrees. But the phase difference between the fluxes is itself dependent upon the magnitude of the series magnetic reactance in relation to the magnetic resistance of the remainder of the air path (as explained earlier in the chapter - see Fig 86). The value of this series transference is in inverse proportion to the electrical resistance of

the current flow paths within the shading sheet. Thus a shading sheet with paths of low resistance is seen as a large transference, causing a large phase lag and inducing a powerful sideways travelling field, while conversely a high-resistance electric circuit constitutes a small transference, with a correspondingly small shading effect.

Just such a pair of contrasting circuits is found in a laterally displaced sheet rotor above an electromagnetic river. Fig 91(b) shows the familiar situation. The main induced current above the central slot of the stator has two return paths, one a narrow, constricted path (on the left in the diagram) of high resistance relative to the other, spacious path along which most of the return current flows. Thus the inner edge of the plate, although in a region of higher flux density than the outer, can have considerably less shaded-pole effect on account of its higher electrical resistance. The low resistance current path at the outer edge constitutes a high transference, resulting in a strong shading action that provides overall lateral stability for the whole machine.

Once again it is seen that the simple theory, taking into account only the positions of the edges, is valid only when the pattern of secondary induced currents is not dependent on rotor position. As soon as an extra degree of freedom is allowed - moving rotor current patterns - an extra degree of complication is introduced into the situation. In the particular case just discussed explanation is possible only with foreknowledge of the pattern of rotor currents after displacement. Again it must be admitted that progress is still at the stage of adjusting a theory to fit observed behaviour rather than of using an established theory to predict the behaviour of an untried configuration.

There is one further experimental effect observed during the researches described in this thesis that is interesting to consider from the viewpoint of shaded-pole action. At the beginning of Chapter 2 an electromagnetic levitator was described consisting of a single pair of long pole-pieces embraced by a coil passing along

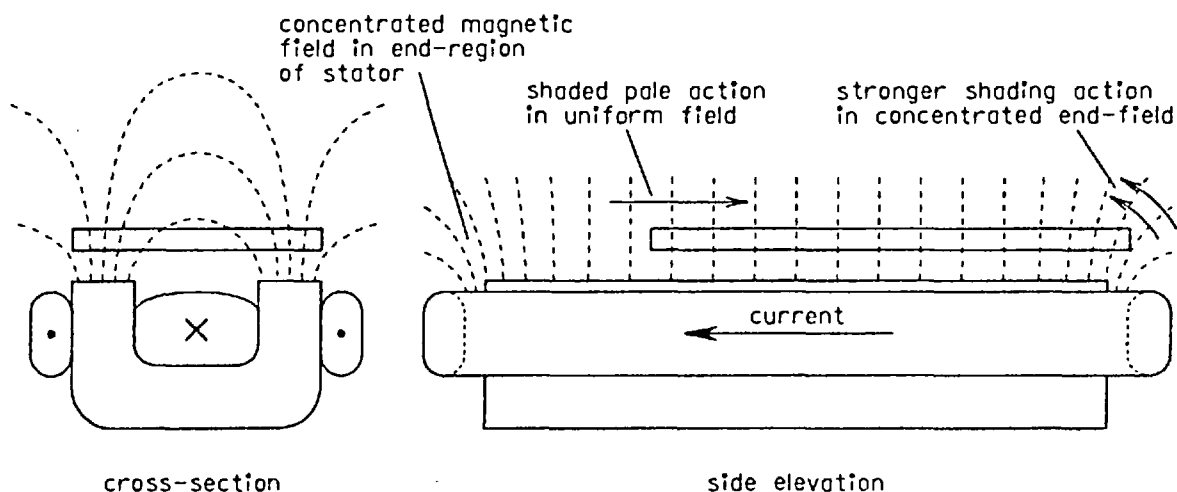


Fig 92. Longitudinal stabilisation of plate over long pole-pair machine.

the centre slot and splitting to return down the two sides (see Fig 20). It will be recalled that a critical length of rotor was found, below which plates were capable of stabilising themselves longitudinally as well as laterally. It may be that explanation of this stabilisation is possible in terms of the shading effects of the plate ends.

Fig 92 shows a cross-section and a side elevation of the machine. It seems reasonable to assume that the longitudinal distribution of the stator field might be uniform over most of the length of the machine, but would become more concentrated at the two ends as a result of the fringing fields. If this is so then the stabilising action of the plate as it approaches one end of the machine consists merely of the leading edge entering the more concentrated field and experiencing an increased inwards-travelling field from the shading action of its own end. The critical length of plate for longitudinal stability is such that when the plate is in a position of longitudinal equilibrium, each of its ends is at the region of maximum flux density within the corresponding end-region of the stator.

Thus stated the theory sounds convincing, until it is remembered that precisely the same argument should apply also to the original

flat-plate floater described in Chapter 1 (see Figs 1 and 2). This machine, however, behaves in just the opposite manner - a plate of any length approaching either end of the stator is drawn into the end region, through it, and thrown off beyond. Again the only conclusion to be drawn is that the shaded-pole approach is not sufficient to explain all the observed facts. Further investigation into the end effects of these two machines, while of no particular relevance to electromagnetic rivers, might prove interesting as a minor project for some future time.

9.7 Stability by Rules of Thumb

To return to the subject of the lateral stability of the electromagnetic river, a third approach to the problem is one making use of no more than simple "rules of thumb" such as are found in elementary teachings of electromagnetism. To begin with it is necessary to make two assumptions - that all magnetic flux produced by the electromagnetic river is composed only of vertical and transverse components, and that all rotor currents have only longitudinal and transverse components. The latter assumption is certainly true for most rotors since thin sheets are not conducive to the flow of vertical current (trough-shaped rotors being ignored for the time being). In regions remote from the stator ends it is also reasonable to assume low longitudinal components of flux.

The machine to be considered is an electromagnetic river complete with a polyphase stator supply creating a longitudinally-travelling field. Over such a stator there exist sets of transverse rotor currents spaced at regular intervals of one longitudinal pole-pitch throughout the length of the rotor. These serve to link the sets of main and return longitudinal currents. (The contrast might be noted here with machines of long pole-pair single-phase design such as that considered in the previous section (Fig 92), in which transverse rotor currents exist only in the end regions.)

In this situation two equations can be written relating the vector products of individual pairs of components of flux and induced current to the forces produced by them on the rotor, as follows:

$$\begin{array}{lcl} \text{Transverse current} \times \text{Vertical flux} & = & \text{Longitudinal force} \\ & & \text{i.e. Thrust} \quad \dots (1) \end{array}$$

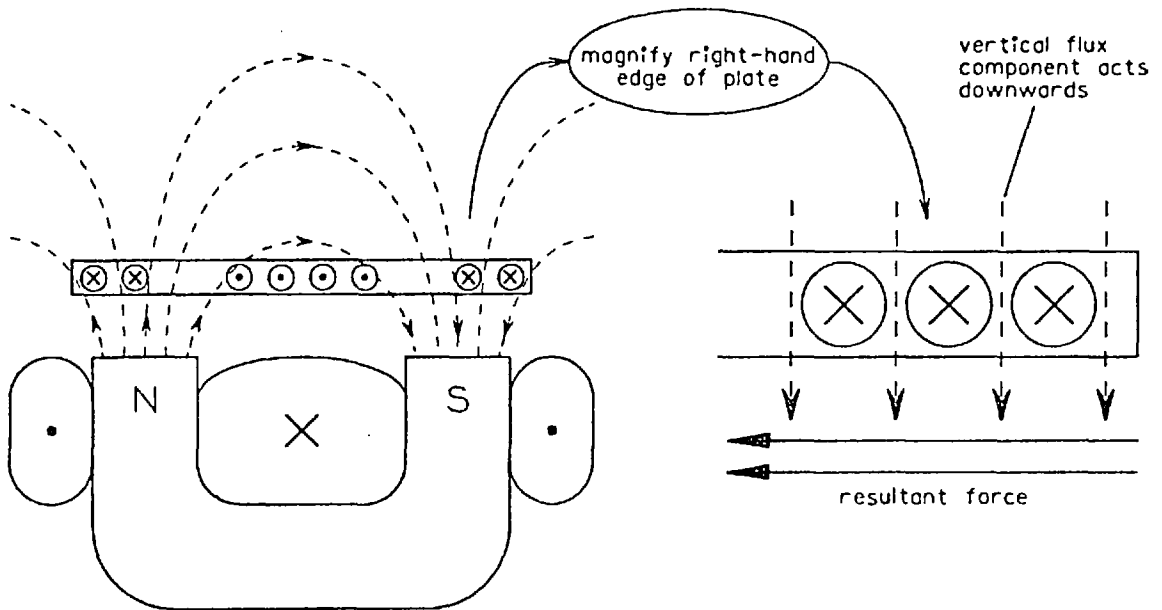
$$\begin{array}{lcl} \text{Longitudinal current} \times \text{Transverse flux} & = & \text{Vertical force} \\ & & \text{i.e. Lift} \quad \dots (2) \end{array}$$

Both these formulae, of course, are expressions of Fleming's Left Hand Rule. Such formulae of expression for forces produced by electromagnetic means may seem a little unusual, but the equations predict directly two effects with which the linear motor designer is well familiar. Firstly, equation (1) states in effect that only the transverse components of rotor current produce thrust - which is another way of saying that the longitudinal current components, often referred to as "end ring currents" in imitation of the terminology applied to their counterparts in rotary machines, are wasteful. Secondly equation (2) states that the horizontal component of magnetic flux (transverse in an electromagnetic river, longitudinal in a conventional linear motor) is alone responsible for levitation of the rotor. This explains why no lift is produced on a rotor symmetrically positioned within the horizontal airgap of a double-sided linear motor, whose flux comprises only vertical components passing across the air gap directly from one pole face to its opposite member.

But a third equation, closely analogous to the first two, can be formulated from the flux and current components existing over an electromagnetic river, as follows:

$$\begin{array}{lcl} \text{Longitudinal current} \times \text{Vertical flux} & = & \text{Transverse force} \\ & & \text{i.e. Stability} \quad \dots (3) \end{array}$$

This third equation can be used as the basis for another approach towards understanding the electromagnetic river. (The last remaining pairing of products - Transverse current \times Transverse flux - of course gives nothing since the vector product of two parallel vectors is zero.)



(a) Stator currents, rotor currents and magnetic field have directions instantaneously as shown.

(b) Right-hand edge of plate - Fleming's Left Hand Rule predicts that resultant force is to left.

Fig 93. Components of flux and rotor currents acting on plate over electromagnetic river.

Once again, the first step is to investigate from this viewpoint the forces acting on a plate in lateral equilibrium. Take, for example, a section of the electromagnetic river for which at some instant of time the effect of the poly-phase stator windings is equivalent to a pair of coils carrying currents of directions shown in Fig 93(a). Then at that instant the magnetic polarities, the directions of the lines of flux, and the pattern of rotor currents are also as shown.

Fig 93(b) shows the resulting situation for the right-hand edge of the plate. The vertical component of magnetic flux in this region is downwards (the horizontal component being ignored as irrelevant for stability purposes) and the rotor current flows into the plane of the diagram, from which Fleming's left hand rule predicts that the resulting force is to the left, i.e. inwards. On the other edge of the plate, the flux component is upwards but the current flows in

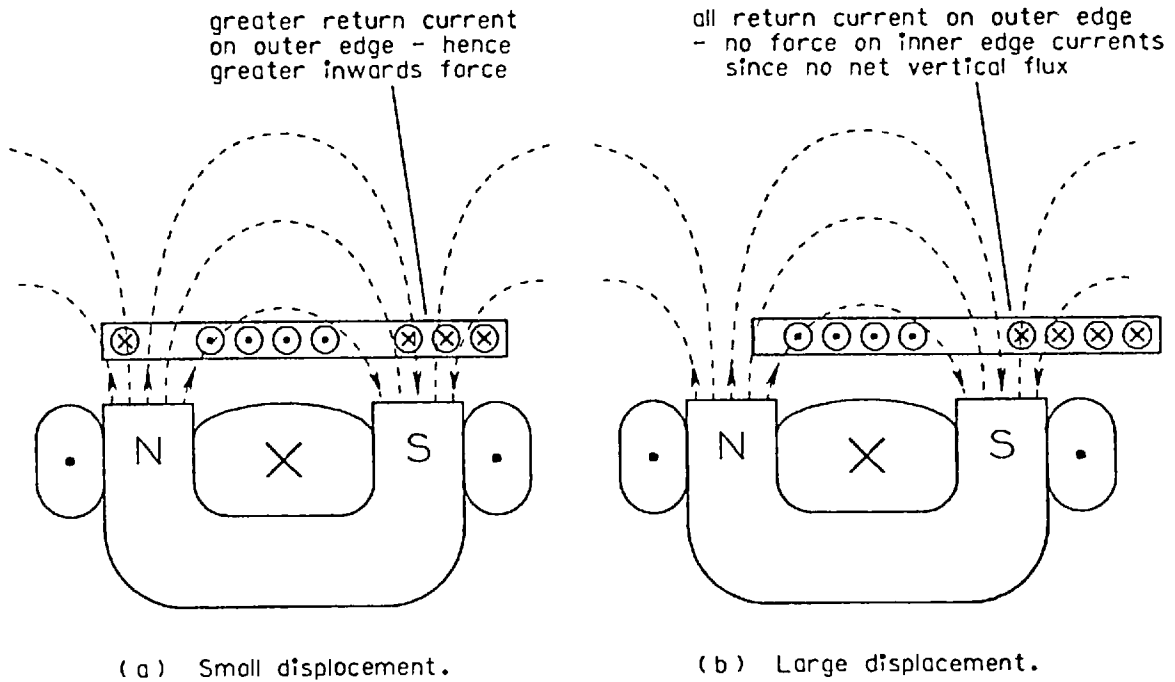


Fig 94. Flux and current components for displaced plates.

the same direction as before, so that the horizontal force is in the opposite direction - i.e. again inwards. (The horizontal force on the centre region of current is of course zero since the net vertical flux over this region is zero.)

A simple extension takes the argument to the next stage, which is to consider a displaced plate. Instead of considering a small displacement such as shown in Fig 94(a), it is more interesting to examine the effect of a large horizontal movement - sufficiently great for the return currents along the inner edge of the plate to have been reduced to zero, leaving only a single-loop pattern of rotor current as shown in Fig 94(b). In this situation the net vertical flux over the current-carrying region near the inner edge of the plate is small or zero. The horizontal force on this region is therefore likewise small. The outer edge of the plate, on the other hand, is in a region of flux whose vertical component is downwards. The resulting force is inwards, tending to return the plate to its central position.

A point of interest is that on this basis it is possible to gain a feel for the condition at which the displacement becomes so great that stability is lost. Further outward movement beyond the position shown in Fig 94(b) will result in the inner edge of the plate (the left hand edge in the figure) entering the region of downwards flux. The rotor current is here opposite in direction to that at the outer edge, and the resulting force is therefore to the right, i.e. of de-stabilising action.

The critical position, at which stability is just lost, is reached when the inner plate edge has moved sufficiently far into the downward field for the magnitude of the de-stabilising force to equal that of the stabilising action of the outer edge. Precisely how far this is is not readily predictable; the theory does not lend itself to numerical calculations. It is encouraging, however, to have found a viewpoint giving at least some insight into the loss of stability beyond a certain value of displacement, for considerations neither of attracting and repelling currents nor of shaded-pole action give any clear indication of how or where the change occurs.

In general, however, the method based on the simple "rules of thumb" suffers from the same deficiency as the shaded-pole approach - that foreknowledge is required of the field pattern, the rotor current pattern, and the way that both change as the plate is displaced, before an explanation of observed phenomena can be attempted. Prediction of the behaviour of untried machines seems equally beyond the reach of either approach.

9.8 "Hills of flux"

In a situation where theoretical techniques established elsewhere in electrical engineering prove to be of such limited value, it may be thought justifiable to consider any theory or idea, however dubious its foundation, that can help to give a feel for the phenomena involved. The following idea is one such dubious approach; it has no established theoretical basis whatsoever, only the justification that at least up to a point "it works".

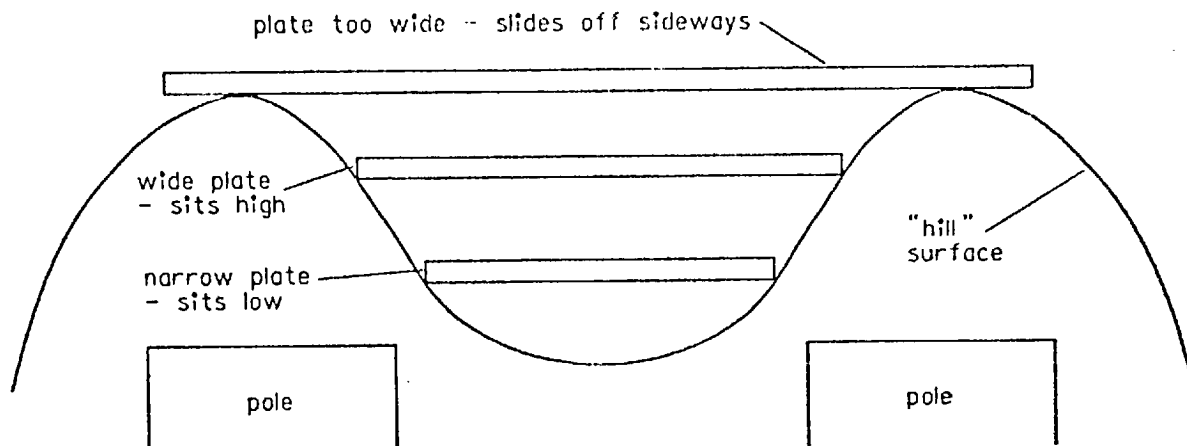


Fig 95. "Hills of flux" above a C-core stator.

Let it be assumed then, that for some reason which need not be understood, the levitation force acting upon a small region of conducting material in position above a stator is proportional only to the magnitude of the flux density within that region. A simple plot of flux density magnitude across the poles of an electromagnetic river has roughly the shape shown in Fig 95; for the purposes of this argument this is then assumed to be a plot of "levitation force distribution" across the stator. It is difficult to define any precise quantity that corresponds to the height of the resulting "hills" in the figure, and it is not suggested that the idea can be justified in any numerical manner. It is rather a question of doing "something" than "nothing".

The mechanism of stability of a floating plate is then explainable simply in terms of the action of gravity. Any conductor initially above the centre of the stator finds itself in a region of greater levitation when pulled to one side, and therefore tends to float higher. Release from the displacing influence allows gravity to pull the conductor back down to the position of minimum potential energy, symmetrically in the centre. The regions above the poles can almost be thought of as "hills of flux", creating between them a valley in which conducting plates position themselves. Narrow plates will then tend to position themselves well down within the groove, the lower

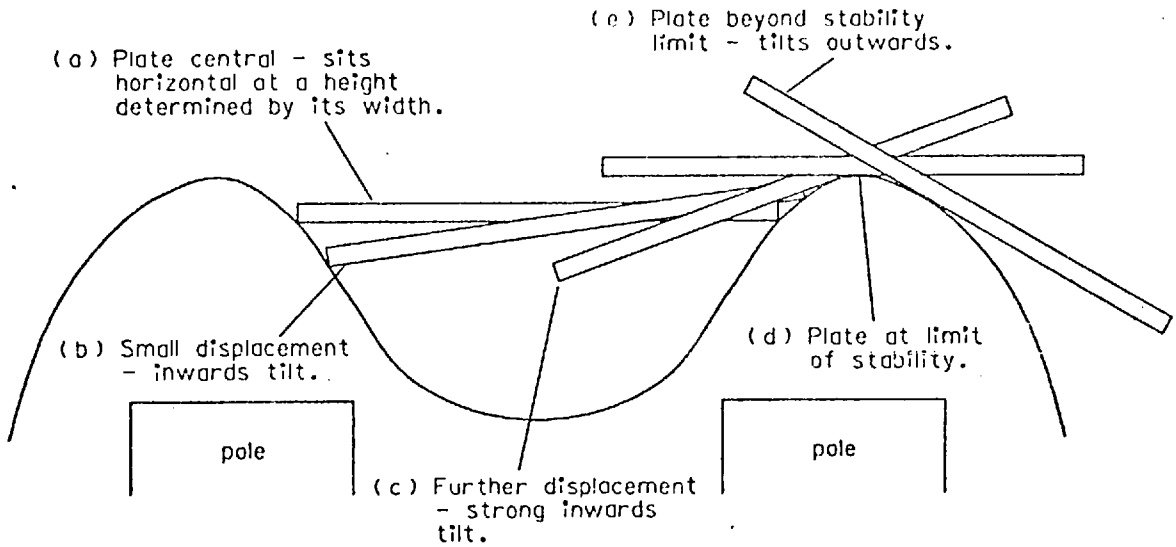


Fig 96. Progressive displacement of a plate over a "hill of flux".

limit on width being that for which the plate settles at the level of the pole pieces, and wide plates will settle higher in the groove.

The maximum width for stability is given by the distance between the "peaks" of the flux hills, since any plate wider than this distance will rest across the tops of the hills and will not have its potential energy changed after displacement - see Fig 95. This concept also explains the feeling mentioned in Chapter 1 and referred to several times since, that wide plates are generally "floppier" in their stability than narrower ones - evidently so on the above basis since they cannot sit so deeply in the valley.

Similar considerations can predict the sequence of roll motions of a plate as it is displaced progressively to one side. Fig 96 shows a plate (a) in the central position, and (b) and (c) after progressive lateral displacement to the right. It is seen that the outer edge of the plate has been made to rise up the surface of the hill, giving the plate an overall inwards tilt. Position (d) is attained when the centre of the plate reaches the top of the hill - the limit of stability. Note that the plate is again horizontal. Further displacement, into the unstable region(e) on the far side, is accompanied by an outward tilt, as shown.

When the corresponding experiment is carried out in the laboratory, it is found that the plate behaves in precisely the manner described. The "feel" of the initial strong inwards tilt upon lateral displacement, reducing back to the level position as the limit of stability is approached, is particularly striking. Indeed the theory predicts the observed behaviour so well that the "hills of flux" approach is regularly the first to be invoked for an explanation of any new stability phenomenon observed in the laboratory. It was, of course, from just such a feeling of hills, albeit from two long hills running parallel and a short distance apart, that the name "electromagnetic river" was derived.

It now becomes possible to attempt an explanation of the failure of one of the machines described in the previous chapter. Fig 78 showed the machine in question, comprising four steel blocks each surrounded by its own electric coil, mounted upon a backing sheet of steel. It will be remembered that the intention was for each pair of poles to provide stability against displacements in directions parallel to the lines joining their own centres, so that the action of all four poles together should be to stabilise in all directions a sheet floating in the middle.

The appropriate mechanical system analogous to the electromagnetic "hills" seems to be to attempt to stabilise, say, a small sphere in the hollow between four surrounding hills. It should be evident that such stabilisation is possible only if the centre point of the system is lower than the four points mid-way between adjacent hills. The observed behaviour of the electromagnetic machine suggests that it is this requirement that is lacking. Rather the system appears to resemble a situation where the centre of the machine is at a level intermediate between the summits of the hills and the points mid-way between them, so that four valleys are formed, each sloping downwards away from the centre point. The centre becomes an unstable position so that any sphere placed there will always roll away, down one of the four valleys. This corresponds with the observed behaviour of sheets

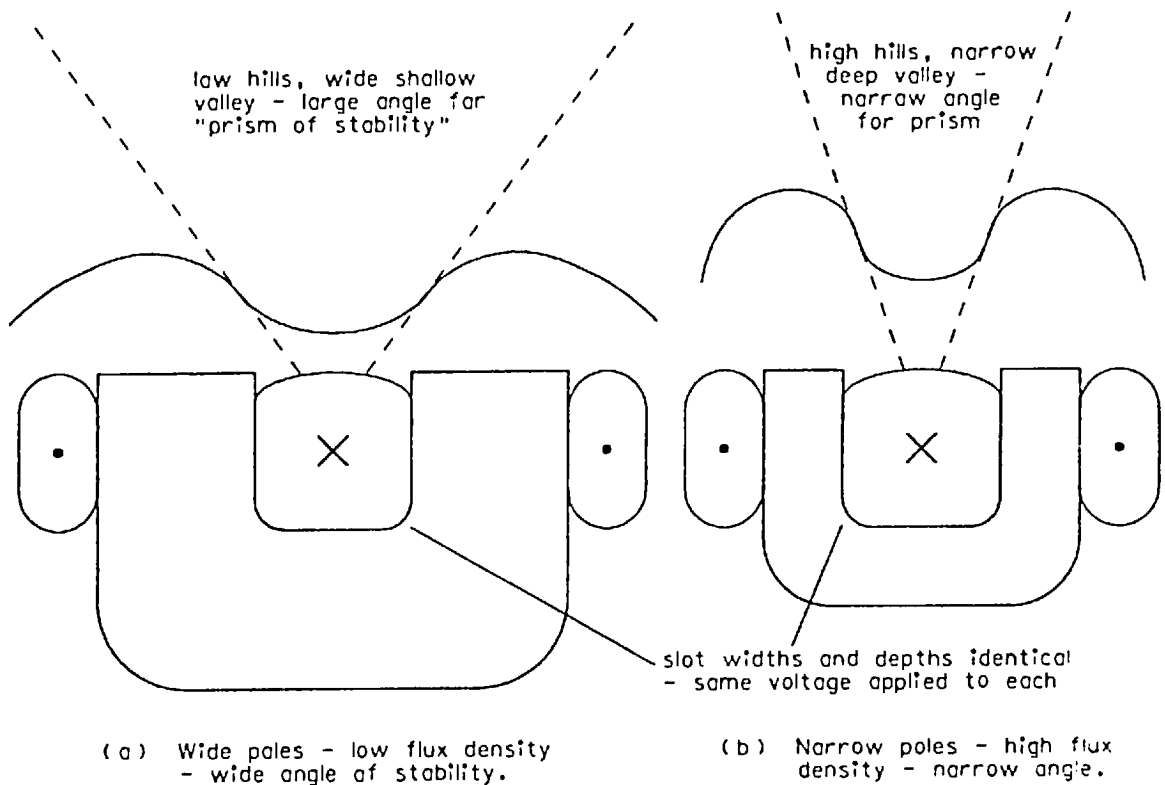


Fig 97. Effect of pole width upon "hills of flux".

of aluminium placed over the original machine, for they too always fell out of the machine along one of the four lines passing mid-way between the poles.

One further phenomenon that can usefully be considered from the point of view of "hills of flux" is that discovered during initial experiments with the gramme-ring wound linear motor blocks - that the "steepness" of the boundaries of stability of an electromagnetic river is affected by the widths of the pole faces below (see section 2 of Chapter 7 - Fig 62). If the angle of the inverted prism of stability is considered as being the maximum angle attained by the walls of the valley formed between the hills of flux, then the higher the hills, the narrower this angle will be. For two stators with identical central slots but different pole widths, such as those shown in Fig 97, the same value of voltage applied to each excitation coil

induces the same total flux to pass around each of the magnetic circuits.* This results in regions of greater flux density over the narrower pair of poles, and hence higher hills. Thus the narrow-poled machine has the narrower angle of stability.

The "hills of flux" approach completes the list of different theoretical methods and ideas developed to date for understanding the stability properties of the electromagnetic river. It is clear from the elementary nature of these explanations that the whole subject is one where practical work has gone well ahead of theoretical understanding. By methods consisting almost exclusively of trial and error (and happy accident) the original discovery of stability over only a single coil system (see Chapter 1, Fig 10) has been developed through all the stages described in this thesis into a whole new branch of electrical machine engineering.

By contrast few of the theoretical approaches described are capable of explaining much more than the simplest of the phenomena observed, and none seems likely to form the basis of a universal theory of electromagnetic-stability. Continued haphazard practical research may well lead to further developments at laboratory scale, but progress to larger and better machines is likely to be severely hampered until more adequate theoretical support is obtained. The need for further work in this field is evident.

* Total flux induced by a given a.c. voltage is independent of magnetic path reluctance (see reference 35).

CHAPTER 10

CONCLUSIONS AND RECOMMENDATIONS



A full-scale wooden model of a transverse-flux E-core linear motor design to lift and propel (but not guide) a 50-tonne vehicle.

CHAPTER 10. CONCLUSIONS AND RECOMMENDATIONS

In Chapter 1, in place of the more normal "review of relevant research conducted by others", was presented the story of the invention of a new machine. No review section appeared until Chapter 6. Continuing these slight departures from convention the present chapter, though not the last, forms the "conclusions and summing-up" section of the thesis. The reason for this is that the chapter to follow describes a further new machine, upon which research is only in its infancy; it seemed inappropriate to place an overall summing-up section directly following a chapter to which none of the remarks referred.

10.1 Review and suggestions for further work

General conclusions are in any case few, for the whole project has been one of opening new paths for others to follow rather than of exploring and concluding paths already opened. Indeed almost every chapter has ended with or included recommendations for future work, and it might be helpful to collect these together and elaborate on them a little. This can be conveniently combined with a brief review of the subject matter of each chapter taken in turn.

Chapter 1, as already stated, was the story of the invention of the electromagnetic river - the prologue to the researches described in this thesis. In Chapter 2 a stable levitator was developed, providing longitudinal as well as lateral stabilising fields, and with this levitator were carried out the first experiments into the effects of different widths, thicknesses and materials of plate. Particular attention was paid to the development destined to free electromagnetic levitation from the constraints of "cones and prisms of attraction" - the concept of single-coil levitation systems.

Chapter 3 described the building of the long pole-pair machine, the simplest single-coil levitator, from which was developed the idea of double-loop patterns of induced current existing in rotors

floating over electromagnetic rivers. The importance was also realised of the need for secondary induced currents to be allowed complete freedom of flow within the rotor in order to maintain stability. (This was further confirmed, in a different machine, in Chapter 8 - see Fig 77.) The rest of the chapter was concerned with various rotary forms of the electromagnetic river, such as the electromagnetic bearing and whirlpool - subjects which could prove interesting for further development and research.

An attempt was made in Chapter 4 to put the path of research onto a more formal scientific footing. The chapter began with measurements both of the voltage potentials within a floating plate and of the surrounding magnetic field, and then proceeded to develop a method relating the magnetic flux distribution to the real force distribution across a floating rotor, using the Maxwell Second Stress formulae. Here is a subject that could be a basis of much useful work in the future, for the method is applicable to many situations where the complete distribution of magnetic field around a component can be measured. A small amount of computing was carried out in the calculation of the force distributions using the Maxwell formulae, and computer-based graphical display facilities were employed for direct presentation of the results (see Fig 42).

There is scope here for considerable extension. A start has already been made in the laboratory by linking a tape recorder to a selector system which reads in succession the voltages picked up by the search coils measuring the magnetic field components. These search coil readings are transferred in sequence onto the tape, and in this form they become data that can be read directly by the computer. Further development of this technique, such as linking the selector output directly to a computer interface, might lead to an invaluable "on-line" system where the force distribution over a plate could be viewed on a cathode ray tube while the plate itself is being moved about over the electromagnetic river.

Chapter 5 described the introduction of phase-mixing into the electromagnetic river in order to create a more effective propulsion unit. The subsequent extension of the resulting new machine to a length of seven metres allowed the possibility of dynamic tests, followed by operation of the machine in back-to-back oscillation mode. One example of a possible industrial application of the device - shuttle propulsion - was examined at some length, and again there is scope for continued work on this and other industrial uses.

Chapter 6 was concerned with the "glamorous engineering" of high-speed transport. Full scale practical work on a subject such as this clearly falls outside the scope of a university laboratory, being rather the province of large industry or government. A number of relevant laboratory-scale experiments were described in Chapter 7, including in particular the double-stator "catamaran" motor, the use of gramme-ring wound stator blocks for simulation of various machines, and the application of static variable-frequency tests to simulate increases in scale.

A gap remaining to be filled is the investigation of changes in lift and thrust forces under conditions of relative velocity between the rotor and stator of an electromagnetic river. This and other desirable measurements suggest that a useful project might be the construction of a dynamic test rig, probably in the form of an annulus-rig. Chapter 7 ended with a description of a brief series of tests attempting to measure the dynamic stability behaviour of floating plates. Results obtained proved most difficult to interpret, and suggested that the subject is one about which far too little is known - again a good topic for some pioneering work.

Chapter 8 was complete in itself, in that it set out to design a machine for a specific purpose - to float a set of lecture notes - and eventually succeeded in its purpose. Finally Chapter 9 presented some of the ideas that have been put forward for explanation of the phenomenon of electromagnetic stability. None of these ideas carries

any pretence at completeness, and perhaps here lies the greatest scope for future work, since levitation machines and linear motors in general are poorly supported by workable theoretical backing.

It will now be appreciated why little attempt has been made to adhere to one of the accepted "fashions" of present day research in science and engineering - the use of the computer. Computing is useful only if there are established theories or numerical techniques on which to base computer programmes. Since none such existed, any computing work would necessarily have been in the nature of the development of workable programmes, which would indeed have been a valuable contribution to the subject as a whole. However the work involved in such a project could have been easily sufficient to absorb all of the three years available, and the decision had to be taken early on whether to make the research programme a practical or a computing one. Choice fell on the former.

10.2 Addition of backing steel

There remains a further major line of research which has not been tackled, and that is investigations involving the addition of backing steel to the far side of the rotor. A linear motor built to be an effective propulsion unit must have its rotor backed by iron or steel to reduce the reluctance of the magnetic circuit to a value sufficiently low to permit a workable goodness factor. The addition of a sheet of backing steel to the top surface of a floating rotor, however, introduces an additional effect, for the steel is of course magnetically attracted to the stator.

At the same time the extra flux passing through the aluminium as a result of the improved magnetic path induces larger secondary currents, which in turn act to increase the repulsion force experienced by the aluminium. Which of the two effects, the attraction or the repulsion, is the greater is determined almost solely by the overall scale of the whole system. The repulsion force between the primary and secondary currents is an electromagnetic effect, which becomes

greater with increasing size of machine, while the attraction of steel is a magnetic effect which reduces with increasing scale.* For any given proportions of steel and aluminium in the rotor, therefore, there is a critical size of machine at which the presence or absence of the steel makes no difference to the lift force. For machines smaller than this critical size, the addition of steel causes greater attraction to the stator, and for larger machines the result is greater repulsion.

Now the long electromagnetic river, the Washington model, and the associated machines present in the laboratory are all well below the critical size for a realistic amount of steel behind their respective designs. This has meant that any attempt to introduce backing steel behind a stabilised floating sheet has resulted in an immediate violent clamping down of both metal sheets to the stator. With the steel and aluminium free to move separately, the aluminium is usually ejected sideways from between the steel and the stator; if bolted together the compound rotor tends to tip over sideways to bring one edge into contact with one of the rows of pole-pieces, so that at least that edge of the steel is as close as possible to the stator. Under these conditions research into levitation is of course impossible.

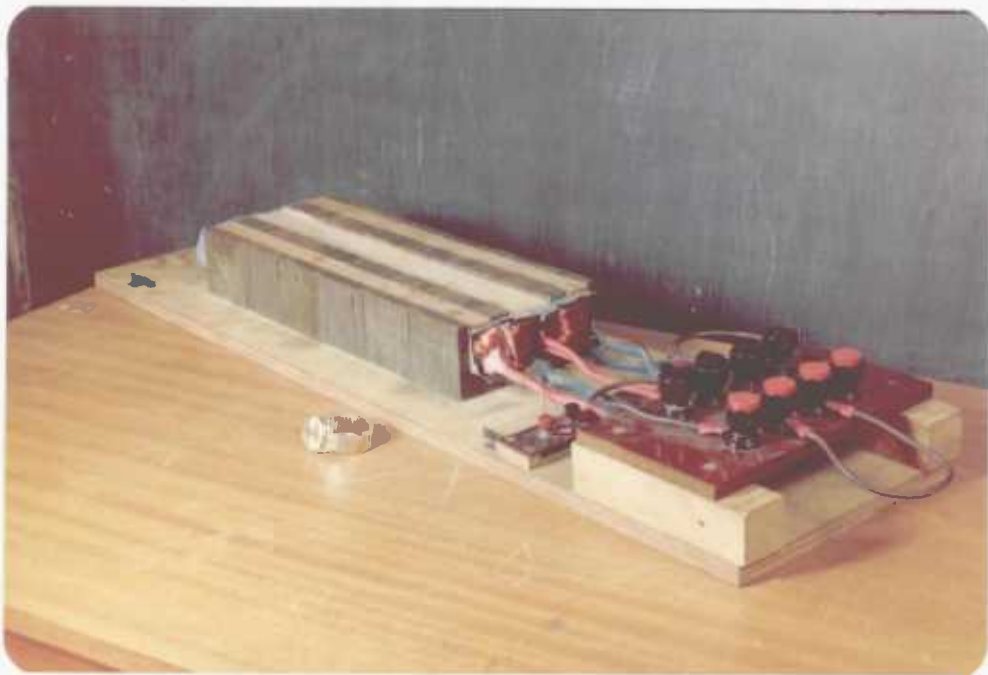
However the subject is an important one; a full-scale transport system, for example, would inevitably require backing steel behind the aluminium track, and it will become essential to discover the effects that this will have on the stability properties of a floating stator. The most promising approach to the problem would probably be to employ high-frequency supplies to simulate increases in scale, and to use these to find the critical size at which the addition of backing steel has no effect upon lift. The next stage might then be to build a machine as big as, or bigger than, this critical size, for testing at mains frequency. Such a project would undoubtedly prove a worth-while subject for further research. .

* see section 2 of Chapter 6 (p 121) and reference 18 for definitions of the terms "electromagnetic" and "magnetic" in this context.

In conclusion let it be repeated that in the electromagnetic river is found a truly remarkable machine - a machine capable of providing lift, guidance and propulsion all from one set of electromagnetic coils, capable like all transverse-flux motors of propelling at speeds of 400 km/h and beyond from a mains frequency supply, able to perform as a frictionless rotary bearing or as a linear self-sustaining floating shuttle, and no doubt capable of being applied in many ways yet to be discovered. Moreover all these applications, with the exception of velocities greater than 50 km/h, have been demonstrated on a laboratory machine of width only ten centimetres. The machine is an electromagnetic one, which must necessarily improve with increasing scale. It is to be hoped that the work described in this thesis will form the beginnings of the development of an important new subject in electrical engineering - an exciting subject and possibly a profitable one for industry, certainly a fascinating one for research - the subject of electromagnetic rivers.

CHAPTER 11

POSTSCRIPT - THE XI-CORE MOTOR



The prototype Xi-core levitator (p 246).

CHAPTER 11. POSTSCRIPT - THE XI-CORE MOTOR

In this chapter a machine is described that does not form part of the sequence of machines discussed in Chapters 1 to 10. Rather it stands on its own, as the prototype of a whole new category of motors, much as the Washington model stands as the prototype C-core electro-magnetic river. The new machine was invented and patented⁽³⁶⁾ towards the end of the three-year period of research, and the available time remaining allowed no more than a preliminary appraisal of its capabilities. It is for this reason that the chapter has been headed "postscript", for most of the subject matter to be presented would be well placed as "Chapter 1" of a thesis based on research yet to be carried out in continuation of these initial investigations.*

11.1 Kilowatts per tonne

The train of thought leading to the invention of the new machine was somewhat more logical than the sequence of events which produced the Washington model - indeed in retrospect the idea appeared so simple that its only remarkable feature was that the time of invention had been so long delayed. To understand the process of development it is necessary to introduce a new concept, which for want of a better term is usually referred to by the units in which it is expressed - "kilowatts per tonne". This is simply a measure of the input power required to a machine per unit weight of rotor lifted. Evidently the quantity is measurable for any levitating device, and for an electromagnetic machine its numerical value will in general change with different designs of rotor over a given stator. Its value will also be highly dependent upon the clearance between rotor and stator at which the measurement is taken.

As it stands the quantity is particularly relevant to designs of the various high-speed ground transport systems described in Chapter 6. Four systems were described in section 2 of that chapter. Of these, the air cushion support, the magnetic suspension and the superconducting

* see reference 37 for some continuation work recently completed.

d.c. coil systems all require considerable power inputs simply to float their respective vehicles. In the case of the Hovertrain the power requirement for support is simply that drawn by the air pads, and this is essentially constant for all vehicle speeds. The superconducting system appears to absorb only small quantities of refrigeration power to maintain the d.c. currents in the superconductor, but as the vehicle accelerates the linear motor propulsion unit has to work against the electromagnetic drag of the strong d.c. field sweeping through the secondary conductor. The resulting extra power drawn by the motor must be attributed solely to the provision of support and guidance, since it has to be supplied in addition to the normal requirements of the motor for propulsion.

The magnetic attraction system claims a low value of support power input, being merely that dissipated by the current in the solenoid providing the levitation force. Here however the relevant quantity is rather the power absorbed in the feedback amplifier system that controls the currents in the solenoid so as to maintain a constant air gap. This last figure, particularly as applied to a moving vehicle exposed to all the disturbances entailed by high velocity travel, can be many times the value required by the system undisturbed at standstill.

The fourth of the systems, using repulsion forces between permanent magnets, of course requires zero power in order merely to obtain lift. But once again another consideration must be taken into account - in this case the power absorbed by whatever guidance system operates to overcome the powerful instability tendencies of the main support.

Each of the power input quantities outlined above must be supplied to the respective vehicle in addition to the power required by the propulsion unit. But the electromagnetic river is different. In general the concept of kilowatts input per tonne weight lifted has meaning only for configurations of the machine built to provide levitation without propulsion. A number of such machines have been

described in earlier chapters; for example the "magic carpet" machine of Chapter 2 (see Fig 13), the long pole-pair and the various circular machines of Chapter 3 (see Figs 20, 26(b) and 27), and all the motors of Chapter 8. Some of these machines employ a single-phase current supply while others create two or more opposing travelling fields arranged so that the net motion of the rotor is zero. For either type the input power is drawn solely for the purpose of floating the rotor, and the number of kilowatts drawn per unit weight supported can be measured.

In a true electromagnetic river, however, in which the rotor is propelled by a travelling field while simultaneously experiencing lift and guidance, the situation is less simple. The power input is that required to supply the losses involved in setting up the stator and rotor currents which between them produce the forces of lift, guidance and propulsion, and any attempt to specify the distribution of input power between these three functions is usually meaningless. Only in a few selected cases can a sensible assessment be made. For example although the original Washington model of Chapter 1 provided weak longitudinal propulsion, it was clear that the great majority of the input power was used merely to lift the rotor. Measurements later confirmed this when it was found that only five per cent of the input power appeared as "synchronous rotor power" - the theoretical maximum output power able to be developed by the rotor for the production of thrust (see section 1 of Chapter 5).

At the other end of the scale is the sophisticated electromagnetic river in use as a system for high-speed ground transport. Here it is necessary to provide large quantities of power just to maintain a high velocity against air resistance, and it is the "magic" of the electromagnetic river that without dissipating any extra power the forces of guidance and lift are extracted from the very currents that are reacting against each other to produce thrust. The "kilowatts per tonne" value for this machine under these conditions is zero.

Lift and guidance for zero power input is not, however, the complete story. Since the time of the Washington model it has been recognised that all the "expanding geometry" machines built in the laboratory, whether circular or linear, propulsive or static, have suffered from a considerably lower value of power factor than most of their counterparts of earlier design. In the testing of small laboratory models this is of little consequence unless the resulting current requirements exceed the rating of the available supply. But on board a vehicle the motor power factor becomes of prime importance, since once the necessary power rating and the maximum voltage rating of the machine have been fixed it is the power factor that determines the input current - which in turn defines the ratings of the brushes, pantographs, catenaries or whatever system is used to convey power into the moving vehicle.

The term used to quantify these new considerations is similarly expressed as the name of the units in which it is measured - "kilovolt-amperes per tonne" or "kVA per tonne". It is this term, rather than the simpler "kilowatts per tonne", which the engineer must seek to minimise in the design of a high-speed vehicle.

11.2 A new geometry

During discussions about various means to improve the power factor of the long electromagnetic river it was pointed out that some years beforehand a change in geometry had resulted in a considerable improvement to the single-sided conventional linear motor. Perhaps a similar change could be applied to the electromagnetic river. The change in geometry involved new shapes of iron core, and there eventually emerged a logical sequence of shapes whose first three steps included the longitudinal and transverse-flux conventional linear motors and the electromagnetic river, and whose fourth step became the new machine that is the subject of this chapter.

Fig 98 shows cross-sectional representations of the first four basic machines of the progression. Fig 98(a) is a conventional

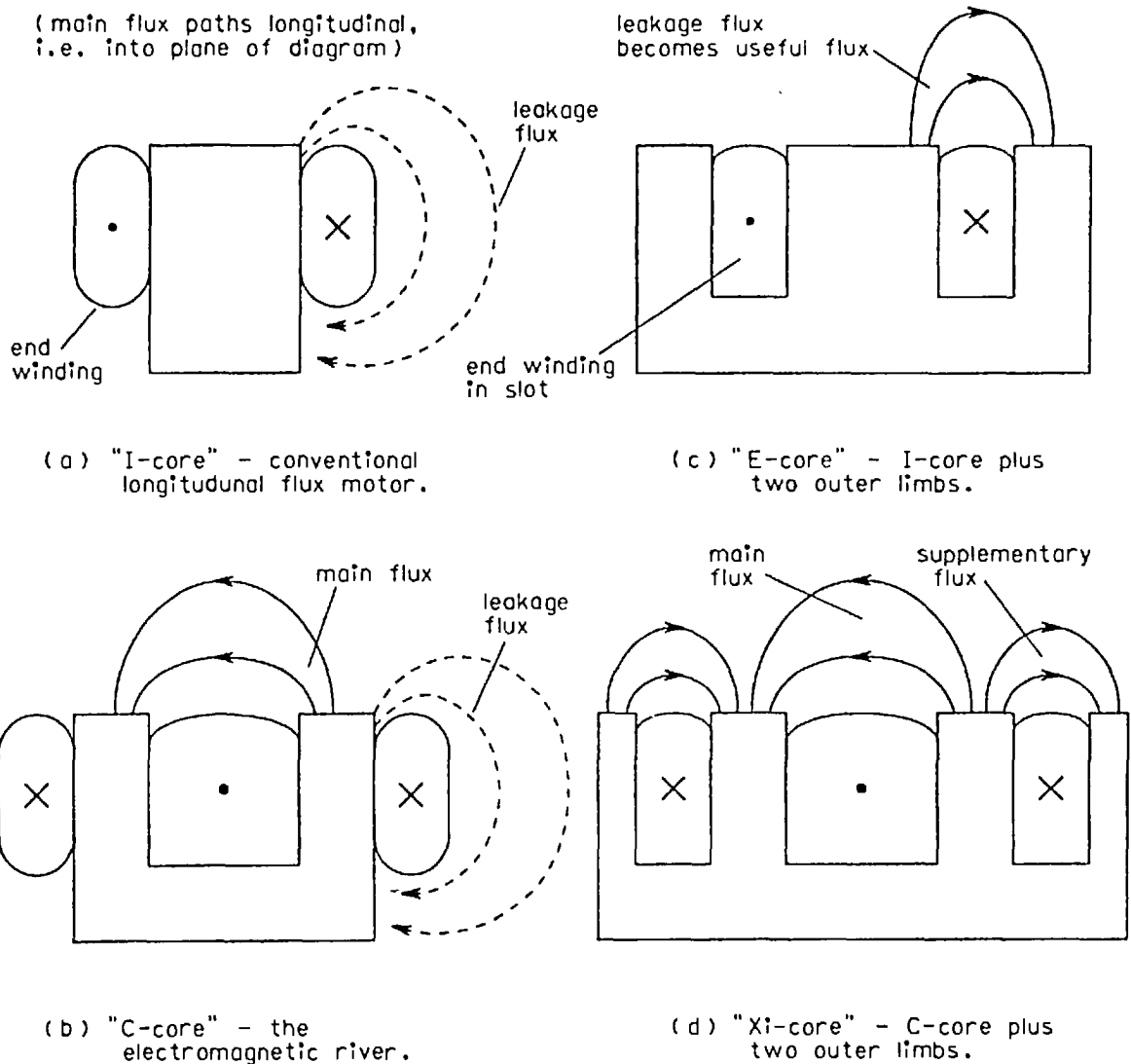


Fig 98. Origin of the Xi-core motor.

longitudinal-flux linear motor built on an "I-core" of laminated iron. Fig 98(b) is the electromagnetic river - the C-core stator. Now even in an I-core longitudinal flux motor a considerable quantity of magnetic flux can "leak" transversely from the top of the pole faces, passing around the outside of the end-windings, below them and back into the core. The idea had occurred several years ago to modify the shape of the iron core in such a way as to make use of this wasted flux.

Fig 98(c) shows the modification. Two extra limbs were added, transversely laminated, each extending sideways from the base of the "I-core" and upwards round the outside of the end winding to form new pole faces at the same level as the original limb. The end windings became enclosed in slots, and the "leakage" flux was made to pass across the top of the motor with a much shorter air-path than before, thereby improving the power factor of the machine. In addition some of the re-directed flux passed through the secondary conductor, providing extra lift and thrust. This kind of motor has become known as the "hybrid" machine because it has both longitudinal and transverse flux paths. Its E-core stator is also seen with all its laminations transversely aligned to eliminate longitudinal flux entirely, this being of course the basic design of a transverse-flux motor. (28 and 29)

The same process can be applied to the C-core of Fig 98(b). The addition of two extra limbs to enclose the leaky end-windings in slots results in a four-limbed machine, which was given the name "Xi-core", derived from the Greek letter ξ (Xi) which could be considered to have the form of an elaborate E.

There seemed no reason to suppose that the effects of the change on the lift and thrust capabilities and on the overall power factor of the machine would not correspond to the improvements in developing the I-core to the E-core design. But prediction of the effects on properties of stability or guidance was a different matter. As has been discussed in Chapter 9, analytical procedures capable of handling changes of this kind have not yet been forthcoming, and even simplified semi-practical considerations (such as magnetic field plotting by the use of a conducting paper analogue) were of no help in a situation where one main stator flux path had been replaced by three. It was decided therefore to build and test a Xi-core motor.

11.3 Design of the Xi-core motor

The design of the model was planned with rather more care than had been the case with some of the earlier models already described (many of which were conceived and hurriedly constructed to meet deadline dates for various lectures or exhibitions that called for live demonstration machinery). Firstly, to allow as easy as possible a comparison between the new machine and its predecessors, the central two limbs, the slot between them and the backing section below were designed with the same cross-sectional dimensions as the C-cores used in the long electromagnetic river. The two outer slots were made the same depth and half the width as the centre slot (since each was to embrace windings carrying half the return current), while the two outer limbs were somewhat arbitrarily given half the width of the two central limbs. Finally the longitudinal dimension of each block of laminations was made similar to (in fact slightly longer than) that of the long electromagnetic river blocks, so that similar electric coils could be used in the construction of the complete motor, arranged in the same manner as shown in Fig 44 for the long C-core machine.

One complete stator block for the new motor is illustrated in Fig 99. Six similar blocks were constructed, with the intention eventually of building a three-phase machine two pole-pitches in length. However it was felt prudent to construct a single-phase version first, so that initial investigations could be carried out without the complication of a longitudinal travelling field. The six blocks were therefore mounted together, to form four long poles carrying two windings both passing the whole length of the machine.

Before proceeding with construction of the coils, an attempt was made to estimate the probable inductance of the windings embracing all six stator cores, so that sensible quantities could be chosen for the number of turns required per coil and for the current rating of the wire. The method used was an extension of a well-known formula for estimating the approximate inductance of a group of wires

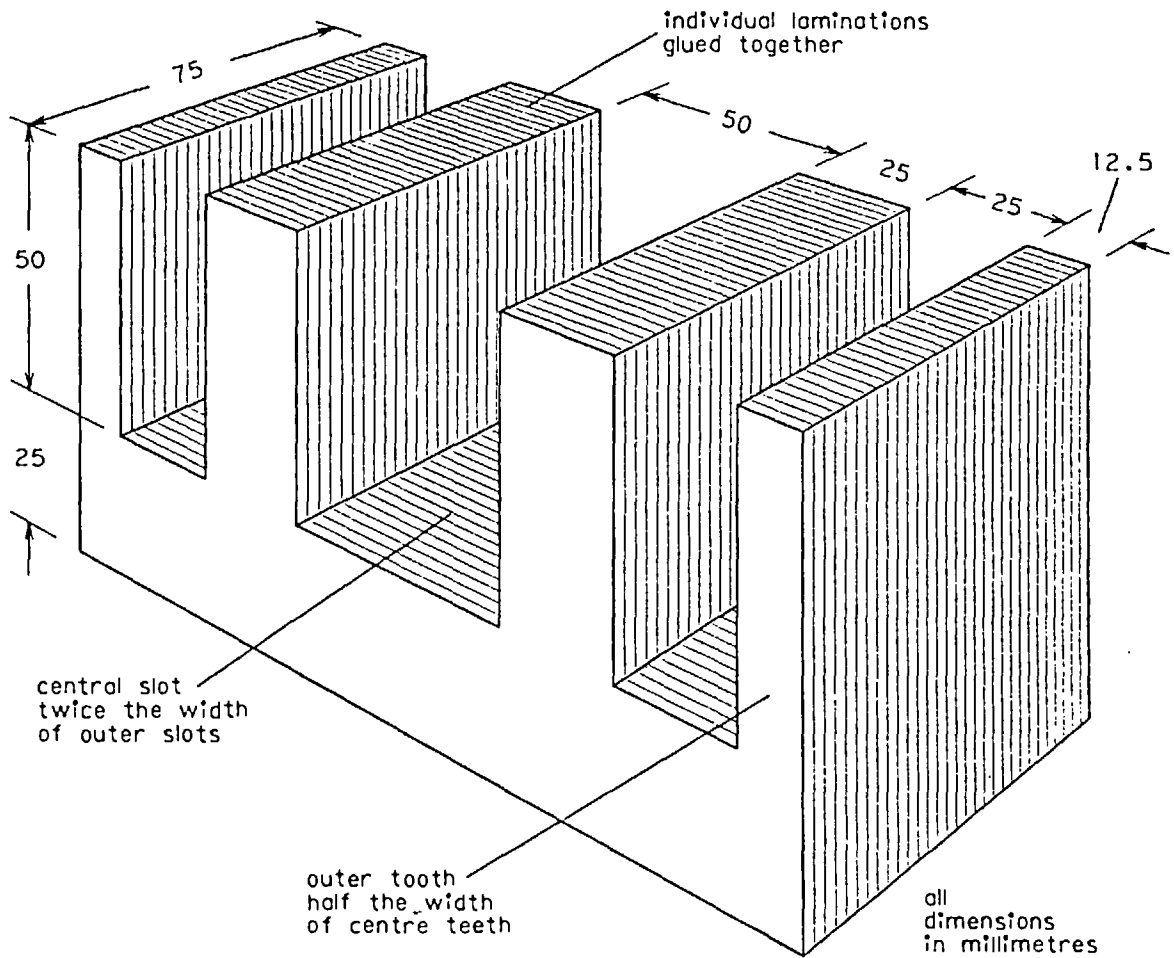


Fig 99. One stator block of the Xi-core motor.

in a single slot. The standard formula is that the inductance of a coil in a slot such as that shown in Fig 100(a) is given by:*

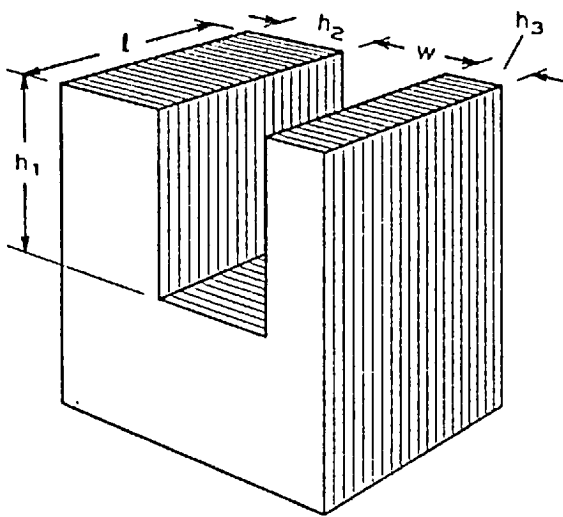
$L = N^2 \lambda$ where L is the inductance,
 N is the number of turns in the slot,
and λ is given by:

$$\lambda = \ell \mu \cdot \left\{ \frac{h_1}{3w} + \frac{h_2}{w} + \frac{h_3}{w} \right\}$$

where ℓ , h_1 , h_2 , h_3 and w are the dimensions defined on the diagram of Fig 100(a),

and μ is the absolute permeability of the space inside the slot (normally μ_0 for "free space").

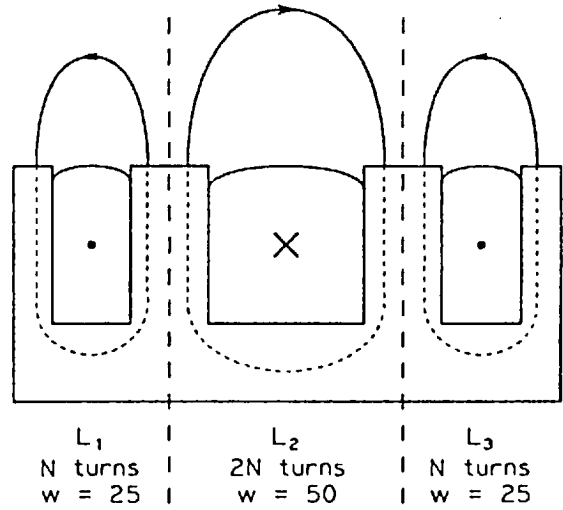
* see footnote on derivation of formula on next page.



approximate inductance of N turns in slot is

$$L \approx N^2 l \mu \left\{ \frac{h_1}{3w} + \frac{h_2}{w} + \frac{h_3}{w} \right\}$$

(a) Single slot - C-core



$h_1 = 50$, $h_2 = h_3 = 12.5$
(all dimensions in millimetres)

(b) Xi-core considered as three slots in series.

Fig 100. Dimensions used in formula for estimating inductances of C-core and Xi-core.

Adaptation of this formula to the four-limbed block was made by considering the total inductance of the Xi-core to be the sum of the inductances L_1 , L_2 and L_3 of the three component slots taken

Footnote on derivation of approximate inductance formula:

The derivation of the inductance expression of the previous page is straightforward. The first term is the self inductance of a slot of depth h_1 , filled with N turns of conductor, ignoring the mutual coupling between individual turns. This is obtained by integrating the expression for the elemental inductance $\delta L = \frac{n^2 \ell \mu}{w} \cdot \delta y$ of an element of slot of depth δy at height y from the bottom of the slot, over the range 0 to h_1 (where n is the number of turns enclosed up to height y , equal to $\frac{y}{h_1} \cdot N$).

The second two terms take account of the widths h_2 and h_3 of the pole faces on either side of the slot, on the assumption that their effect is the same as if the slot were extended to a depth $\{h_2 + h_3\}$ above the top of the conductors, all flux then being contained within this depth. The term $\frac{N^2 \ell \mu}{w} \cdot \{h_2 + h_3\}$ is the expression for the extra inductance so introduced.

in series, as shown in Fig 100(b). Clearly L_1 and L_3 are equal, so that the total inductance L_T is given by:

$$\begin{aligned} L_T &= 2L_1 + L_2 \\ &= 2N^2\lambda_1 + (2N)^2\lambda_2 \end{aligned}$$

where λ_1 and λ_2 are the relevant quantities appropriate to L_1 and L_2 respectively,

$$\text{or } L_T = N^2\lambda_T$$

$$\text{where } \lambda_T = 2\lambda_1 + 4\lambda_2.$$

Using the dimensions given in Fig 100(b),

$$\lambda_1 = \frac{5}{3} \cdot \ell\mu$$

$$\lambda_2 = \frac{5}{6} \cdot \ell\mu$$

$$\text{whence } \lambda_T = \frac{20}{3} \cdot \ell\mu.$$

With the six stator blocks making a total length of $\ell = 0.45$ m (and taking the permeability to be that of free space, i.e. $\mu = 4\pi \times 10^{-7}$ H/m), the resulting value for λ_T is:

$$\lambda_T = 3.77 \text{ } \mu\text{H}.$$

A quick practical test was made to verify this result. A length of heavy-duty double flexible mains conductor, p.v.c. plastic insulated, was wrapped several times around each of the two centre poles of the Xi-core, passing along the centre slot and back along both side slots exactly as would a normal winding. Twenty turns were required around each pole to fill the slots. The theoretically predicted inductance of twenty turns of winding on a Xi-core is given by $(20)^2\lambda_T$, which with the value for λ_T calculated above gives an inductance of 1.51mH. The practical measurement was made by passing a known current through one circuit of the double conductor while reading the voltage induced in the other. This gave the result that 13 volts were induced by a current of 29 amps (at 50 Hz), yielding a self-inductance of 1.43mH.

Such agreement was taken to indicate that the theoretical value obtained for λ_T was sufficiently reliable for design to proceed. (In fact this "instant plastic winding" test technique can in itself be a valuable aid to design, applicable to many types of machine. Its particular feature is that by filling each slot to capacity the space distribution of each winding is properly simulated.)

The rest of the design for the Xi-core winding was straightforward. In view of the usefulness of high-frequency test procedures such as those described in section 8 of Chapter 7, it had been decided from the outset to build the stator of the new motor with electrical characteristics matching the output of the only available high-frequency generator. This dictated a winding reactance at 50 Hz of 0.3Ω , from which it followed that the necessary number of turns round each pole was sixteen (given by $0.3 = 2\pi f N^2 \lambda_T$). It happened that about 700 strands of a conveniently available size of enamelled copper wire would fill comfortably the space within the slots, giving 44 strands per turn of the winding.

In practice the coils were constructed with each turn composed of 41 strands, arranged in two independent groups each of 20, and one individual strand. The two groups could then be connected in parallel to match the frequency-changer, or in series giving an impedance of 1.2Ω , being rather more suitable for connection to the 50 Hz laboratory supply. The remaining strand was intended as a "shadow coil", having induced in it a directly measurable voltage equal to the "back e.m.f." present in the main coils (i.e. the "shadow voltage" as measured is the component of supply voltage remaining after deduction of stator resistive drop). Fig 101 shows the completed machine, with its electrical connections.

11.4 Performance of the Xi-core motor

Upon initial testing of the complete machine the most immediate impression was that the guidance forces acting upon floating plates were far stronger than their counterparts produced by the long

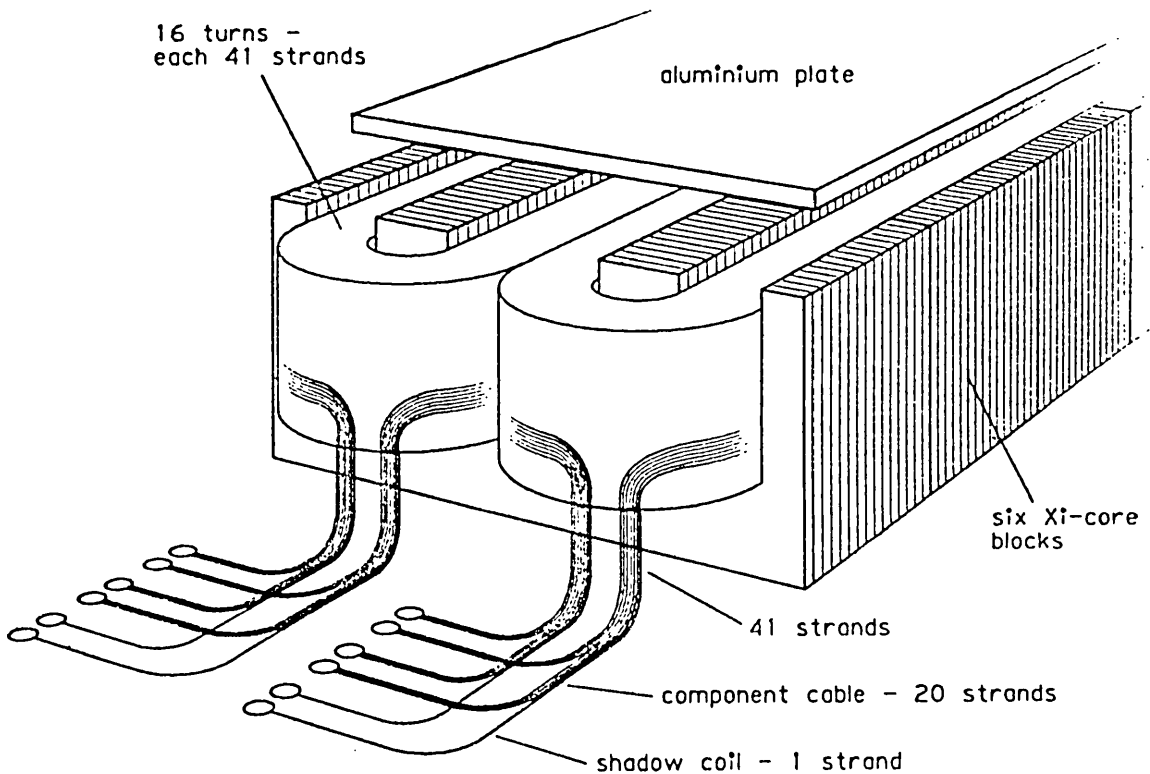


Fig 101. The single-phase Xi-core motor.

electromagnetic river and its predecessors. The lift force for a given input current also appeared to have been considerably improved. It seemed probable that both these effects were the result of the extra flux produced above the two side slots acting on the edge regions of the plate, this action being in addition to the main flux acting in the centre region.

However the expected improvement in power factor was not quite as great as had been hoped. The measured value at 50 Hz, with no secondary plate present, was 0.1 pf, compared with about 0.03 for the long electromagnetic river. Both figures would of course be greatly improved with the addition of backing steel to an aluminium secondary, but as explained briefly in Chapter 10 (pp 237 and 238) experiments involving the use of steel are impracticable on a small scale.

It was soon realised that, as so often happens in researches of this kind, the effects originally considered mere fortunate bonuses incidental to the main purpose of the Xi-core were in fact ample justification in their own right for continued interest in the machine. The series of investigations that followed revealed the Xi-core motor as a powerful levitator with guidance properties far superior to any machine hitherto constructed.

One of the first series of measurements to be made on the completed motor was of the kilowatts input required per tonne weight of secondary floated, for various widths and thicknesses of aluminium plate. (A set of plates was prepared for the purpose, similar to the test sets described for the "magic carpet" machine in Chapter 2. All were of the same length, and all plates of the same thickness were cut from a single sheet to ensure equal resistivities of aluminium.) For each plate the voltage applied to the stator was increased gradually until the plate just floated, and measurements of voltage, current and power input were taken at that point. A simple mechanical structure was built around the machine to maintain the longitudinal position of floating plates (since the machine provided of itself no action in a longitudinal direction), and also to restrain laterally those plates that were not themselves inherently stable when floating at only a small clearance. Sets of measurements were taken at several frequencies, from 50 Hz to 250 Hz.

Fig 102 shows a selection of the results, obtained for two thicknesses of plate and at two frequencies. An obvious deduction from the shape of the curves is that the criterion for minimum power input per unit weight lifted is simply "the wider the better", at least for widths of plate up to about 15 cm. This of course is in direct conflict with the criterion for maximum lateral stability, which in all machines of the expanding-geometry type requires the plates to be as narrow as possible. Fifteen centimetres was found to be the maximum width of plate that could be stabilised over the Xi-core without resorting to unduly large currents.

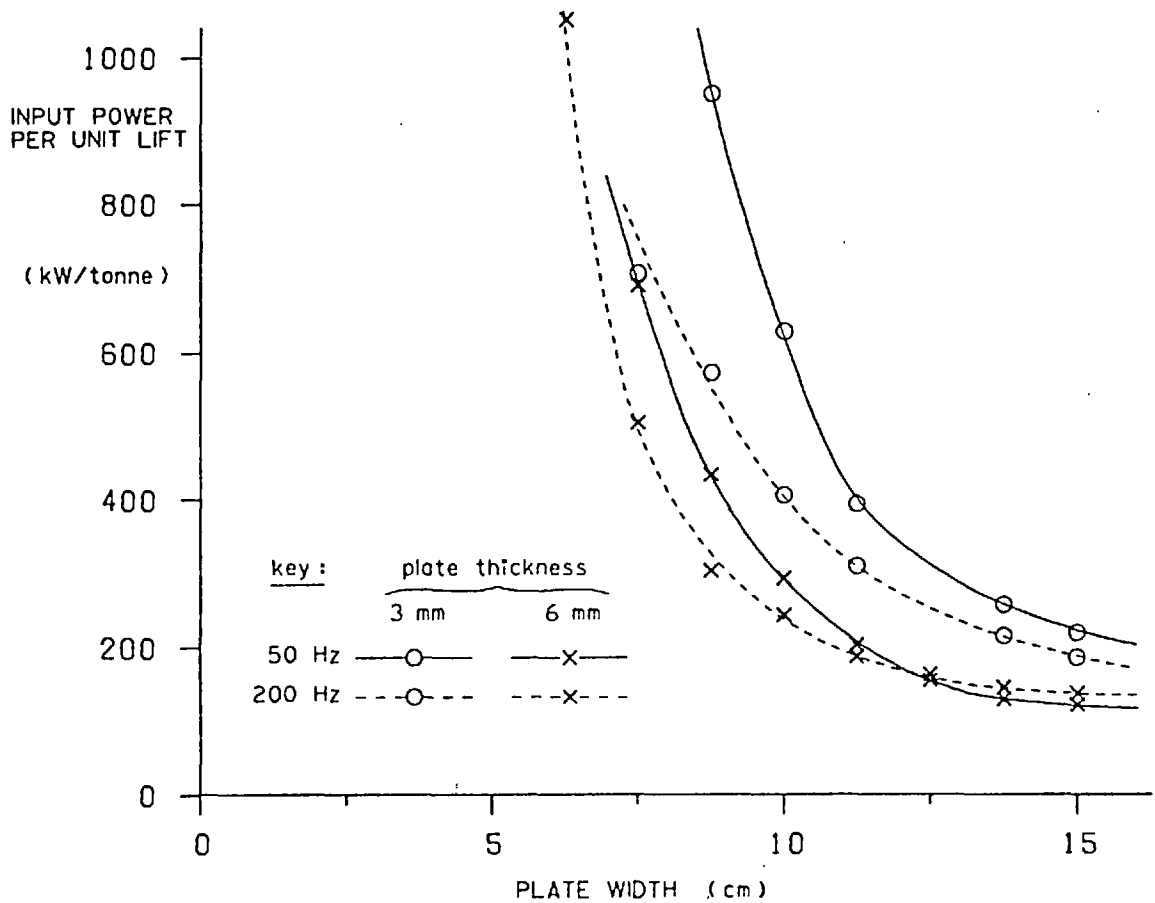


Fig 102. Graph of kilowatts input per tonne weight lifted plotted against plate width, with plates just lifting off Xi-core motor.

For a three-phase Xi-core motor, however, built as an efficient propulsion unit such as might be required for purposes of high-speed transport, the information displayed in Fig 102 is of little value since the effective power input per unit weight lifted is in any case zero (as explained earlier in this chapter). Relevant data for this situation is total volt-amperes per unit weight of secondary. A display of such data is given in Fig 103, taken for the same two thicknesses of aluminium plate over the same range of widths and under the same sets of conditions as the results of Fig 102. (Note that the numerical values for the vertical scale of Fig 103 are ten times greater than those for the corresponding scale of Fig 102, horizontal scales being equal.)

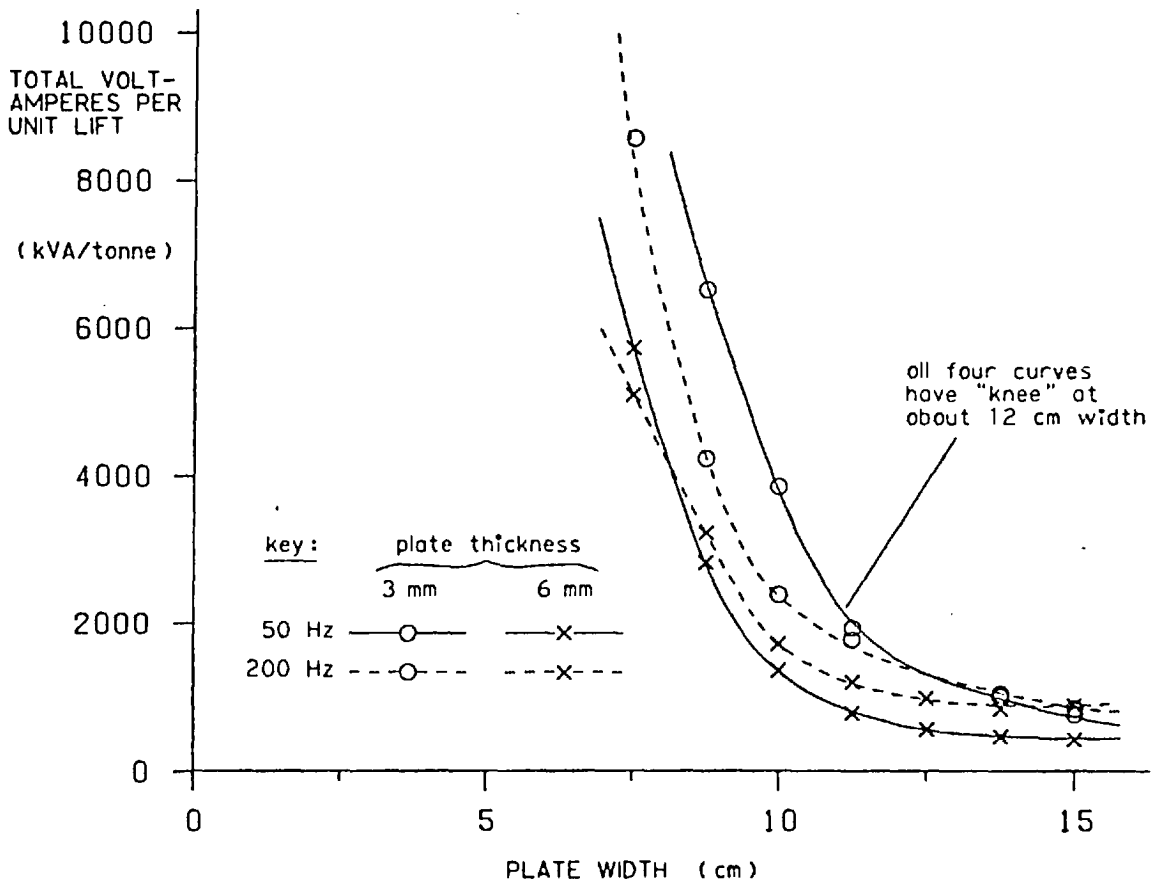


Fig 103. Kilovolt-amperes per tonne weight lifted plotted against plate width, with plates just lifting off Xi-core motor.

A particular feature about the kVA/tonne data is that each of the curves displayed has a "knee" at a width of about 12 cm. Below this width the kVA input increases rapidly while above it decreases only slowly if at all. The curve for plates 6 mm thick excited at a stator frequency of 200 Hz reaches a definite minimum value of kVA input, at a width of about 14 cm. Beyond this point, increases in width have an adverse effect on capabilities of lift - the first observation of such a trend.

Taken together, the curves of Fig 103 suggest that the centre two poles of the Xi-core (whose edges are 10 cm apart) should be well covered by the floating plate in order to achieve reasonable values of kVA/tonne. Indeed an empirical criterion might be that the edges of the plate should "split" the outer two slots, whose centres are

12.5 cm apart. (There is an interesting inverse comparison here between this, the new expanding-geometry machine, and the flat-plate floater of Chapter 1, one of the previous generation of levitation machines. For the latter it was found that the optimum width of plate was that which "split" the centre pole of each E-core stator block - see Fig 3.)

With regard to the numerical values of volt-amperes per tonne (Fig 103), it can be seen that all the curves have regions falling well below the 1000 kVA/tonne mark. This fact is encouraging in itself since the majority of earlier electromagnetic levitators of corresponding size required inputs considerably in excess of this. Even more promising, however, is the series of results obtained for the 6 mm plate at 50 Hz, for which the far end of the curve drops below 500 kVA/tonne. The minimum value obtained was 421 kVA/tonne, achieved with a plate 15 cm wide. The corresponding power input was 125 kW/tonne, yielding a power factor of almost 0.3. It is to be expected that continued progress of design will result in further improvements to these figures.

11.5 Boundaries of stability

The remaining series of tests carried out on the Xi-core motor was performed with much haste and little planning, the objective being simply to collect sufficient information in the limited time remaining to point the way for future research. For example, Fig 104 shows the variations of height of flotation with width of plate, and of maximum available lateral restoring force at that height, taken at constant stator current (at 50 Hz). The increase in height as wider plates are substituted, shown in Fig 104(a), follows the pattern that would be expected. Starting with a rapid rise, each curve then tails off to approach a maximum height, reached as the plate area covers the useful extent of magnetic field. Less expected, perhaps, is that the curve for the 3 mm plates crosses that for the thicker plates, resulting in a region where thinner plates are the better performers in lift.

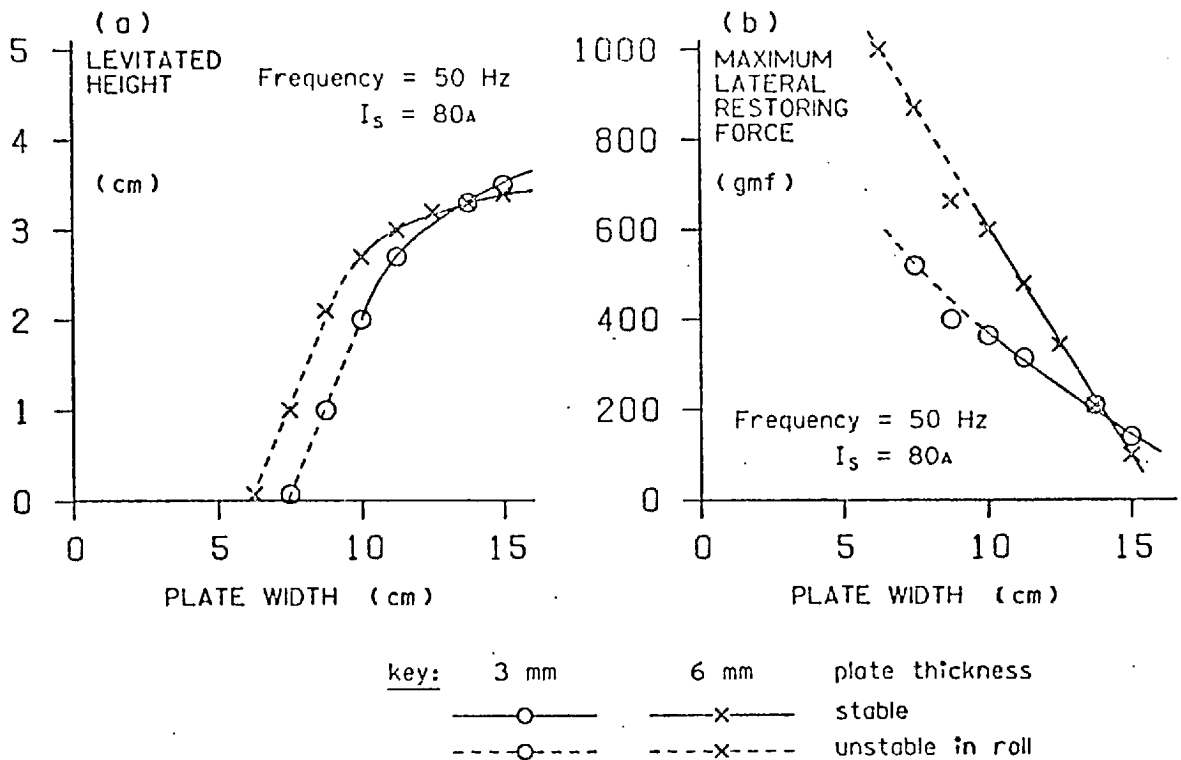


Fig 104. Variations of levitated height and of maximum lateral restoring force with width of plate, for constant stator current.

Predictable also is the general shape of Fig 104(b), showing a decrease in the lateral stabilising forces with increasing width. The particular results displayed appear to indicate an approximately linear variation, but there is as yet insufficient data to deduce that such a rule is general. Extrapolation of the two straight lines to the horizontal axis suggests that the limiting widths of plate before encountering lateral instability are about 18 cm and 16 cm for plates 3 mm and 6 mm thick respectively (at that particular value of stator current). Practical experiment confirms this.

Note that all the results displayed were obtained for a stator current of 80 amps. A change in current of course modifies both sets of curves of Fig 104, the general trends being those observed in all expanding-geometry machines - i.e. that increases both in height of levitation and in magnitude of restoring forces result from increased stator currents.

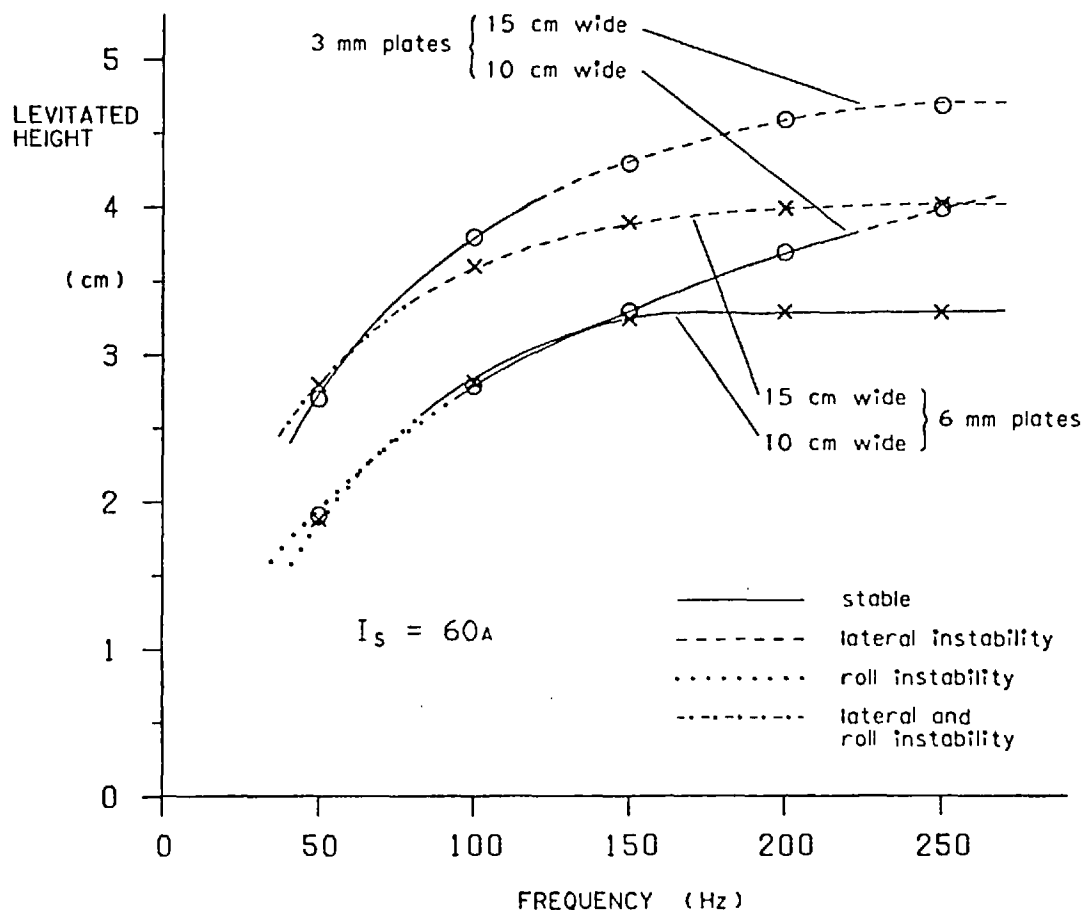


Fig 105. Variation of height with frequency, showing modes of instability, for four plates, at constant stator current.

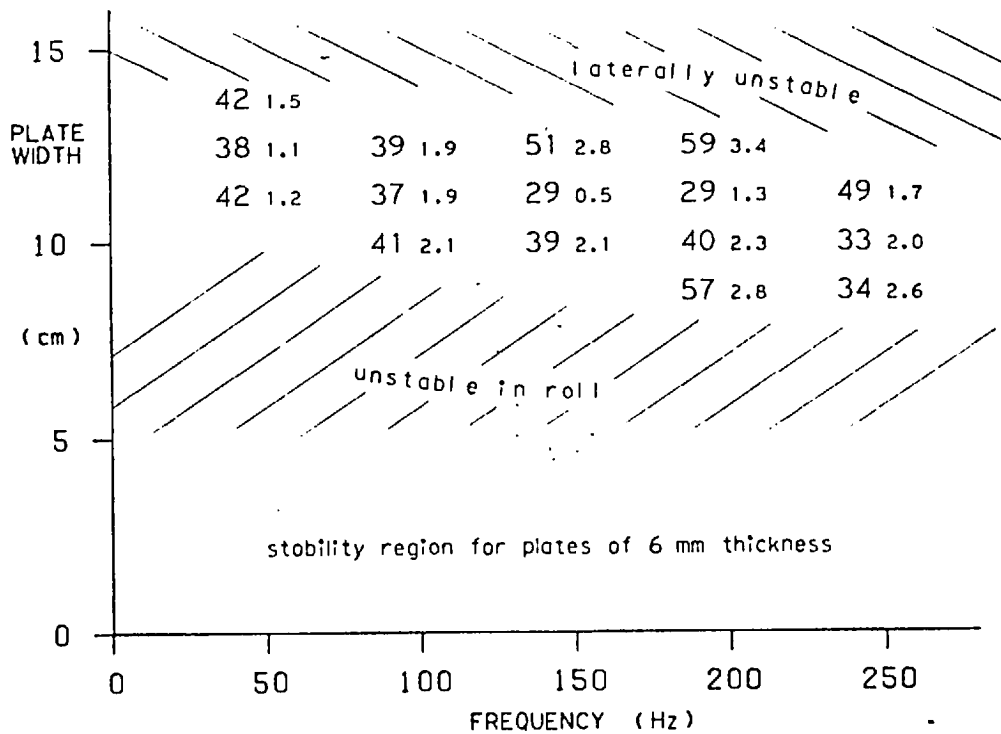
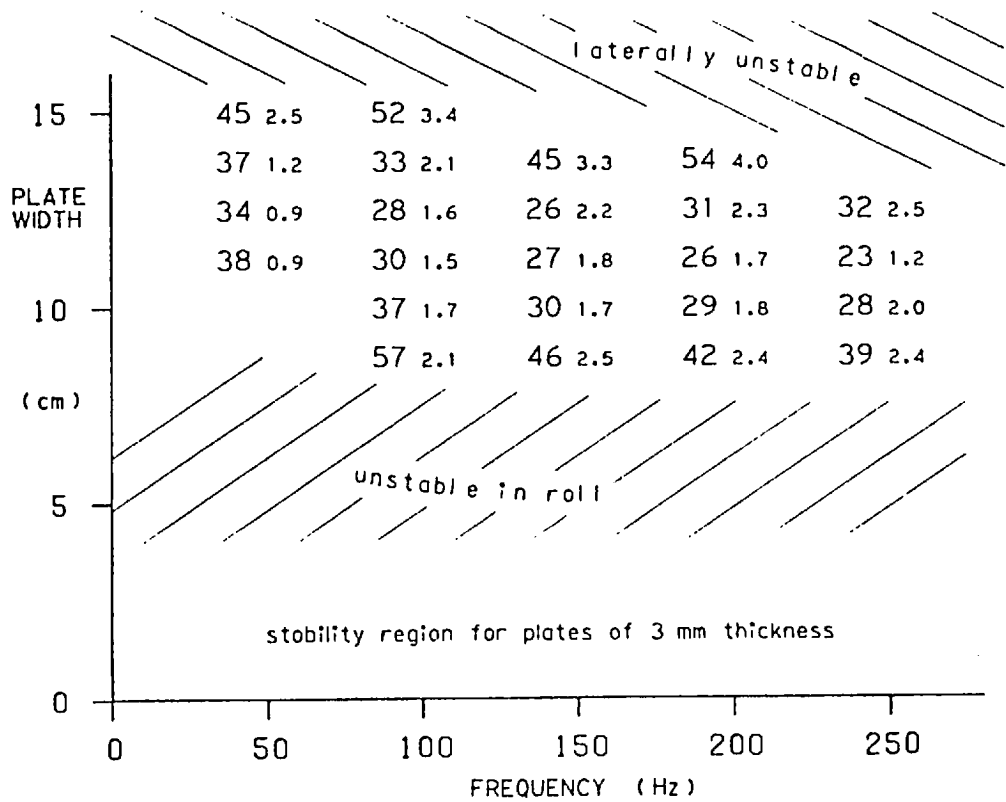
The graphs of Fig 104 also illustrate regions of instability in roll. It will be observed that the overall trend here is opposite to that for lateral stability, in that decreases of width lead to roll instability. Behaviour of this kind was first observed during experiments with the Washington model of Chapter 1, and appears to be a further general feature of expanding-geometry levitators.

Regions of both kinds of instability are indicated by the curves shown in Fig 105. On this graph are shown the variations of levitated height with frequency, taken for four different plates at the same value of stator current. The general shapes of the curves are again as expected; the similarity will be noticed between these and the corresponding measurements taken for plates over a length of the long

electromagnetic river (see section 8 of Chapter 7, Fig 68). In particular the same tendency is exhibited for the thicker plates to reach their limiting value of height at a lower frequency, the determining factor again being the decrease in skin depth with increasing frequency. The distribution of regions of stability, however, is complex. General trends are that wide plates tend to be the first to lose lateral stability, while narrow ones tend to meet roll instability first, but there is little obvious pattern relating the specific points on the four curves at which stability of either kind is lost.

It will have been realised by now that the conditions under which plates can be floated with complete stability are bounded in several directions by a number of differing criteria. In addition to the effects of width of plate mentioned above, it has been established that the magnitude of stator current has a large effect on lateral guiding forces, but appears to influence roll stability scarcely, if at all. The precise effects of changes in plate thickness are not yet clear. It seemed that a valuable presentation of the experimental data obtained from the Xi-core, and indeed from a number of other expanding-geometry levitating machines, might be one showing general regions of stability, and defining in particular as many as possible of the different stability boundaries.

An attempt at such a presentation is made in Fig 106. The tests from which the display was obtained consisted of selecting each combination of plate width and stator frequency, and reducing the stator current to find the point at which stability was just lost. The current, the height of flotation and the mode of instability at this point were recorded. Resulting information can of course be displayed in many different ways, since at least six variables are involved (plate width, thickness, height of flotation, stator current, frequency and mode of instability). Fig 106 presents a separate display for each thickness of aluminium, setting plate width and excitation frequency as the co-ordinate axes. For each combination of width and frequency a pair of figures is quoted, being the minimum



Large figures indicate minimum current (in amps) for stability.
Small figures indicate corresponding minimum levitated height (cm).

Fig 106. Regions of total stability over the Xi-core motor for stator currents up to 60 amps.

stator current (in amperes) for the chosen plate to remain stable (large figures), and the corresponding minimum levitated height (in cms - small figures).

Regions shown shaded are those for which stability was not possible at all within the chosen stator current limit of 60 amps. An increase in this limit would push back the boundary of lateral instability, since lateral restoring forces rise with stator current, but the roll stability boundary would remain substantially unchanged since this appears to be dependent on the shape rather than on the size of the "electromagnetic river banks" above the stator poles.*

It is difficult to assess as yet the eventual usefulness of data displayed in the form of Fig 106. However a number of valuable deductions can immediately be made upon scanning the figures. For example the optimum width of 3 mm aluminium plate for use at 50 Hz is seen at a glance to be 12.5 cm, since this is the width requiring minimum stator current to create stability. It is interesting to note that at 250 Hz the optimum width is slightly less, at about 11 cm, while the height at which the corresponding optimum plate can float is slightly greater, at 1.2 cm in place of 0.9 cm. On the basis of scale-modelling by frequency control, these observations might be interpreted as suggesting that a machine 2.2 (i.e. $\sqrt{250/50}$) times the size of the motor under test, built to operate at 50 Hz, would have for the appropriate plate thickness an optimum rotor width

* There is another kind of roll instability, mentioned in Chapter 7 (section 1, Fig 55) and observed in Chapter 8 (section 3, Fig 81), the investigation of which has not been attempted here. This is the kind encountered in machines having a "wide-angled prism of stability" (Figs 62 and 81) where an increase of stator current can result in the edges of a floating plate being too far removed from the stability boundaries, causing the plate to become unstable in roll. In fact none of the plates investigated became unstable in this fashion over the Xi-core motor, though the reason for this is almost certainly that adequately large stator currents were not tested. Inclusion of such behaviour as a further boundary on Fig 106 could be effected by adding a second pair of figures to each combination of width and frequency, denoting the maximum stator current and the corresponding maximum height before stability is lost in this way.

proportionally slightly smaller than the present machine, but the minimum float height would be proportionally greater.

The inherently better performance obtained by increases in size can be seen across the whole range of data for the 3 mm plates. Inspection of the minimum current capable of stabilising the optimum width of plate reveals a steady decrease as higher frequencies are selected (simulating larger machines) from a value of 34 amps at 50 Hz to 23 amps at 250 Hz. The corresponding heights of levitation, by contrast, change by only a little. The effect is masked somewhat in the data relevant to 6 mm plates by the approach of skin depth with increasing frequency.

The stability region display of Fig 106 and the deductions made from it conclude the work carried out on the Xi-core motor up to the time of composition of this thesis. As was stated at the beginning of the chapter the investigations have been only of a preliminary kind, rather in the nature of the experiments described in Chapter 1 in connection with the first expanding-geometry machines. It appears that a major line of development of the linear motor may have been opened up by the invention of the Xi-core, and a programme of detailed investigations into the machine might prove to be a worthwhile project. Particular recommendations for future work are firstly to split the original Xi-core motor back into its six component blocks and re-build it with a three-phase winding to create a Xi-core electromagnetic river, and secondly to develop further methods defining regions and boundaries of stability applicable to all expanding-geometry machines.⁽³⁷⁾

It is to be hoped that improved designs of Xi-core motors will be built and tested, and it may be that investigations into changes of topology, perhaps circularising procedures such as those described in Chapter 3, could lead to a whole new family of electromagnetic machines. An example is the electromagnetic whirlpool of Fig 28, where the vertical lift forces are provided by the same shearing

mechanism as the horizontal guidance forces of a standard electromagnetic river. The Xi-core is already known to provide considerably stronger forces of guidance.

But perhaps most of all it is to be hoped that advantage will be taken of any opportunity to build machines on a larger scale, for it is in large sizes that electromagnetic devices are shown to their maximum advantage. High-speed transport is again the obvious application, and it would be a fitting end indeed to the work begun in this chapter to see a fifty-tonne passenger-carrying vehicle being supported, guided and propelled at 400 km/h on the silent, invisible, non-polluting magnetic field of a Xi-core electromagnetic river.

REFERENCES

1. - analogy between real and electromagnetic rivers
(pp 15 and 208):
Eastham, J.F. and Laithwaite, E.R., "Linear induction motors as electromagnetic rivers". Proc IEE, Vol 121, No 10, pp 1099-1108, Oct 1974.
2. - the Russell and Norsworthy factor (pp 19 and 48):
Russell, R.L. and Norsworthy, K.H., "Eddy currents and wall losses in screened-rotor induction motors". Proc IEE, Vol 105A, Paper 2525U, pp 163-175, Apr 1958.
- see also:
Laithwaite, E.R., "Induction Machines for Special Purposes", p 107. Newnes, 1966.
3. - levitation of 1 m aluminium sphere (p 28):
Laithwaite, E.R., "The Engineer in Wonderland", Chapter 6 and prologue, pp 138-168. English Universities Press, 1967.
4. - an exposition on Magic Carpets (p 34) - see for example:
"The Tale of Ala al-Din Abu Shamat" from The Book of the Thousand Nights and One Night (Arabian Nights Entertainments). Translated into French by Mardrus and thence into English by Lane (1840), Burton (1888), Mathers and others.
5. - free rotor over single-sided linear induction motor has same power and lift for all stator currents (p 38):
Laithwaite, E.R., "Induction Machines for Special Purposes", pp 165-166 and Fig 7.13. Newnes, 1966.
6. - derivation of goodness factor (pp 39 and 121):
Laithwaite, E.R., "The goodness of a machine". Proc IEE, Vol 112, No 3, pp 538-541, Mar 1965.
7. - criterion for self-oscillation is $G > 1.0$ (p 40):
Laithwaite, E.R., "Induction Machines for Special Purposes", p 185. Newnes, 1966.

8. - elementary experiments with permanent magnets (p 46):
Laithwaite, E.R., "Propulsion Without Wheels", Section 2.5, pp 24-26. English Universities Press, 1966.
9. - tubular transverse-flux motors (p 55):
Eastham, J.F. and Alwash, J.H., "Transverse-flux tubular motors". Proc IEE, Vol 119, No 12, pp 1709-1718, Dec 1972.
10. - derivation of the Maxwell Second Stress formulae (p 75):
Stratton, J.A., "Electromagnetic Theory", pp 153-159. McGraw-Hill, 1941.
11. - presence of large non-force-producing losses in windings with only 1 slot per pole per phase (p 90):
Laithwaite, E.R., Eastham, J.F., Bolton, H.R. and Fellows, T.G., "Linear motors with transverse flux". Proc IEE, Vol 118, No 12, pp 1761-1767, Dec 1971.
12. - the two-layer concentric winding (p 91):
Eastham, J.F., "Linear induction motor stator". U.K. Patent number 1340860 (Feb 1970).
13. - general theory of back-to-back oscillating motors (p 105):
Laithwaite, E.R., "Induction Machines for Special Purposes", Ch 8, pp 174-195. Newnes, 1966.
14. - mechanism of back-to-back oscillation (p 105):
Laithwaite, E.R. and Nix, G.F., "Further developments of the self-oscillating induction motor". Proc IEE, Vol 107A, Paper 3273U, pp 476-486, Oct 1960.
15. - early work on back-to-back oscillation (p 106):
Laithwaite, E.R. and Lawrenson, P.J., "A self-oscillating induction motor for shuttle propulsion". Proc IEE, Vol 104A, Paper 1988U, pp 93-101, Feb 1956.
16. - magnitude of dynamic forces on railway track (p 116):
Jones, S., "Economic and high-speed running of railways". Electronics and Power, Vol 21, No 2, pp 100-104, 6 Feb 1975.

17. - comprehensive review of worldwide progress on high-speed ground transport (p 117):
Ellison, A.J. and Bahmanyar, H., "Surface-guided transport systems of the future". IEE Review: Proc IEE, Vol 121, No 11R, pp 1224-1248, Nov 1974.
18. - definitions of the terms "electromagnetic" and "magnetic" (pp 121, 159 and 238):
Laithwaite, E.R., "Magnetic or electromagnetic? - the great divide". Electronics and Power, Vol 19, No 4, pp 310-312, 9 Aug 1973.
19. - derivation of "the smaller the better" for magnetic machines (p 121):
Laithwaite, E.R., "Linear Electric Motors", Ch 2, p 39.
Mills and Boon, 1971.
20. - derivation of Earnshaw's theorem (p 122):
Earnshaw, S., "On the nature of the molecular forces which regulate the constitution of the luminiferous ether". Trans. Cambridge Phil. Soc., Vol 7, Part 1, pp 97-112, 1842.
- see also:
Geary, P.J., "Magnetic and electric suspensions", Section 1.4, pp 5-6. British Scientific Instrument Research Association, 1964.
Stratton, J.A., "Electromagnetic Theory", Section 2.12, pp 116-117. McGraw-Hill, 1941.
21. - original work on variation of normal force over linear induction motor (p 128):
Lowther, D.A., "A study of the 3-axis forces in linear induction machines using electromagnetic scale models", Ch 8, pp 241-269. PhD Thesis, Brighton Polytechnic, 1973.
22. - publication of work of reference 21:
Freeman, E.M. and Lowther, D.A., "Normal force in single-sided linear induction motors". Proc IEE, Vol 120, No 12, pp 1499-1506, Dec 1973.
23. - speed control of induction motors (p 129):
Laithwaite, E.R., "Induction Machines for Special Purposes", Ch 12, pp 265-300. Newnes, 1966.

24. - regenerative braking of induction motor after external supply failure to vehicle (p 130):
Bliss, D.S., "Improvements in and relating to traction systems". U.K. Patent number 1002588 (May 1962).
Bliss, D.S., "Improvements in and relating to traction systems comprising vehicles for travelling along a prepared track". U.K. Patent number 1033925 (July 1962).
25. - explanation of an induction generator (p 131):
Eastham, J.F., "Principles and characteristics of induction generators". Electrical Review, 11 Nov 1960, pp 809-813.
26. - explanation of regenerative linear induction motor braking without external supply to vehicle (p 133):
Laithwaite, E.R., "Propulsion Without Wheels", Section 9.4, pp 161-163. English Universities Press, 1966.
27. - the electromagnetic track joint (pp 137 and 163):
Laithwaite, E.R. and Fellows, T.G., "Linear induction motor secondary member". U.K. Patent number 1371266 (Mar 1972).
28. - development and properties of transverse-flux motors (pp 138 and 245):
Laithwaite, E.R., Eastham, J.F., Bolton, H.R. and Fellows, T.G., "Linear motors with transverse flux". Proc IEE, Vol 118, No 12, pp 1761-1767, Dec 1971.
29. - the Waffle motor and other linear motor variations (pp 145 and 245):
Eastham, J.F. and Laithwaite, E.R., "Linear motor topology". Proc IEE, Vol 120, No 3, pp 337-343, Mar 1973.
30. - differences between series and parallel connections of linear induction motors (p 162):
Laithwaite, E.R. "Differences between series and parallel connection in machines with asymmetric magnetic circuits". Proc IEE, Vol 112, No 11, pp 2074-2082, Nov 1965.
- see also:
Laithwaite, E.R., "Induction Machines for Special Purposes", pp 16-21, 49, 51-54, 78-82, 83-85, 179. Newnes, 1966.

31. - representation of large machines by electromagnetic scale modelling (p 167):
Lowther, D.A., "A study of the 3-axis forces in linear induction machines using electromagnetic scale models", Ch 4, pp 99-128. PhD Thesis, Brighton Polytechnic, 1973.
32. - subsequent work on electromagnetic scale models (p 167):
Freeman, E.M., Lowther, D.A. and Laithwaite, E.R., "Scale-model linear induction motors". Proc IEE, Vol 122, No 7, pp 721-726, July 1975.
33. - derivation of magnetic equivalent circuits (pp 205 and 207):
Laithwaite, E.R., "Magnetic equivalent circuits for electrical machines". Proc IEE, Vol 114, No 11, pp 1805-1809, Nov 1967.
34. - explanation of production of travelling field from polyphase supply (p 208):
Laithwaite, E.R., "Propulsion Without Wheels", Sections 1.3 and 3.1, pp 4-10 and 29-32. English Universities Press, 1966.
35. - derivation of "the voltage sets up the flux" (p 233):
Laithwaite, E.R., "Induction Machines for Special Purposes", Ch 1, p 12. Newnes, 1966.
36. - the Xi-core motor (p 240):
Attwood, A. and Laithwaite, E.R., "Electromagnetic levitation". U.K. Patent application number 41421/74 (Sep 1974).
37. - continued research on electromagnetic rivers (pp 169, 240 and 261):
Greatorex, N., "A study of transverse-flux linear motor performance". PhD Thesis, Imperial College, London, Dec 1977.

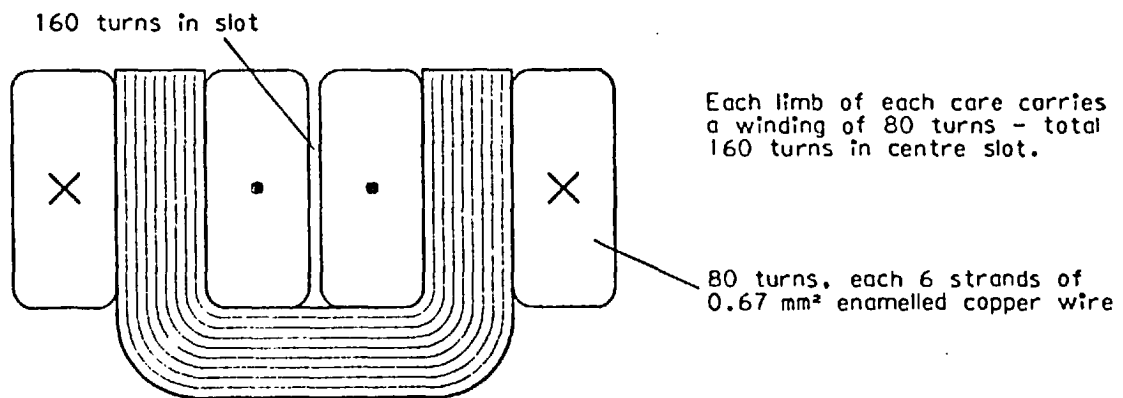
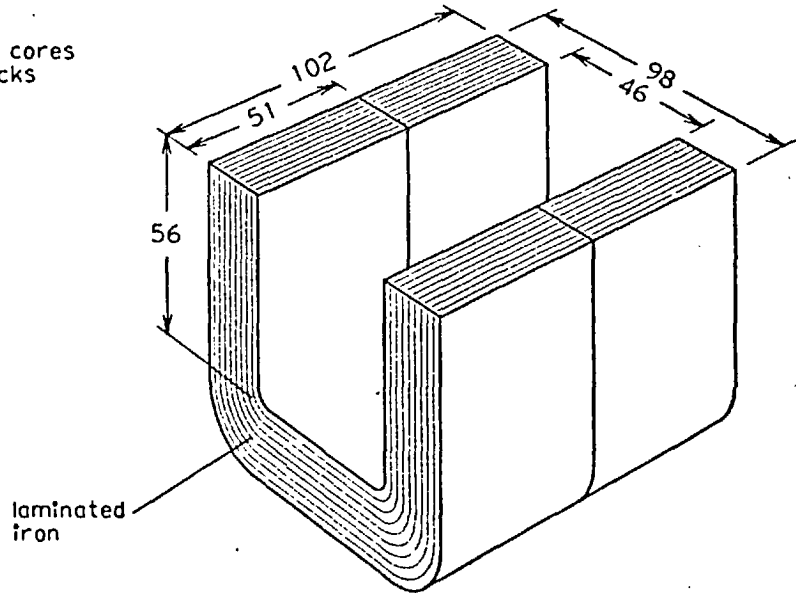
APPENDIX A. ENGINEERING DETAILS OF FOUR MACHINES

A.1 The "magic carpet" machine

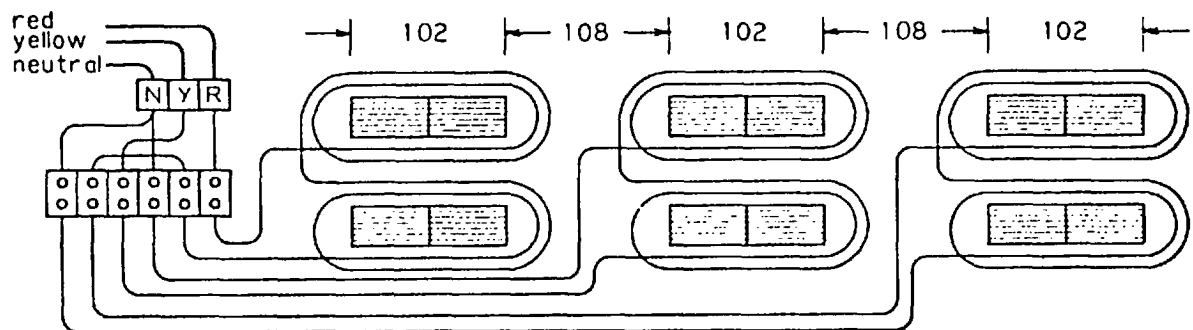
(see figures 13, 14, 15 and 16)

Each of the three magnetic cores comprises two laminated blocks mounted end-to-end:

(all dimensions
in millimetres)



Inter-core spacing and winding connections:



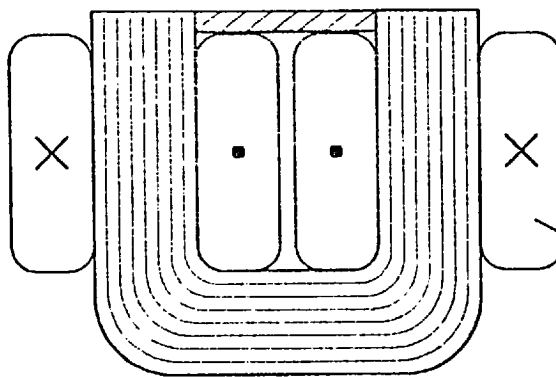
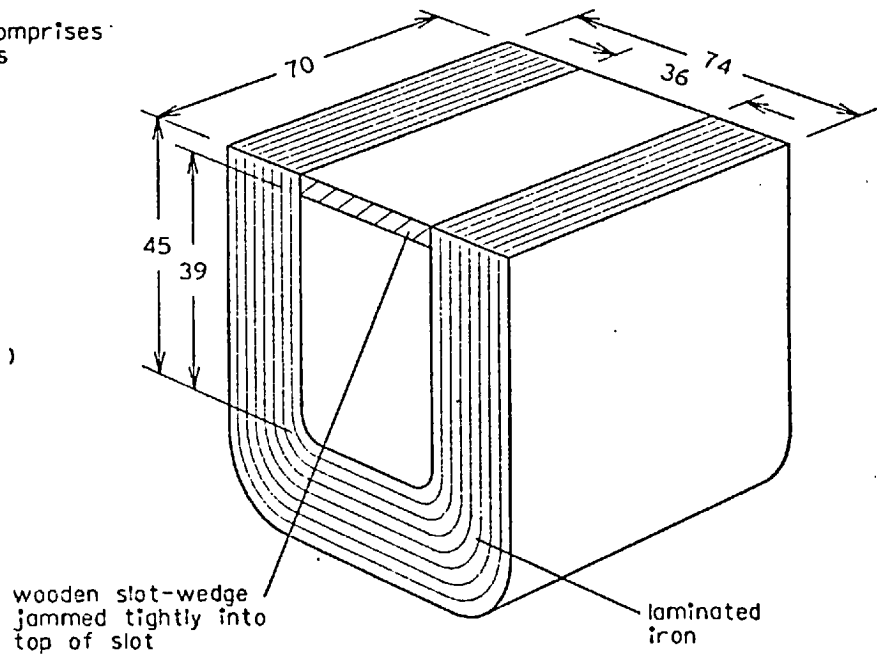
End two windings in series, connected Red-to-Neutral.
Centre winding connected Neutral-to-Yellow.

A.2 The long pole-pair machine

(see Figs 20, 29, 33 and 92)

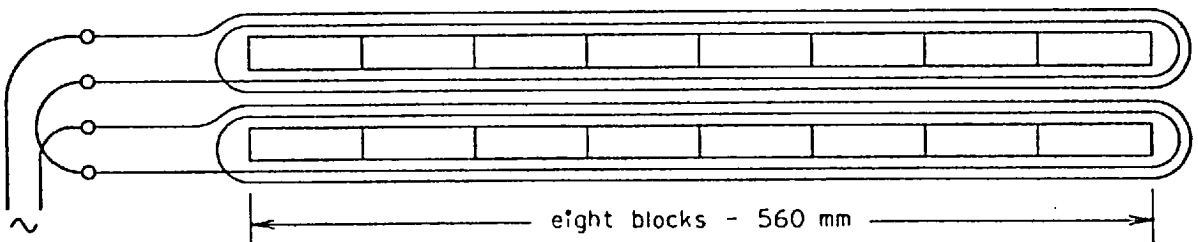
The magnetic core comprises eight laminated blocks mounted end-to-end, each block as shown:

(all dimensions
in millimetres)



Each limb carries a winding of 47 turns - total 94 turns in centre slot.

47 turns, each 10 strands of 0.67 mm² enamelled copper wire

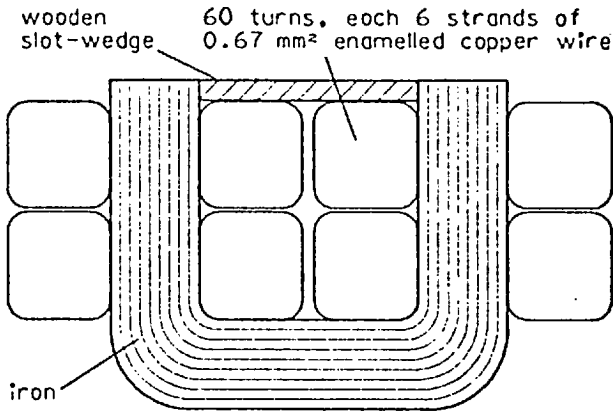


A.3 The phase-mixed electromagnetic river

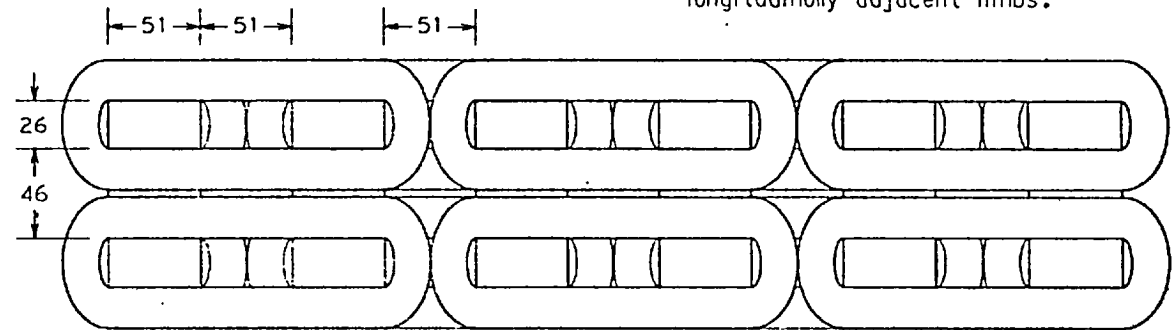
(see Fig 44)

Each of the six magnetic cores is a single block of iron laminations of the same dimensions as those used in the "mogie carpet" machine (see section A.1).

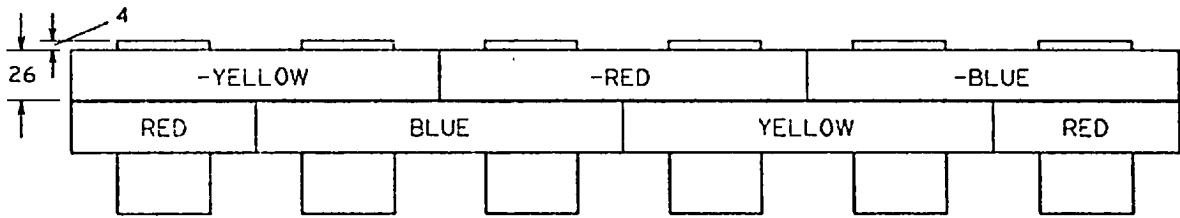
(all dimensions in millimetres)



Each limb carries two coils, and each coil embraces two longitudinally adjacent limbs.



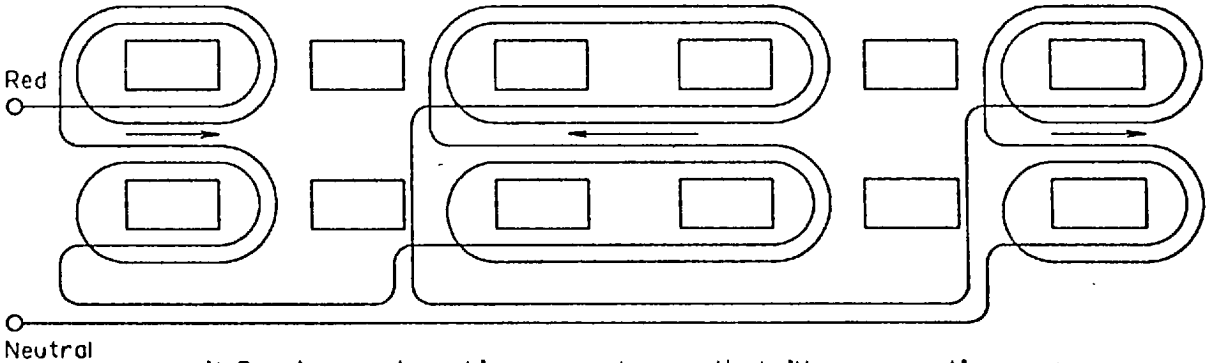
plan view



side elevation

Wiring connections
e.g. Red phase:

All coils of the same phase connected in series throughout. Machine as a whole is in "star" connection.



N.B. A second machine was subsequently built on magnetic cores of identical dimensions and layout, but a better electrical characteristic was obtained by winding each coil with 120 turns of three strands instead of 60 turns of six strands.

A.4 The seven-metre stator (see Fig 46)

The phase-mixed electromagnetic river (see section A.3) was extended to a length of seven metres by repeating its pattern of laminated blocks to make a total of 60 magnetic C-cores.

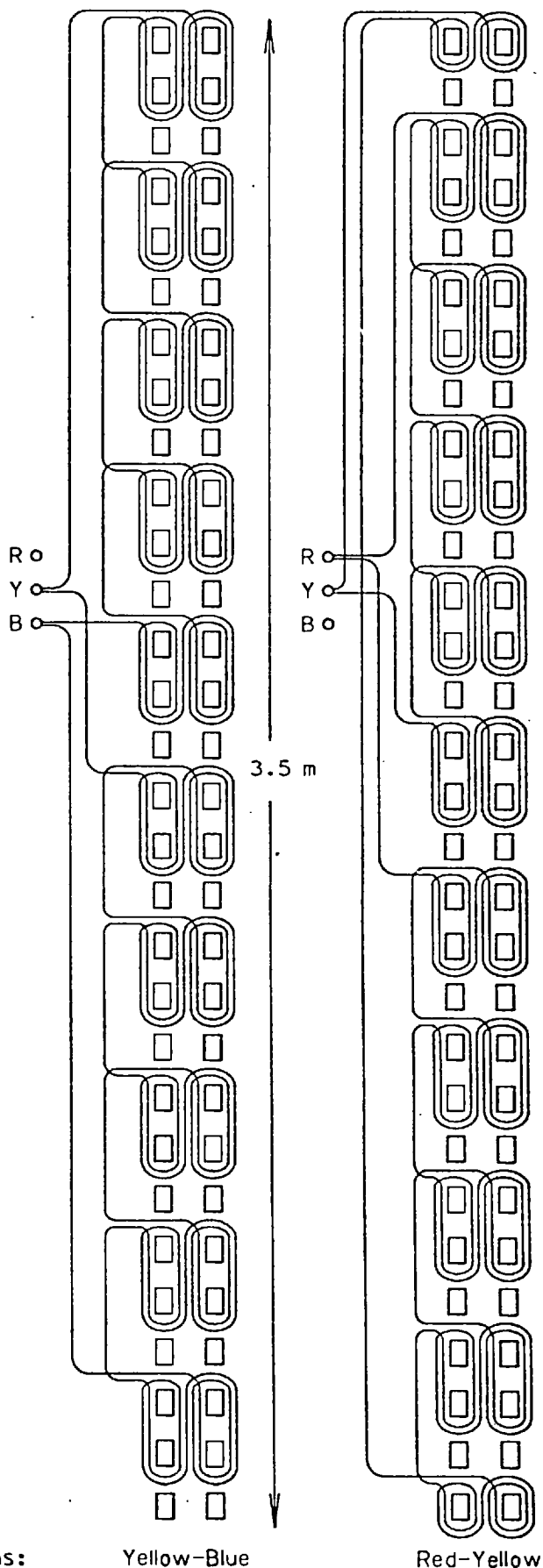
These were mounted in two mechanically-independent sections, each of 30 cores. The adjacent diagrams show one of these sections, i.e. half the length of the machine.

Each mechanical section was further divided electrically into two independent parts, making four electrical ports to the entire machine. Within each part, all coils of the same phase were connected in series (ten coils in all), embracing five pairs of C-cores.

The four groups of series coils were then combined in parallel to form one "phase" of the electromagnetic river. The three resulting "phases" were connected in delta formation (unusual in a linear motor) for use with a 415-volt three-phase supply.

The "extro" half-sized coils on the Red-Yellow phase of each section were included by connecting four full-sized pairs and one small pair at one end of the section in series with the small-sized pair at the opposite end.

The completed machine drew approximately 240 amps from a 415 volt supply. Parallel connection of 1200 μ F of capacitance per phase (connected in delta in the manner of Fig 65) reduced this input current by a factor of eight, thus bringing voltage control of the machine within the capability of a 30-amp three-phase variac.



Example phase connections:

Yellow-Blue

Red-Yellow

LEVIDUCTION - A STUDY IN ELECTROMAGNETIC LEVITATION

VOLUME II

by

Alan Attwood, B.Sc.(Eng.), A.C.G.I.

April 1980

A thesis submitted for the degree of Doctor of Philosophy
of the University of London and for the Diploma of Imperial College

Electrical Engineering Department,
Imperial College,
London SW7.

VOLUME II CONTENTS

	<u>page</u>
APPENDIX B. AN ALTERNATIVE THEORETICAL APPROACH	273
B.1 Introduction	273
B.2 An elementary theoretical model using strip conductors	277
B.3 Preliminary results from the elementary strip conductor analysis	283
B.4 Extensions and conclusions	292
APPENDIX C. ANALYTICAL DERIVATIONS OF THE MATHEMATICAL EXPRESSIONS USED IN APPENDIX B	297
C.1 Conventions for co-ordinates, currents and fluxes	297
C.2 Field set up by a current in a horizontal strip conductor	299
C.3 Field components set up by a horizontal coil of strip conductors	301
C.4 Force exerted upon a strip conductor in the field set up by a coil of two strip conductors	301
C.5 The calculation of mutual inductance	306
APPENDIX D. COMPUTER SUBROUTINES, FUNCTIONS AND PROGRAMS	309
D.1 The functions AATAN and AALOG	309
D.2 AASORS - the function and subroutine library	311
D.3 FORDIS and CONDAT - two computer programs to analyse an electromagnetic levitator	319
D.4 Keyboard commands for running FORDIS and CONDAT	330
APPENDIX E. COMPUTER SOURCE CODE LISTINGS	336
E.1 Source code listing of library AASORS	336
E.2 Source code listing of program FORDIS	341
E.3 Source code listing of program CONDAT	346

APPENDIX B. AN ALTERNATIVE THEORETICAL APPROACH

B.1 Introduction

The main text of this thesis was principally devoted to a discussion of some practical and experimental aspects of expanding-geometry levitating machines. Two substantial portions, however, were concerned with theoretical considerations. The first of these was in Chapter 4, where an analytical representation of the "long pole-pair" machine was proposed (see section 4.3, pages 70 to 74). This analysis was ultimately abandoned in view of the lack of an effective theoretical means for evaluating the practical constants of self- and mutual inductance. The second theoretical portion of text was the whole of Chapter 9. The objective of this chapter was to find a straightforward physical explanation for the mechanism of stability forces, which could have been used to predict the stability behaviour of new designs of levitator. Such an explanation, had it been found, might hopefully have proved possible to represent in terms of mathematical equations, thus allowing an analytical solution for stability.

Neither of the above approaches was particularly successful. Nor, however, was a large effort expended upon either, since it was evident that the limited time available could be more profitably spent on creative experimental work. The justification can be seen in the results achieved. Indeed it is fair to say that in the entire sequence of discoveries from the Washington model of Chapter 1 to the Xi-core levitator of Chapter 11, theoretical analysis and analytical considerations played no useful part whatsoever.

Following the invention of the Xi-core motor, experimental progress became rather slower, and it was evident that a complementary background of workable theory was needed. The work presented in this Appendix is the third effort at providing the beginnings of such a background. Since there seemed little purpose in restarting along the lines of either of the previous two efforts, a new approach was taken with a rather different initial objective. This was to show

that by suitable choice of theoretical model, force distributions may be derived of the same kind as those created in practice by the electromagnetic river and other expanding-geometry levitating machines, even though the model may fall far short of simulating any practical machine.

In the first instance the objective is merely to derive a shape - the characteristic "river bank" double-hump shape of forces that gives the electromagnetic river its name. It was decided to begin by disregarding all practical considerations and searching for a theoretical model of the simplest possible kind that would produce the required patterns of force. The model as finally chosen was indeed simplified to the extent of bearing a closer resemblance to an O-level examination question than to any conceivable working machine. Both the primary and the secondary comprise conductors of infinite length and zero cross-sectional area; the secondary plate has width but no thickness; iron is both infinitely laminated in all directions and infinitely permeable to magnetic flux - if indeed it is present at all! Such simplification is, of course, to be regarded only as the first of a series of increasingly sophisticated models, each additional complexity bringing the representation one stage closer to a practical working machine. A parallel might be drawn with the simplicity of Ohm's Law, which was a prerequisite to the generality of Maxwell's Equations.

The form of model employed in the analysis stemmed from discussions with Messrs R.J. Jackson and J.G. Steel of the Central Electricity Research Laboratories, Leatherhead. They suggested that a particular theoretical method which had been applied by them in cylindrical co-ordinates to rotating synchronous machines might also be applicable in linear co-ordinates to static expanding-geometry levitators. A feature of their work was the use throughout of "strip" conductors, and this feature has been extended here to its linear application. The strip conductor is considered to be a conductor of infinite length, finite width and infinitesimal thickness. Its perpendicular cross section is thus a finite straight

line. The conductivity of such a conductor is necessarily infinite, but the resistance per unit length resulting from the product of infinite conductivity with infinitesimal cross-sectional area is chosen to be finite and equal to the corresponding resistance of the practical conductor or set of conductors being modelled.

The reason for the introduction of strip conductors in the original cylindrical work was that the magnetic field set up by a uniformly distributed current in a strip conductor placed immediately across the top of a slot in iron is generally an excellent representation of the field set up by a similar current distributed throughout the conductors filling the slot. The substitution of an infinitely thin current sheet to represent a set of currents flowing in a slot is indeed an established technique used to make the analysis of electromagnetic problems tractable. The case is succinctly argued in a paper by Saunders*. To quote Saunders directly:-

"The transition from conductors embedded in slots to an infinitely thin current sheet on the smooth surface of the rotor or stator has been demonstrated by Hague**. He shows that, as far as the air gap field is concerned, the slot-embedded conductors may be replaced by a current sheet consisting of a very thin continuous conductor fastened to the surface of an otherwise uniform steel surface, as shown in Fig B.1. Hague argues that the field conditions in the air gap just over the slot of Fig B.1(a) and those just over the current element of Fig B.1(b) must be the same, since the line integral represented by the paths shown will be the same. Of course, this argument does not take into account the field associated with the slot itself, which in this paper is being considered as a non-interacting energy storage realm with respect to the air-gap fields. Thus, using Hague's reasoning, the slot-embedded conductors may be replaced by a current sheet of infinitesimal thickness having the same distribution of

* Saunders, R.M., "Electromechanical Energy Conversion in Double Cylindrical Structures". Trans I.E.E.E., Vol 82, pp 631 - 638, Oct 1963.

** Hague, B., "Electromagnetic Problems in Electrical Engineering", pp 183 - 185, 297. Oxford University Press, New York, 1929..

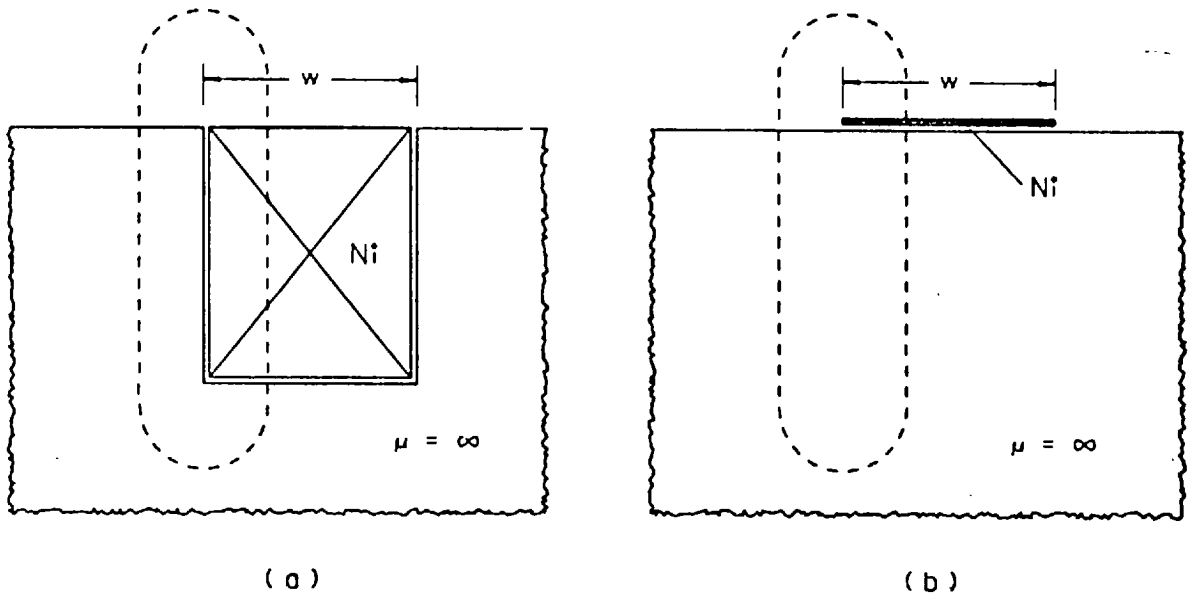


Fig B.1 Replacement of embedded conductors with a surface current element.

surface current as the slot-embedded conductor configurations. While it may be difficult to formulate the exact equivalent current sheet, such a current sheet is a helpful adjunct to the analytic solution of the fields within the air-gap machine."

Both the rotor and the stator of a rotating synchronous machine normally comprise sets of conductors arranged within slots in iron. In the original cylindrical analysis by Jackson and Steel, the use of strip conductors in the manner of Saunders and Hague was therefore appropriate to the modelling of both parts of the machine. Likewise, when applying the theory to linear expanding-geometry machines, the use of strip conductors to model the stator is appropriate.

The rotor, however, comprises a thin sheet of continuously conducting material, possibly backed by a sheet of iron. The use of strip conductors here, in the absence of slots of any kind, is based on rather more intuitive reasoning. By the nature of the analysis to follow it is necessary to model the continuous rotor material by a set of equivalent discrete conductors. The analysis will solve for the currents within these. The number of discrete conductors may of

course be as large as desired (limited only by the available computational facilities), and in general the larger the number the more accurate the representation. The shape of the conductors must also be specified. The choice is great - circular, square, rectangular, "line" conductors whose cross-section is a mathematical point - but it seems intuitively satisfying to represent a wide, thin rotor sheet in terms of wide, thin equivalent conductors. Taking the limiting case as the thickness tends to zero, these thin rectangular conductors become the same strip conductors as those already proposed for the representation of the stator.

A set of such strip conductors placed horizontally side by side then comprises a theoretical rotor sheet that is infinitely long and infinitely thin. Since the current within each strip conductor is uniformly distributed, this arrangement simulates a practical system in which the horizontal rotor plate is sufficiently thin for any variations in the vertical distribution of current flow to be considered insignificant. However the concept may readily be extended to simulate thick plates, by specifying an array of strip conductors comprising several rows one above another. Solution for the individual currents will then allow for non-uniform vertical current distributions. This approach becomes particularly valuable when the plate thickness becomes a significant fraction of the skin-depth of the rotor material, since the action of the internal eddy currents opposing the penetration of the externally applied field can be properly simulated.

B.2 An elementary theoretical model using strip conductors

The first attempt to model an expanding-geometry levitator by means of discrete strip conductors is shown in Fig B.2. If this representation can be said to have any practical basis, it would be the "long pole-pair" levitator discussed in Chapters 3 and 4 (see Figs 20 and 29). The practical machine was made "long" so that measurements taken near the centre of its length could be assumed to be free of any electromagnetic distorting effects from the end

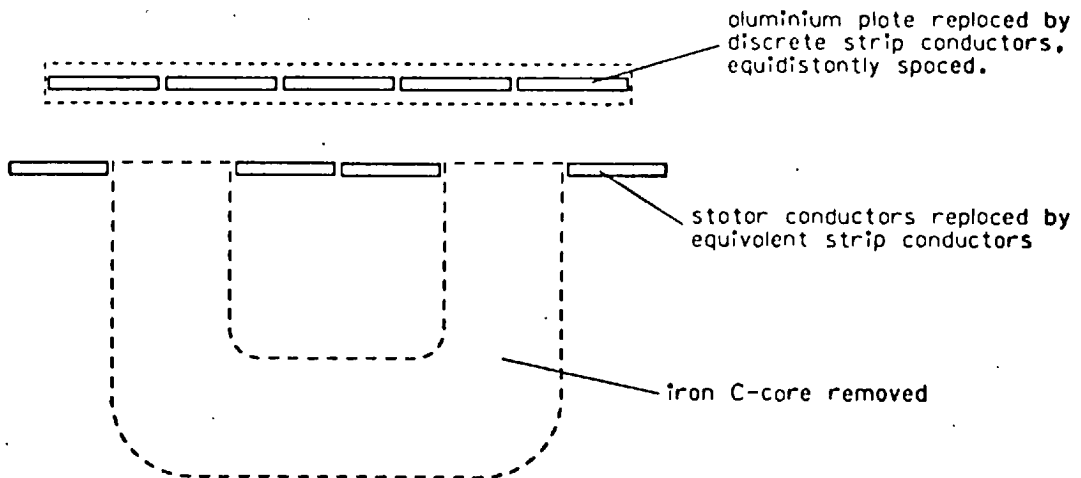


Fig B.2 Elementary system using strip conductors.

regions. It should be emphasised, however, that in the first instance the theoretical model is less concerned with practical details than with finding the ultimate expression of simplicity consistent with the generation of laterally stabilising forces. The complexities of the practical world may be considered later.

In the interests of theoretical simplicity, then, "long" becomes "infinite" and the iron stator core is removed. This latter step may seem rather drastic, but it was pointed out that the process of replacing slot-embedded conductors by strip conductors has already robbed the iron of its "shape" by simplifying it to a semi-infinite block, and it seems unlikely that a semi-infinite block of iron could play a fundamental part in the mechanism of stability. This view led to considerable discussion on whether an air-cored levitator could ever be expected to generate lateral stabilising forces. Such a machine has never been tried in practice, and would probably prove impracticable to build on account of the high current densities that would be required to produce a significant force of lift. Nevertheless it was considered an interesting point to determine, at least in theory, whether the lateral stability forces depend for their production on the presence of "edges" of iron, or whether they are a direct consequence of the topology of the stator and rotor currents.

Referring to Fig B.2, the stator current system may conveniently be represented by four strip conductors, forming two coils. The conductor widths and spacings are chosen such that the two adjacent conductors in the centre just span the central slot of the original iron C-core (now removed) and each coil just embraces the space formerly occupied by an iron tooth. Note that two coils alone are sufficient to represent the stator currents since in this case the current pattern is "known". By the nature of the wound coil system which is being represented, all current flowing in the left-hand central strip conductor of the stator is known to return in the left-hand outer conductor, and likewise for the right-hand coil.

By contrast the current pattern in the rotor is unknown. For this reason it was decided to represent the rotor currents by a general series of inter-dependent loop currents, as shown in Fig B.3. The figure is in fact a representation of one of the infinitely distant "ends", where the currents in the infinitely long strip conductors turn around to return in other conductors. Note that for simplicity a single row of strip conductors has been used in the rotor simulation. The vertical distribution of current flow is thus assumed to be uniform at this stage.

The close resemblance may be noticed between Fig B.3 and Fig 36 of Chapter 4 (page 72), where in particular the rotor "bars" in the latter figure correspond to the strip conductors in the former. The parallel can be extended further if the strip conductors are assumed to butt up against one another with no gaps in between, for then each conductor can be assigned a finite resistance, equal to the resistance of a single "bar" of Fig 36 of width equal to the width of the strip conductor and thickness equal to that of the plate.

A series of equations may now be written down for the various loops of current. Any number of loops may be chosen to represent the rotor - the more loops the better the representation. The general set of equations for Fig 36 is set out on page 71 of Chapter 4, and the same set applies without modification to Fig B.3. However the development of the equations in the remainder of this section will

be presented for the particular number of four current loops in the rotor (i.e. five strip conductors); the generalisation to any number of loops is obvious throughout.

Consider firstly the rotor loop currents I_1 , I_2 , I_3 and I_4 as shown in Fig B.3. The total voltage around each loop is evidently zero, hence applying Kirchoff's voltage law to the four loops in order:

$$RI_1 + R(I_1 - I_2) + j\omega L_1 I_1 + j\omega M_{12} I_2 + j\omega M_{13} I_3 + j\omega M_{14} I_4 + j\omega M_{S11} I_{S1} + j\omega M_{S12} I_{S2} = 0$$

$$R(I_2 - I_1) + R(I_2 - I_3) + j\omega M_{21} I_1 + j\omega L_2 I_2 + j\omega M_{23} I_3 + j\omega M_{24} I_4 + j\omega M_{S21} I_{S1} + j\omega M_{S22} I_{S2} = 0$$

$$R(I_3 - I_2) + R(I_3 - I_4) + j\omega M_{31} I_1 + j\omega M_{32} I_2 + j\omega L_3 I_3 + j\omega M_{34} I_4 + j\omega M_{S31} I_{S1} + j\omega M_{S32} I_{S2} = 0$$

$$R(I_4 - I_3) + RI_4 + j\omega M_{41} I_1 + j\omega M_{42} I_2 + j\omega M_{43} I_3 + j\omega L_4 I_4 + j\omega M_{S41} I_{S1} + j\omega M_{S42} I_{S2} = 0$$

where R = resistance of one rotor "bar",

L_x = self-inductance of the x^{th} rotor loop,

$M_{xy} = M_{yx}$ = mutual inductance between rotor loop x and rotor loop y ,

M_{Sxz} = mutual inductance between rotor loop x and stator loop z ,

$\omega = 2\pi \times \text{frequency}$,

$j = \sqrt{-1}$, representing a phase lag of 90 degrees.

Similarly for the two stator loop currents I_{S1} and I_{S2} :

$$I_{S1} R_S + j\omega M_{S11} I_1 + j\omega M_{S21} I_2 + j\omega M_{S31} I_3 + j\omega M_{S41} I_4 + j\omega L_S I_{S1} + j\omega M_{SS} I_{S2} = V_1$$

$$I_{S2} R_S + j\omega M_{S12} I_1 + j\omega M_{S22} I_2 + j\omega M_{S32} I_3 + j\omega M_{S42} I_4 + j\omega M_{SS} I_{S1} + j\omega L_S I_{S2} = V_2$$

where R_S = total resistance of one stator coil,

L_S = self-inductance of one stator coil,

M_{SS} = mutual inductance between the two stator coils,

V_1 and V_2 = voltages applied to stator coils.

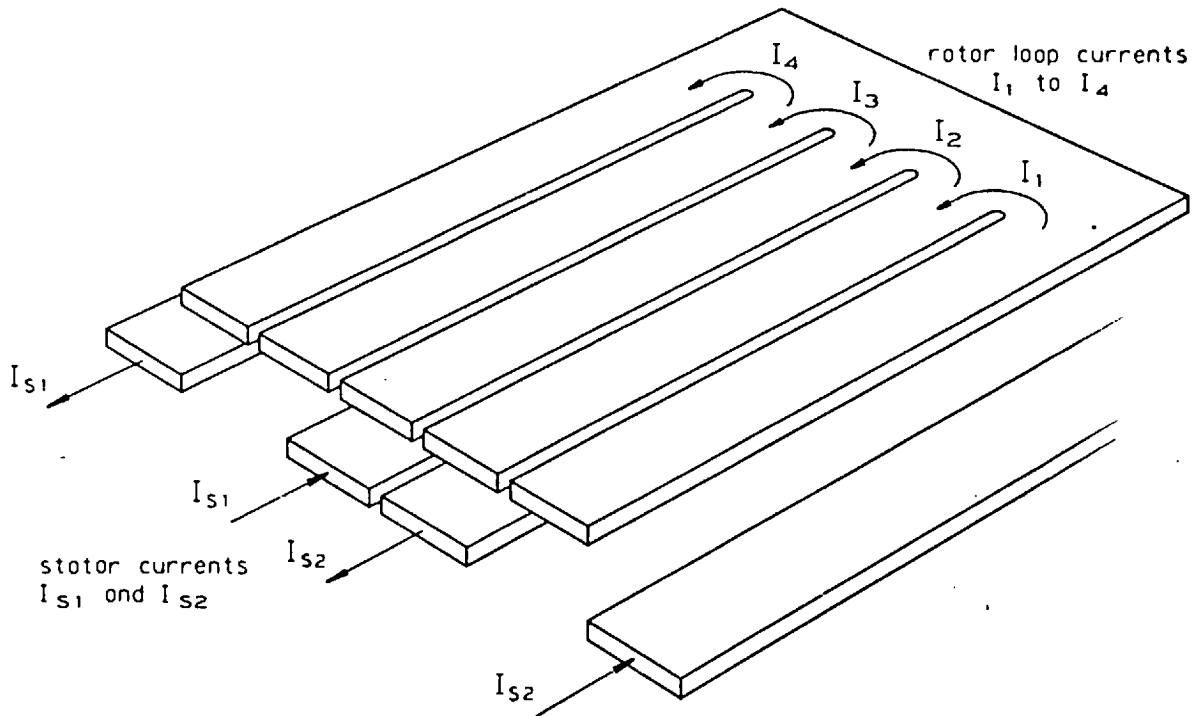


Fig B.3 Example system comprising four inter-dependent rotor current loops above two independent stator current loops.

A final pair of equations depends upon the connection of the stator coils. For coils in series $V_1 + V_2 = V_m$ where V_m is the applied mains voltage, and $I_{s1} = -I_{s2}$. For coils in parallel $V_1 = V_2 = V_m$.

As explained in Chapter 4, this complete set of equations may be solved by using a standard matrix inversion routine on a computer, yielding the rotor and stator currents as functions of the applied stator voltages. Such a solution is termed "voltage forced", since the stator voltages are the independent variables. Each new position of the rotor changes the values of all the mutual inductances between the rotor and stator current loops, and a complete re-working of the matrix inversion is thus necessary for every rotor position examined.

However the amount of computation may be much reduced by solving for a "current forced" system, where the stator currents are specified together as the single independent variable. This corresponds in practice to a series-connected stator coil system such that the current in one coil

is the negative (by the chosen convention) of the current in the other, and to a rotor which is "short" compared with the stator so that variations in rotor position have an insignificant effect upon the stator currents. Alternatively the current forced option corresponds to the common experimental technique of adjusting the stator current to a constant reference value for each experimental reading.

With the stator currents defined as I_S and $-I_S$ in stator coils 1 and 2 respectively, the four equations for the rotor current loops may be re-written thus:

$$I_1(2R + j\omega L_1) + I_2(-R + j\omega M_{12}) + I_3 \cdot j\omega M_{13} + I_4 \cdot j\omega M_{14} = -j\omega M_{S11}I_S + j\omega M_{S12}I_S$$

$$I_1(-R + j\omega M_{21}) + I_2(2R + j\omega L_2) + I_3(-R + j\omega M_{23}) + I_4 \cdot j\omega M_{24} = -j\omega M_{S21}I_S + j\omega M_{S22}I_S$$

$$I_1 \cdot j\omega M_{31} + I_2(-R + j\omega M_{32}) + I_3(2R + j\omega L_3) + I_4(-R + j\omega M_{34}) = -j\omega M_{S31}I_S + j\omega M_{S32}I_S$$

$$I_1 \cdot j\omega M_{41} + I_2 \cdot j\omega M_{42} + I_3(-R + j\omega M_{43}) + I_4(2R + j\omega L_4) = -j\omega M_{S41}I_S + j\omega M_{S42}I_S$$

or equivalently in matrix form:

$$\begin{pmatrix} 2R + j\omega L_1 & -R + j\omega M_{12} & j\omega M_{13} & j\omega M_{14} \\ -R + j\omega M_{21} & 2R + j\omega L_2 & -R + j\omega M_{23} & j\omega M_{24} \\ j\omega M_{31} & -R + j\omega M_{32} & 2R + j\omega L_3 & -R + j\omega M_{34} \\ j\omega M_{41} & j\omega M_{42} & -R + j\omega M_{43} & 2R + j\omega L_4 \end{pmatrix} \cdot \begin{pmatrix} I_1 \\ I_2 \\ I_3 \\ I_4 \end{pmatrix} = j\omega I_S \cdot \begin{pmatrix} -M_{S11} + M_{S12} \\ -M_{S21} + M_{S22} \\ -M_{S31} + M_{S32} \\ -M_{S41} + M_{S42} \end{pmatrix} \quad \dots (1)$$

Note that the matrix on the left-hand side of equation (1) comprises only terms relating to the rotor, i.e. resistances, self-inductances and mutual inductances. Thus for any given simulation of the rotor this matrix has to be assembled and inverted only once. Different positions of the rotor then involve different values for

the elements of the column vector on the right-hand side, and assembly and multiplication of this column vector with the inverted rotor matrix is all that is necessary to determine the set of currents for each new rotor position.

Figures B.2 and B.3 and equation (1) together complete the elementary theoretical model of an expanding-geometry electromagnetic levitator. It remains only to derive expressions by which the numerical values of the self- and mutual inductance terms may be calculated. Appendix C presents the analytical derivations of such expressions for coils of horizontal strip conductors, and Appendix D gives details of the computer subroutines written to evaluate these. With the addition of a matrix inversion routine it is then a matter of straightforward programming to compute the elements of equation (1) in terms of a given rotor/stator geometry, assemble the left-hand matrix and the right-hand column vector, invert the matrix and hence solve for the current distribution in the rotor plate.

The obvious next step from the above computation is then to evaluate the forces exerted upon the various currents by the action of the surrounding currents. Clearly the forces exerted by the rotor currents upon each other are of no interest since these can lead only to internal stresses within the rotor material. However the forces exerted upon the rotor currents by the stator currents are of fundamental interest since these comprise the levitating and stabilising (or otherwise) forces upon the rotor plate. It is hoped that from these forces, evaluated at different positions of the rotor across the stator, the "double-hump" pattern of lift and stability forces will emerge.

B.3 Preliminary results from the elementary strip conductor analysis

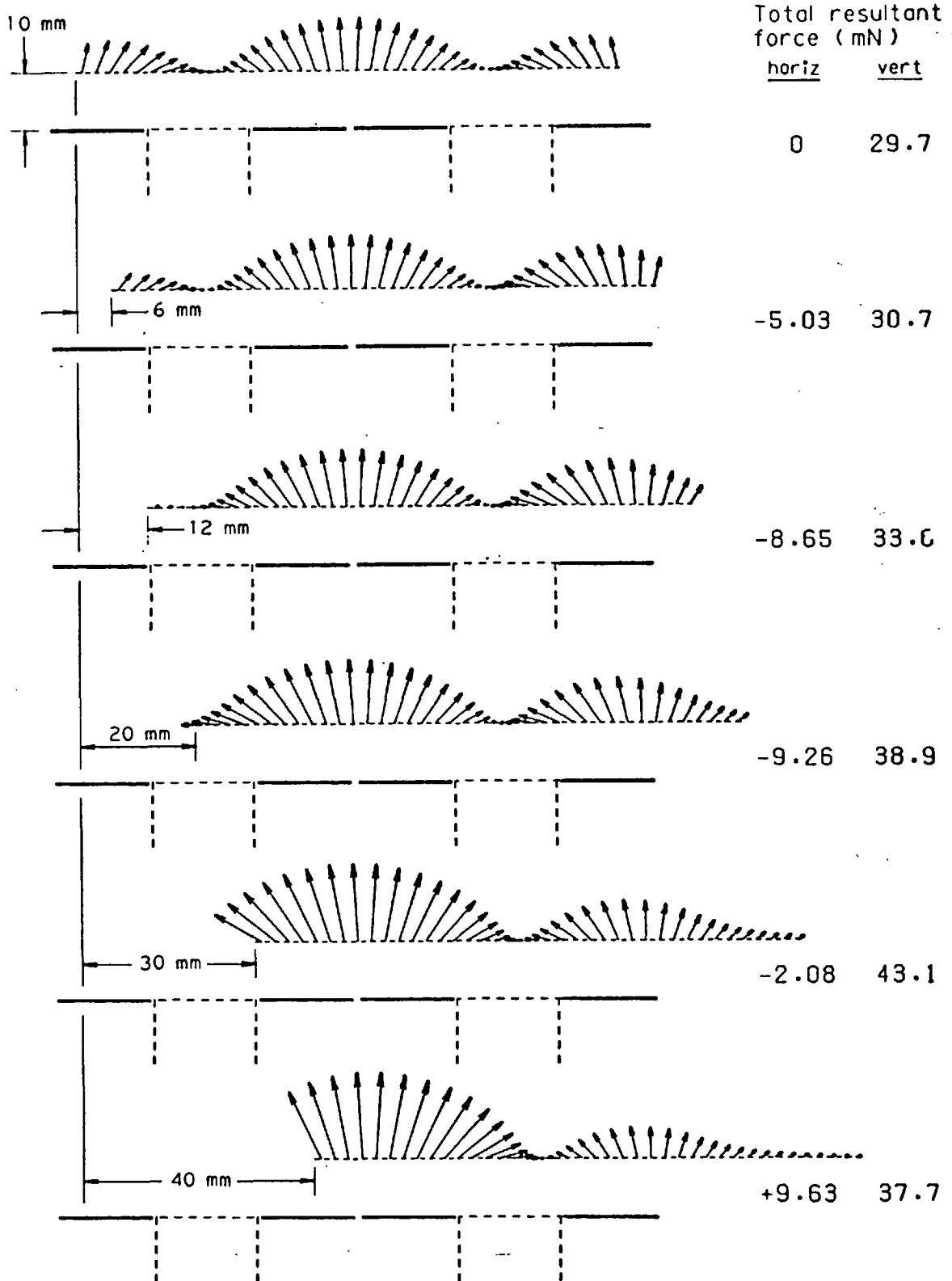
Included in Appendices D and E are descriptions and source code listings of two computer programs which carry the strip conductor analysis through to the point of computing the forces acting upon the rotor plate. Many runs of these two programs were made, producing a large quantity of numerical output. This section presents some of the trends of behaviour observed within the numerical data, and compares these where possible

with the equivalent trends observed on practical machines and discussed in the main text of the thesis. It should be remembered, however, that the comparison is only at a qualitative level - the analysis is too crude as yet to attempt a quantitative comparison between theory and practice. The discussion therefore centres on shapes and trends rather than on direct comparisons of computation with measurement.

The results may conveniently be considered in two parts - firstly the distribution of forces across the width of a given rotor plate in a given position, and secondly the variation of the overall resultant force acting on the rotor for different rotor positions. In view of the many variables involved it was found convenient to define a "standard configuration" exhibiting "average" behaviour, against which the behaviour of other configurations could then be compared. The standard selected for the rotor was 1 metre length of a 40-conductor simulation of an aluminium plate 100 mm wide by 3 mm thick, floating at a height of 10 mm. The standard stator was specified as having a slot width of 36 mm with a tooth width of 19 mm, and carrying a current of 100 amps at 50 Hz.

Fig B.4 shows a selection of force distributions, evaluated for the "standard" rotor plate in a variety of horizontal positions. The representation of the forces in this figure uses the same pictorial display as that presented in Fig 42 of Chapter 4 - the computed value of the force acting on each strip conductor in the rotor simulation is drawn as a vector acting from the centre of that conductor, with length representing magnitude and pointing in the direction of the force. In addition a pair of numbers is given to the right of each display. These are respectively the horizontal and vertical components of the total force (in mN) acting on the rotor plate, i.e. the sums of the components of the forty individual forces in each display.

Many similarities will be noted between Fig B.4 and Fig 42. In the first place the "standard" aluminium rotor plate for the theoretical analysis has the same dimensions (100 mm wide by 3 mm thick) as those of the plate whose practical measurements resulted in Figs 42(b) and (c).



Aluminium rotor plate 100 mm wide by 3 mm thick
 Stator slot width 36 mm and tooth width 19 mm
 Stator current 100 amps at 50 Hz

Fig B.4 Theoretical force distributions across a floating plate.

The stator dimensions are also the same. (This correspondence does not extend, however, to the stator current or the rotor forces, nor to the scale for plotting the force vectors.)

Secondly there is a strong resemblance between the theoretically-derived and the practically-derived force distributions for the plate in its central (symmetrical) position - these are respectively the top display of Fig B.4 and the central display of Fig 42. In both cases, allowing for the difference in scales, there is a central region of upwards levitation forces bounded on either side by smaller regions of mainly upwards and inwards forces. It is interesting, however, that the theoretical distribution fails to show the small regions of downwards force that are apparent on the practical display. Indeed for no size of plate in any position so far tried has the theoretical analysis predicted any such regions.

The second display of Fig B.4 and the bottom display of Fig 42 may also be compared directly since the plate is in each case displaced 6 mm to the right. The same effect can be seen in both - that the central region of upwards force shifts within the plate so as to remain above the centre stator conductors, the cluster of forces on the left-hand edge of the plate shrinks and the cluster on the right grows. These latter, having their horizontal components of force to the left, appear to provide the main stabilising influence on the plate. It will be appreciated, of course, that a negative horizontal component of force (i.e. one to the left) is required to stabilise a displacement to the right.

The remaining displays of Fig B.4 show the plate in four more positions, displaced successively further to the right. The shrinking of the left-hand "destabilising" group of forces continues to the point of complete extinction at displacements of over 20 mm. The right-hand "stabilising" group correspondingly grows, until by 20 mm displacement it is approaching the proportions of the original central group (itself noticeably larger than with the plate in its symmetrical position). Beyond 20 mm, however, the growth stops, and between 30

and 40 mm the stabilising group begins to shrink again. At this stage the group of forces above the stator centre conductors is also beginning to shrink, helped by the truncating action as the left-hand edge of the rotor plate intrudes upon the stator centre area.

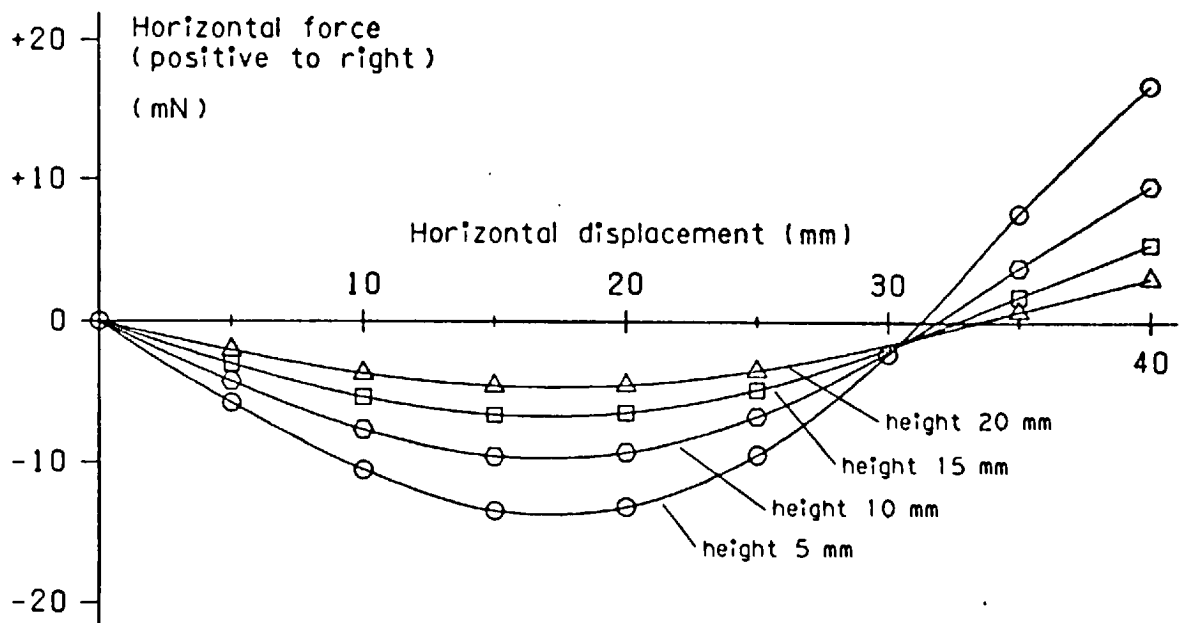
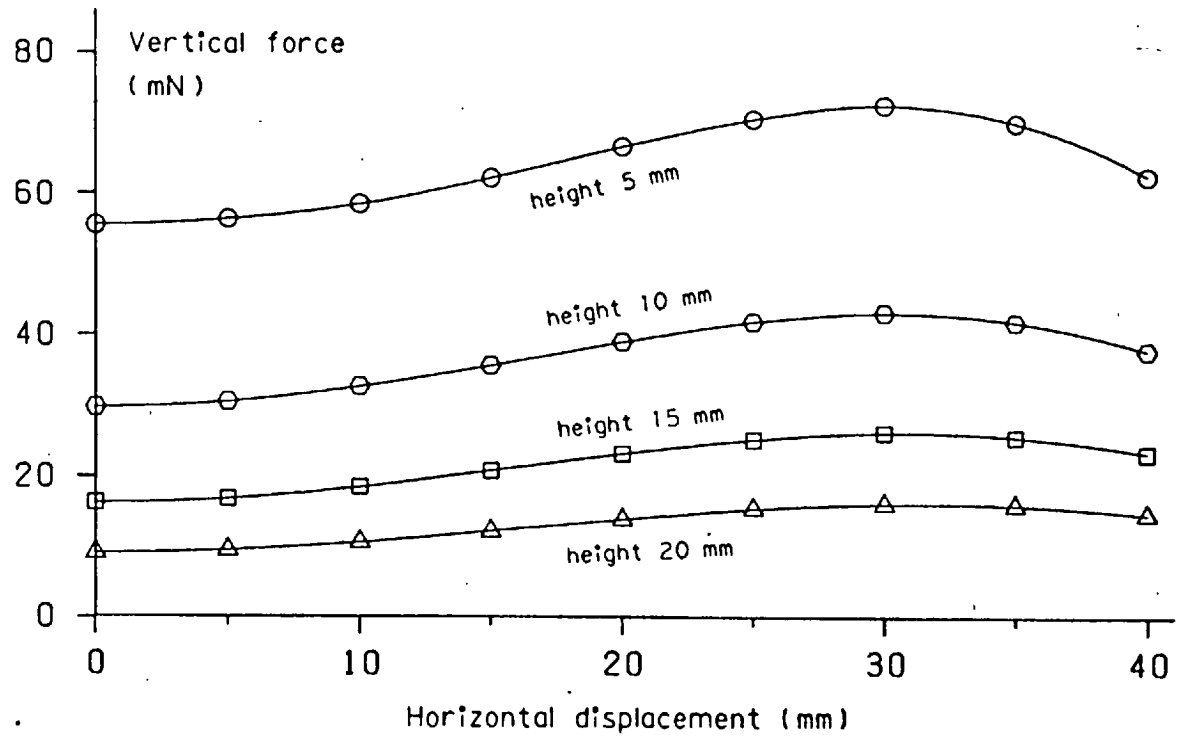
All these observations are encouraging indications of the validity of the theoretical approach, since they compare well with the corresponding observations made from practical measurements. The similarities between the two sets of force distributions are the more notable because their derivations are fundamentally different. The practical derivation of Fig 42 was made by applying the Maxwell Second Stress formulae to measurements only of the magnetic field made at many positions around the surface of the rotor plate, while the theoretical derivation of Fig B.4 involved the computation of a set of equivalent rotor currents and the evaluation of the forces on each of these by reaction with the stator currents. Indeed it could be argued that these results are further justification for the somewhat unconventional extension to the application of the Maxwell Second Stress formulae employed in the derivation of the practical force distributions (see section 4 of Chapter 4, pages 75 to 85).

Some even more encouraging results for the theoretical analysis are those deriving the horizontal and vertical components of the total resultant force acting on the rotor plate, for various positions of the rotor. Referring again to Fig B.4, it may be seen from the numbers to the right of each display (representing the sums of the components of the forty forces displayed) that the overall horizontal restoring force increases with displacement for plate movements of up to about 20 mm. It then decreases rapidly as the displacement progresses to 30 mm, and changes sign to become a destabilising force shortly after 30 mm. Correspondingly the upwards lift force increases slowly with displacement for movements of up to 30 mm, then begins to decrease again. These patterns of force variation are precisely the "river bank" shape that was described in Chapter 1 (see Fig 7). This, then, is the achievement of the objective stated at the beginning of this Appendix - to derive from theoretical considerations alone the characteristic "river bank" double-hump shape of forces that gives the electromagnetic river its name.

The variation of total force on the rotor with rotor position may be more clearly represented by a graphical rather than a pictorial display. For example Fig B.5 shows the vertical (lifting) and horizontal (stabilising) forces acting upon the "standard" rotor plate in a series of nine horizontal positions at each of four heights. These include four of the positions for which the complete force distributions were presented in Fig B.4 (all at a height of 10 mm). Note in particular that regions of static stability at a given rotor height appear on the lower graph as the range of horizontal positions for which the appropriate curve is below the horizontal axis.

Several characteristics of expanding-geometry levitating machines may be deduced from Fig B.5. The four curves of the top graph give the obvious result that the lift force decreases with height, at all positions of lateral displacement investigated. They also show that at a given height the lift force initially increases slightly with displacement, reaches a maximum value, and then decreases rather more rapidly after the peak is passed. This "hump" effect is more noticeable on the curves plotted for lower heights.

The curves of the lower graph show that over almost all of their respective regions of stability, plates experience lesser stabilising forces at greater heights. The exception is for positions at the extreme edges of the stable regions. The four curves cross over one another shortly before crossing the zero axis into the regions of instability (positive lateral force), indicating a small range of lateral displacements within which the stabilising force increases with height. (No significance, incidentally, is to be attached to the fact that all four curves seem to cross at the same point - this appears to be co-incidental to the particular choice of parameters selected for Fig B.5.) It might be noted that the limiting displacement for lateral stability - the position at which the horizontal force curve crosses the horizontal axis - increases slightly at increasing heights. This might be taken as an example of an expanding geometry, since the range of stable positions is thus wider for plates that float higher. The effect is, however, small, and is not the behaviour that originally led



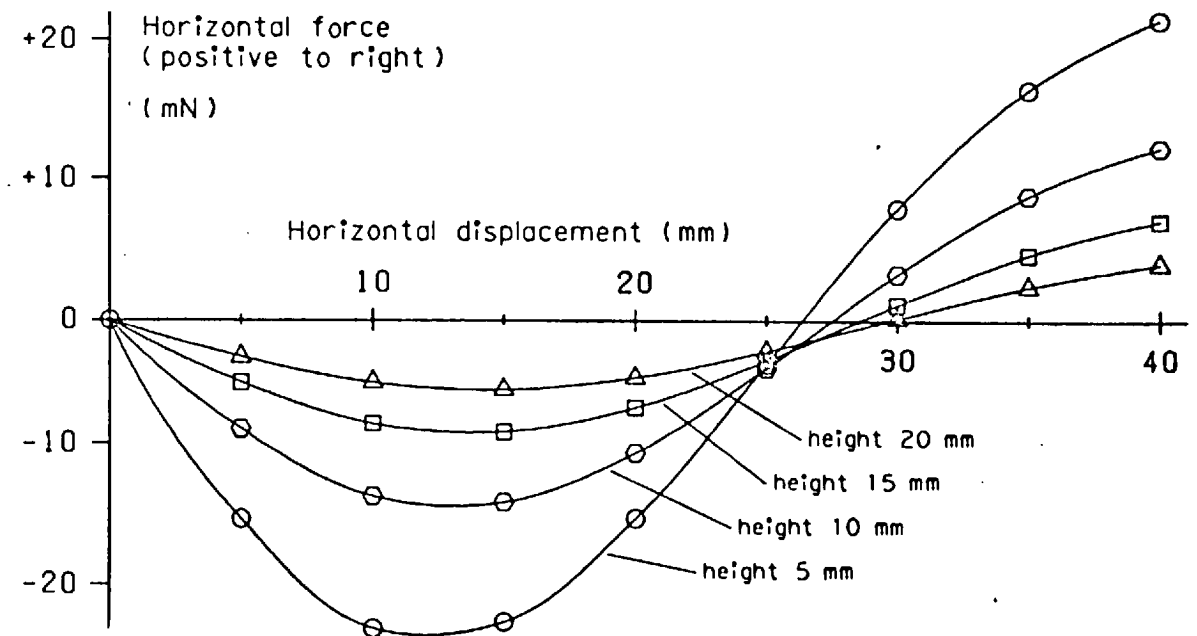
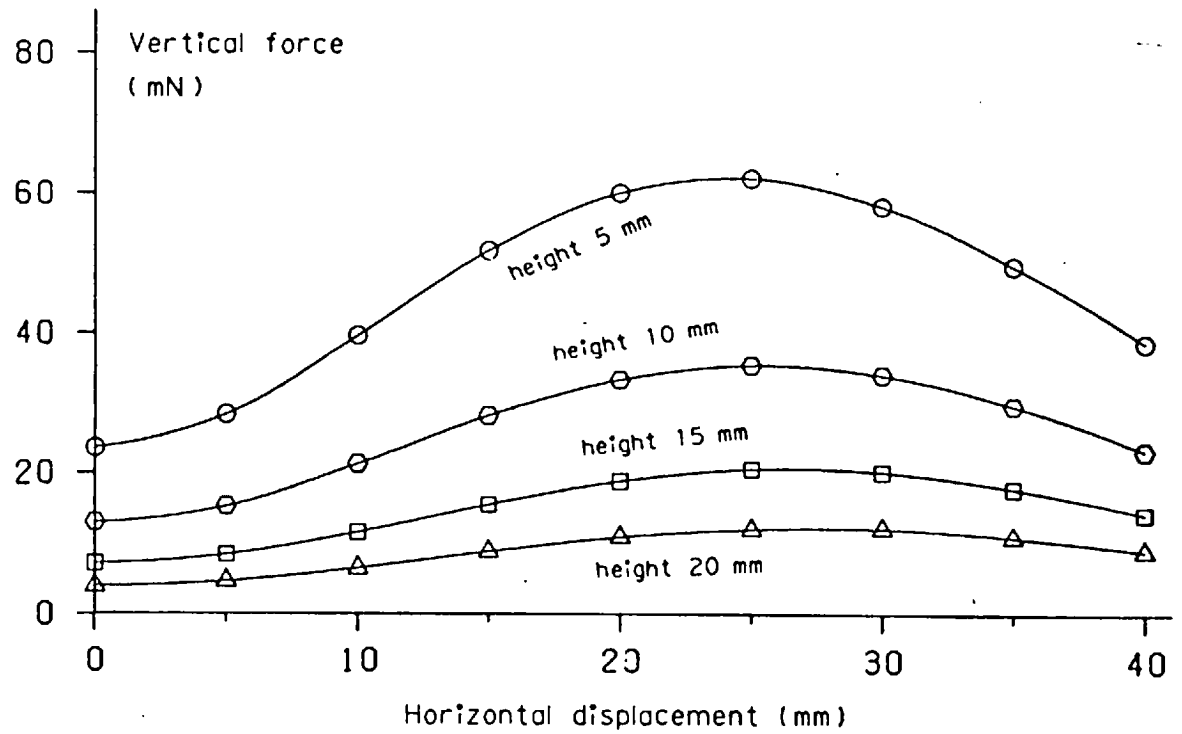
Aluminium rotor plate 100 mm wide by 3 mm thick
 Stator slot width 36 mm and tooth width 19 mm
 Stator current 100 amps at 50 Hz

Fig B.5 Variations of total horizontal and vertical forces acting upon a "standard" rotor plate, plotted against horizontal rotor displacement.

to the concept of expanding geometry (which was that greater stator currents may be used to float wider plates at greater heights - see Chapter 1, page 25).

A further series of computed results is presented in Fig B.6. These were evaluated for a plate only 80 mm wide (compared with the 100 mm plate of Fig B.5), in order to see how well the theoretical analysis reflected the known practical behaviour of a narrower plate. Comparing the top set of curves of Fig B.6 with the corresponding set of Fig B.5, it is immediately apparent that the narrower plate experiences rather less lift in positions of zero displacement. For each of the four heights plotted this reduction in lift is greater than the corresponding reduction in the weight of the plate (proportional to the change in width from 100 mm to 80 mm), implying that the height at which an unconstrained narrow plate would float is lower than that for a wider plate. This is certainly known to be the case in practice (see section 3 of Chapter 2, Fig 17). The top set of curves also shows that as the plate is displaced laterally the lift force initially increases more rapidly than it did for the 100 mm plate. The "hump" of the river bank thus appears to have steeper sides. A similar effect was noted during practical experiments with annular rotors above a single C-core stator - see Chapter 8, pages 188 - 189.

The lower set of curves of Fig B.6 shows that at low heights the 80 mm plate experiences a rather stronger lateral restoring force over its stable region than did the 100 mm plate. The remarkable fact thus emerges from the analytical derivation, as it did from practical observations, that the smaller plate experiences a greater restoring force although there is less material on which the eddy currents can act. It will be further appreciated that the effectiveness of this force is increased in proportion to the reduction in the mass of the plate. At greater heights of levitation the change in the restoring force for the smaller width of plate is less marked. At all heights, however, the region of stability is less extensive than for the wider plate. Corresponding observations were made in practice during measurements of the restoring forces acting on two plates of different widths under various conditions of mechanical loading - see section 9 of Chapter 7, Fig 73 (page 178).



Aluminium rotor plate 80 mm wide by 3 mm thick
Stator slot width 36 mm and tooth width 19 mm
Stator current 100 amps at 50 Hz

Fig B.6 Variations of total vertical and horizontal forces with rotor position, plotted for a plate 80 mm wide.

The comparison between Figs B.5 and B.6 may be summarised as showing that the theoretical analysis based on strip conductors agrees with the practical observation that for a given stator current wide plates tend to float higher than narrow ones, but are rather less stable (see section 2 of Chapter 2, page 33). Each figure on its own clearly shows the "river bank" shape of forces described in Chapter 1 (Fig 7). Taken together these are encouraging indications of the validity of the strip conductor analysis as applied to the modelling of practical expanding-geometry levitators.

B.4 Extensions and conclusions

The latter part of section B.3 concentrated upon a comparison between two sets of data showing the effect of a change in the width of the rotor. It is, of course, possible to use the strip conductor analysis to investigate the effect of varying other parameters, such as plate thickness, resistivity, stator dimensions, stator current or supply frequency. The associated computer programs were used many times during the course of such investigations, and again the trends of behaviour deduced agreed well with those observed in the laboratory. However the voluminous results obtained do no more than further prove the strip conductor analysis and they are considered of insufficient interest to warrant presentation here. The final section of this Appendix therefore concentrates instead on outlining the limitations of the theoretical method, and suggests some extensions and improvements which might lead to a more refined analysis.

An obvious limitation of the analysis as presented in section B.2 is the use of only a single row of strip conductors in the representation of the rotor. As explained in section B.1, the use of several horizontal layers of equivalent conductors would permit a more realistic simulation of rotor thickness, and hence could take account of skin depth in the rotor material. Note that nothing is to be gained by applying the same process to the stator conductors in an attempt to simulate the space distribution of the stator windings in their slots. In the paper by Saunders quoted earlier (page 275), the discussion about replacing slot-embedded conductors by an equivalent strip conductor made no

assumptions regarding the space distribution of the conductors within the slot. The current flowing in a single strip conductor spanning the top of a slot has the same effect within the region above it as any space distribution of the equivalent current flowing in the slot below.

Extensions such as additional rows of rotor loop currents would, of course, involve the solution of a larger set of equations, and a limit must ultimately apply to the size of complex rotor matrix that can be stored and inverted by a computer. The two programs that produced the data presented in section B.3 are both complete in themselves, and therefore each has to contain the entire sequence of instructions necessary to assemble the rotor matrix, invert it, and use it in the subsequent calculations. This makes a heavy demand on storage space within the computer memory. However since the investigation of a given rotor configuration requires the construction and inversion of the matrix only once, it might be worthwhile to split such programs into three separate parts, to be executed independently by the computer. The first part would construct the rotor matrix and write it to a data file; the second part would then invert the matrix, the whole of the computer memory being available for this task. Indeed use could if necessary be made here of more "exotic" inversion routines which do not need to hold the entire matrix in memory in order to perform the inversion. The third part could then use the inverted matrix as an operator on the remaining parameters calculated for the rotor in a variety of positions.

In Appendix C the analytical derivations are given of the expressions used to determine the magnetic field set up by a horizontal coil of strip conductors, the force experienced by another horizontal strip conductor within such a field, and the mutual inductance between two horizontal coils. Several integrals are involved in the derivations, all of which are evaluated only for horizontal conductors and coils since this is sufficient for the analysis of section B.2. Extensions to the theory could be made, however, by evaluating further integrals to give the fields, forces and mutual inductances for conductors and coils in planes other than

horizontal. For example the evaluation of such quantities for vertically-aligned rotor coils might allow the investigation of U-shaped rotors (plates with turned-up edges). Generalisation to rotor coils tilted at any angle would permit the examination of rotors in positions of angular displacement about their longitudinal axes, and this could develop into an investigation of the roll-stability of floating plates.

A limited amount of information on roll effects could in fact be obtained from a minor extension to the last stages of the horizontal analysis presented, without the evaluation of new sets of integrals. This merely involves summing the moments of the individual vertical force components about the longitudinal rotor axis, to give the magnitude and angular direction of the roll torque acting upon the horizontal rotor. Such an evaluation could predict only the strength and angular direction by which the rotor tends to tilt from its horizontal position; it could give no information about the existence of an equilibrium angle of tilt or about roll stability. However it might at least confirm (or otherwise) the sequence of roll motions displayed in Fig 96 (page 230), for a plate in several positions of lateral displacement.

Of the simplifications made in the analysis of section B.2, perhaps the most significant was the complete removal of all the iron. This was justified in the original analysis by the search for the simplest theoretical system capable of producing expanding-geometry stability forces. Moreover it was considered improbable that a semi-infinite iron block (itself a simplification resulting from the use of strip conductors) could play a fundamental part in the stability mechanism. It is certain however, that the absence of the iron has a profound effect upon the overall absolute magnitudes of the forces calculated, and it is largely for this reason that no quantitative comparison of calculated with measured results has been attempted.

Reconstruction of the analysis to include the shape of the iron core (e.g. a C-core block of laminations) may be considered in two stages. The first is to re-introduce the semi-infinite block of iron

below the stator strip conductors and the second is then to transform this into the original iron shape. Stage 1 may be accomplished by using the method of image currents to simulate the semi-infinite block of iron. The iron would here be considered infinitely permeable to magnetic flux but infinitely laminated against the flow of electric current, extending to infinity vertically downwards from the plane of the stator strip conductors and horizontally in all directions.

Such a system may be analysed by replacing the iron by a second set of stator and rotor conductors. The positions of these are found by considering the top surface of the iron to be a mirror, and placing a new "image" conductor in the position of the image of every original conductor as seen in the mirror. Each new conductor carries the same current in the same direction as its image. The semi-infinite block is thus replaced by a second set of stator conductors superimposed upon the original set (since both are at the surface of the "mirror"), and a second set of rotor currents vertically in line with the original set but as far below the iron surface as the original set is above. The use of image currents does, of course, require the assembly and inversion of a complex rotor matrix twice the size of that for a solution without semi-infinite iron.

The second stage in the re-instatement of "real" iron is less straightforward. Many factors are involved. Apart from the simulation of three-dimensional features such as slots, limbs and teeth, a comprehensive analysis should aim to take into account parameters such as non-infinite permeability, non-ideal lamination and hence eddy currents in certain planes, and saturation of the iron. It seems improbable that an analysis based on equivalent circuits and discrete mutual inductances can be extended to include complexities such as these.

However even without the last stage, there is at least one practical machine that may be sufficiently similar to a set of strip conductors over semi-infinite iron for a quantitative comparison to be possible. This is the Xi-core motor (see Figs 98 and 99). Three features of the Xi-core motor are particularly relevant in this connection. Firstly the iron core has four vertical limbs whose tops all lie in one

horizontal plane. This plane readily transforms into the top plane of a semi-infinite block of iron. Secondly the arrangement of the four limbs ensures that all three sets of stator conductors are fully embedded in slots, and are thus immediately suitable for modelling by the strip conductor technique. Thirdly the two outer limbs were originally provided to turn wasteful "leakage" flux into useful flux (see Fig 98). As such their precise dimensions are largely irrelevant. Extending their widths to infinity outwards may prove to have little significant effect upon the behaviour of the levitator.

In conclusion, an elementary analysis based on strip conductors has been shown to be possible, and a system of conductors has been found from which forces may be derived that behave in ways similar to those measured on practical expanding-geometry levitators. The contrast, incidentally, might be appreciated between the "circuit theory" approach employed in this analysis and the "field theory" approach that is perhaps more commonly used in attempts to analyse the behaviour of machines of this kind. Several suggestions have been made for extensions and refinements to the analysis and some of these extensions might be considered worthwhile for research in the future. Whether the analysis can be developed to the point of quantitative simulation remains to be seen.

APPENDIX C. ANALYTICAL DERIVATIONS OF THE MATHEMATICAL EXPRESSIONS USED IN APPENDIX B

Appendix B described how a circuit-theory approach could be employed to construct a theoretical model of a simple expanding-geometry levitator. The model featured the use of strip conductors, i.e. conductors considered to be of infinite length, finite width and infinitesimal thickness. The method involved the construction of a matrix relating each current in the model to every other current, in terms of resistances, self-inductances and mutual inductances. The matrix was inverted in order to solve for the rotor currents, and the forces between the rotor and stator currents were then evaluated to determine the total force on the rotor.

This Appendix presents analytical derivations of the mathematical expressions used to evaluate the self- and mutual inductance terms in the matrix and the forces on current-carrying strip conductors. Firstly the derivation is given of the magnetic field around a strip conductor set up by a current flowing in the conductor. This is easily extended to give the field set up by a coil comprising a pair of horizontal strip conductors. The force is then evaluated upon a third current-carrying strip conductor placed within the field set up by such a coil. Finally the expressions for the mutual inductance between two horizontal coils of strip conductors is derived, and this of course also gives the self-inductance of a single coil when the two coils are superimposed. It should be noted that all the derived equations have been expressed in a form suitable for numerical evaluation by a digital computer.

C.1 Conventions for co-ordinates, currents and fluxes

The conventions for co-ordinates, current flows and flux directions employed in the following analytical derivations are given here. Since the hypothetical machine of the model is infinitely long and all current flow is axial, i.e. parallel to this infinite length, it is convenient to present all diagrams in the form of transverse cross sections. The x-axis on each diagram is thus the horizontal direction

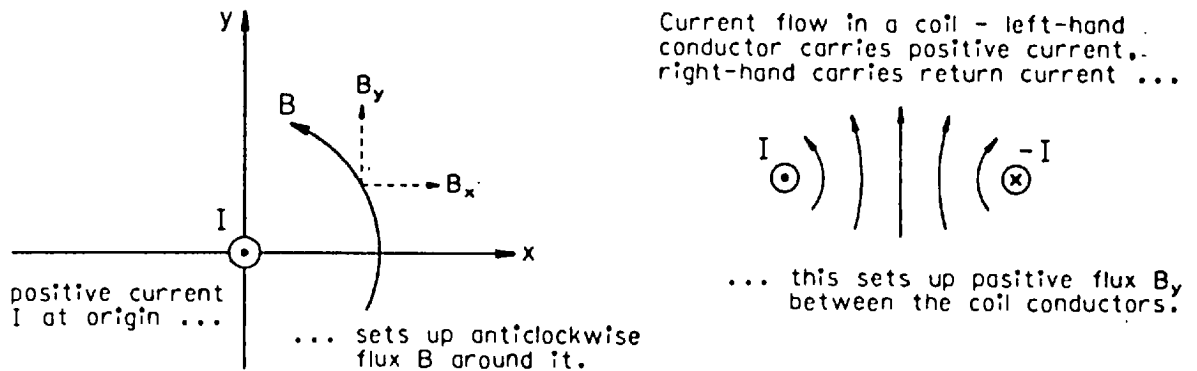


Fig C.1 Current and flux conventions.

transverse to the machine; the y-axis is the vertical direction, and the z-axis, perpendicular to the plane of the diagram, is the horizontal axial direction along the machine. To maintain a right-handed co-ordinate system consistent with the accepted positive x and y directions on the paper, the positive z direction is out of the front surface of the paper, towards the observer.

Positive axial current is defined to be in the direction of the z-axis, i.e. also towards the observer. Thus a positive current sets up a magnetic field around it which is anticlockwise in the x-y plane as viewed on the paper - see Fig C.1. Note that by this convention the horizontal component of field B_x set up by positive axial current I at the origin is negative in the first quadrant of the x-y plane, while the vertical component B_y is positive.

The convention taken for positive current flow in a pair of axial conductors forming an infinitely long coil in the x-z plane is that the circulation of current is clockwise as viewed along the y-axis. The left-hand conductor of a horizontal coil therefore carries current out of the plane of the paper (positive) and the right-hand conductor carries the return current into the paper (negative) - see Fig C.1. This convention produces a positive vertical component of flux B_y between the two conductors.

C.2 Field set up by a current in a horizontal strip conductor

Fig C.2 shows a horizontal strip conductor of width $2c$, centred on the origin, carrying current I . The objective is to derive the horizontal field component B_x and the vertical component B_y set up by the current at a general point P , co-ordinates (p, q) .

Consider an elemental width δx of the strip conductor, at position x from the origin. The current carried by this width of conductor is $\frac{I\delta x}{2c}$, therefore the elemental field δB set up at P by the current in the element is given by:

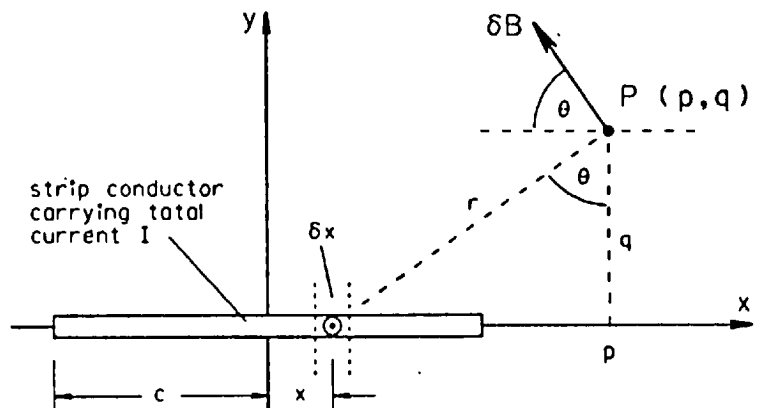
$$\delta B = \frac{\mu_0}{2\pi r} \cdot \frac{I\delta x}{2c} \quad \text{where } r \text{ is the distance of } P \text{ from the element of the conductor, and } \delta B \text{ acts in direction } \theta, \text{ as shown.}$$

Resolving into horizontal and vertical components δB_x and δB_y :

$$\begin{aligned} \delta B_x &= -\frac{\mu_0 I}{4\pi c} \cdot \frac{\cos\theta}{r} \delta x \\ &= -\frac{\mu_0 I}{4\pi c} \cdot \frac{q}{r^2} \delta x \\ &= -\frac{\mu_0 I}{4\pi c} \cdot \frac{q}{(p-x)^2 + q^2} \delta x \end{aligned} \quad \left| \quad \begin{aligned} \delta B_y &= \frac{\mu_0 I}{4\pi c} \cdot \frac{\sin\theta}{r} \delta x \\ &= \frac{\mu_0 I}{4\pi c} \cdot \frac{p-x}{r^2} \delta x \\ &= \frac{\mu_0 I}{4\pi c} \cdot \frac{p-x}{(p-x)^2 + q^2} \delta x \end{aligned} \right.$$

Fig C.2

Field set up by strip conductor.



Integrating across the width of the conductor to give the field components B_x and B_y at P:

$$\begin{aligned}
 B_x &= -\frac{\mu_o I}{4\pi c} \cdot \int_{-c}^c \frac{q}{(p-x)^2 + q^2} dx \\
 &= +\frac{\mu_o I}{4\pi c} \cdot \int_{p+c}^{p-c} \frac{q}{x^2 + q^2} dx \\
 B_x &= \frac{\mu_o I}{4\pi c} \cdot \left[\tan^{-1} \left\{ \frac{x}{q} \right\} \right]_{p+c}^{p-c}
 \end{aligned}
 \quad \left| \quad
 \begin{aligned}
 B_y &= \frac{\mu_o I}{4\pi c} \cdot \int_{-c}^c \frac{p-x}{(p-x)^2 + q^2} dx \\
 &= -\frac{\mu_o I}{4\pi c} \cdot \int_{p+c}^{p-c} \frac{x}{x^2 + q^2} dx \\
 B_y &= -\frac{\mu_o I}{4\pi c} \cdot \left[\frac{1}{2} \log (x^2 + q^2) \right]_{p+c}^{p-c}
 \end{aligned}$$

It is convenient at this point to define two functions. Let AATAN (x, y) be defined as $\tan^{-1} \left\{ \frac{x}{y} \right\}$ and AALOG (x, y) be defined as $\frac{1}{2} \log (x^2 + y^2)$. Then the field components B_x and B_y are given by:

$$\begin{aligned}
 B_x &= \frac{\mu_o I}{4\pi c} \cdot \left\{ \text{AATAN} (p-c, q) - \text{AATAN} (p+c, q) \right\} \\
 B_y &= -\frac{\mu_o I}{4\pi c} \cdot \left\{ \text{AALOG} (p-c, q) - \text{AALOG} (p+c, q) \right\}
 \end{aligned}$$

The two equations in this form are particularly suitable for use on a computer, since the functions AATAN and AALOG may be defined as Fortran functions, and evaluated with the appropriate numerical arguments whenever required. (Indeed computer users may recognise that the names of the two functions were chosen with Fortran naming conventions in mind, and in deliberate imitation of the standard Fortran functions ATAN and ALOG.) It should be noted that each function has a singularity when $x = y = 0$. The computer must therefore be instructed to detect and handle these special conditions (see section 1 of Appendix D for the details and justification of the method employed).

C.3 Field components set up by a horizontal coil of strip conductors

A simple extension to the derivation given in section C.2 above gives the magnetic field set up by a horizontal coil of two strip conductors. Consider the system shown in Fig C.3, where the coil spacing is $2a$ between the centres of its conductors, and each conductor is of width $2c$. The coil is centred on the origin, the left-hand conductor carries current I and the right-hand conductor carries current $-I$. The field components at point $P(p, q)$ are given by the sum of the contributions from the two currents:

$$B_x = \frac{\mu_0 I}{4\pi c} \cdot \left\{ \text{AATAN}(p+a-c, q) - \text{AATAN}(p+a+c, q) \right\} \\ - \frac{\mu_0 I}{4\pi c} \cdot \left\{ \text{AATAN}(p-a-c, q) - \text{AATAN}(p-a+c, q) \right\} \dots\dots (1)$$

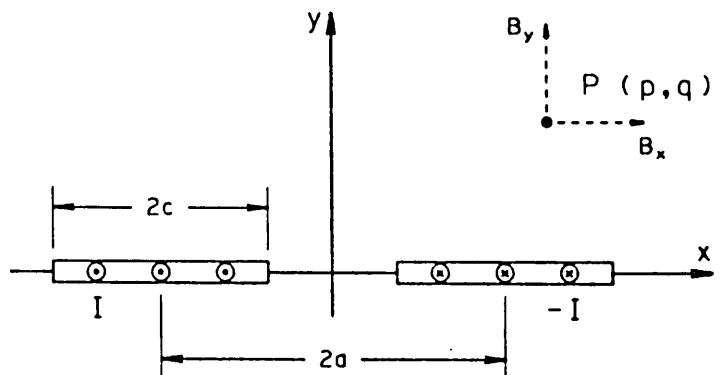
$$B_y = - \frac{\mu_0 I}{4\pi c} \cdot \left\{ \text{AALOG}(p+a-c, q) - \text{AALOG}(p+a+c, q) \right\} \\ + \frac{\mu_0 I}{4\pi c} \cdot \left\{ \text{AALOG}(p-a-c, q) - \text{AALOG}(p-a+c, q) \right\} \dots\dots (2)$$

C.4 Force exerted upon a strip conductor in the field set up by a coil of two strip conductors

The objective of this section is to find an expression for the force exerted upon a horizontal current-carrying strip conductor within the magnetic field set up by the current flowing in a horizontal coil of two strip conductors. The general expression for the force \underline{F} acting on a current \underline{I} in a field \underline{B} is $\underline{F} = \underline{I} \times \underline{B}$,

Fig C.3

Flux components set up by a coil of two strip conductors.



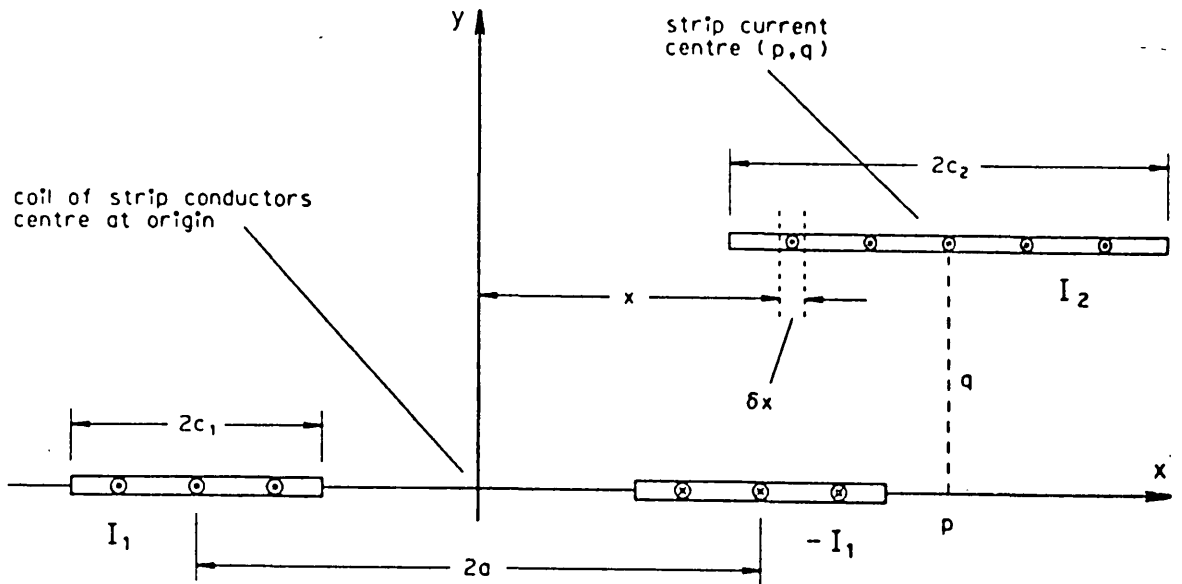


Fig C.4 Force on a strip conductor in the field set up by a coil of strip conductors.

where \underline{F} , \underline{I} and \underline{B} are all vectors, and \times is the vector cross product. For the present purpose, where all current flow is parallel to the z-axis, it is convenient to use the component co-ordinate forms:

$$F_x = -B_y \cdot I_z$$

$$F_y = B_x \cdot I_z .$$

Fig C.4 shows a strip conductor in the vicinity of a coil of strip conductors. The coil is centred at the origin, is of conductor spacing $2a$, of conductor width $2c_1$ and carries current I_1 . The separate conductor is at centre (p, q) , of width $2c_2$ and carries current I_2 . Consider first the force δF acting on an element of the conductor of width δx at position (x, q) , carrying current δI_2 . The horizontal component of force δF_x acting on the element is given by:

$$\begin{aligned} \delta F_x &= -B_y \cdot \delta I_2 \\ &= \frac{-B_y I_2 \delta x}{2c_2} . \end{aligned}$$

Integrating across the conductor width to give the horizontal force F_x on the entire conductor:

$$F_x = - \frac{I_2}{2c_2} \cdot \int_{p-c_2}^{p+c_2} B_y \, dx \quad \dots\dots (3)$$

Likewise the vertical component of force F_y acting on the entire conductor is given by:

$$F_y = \frac{I_2}{2c_2} \cdot \int_{p-c_2}^{p+c_2} B_x \, dx \quad \dots\dots (4)$$

These two expressions for the components of force include definite integrals of the flux components B_x and B_y , which are themselves functions in AATAN and AALOG (see equations 1 and 2 on page 301). These latter, it will be recalled, were defined by:

$$\begin{aligned} \text{AATAN} (x, y) &= \tan^{-1} \left\{ \frac{x}{y} \right\} \\ \text{AALOG} (x, y) &= \frac{1}{2} \log (x^2 + y^2) . \end{aligned}$$

The function $\text{AATAN} (x, y)$ may be integrated thus:

$$\begin{aligned} \int_{\alpha}^{\beta} \text{AATAN} (x, y) \, dx &= \int_{\alpha}^{\beta} \tan^{-1} \left\{ \frac{x}{y} \right\} \, dx \\ &= \left[x \cdot \tan^{-1} \left\{ \frac{x}{y} \right\} - \frac{y}{2} \cdot \log (x^2 + y^2) \right]_{\alpha}^{\beta} \\ &= \left[x \cdot \text{AATAN} (x, y) - y \cdot \text{AALOG} (x, y) \right]_{\alpha}^{\beta} \\ &= \left[\text{TANINT} (x, y) \right]_{\alpha}^{\beta} \quad (\text{say}) \end{aligned}$$

where $\text{TANINT} (x, y)$ is a new function, defined by:

$$\text{TANINT} (x, y) = x \cdot \text{AATAN} (x, y) - y \cdot \text{AALOG} (x, y) .$$

Likewise the function AALOG (x, y) may be integrated thus:

$$\begin{aligned}
 \int_{\alpha}^{\beta} \text{AALOG} (x, y) \, dx &= \int_{\alpha}^{\beta} \frac{1}{2} \log (x^2 + y^2) \, dx \\
 &= \left[\frac{x}{2} \cdot \log (x^2 + y^2) + y \cdot \tan^{-1} \left\{ \frac{x}{y} \right\} - x \right]_{\alpha}^{\beta} \\
 &= \left[x \cdot \text{AALOG} (x, y) + y \cdot \text{AATAN} (x, y) - x \right]_{\alpha}^{\beta} \\
 &= \left[\text{ALNINT} (x, y) \right]_{\alpha}^{\beta} \quad (\text{say})
 \end{aligned}$$

where ALNINT (x, y) is another new function, defined by:

$$\text{ALNINT} (x, y) = x \cdot \text{AALOG} (x, y) + y \cdot \text{AATAN} (x, y) - x.$$

Like the functions AATAN and AALOG, the two functions TANINT and ALNINT are suitable for programming directly into a computer as Fortran functions. (Again Fortran users will recognise that the name ALNINT was chosen instead of the more obvious LOGINT bearing in mind the Fortran naming conventions for floating-point functions.) Note that since TANINT and ALNINT are defined in terms of AATAN and AALOG, no special handling of singularities is necessary beyond that already contained in AATAN and AALOG (see Appendix D).

The force components F_x and F_y on the horizontal strip conductor of Fig C.4 may now be evaluated using equations 3 and 4 as follows:

$$\begin{aligned}
 F_x &= - \frac{I_2}{2c_2} \cdot \int_{p-c_2}^{p+c_2} B_y \, dx \\
 &= - \frac{I_2}{2c_2} \cdot \frac{\mu_0 I_1}{4\pi c_1} \cdot \int_{p-c_2}^{p+c_2} \left\{ \begin{aligned} &-\text{AALOG} (x+a-c_1, q) + \text{AALOG} (x+a+c_1, q) \\ &+\text{AALOG} (x-a-c_1, q) - \text{AALOG} (x-a+c_1, q) \end{aligned} \right\} \, dx \\
 &= - \frac{\mu_0 I_1 I_2}{8\pi c_1 c_2} \cdot \left[\begin{aligned} &-\text{ALNINT} (x+a-c_1, q) + \text{ALNINT} (x+a+c_1, q) \\ &+\text{ALNINT} (x-a-c_1, q) - \text{ALNINT} (x-a+c_1, q) \end{aligned} \right]_{p-c_2}^{p+c_2}
 \end{aligned}$$

$$F_x = \frac{\mu_0 I_1 I_2}{8\pi c_1 c_2} \cdot \left\{ \begin{array}{l} \text{ALNINT} (p+a-c_1+c_2, q) - \text{ALNINT} (p+a+c_1+c_2, q) \\ - \text{ALNINT} (p-a-c_1+c_2, q) + \text{ALNINT} (p-a+c_1+c_2, q) \\ - \text{ALNINT} (p+a-c_1-c_2, q) + \text{ALNINT} (p+a+c_1-c_2, q) \\ + \text{ALNINT} (p-a-c_1-c_2, q) - \text{ALNINT} (p-a+c_1-c_2, q) \end{array} \right\} \dots (5)$$

$$\begin{aligned} F_y &= \frac{I_2}{2c_2} \cdot \int_{p-c_2}^{p+c_2} B_x dx \\ &= \frac{I_2}{2c_2} \cdot \frac{\mu_0 I_1}{4\pi c_1} \cdot \int_{p-c_2}^{p+c_2} \left\{ \begin{array}{l} \text{AATAN} (x+a-c_1, q) - \text{AATAN} (x+a+c_1, q) \\ - \text{AATAN} (x-a-c_1, q) + \text{AATAN} (x-a+c_1, q) \end{array} \right\} dx \\ &= \frac{\mu_0 I_1 I_2}{8\pi c_1 c_2} \cdot \left[\begin{array}{l} \text{TANINT} (x+a-c_1, q) - \text{TANINT} (x+a+c_1, q) \\ - \text{TANINT} (x-a-c_1, q) + \text{TANINT} (x-a+c_1, q) \end{array} \right]_{p-c_2}^{p+c_2} \\ &= \frac{\mu_0 I_1 I_2}{8\pi c_1 c_2} \cdot \left\{ \begin{array}{l} \text{TANINT} (p+a-c_1+c_2, q) - \text{TANINT} (p+a+c_1+c_2, q) \\ - \text{TANINT} (p-a-c_1+c_2, q) + \text{TANINT} (p-a+c_1+c_2, q) \\ - \text{TANINT} (p+a-c_1-c_2, q) + \text{TANINT} (p+a+c_1-c_2, q) \\ + \text{TANINT} (p-a-c_1-c_2, q) - \text{TANINT} (p-a+c_1-c_2, q) \end{array} \right\} \dots (6) \end{aligned}$$

Once again the two expressions for the forces F_x and F_y are suitable for definition on the computer as Fortran functions. The names chosen were XFORCE and YFORCE, each function having the five arguments p, q, a, c_1 , and c_2 . With these changed to upper case to suit the limited Fortran character set, and with each of the functions comprising the term $\frac{\mu_0}{8\pi c_1 c_2}$ multiplied by one of the large curly brackets, the evaluation of the components of force acting on a strip conductor in the field of a coil of strip conductors becomes the execution of two statements in Fortran:

$$FX = CURNT1 * CURNT2 * XFORCE (P, Q, A, C1, C2)$$

$$FY = CURNT1 * CURNT2 * YFORCE (P, Q, A, C1, C2)$$

where CURNT1 and CURNT2 are the Fortran variables corresponding to I_1 and I_2 .

C.5 The calculation of mutual inductance

The final piece of mathematical analysis needed for Appendix B is the derivation of an expression for the mutual inductance between two horizontal coils of strip conductors. The mutual inductance may be found by evaluating the total flux linking the current in one coil per unit current in the other. It is necessary, of course, to make allowance for those flux paths set up by the primary current which intersect the secondary strip conductors and therefore link only a portion of the secondary current.

Fig C.5 shows two horizontal coils of strip conductors. The primary coil is centred on the origin, has conductor spacing $2a_1$ and conductor width $2c_1$, and carries unit current I . The secondary coil is at centre (p, q) , of conductor spacing $2a_2$ and width $2c_2$. Consider an elemental coil, part of the secondary main coil, at centre (x, q) , of conductor spacing $2a_2$ and conductor width δx , as shown. The flux passing through this elemental secondary coil set up by the unit current in the primary coil is $\int_{x-a_2}^{x+a_2} B_y dx$, and this links $\frac{\delta x}{2c_2}$ of any current flowing in the main secondary coil. Thus the elemental mutual inductance δM contributed by the elemental coil is given by:

$$\begin{aligned}
 \delta M &= \frac{\delta x}{2c_2} \cdot \int_{x-a_2}^{x+a_2} B_y dx \\
 &= \frac{\delta x}{2c_2} \cdot \frac{\mu_0}{4\pi c_1} \cdot \int_{x-a_2}^{x+a_2} \left\{ -\text{AALOG}(x+a_1-c_1, q) + \text{AALOG}(x+a_1+c_1, q) \right. \\
 &\quad \left. + \text{AALOG}(x-a_1-c_1, q) - \text{AALOG}(x-a_1+c_1, q) \right\} dx \\
 &= \frac{\mu_0 \delta x}{8\pi c_1 c_2} \cdot \left[-\text{ALNINT}(x+a_1-c_1, q) + \text{ALNINT}(x+a_1+c_1, q) \right]_{x-a_2}^{x+a_2} \\
 &= \frac{\mu_0 \delta x}{8\pi c_1 c_2} \cdot \left\{ \begin{aligned} &-\text{ALNINT}(x+a_1+a_2-c_1, q) + \text{ALNINT}(x+a_1+a_2+c_1, q) \\ &+ \text{ALNINT}(x-a_1+a_2-c_1, q) - \text{ALNINT}(x-a_1+a_2+c_1, q) \\ &+ \text{ALNINT}(x+a_1-a_2-c_1, q) - \text{ALNINT}(x+a_1-a_2+c_1, q) \\ &-\text{ALNINT}(x-a_1-a_2-c_1, q) + \text{ALNINT}(x-a_1-a_2+c_1, q) \end{aligned} \right\} \\
 &\quad \dots\dots (7)
 \end{aligned}$$

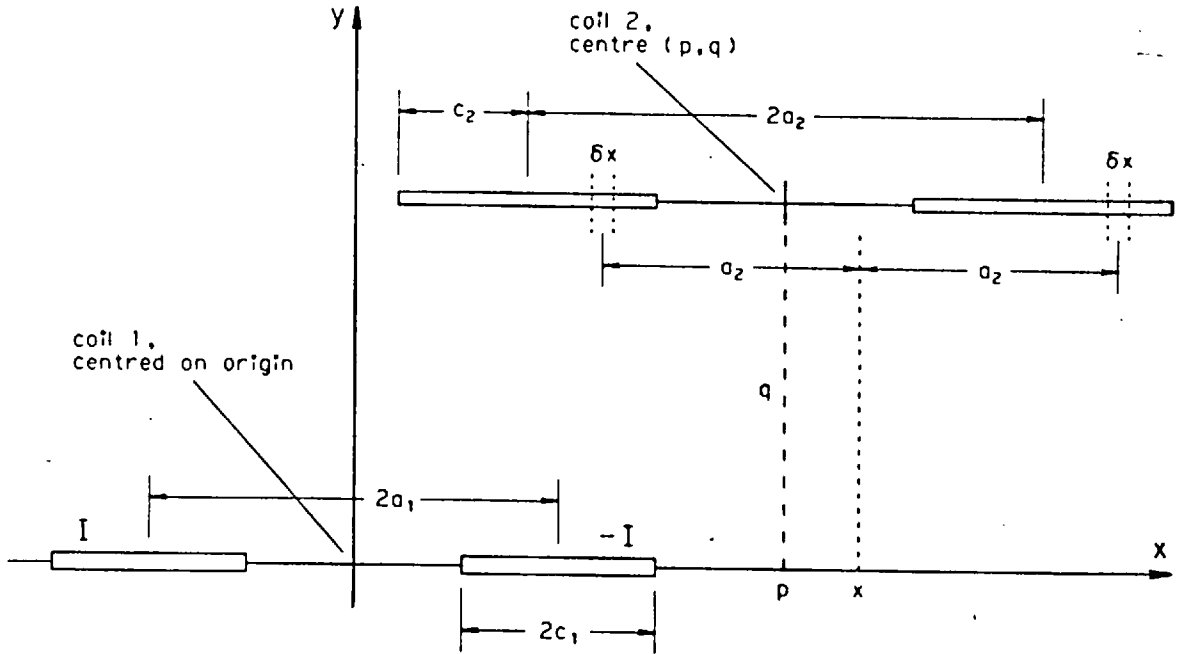


Fig C.5 Mutual inductance between coils of strip conductors.

The total mutual inductance M between the two coils is then obtained by integrating this elemental coil inductance across the width of the secondary coil, i.e. from $x = p - c_2$ to $x = p + c_2$. This requires the definite integral of the function ALNINT. The integral of ALNINT may be handled in general as follows:

$$\begin{aligned}
 \int_{\alpha}^{\beta} \text{ALNINT}(x, y) dx &= \int_{\alpha}^{\beta} \left\{ x \cdot \text{AALOG}(x, y) + y \cdot \text{AATAN}(x, y) - x \right\} dx \\
 &= \int_{\alpha}^{\beta} \left\{ \frac{x}{2} \cdot \log(x^2 + y^2) + y \cdot \tan^{-1} \left\{ \frac{x}{y} \right\} - x \right\} dx \\
 &= \left[\frac{1}{4}(x^2 - y^2) \cdot \log(x^2 + y^2) + xy \cdot \tan^{-1} \left\{ \frac{x}{y} \right\} - \frac{3}{4}x^2 \right]_{\alpha}^{\beta} \\
 &= \left[\frac{1}{2}(x^2 - y^2) \text{AALOG}(x, y) + xy \text{AATAN}(x, y) - \frac{3}{4}x^2 \right]_{\alpha}^{\beta} \\
 &= \left[\text{DUBINT}(x, y) \right]_{\alpha}^{\beta} \quad (\text{say})
 \end{aligned}$$

where DUBINT is another new function, defined by:

$$\text{DUBINT}(x, y) = \frac{1}{2}(x^2 - y^2) \cdot \text{AALOG}(x, y) + xy \cdot \text{AATAN}(x, y) - \frac{3}{4}x^2.$$

Function DUBINT is again suitable for direct programming into the computer as a Fortran function. The function may now be used to integrate the elemental inductance of equation 7 across the span of the secondary coil, to give the total mutual inductance M thus:

$$\begin{aligned}
 M &= \frac{\mu_o}{8\pi c_1 c_2} \cdot \int_{p-c_2}^{p+c_2} \left\{ \begin{aligned} &- \text{ALNINT}(x+a_1+a_2-c_1, q) + \text{ALNINT}(x+a_1+a_2+c_1, q) \\ &+ \text{ALNINT}(x-a_1+a_2-c_1, q) - \text{ALNINT}(x-a_1+a_2+c_1, q) \\ &+ \text{ALNINT}(x+a_1-a_2-c_1, q) - \text{ALNINT}(x+a_1-a_2+c_1, q) \\ &- \text{ALNINT}(x-a_1-a_2-c_1, q) + \text{ALNINT}(x-a_1-a_2+c_1, q) \end{aligned} \right\} dx \\
 &= \frac{\mu_o}{8\pi c_1 c_2} \cdot \left[\begin{aligned} &- \text{DUBINT}(x+a_1+a_2-c_1, q) + \text{DUBINT}(x+a_1+a_2+c_1, q) \\ &+ \text{DUBINT}(x-a_1+a_2-c_1, q) - \text{DUBINT}(x-a_1+a_2+c_1, q) \\ &+ \text{DUBINT}(x+a_1-a_2-c_1, q) - \text{DUBINT}(x+a_1-a_2+c_1, q) \\ &- \text{DUBINT}(x-a_1-a_2-c_1, q) + \text{DUBINT}(x-a_1-a_2+c_1, q) \end{aligned} \right]_{p-c_2}^{p+c_2} \\
 &= \frac{\mu_o}{8\pi c_1 c_2} \cdot \left[\begin{aligned} &- \text{DUBINT}(p+a_1+a_2-c_1+c_2, q) + \text{DUBINT}(p+a_1+a_2+c_1+c_2, q) \\ &+ \text{DUBINT}(p-a_1+a_2-c_1+c_2, q) - \text{DUBINT}(p-a_1+a_2+c_1+c_2, q) \\ &+ \text{DUBINT}(p+a_1-a_2-c_1+c_2, q) - \text{DUBINT}(p+a_1-a_2+c_1+c_2, q) \\ &- \text{DUBINT}(p-a_1-a_2-c_1+c_2, q) + \text{DUBINT}(p-a_1-a_2+c_1+c_2, q) \\ &+ \text{DUBINT}(p+a_1+a_2-c_1-c_2, q) - \text{DUBINT}(p+a_1+a_2+c_1-c_2, q) \\ &- \text{DUBINT}(p-a_1+a_2-c_1-c_2, q) + \text{DUBINT}(p-a_1+a_2+c_1-c_2, q) \\ &- \text{DUBINT}(p+a_1-a_2-c_1-c_2, q) + \text{DUBINT}(p+a_1-a_2+c_1-c_2, q) \\ &+ \text{DUBINT}(p-a_1-a_2-c_1-c_2, q) - \text{DUBINT}(p-a_1-a_2+c_1-c_2, q) \end{aligned} \right] \\
 &\dots\dots (8)
 \end{aligned}$$

This completes the derivations of the mathematical expressions needed to implement the theoretical analysis presented in Appendix B. Referring to the matrix equation on page 282 of Appendix B, equation 8 above may be used to determine the numerical values of all the mutual and self-inductance terms in the matrix, for any given rotor/stator geometry. Inversion of the matrix allows solution for the set of equivalent currents in the rotor. Equations 5 and 6 may then be used to evaluate the forces on each of these currents, to give the force distribution across the floating plate. This is the means by which the results presented in Fig B.4 were derived. Finally the forces may be summed to give the total resultant force upon the rotor, giving results of the kind displayed in Figs B.5 and B.6 .

APPENDIX D. COMPUTER SUBROUTINES, FUNCTIONS AND PROGRAMS

This Appendix gives descriptions of the Fortran subroutines, functions and programs written to perform the theoretical analysis of Appendix B. The programming may best be considered in two parts. Firstly a library of Fortran functions and subroutines was developed, containing the computer coding for the five functions AATAN, AALOG, TANINT, ALNINT and DUBINT derived in Appendix C, for five further functions designed to use these to evaluate fields, forces and mutual inductances, and for a subroutine to perform the inversion of a complex matrix. Secondly two programs were written to use the library to perform an analysis of a theoretical machine whose parameters are entered at the computer keyboard. One of these programs gives the resulting force distribution across the rotor at every rotor position examined; the other analyses a multiplicity of rotor positions, giving only the total force on the rotor at each.

The library and programs were developed on the computer system at Imperial College. This comprises a CDC 6500 and Cyber 174 processor linked in a double-mainframe configuration, running under the NOS operating system of Control Data Corporation. It should be noted that no attempt was made to confine the programming to "ANSI Standard Fortran IV"; instead full use has been made of the considerable extensions that are supported by the specialist Fortran compiler "MNF5", written by the University of Minnesota.

D.1 The functions AATAN and AALOG

The two functions AATAN and AALOG were originally defined in the course of the derivation of the magnetic field set up by a current flowing in a strip conductor. They subsequently appeared in the definitions of three further functions TANINT, ALNINT and DUBINT. These are themselves constituent parts of the expressions for the force components acting on a strip conductor within the field set up by a coil of strip conductors, and for the mutual inductance between

two such coils. AATAN and AALOG are thus fundamental to the analysis of any system involving strip conductors.

The definitions of AATAN and AALOG (first given in section 2 of Appendix C, page 300) were:

$$\text{AATAN}(x, y) = \tan^{-1}\left\{\frac{x}{y}\right\}$$

$$\text{AALOG}(x, y) = \frac{1}{2} \log(x^2 + y^2)$$

These may be programmed into Fortran by elementary one-line statements, except for the handling of the special case $x = y = 0$. Under this condition the function AATAN(0, 0) becomes indeterminate and AALOG(0, 0) becomes negative infinity.

However in the evaluation of forces and mutual inductances called for in the analysis of Appendix B, functions AATAN and AALOG are referenced only through calls to functions TANINT, ALNINT and DUBINT. These were first defined in sections 4 and 5 of Appendix C (pages 303, 304 and 307) thus:

$$\text{TANINT}(x, y) = x \cdot \text{AATAN}(x, y) - y \cdot \text{AALOG}(x, y)$$

$$\text{ALNINT}(x, y) = x \cdot \text{AALOG}(x, y) + y \cdot \text{AATAN}(x, y) - x$$

$$\text{DUBINT}(x, y) = \frac{1}{2}(x^2 - y^2) \cdot \text{AALOG}(x, y) + xy \cdot \text{AATAN}(x, y) - \frac{1}{4}x^2$$

It will be observed that every occurrence of AATAN(x, y) and AALOG(x, y) in the expressions for TANINT, ALNINT and DUBINT is multiplied either by x or by y or by a simple function of the two, and in every case this multiplying factor has the value zero when $x = y = 0$. Thus in the limit as x and y tend to zero, each term involving AATAN and AALOG becomes one of the forms:

$$\lim_{\substack{x \rightarrow 0 \\ y \rightarrow 0}} x \cdot \text{AATAN}(x, y) = \lim_{\substack{x \rightarrow 0 \\ y \rightarrow 0}} x \cdot \tan^{-1}\left\{\frac{x}{y}\right\}$$

$$\lim_{\substack{x \rightarrow 0 \\ y \rightarrow 0}} x \cdot \text{AALOG}(x, y) = \lim_{\substack{x \rightarrow 0 \\ y \rightarrow 0}} \frac{x}{2} \cdot \log(x^2 + y^2)$$

The first of these limits is evidently zero, since the inverse tangent function is limited to a finite range of values (normally $-\frac{\pi}{2}$ to $\frac{\pi}{2}$), even when its argument is indeterminate. The second limit is a particular case of the standard form $\lim_{x \rightarrow 0} x^n \cdot \log(x)$, which has long been established to have the value zero for all positive n .

Thus in the evaluation of the functions TANINT, ALNINT and DUBINT, the values returned by the computer for functions AATAN and AALOG at the singularity are of no consequence, since they are always multiplied by zero. In fact it was decided to make the functions themselves return the value zero at $x = y = 0$, thus making doubly sure that every product term involving AATAN or AALOG gave the correct result.

D.2 AASORS - the function and subroutine library

Reference may now be made to Appendix E, which includes Fortran source code listings of all the functions and subroutines needed to implement the analysis presented in Appendix B. These have been collected together into a source code library, named AASORS. In addition to the five functions AATAN, AALOG, TANINT, ALNINT and DUBINT, library AASORS contains the following functions and subroutines:

FUNCTION XFLUX (P, Q, A, C) } to evaluate the components of magnetic
 FUNCTION YFLUX (P, Q, A, C) } field at distance (P, Q) from the
 centre of a horizontal coil of two strip
 conductors carrying unit current. The centres of the conductors are
 spaced apart by distance 2A, and each conductor is of width 2C.

FUNCTION XFORCE (P, Q, A, C1, C2) } to evaluate the components of force
 FUNCTION YFORCE (P, Q, A, C1, C2) } acting on unit current flowing in a
 horizontal strip conductor of width
 2C2, positioned at distance (P, Q) from a horizontal coil of two strip
 conductors also carrying unit current. The coil is of conductor spacing
 2A and conductor widths 2C1.

FUNCTION EMLINK (P, Q, A1, C1, A2, C2) to evaluate the mutual inductance between two horizontal coils of strip conductors separated by distance (P, Q). One coil has conductor spacing 2A1 and conductor widths 2C1; the other has spacing 2A2 and widths 2C2.

SUBROUTINE CINVRT (AMAT, BMAT, NSIZE, IFAIL) to invert the complex square matrix AMAT of order NSIZE, and return the inverse matrix in BMAT. IFAIL is used to indicate whether any mathematical difficulties were encountered.

The remainder of this section considers the programming of the above ten functions and one subroutine in detail.

D.2.1 AATAN and AALOG programming.

The first two functions in library AASORS are the two basic functions AATAN and AALOG. The programming of these consists of elementary Fortran expressions of the function definitions (see section D.1). The singularity condition of $x = y = 0$ is detected by testing the function parameters X and Y for magnitudes less than 10^{-25} . This particular choice of small number was made to suit the 60-bit word size of the Imperial College computer. More generally a limit must be chosen sufficiently small, allowing for rounding errors, for the computer never to attempt to evaluate the arctangent of an indeterminate number or the logarithm of zero.

Note that the standard Fortran function ATAN2 (X, Y) has been used instead of the better known ATAN (Z) where $Z = X/Y$. This is because ATAN2 is programmed to handle cases when either X or Y is equal or close to zero, while the division operation necessary before the use of ATAN would fail under some of these conditions. Moreover by accepting the two arguments X and Y independently, function ATAN2 is able to return a result within the complete polar range of $-\pi$ to π . For example the evaluation of $\tan^{-1}\{\frac{-2}{-3}\}$ is returned as π different from $\tan^{-1}\{\frac{2}{3}\}$. Results given by the

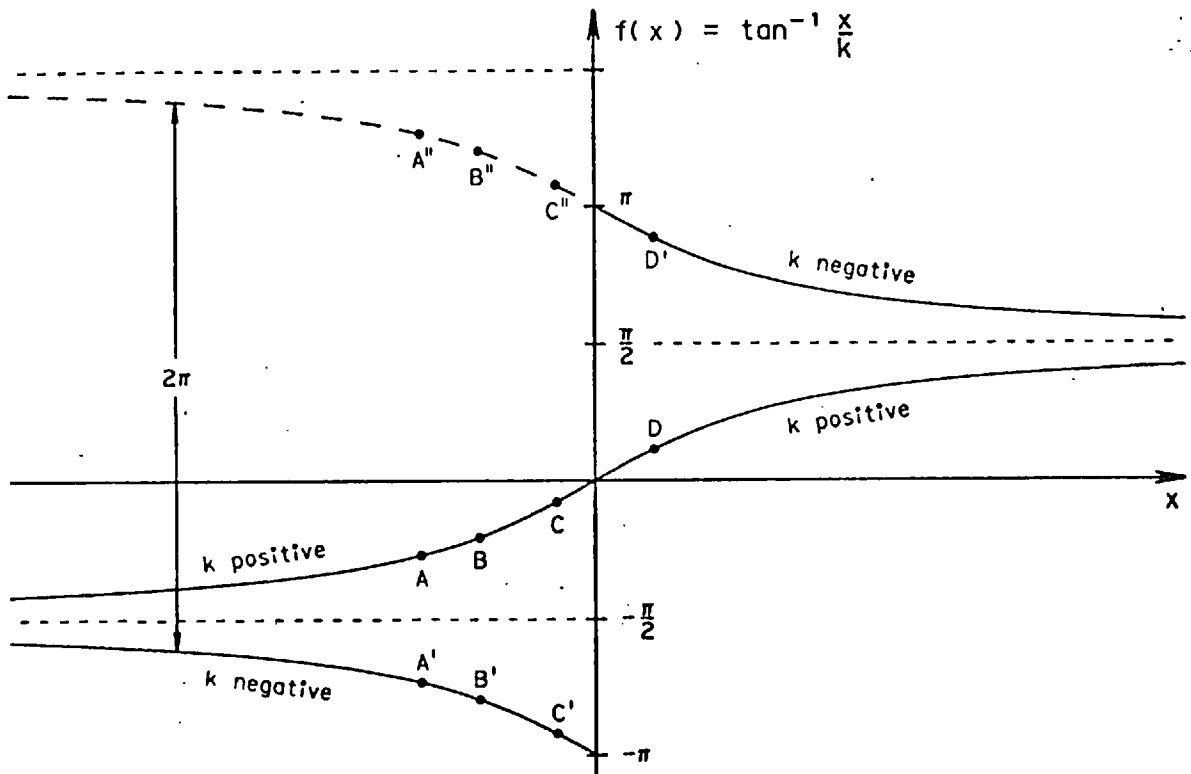


Fig D.1 The function TANINT (x,k).

single-argument function ATAN are limited to the principal values, i.e. those between $-\frac{\pi}{2}$ and $\frac{\pi}{2}$, and further inspection of the original arguments is required to determine the correct quadrant for the result.

Use of the full polar range as returned by ATAN2 does, however, introduce one minor complication. A discontinuity of 2π can occur in the evaluation of AATAN(X,Y) when Y is negative and X passes from negative to positive. The handling of this is simple, necessitating only a single extra line of Fortran in the function definition; nevertheless it warrants an explanation.

Fig D.1 shows the general function AATAN(x,k), where k is a constant. The continuous curve passing through the origin is obtained when k is positive, but the curve with the 2π discontinuity at $x = 0$ is obtained with negative k. Inspection of the definitions given in sections D.1 and D.2 shows that all of the functions within library AASORS that reference function AATAN(X,Y) (whether directly,

as XFLUX does, or indirectly via calls to TANINT, ALNINT or DUBINT) do so via a succession of calls having various numerical values for parameter X but all having the same value for Y. Parameter Y thus corresponds to the constant k on the diagram. Furthermore the calls taken in sequence form a series of pairs each comprising one call subtracted from the other. For example a sequence of calls all with positive k might be AATAN(x,k) evaluated at point A on the diagram subtracted from AATAN evaluated at point B, summed with the evaluation at point D subtracted from that at C. The problem arises when a similar sequence of values of x is required with a negative value of k. This might yield evaluations at points A', B', C' and D', and it can be seen immediately that the subtraction of D' from C' straddles the discontinuity, and is therefore in error by 2π .

The solution employed was to instruct the computer to add 2π to all results evaluated in the quadrant with both x and k negative. The effect of this is to raise the relevant portion of the curve from its position at the bottom left hand side of Fig D.1 to the position of the dashed curve at the top. Points A', B' and C' then become A'', B'' and C''. Clearly this makes no difference to the subtraction of A'' from B'', but the subtraction of D' from C'' now has its spurious 2π removed, and returns with the correct result.

Referring once again to the Fortran source code (see Appendix E), the decision on whether to raise the evaluation by 2π was programmed by testing whether the function result returned by ATAN2(X,Y) is less than $-\frac{\pi}{2}$. This is quicker than doing a double test to detect when parameters X and Y are both negative. On average three out of every four checks will fail the test, causing an immediate return with the value of ATAN2 unmodified, but for the remaining 25% of function calls a second test is applied, to verify that Y is indeed negative. This is done to avoid the remote possibility that rounding errors in the evaluation of ATAN2(X,Y) with a positive Y and a large negative value of X (giving a result close to $-\frac{\pi}{2}$) do not cause 2π to be added in error.

These small points concerning the programming of AATAN and AALOG have been discussed in some detail because the two functions form the core of the numerical calculations called for during the course of any run of an analysis program. For example every call to function EMLINK to calculate a mutual inductance requires sixteen calls to function DUBINT, each of which calls both AATAN and AALOG. Each evaluation of a component of force on a conductor requires a further eight calls. Thus during the course of a program run to analyse a multi-bar rotor simulation, the number of accesses to AATAN and AALOG may run into many hundreds or thousands.

Such usage warrants attention to details with the aim of minimising the time taken by the computer on each access. For example a DATA statement is used to assign the numerical values of variables HALFPI, TWOPI and TINY. By this means each assignment is made only once, during compilation, whereas the use of more obvious Fortran assignment statements (e.g. "TINY = 1.OE-25") would take time to reset the variables at every access during program execution. Similar considerations have been applied to the ordering of tests within multiple-condition "IF" statements. For example Fortran does not expend time unnecessarily testing the second of two conditions related by the ".AND." operator if the first condition has already failed. The condition with the greater likelihood of failure is therefore better placed first.

D.2.2 TANINT, ALNINT and DUBINT programming.

The next three functions in library AASORS are TANINT, ALNINT and DUBINT (see section D.1, page 310 for their definitions). The Fortran programming of these is elementary, comprising only one executable statement in the case of the first two functions and five for the third. Note that none of these routines contains any code to detect the singularity condition $x = y = 0$. Section D.1 showed that all three functions have the value zero under this condition, and it would have been possible to have incorporated an appropriate Fortran test and assignment statement to this effect.

Such programming would, however, have been inefficient since the great majority of function calls would then have undergone, and failed, the test for singularity one more time than necessary.

The only other point of note is the conversion from parameter variables X and Y to local variables XX and YY within routine DUBINT. Use of local variables, internal to the subroutine, is significantly faster on the Imperial College computer than use of parameter variables, accessible from outside. An extra statement for conversion is worthwhile if the same parameter variable is to be used within a routine more than three or four times. (Use of Fortran COMMON variables would have been faster still, but COMMON has been avoided in the interests of simplicity, generality and intelligibility.)

D.2.3 XFLUX and YFLUX programming.

The next two routines, XFLUX and YFLUX, are functions designed to return the horizontal and vertical components of the magnetic field at a chosen point in the vicinity of a horizontal coil of strip conductors. The physical dimensions of the coil and the position relative to it at which the evaluation is required are passed as function parameters (see section D.2, page 311, for the parameter lists). The field components are calculated for unit current in the coil. These two routines have been included in AASORS merely for interest, since the evaluation of the magnetic fields themselves is not in fact required as part of the theoretical analysis presented in Appendix B.

Programming of the functions merely comprises direct Fortran expressions of equations 1 and 2 of Appendix C (see section C.3, page 301). Again the conversion from parameter to local variables is worthwhile, and the only other point to mention is that the term $\frac{\mu_0}{4\pi}$ has been replaced by its numerical value of 10^{-7} .

It should be noted that XFLUX and YFLUX make use of the basic functions AATAN and AALOG directly, and must therefore be handled with care near positions of singularity. More explicitly, each evaluation of a field component calls upon either AATAN(X,Y) or AALOG(X,Y) four times, and this gives rise to four positions of singularity where one of these calls happens to set $X = Y = 0$. These positions coincide with the four edges of the two horizontal conductors comprising the coil. XFLUX and YFLUX may be used to evaluate fields at all other places, including other positions along the horizontal line containing the conductors, but at the four singularity positions the numerical results returned by the computer are invalid. The physical explanation for the singularities is that the field is undergoing infinite curvature as it reverses direction from the top of an infinitely thin conductor, round its end, and back along the bottom. An evaluation of the field at such a point is meaningless.

D.2.4 XFORCE, YFORCE and EMLINK programming.

The last three Fortran functions in the source code library AASORS are XFORCE, YFORCE and EMLINK. These evaluate respectively the horizontal and vertical components of force on a strip conductor in the field set up by a horizontal coil of strip conductors, and the mutual inductance between two such coils. The physical dimensions of conductors and coils, and their relative positions, are passed as function parameters (see section D.2, pages 311 and 312). In the case of the two functions for calculating forces, the evaluations are done for unit current in both the conductor and the coil.

Programming of all three functions again comprises direct Fortran expressions of equations given in Appendix C (see equations 5, 6 and 8 in sections C.4 and C.5, pages 305 and 308). There are no restrictions of singularity on the use of XFORCE, YFORCE or EMLINK. The basic routines AATAN and AALOG are referenced only via calls to TANINT, ALNINT and DUBINT and any singularity evaluations are therefore

properly handled as explained in section D.1. In particular EMLINK may be used to obtain the self-inductance of a horizontal coil of strip conductors simply by evaluating the mutual inductance of two identical coils superimposed.

D.2.5 Subroutine CINVRT programming.

The final routine in library AASORS is subroutine CINVRT, which performs the inversion of a complex matrix. This is defined as a SUBROUTINE rather than as a Fortran FUNCTION since it is the only routine in the library that returns more than one numerical result. The matrix inversion itself is done by one of the subroutines available in the Numerical Algorithms Group library. This latter is a library of mathematical routines that has been installed on many industrial and university computers, and the Mark 6 version of it is currently in operation at Imperial College. Subroutine FO4ADF was selected from the library to perform the matrix inversion. Details of FO4ADF may be found in the NAG software documentation, but its general purpose is to solve a set of complex linear equations with multiple right-hand sides. By specifying the matrix of right-hand sides as the unit complex matrix, the solution obtained is the inverse of the matrix of coefficients on the left-hand sides.

The action of routine CINVRT is to sort out the many parameters required by FO4ADF, copy the matrix to be inverted into a scratch storage area, set up the unit matrix of right-hand sides, and call the NAG inversion routine. Upon return from FO4ADF the solution matrix has overwritten the unit matrix and the scratch storage area has been overwritten during internal computation (this is the reason for the copy operation beforehand). CINVRT then multiplies the original matrix by the solution (inverse) matrix, forming the product in the scratch area again, and checks that this product is a close approximation to the unit complex matrix. This check is done by summing the absolute values of the real and the imaginary parts of all the terms comprising the product matrix - these should of course

all be zero except for the real parts of the terms on the leading diagonal, which should be unity. Thus the resulting sum should equal the size of the matrix being inverted. Such a check is necessary because routine F04ADF does not flag ill-conditioned matrices, i.e. matrices for which an inverse is returned but which have accumulated rounding errors so great that the solution is unreliable.

Four parameters are passed to and from subroutine CINVRT. The first two, AMAT and BMAT, are respectively the given complex matrix to be inverted, and the returned complex inverse. Each of these must be declared as COMPLEX arrays in the calling routine, and each has a size limit of 40 by 40 set upon it within CINVRT. A further 40 by 40 complex matrix, CMAT, is defined internally within CINVRT to form the scratch area for copying and product checking. The third subroutine parameter, NSIZE, is the actual size of the array to be inverted (maximum 40). For any value of NSIZE less than 40, the initial matrix is assumed to lie in the top NSIZE rows and the left-hand NSIZE columns of AMAT, and the solution is returned in the corresponding portion of BMAT. The final subroutine parameter, IFAIL, is normally returned as zero, indicating that a reliable inverse of AMAT has been found. Return with IFAIL = 1 indicates an ill-conditioned matrix (unreliable solution), while return with IFAIL = 2 indicates that routine F04ADF has encountered a numerical error. The latter case is usually the result of trying to invert a singular matrix, i.e. one with a determinant of zero, for which no inverse exists.

D.3 FORDIS and CONDAT - two computer programs to analyse an electromagnetic levitator

This section describes two computer programs which perform analytical investigations of a theoretical model of an expanding-geometry levitator. Each program investigates the elementary strip-conductor model of a levitator described in section 2 of Appendix B (see page 277), by means of the analytical method outlined

in that section. Each therefore makes use of the mathematical derivations of fields, forces and mutual inductances of combinations of strip conductors as presented in Appendix C. Each also makes use of the computer subroutine and function library AASORS, based on the above mathematical derivations. The programs are thus presented as specimen implementations of the theoretical analysis of Appendix B, and as examples of the use of library AASORS.

The first of the two programs, FORDIS, derives the detailed distribution of forces across the width of a conducting plate suspended over a suitable stator. Results from this program were presented in Fig B.4 (see section 3 of Appendix B, page 285). The second program, CONDAT, analyses a similar system for a multiplicity of different positions of the rotor, and derives the total resultant force acting on the rotor in each position. Figures B.5 and B.6 (on pages 289 and 291 of Appendix B) were plotted from results of this kind.

Both programs were designed to be used inter-actively under the Telex subsystem of the NOS operating system on the Imperial College computer. All input parameters (e.g. physical dimensions of stator and rotor, relative positions, stator current) are entered at the terminal in response to appropriate prompts given by the program. Every parameter has a "sensible" default value which may be selected by pressing "carriage return" instead of entering a value in answer to the prompt.

Conversational output and a summary of the program results are directed back to the operating Telex terminal, but the full output of each program is directed to a local file named "TAPE7". This file may be inspected from the terminal upon completion of the program, or it may be listed on the line printer or renamed and saved as a permanent data file for future access. Each new run of either FORDIS or CONDAT writes a new local file TAPE7, overwriting any similarly named local file in the process.

The following two parts of this section describe the two programs in detail. Source code listings of them are presented for reference in Appendix E.

D.3.1 FORDIS - a program to use the simple strip conductor model of an expanding-geometry levitator to derive a theoretical distribution of forces across the rotor.

Program FORDIS may be considered in five parts. The first prompts the terminal for the rotor plate dimensions, the resistivity of the rotor material, the frequency of the current system, and the number of equivalent strip conductors to be used in the modelling of the rotor. The second part constructs the rotor matrix from the information given, and inverts it. This rotor matrix is the left-hand matrix of equation 1 in Appendix B (see page 282). The third part of the program prompts the terminal for the stator dimensions and the stator current. Part 4 asks for the position of the rotor plate relative to the stator, and proceeds to evaluate the terms in the right-hand column vector of equation 1. It then multiplies the inverted rotor matrix by this column vector to solve for the individual currents in the strip conductors. Finally Part 5 evaluates the force on each strip conductor set up by reaction with the stator currents, to give the detailed distribution of force across the rotor. The individual forces are also summed to give the resultant force. The program ends with an option to repeat Parts 4 and 5 for new positions of the rotor plate as many times as required.

In more detail - FORDIS starts by initialising all the input variables to their default values. These are as follows:

WIDTH	=	width of rotor plate	default	10 cm
THICK	=	thickness of rotor plate	"	3 mm
ROE	=	resistivity of rotor material	"	aluminium
OMEGA	=	frequency	"	50 Hz
NBAR	=	number of equivalent strip conductors	"	40

SLOTW	=	slot width of (imaginary) core	default	3.6 cm
TOOTH	=	tooth width of core	"	1.9 cm
SCURNT	=	current in stator coils	"	100 amps
P	=	horizontal rotor displacement	"	0
Q	=	vertical rotor displacement	"	10 mm

Note that the stator coil dimensions are specified in terms of the imaginary iron core which they embrace - see Fig B.2 on page 278 of Appendix B. This was done because it was found easier to visualise the coils in terms of the "slot width" and "tooth width" of the C-core that they embrace rather than in terms of the conductor spacing and conductor widths of the coils themselves. The default values for the stator parameters are the appropriate dimensions of the practical "long pole-pair" machine of Chapters 3 and 4, and the default rotor parameters describe an aluminium plate 10 cm wide by 3mm thick. This forms the "standard levitator" referred to in the discussion on the results of the strip conductor analysis (see section 3 of Appendix B, page 284).

FORDIS then asks the terminal for the width and thickness of the rotor plate to be analysed, the resistivity of the plate, the frequency of the current system and the number of equivalent strip conductors to be used in the rotor simulation. The opportunity is thus given for the investigation of plates of copper or other material or even "superconducting" plates of zero resistivity, and at frequencies other than 50 Hz. The numerical answers to these questions are given in "free-format" style, and any input errors (such as a letter accidentally typed in place of a digit) cause the question to be asked again. Pressing merely "carriage return" in answer to a prompt causes the appropriate default value to be selected for the variable(s) in question.

From the information given (or the default values if selected) the program calculates the width W_{BAR} of each rotor "bar", the half-spacing R_A between the two conductors of each rotor coil, and the half-width R_C of each conductor. Fig D.2 shows these named dimensions on a typical rotor / stator configuration. In practice the

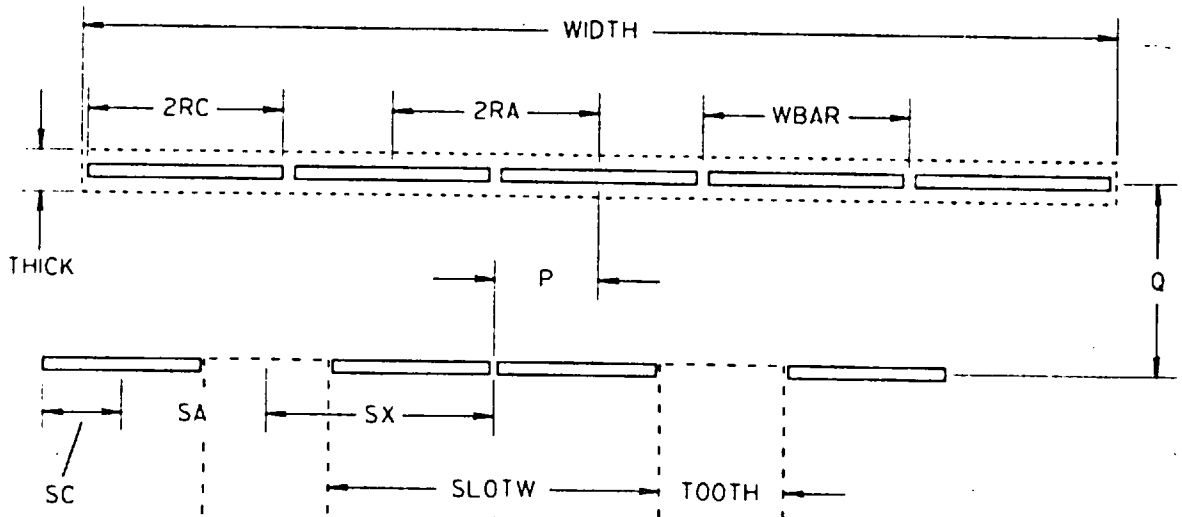


Fig D.2 Geometric parameters in programs FORDIS and CONDAT.

specification that the equivalent strip conductors should together just span the width of the rotor plate, with no gaps between them, means that variables RA and RC both have the numerical value $WBAR/2$, but the distinction between them has been maintained in the interests of clarity and generality. The first part of FORDIS ends by writing all values given and calculated so far to the local output file TAPE7, together with a header giving the date and time of the program run.

The second part of FORDIS assembles the complex rotor matrix AMAT. It will be appreciated that the number of rotor current loop circuits NLOOP is one less than the number of strip conductors NBAR. The rotor matrix is of order NLOOP. A limit of 40 has been placed upon the number of loop circuits, hence AMAT has been dimensioned 40 by 40 at the top of the program. It can be seen from equation 1 of Appendix B (page 282) that the real parts of the matrix elements are all zero except for those on three adjacent diagonals. The program calculates the resistance RESIS of unit length of one rotor bar, and fills in double this value for the real parts of all terms on the leading diagonal, and the negative of RESIS for the elements of one diagonal on either side. The entire matrix is initialised during this process, including all the imaginary terms, which in the first instance are set to zero.

The next step is the computation of the self-inductance of each rotor coil, and the mutual inductances between each and every other coil. There is a large amount of symmetry here, so the program only evaluates the NLOOP mutual inductances between the left-hand coil and all the coils in sequence (the first term of these results being the coil's own self-inductance). The calculations are done inside a DO-loop of calls to function EMLINK in library AASORS, and the results are stored in array RMUT (dimension 40). The imaginary parts of AMAT are then filled by selecting the appropriate value for each matrix element from RMUT, multiplying it by the frequency OMEGA, and adding it to the present element value. The entire matrix is written to TAPE7, and a message "rotor matrix complete" appears on the terminal.

AMAT is inverted by routine CINVRT, the solution being returned in matrix BMAT (also dimensioned 40 by 40). It might be observed that both AMAT and BMAT have been declared as unlabelled COMMON at the top of the program. This uses a particular feature of the Imperial College computer, that unlabelled COMMON occupies that part of the computer memory initially used by the LOADER to load the program. By this means the storage requirements to load the program are reduced by the space taken up by two 40 by 40 complex matrices, i.e. by 6400 words.

On return from CINVRT, the program checks the fail parameter IFAIL for the value 2, indicating that AMAT is singular, and aborts with an appropriate message on the terminal if this condition is found. Otherwise the whole of BMAT is written to TAPE7. IFAIL is then checked for the value 1, indicating an ill-conditioned original matrix, and if this is found the terminal is asked whether program execution is to proceed with the unreliable inverse matrix, and a message is written to TAPE7. Under the normal condition of IFAIL = 0 the message "matrix inversion complete" is printed at the terminal, and the program moves on to part 3.

The third part of FORDIS asks for the stator slot width SLOTH and the tooth width TOOTH. From the values given (or from their defaults) the program calculates the distance SX of the centre of each stator coil from the centre line of the stator, the conductor half-spacing SA of each coil, and the half-width SC of each conductor comprising the coils (see Fig D.2). FORDIS also asks for the stator current SCURNT for which the analysis is to be performed. The values of all variables related to the stator are written to TAPE7. At this point all of the computation that is independent of the displacement between rotor and stator has been completed.

The remaining two parts of FORDIS include all the computation that is dependent upon rotor position, and they may be repeated as many times as desired for different positions of the rotor plate. The beginning of part 4 asks the terminal for the horizontal and vertical displacements P and Q of the rotor centre from the stator centre. The individual rotor coils are then taken in turn. For each rotor coil three distances X, X1 and X2 are calculated, being the horizontal distances from the centre of the coil to the centre of the rotor plate, and to the centres of the two stator coils respectively. The latter two dimensions are used as parameters in function EMLINK, to evaluate the mutual inductances between the rotor coil and each stator coil. These in turn are combined to construct the appropriate element of the right-hand column vector RSIDE of equation 1 in Appendix B. The multiplying factors OMEGA and SCURNT are included in each term of RSIDE. Dimensions X1 and X2 and the corresponding element of RSIDE are written to TAPE7 for each rotor coil.

The inverted matrix BMAT is then multiplied by vector RSIDE to derive the vector of rotor loop currents RCURNT. These are combined again to give the solution vector of bar currents BCURNT. These latter are the individual currents flowing in each of the NBAR strip conductors comprising the simulation of the rotor plate. Note that vectors RCURNT and BCURNT are both Fortran COMPLEX arrays, since in general the alternating rotor currents will differ

in phase from the stator currents. Output of the solution vector of bar currents is held over to part 5 to be combined with the force distribution output.

The fifth and final part of FORDIS takes the rotor bar currents one at a time, and evaluates the forces on each current set up by reaction with the currents in the two stator coils. Functions XFORCE and YFORCE give the components of force acting on unit steady-state current flowing in a strip conductor within the field set up by unit steady-state current in a coil of strip conductors. To obtain the force components between non-unit steady-state currents it is necessary only to multiply the function results by the product of the currents. For alternating currents the situation is a little more complicated in that the scalar product of the two alternating quantities must be used as the multiplying factor (see Chapter 9, page 204 for a similar situation involving the Jumping Ring machine). However for program FORDIS the current in the left-hand stator coil is by definition the phase-zero reference, so the scalar product of any rotor bar current with the left-hand stator current is merely the stator current magnitude multiplied by the real part of the rotor current. The negative of the same quantity is the scalar product of the same rotor current with the (reversed) current in the right-hand stator coil.

Thus for each strip conductor in the rotor simulation, the program calculates the scalar product SCPROD of the conductor current with the current in the left-hand stator coil, and uses this with functions XFORCE and YFORCE. Four components of force are evaluated for each conductor, being FXL and FYL set up by reaction with the left-hand stator coil, and FXR and FYR set up by reaction with the right-hand stator coil. These again are combined to give the total resultant horizontal and vertical components of force FX and FY acting on the strip conductor. FX and FY have been defined as arrays which store the force evaluations for all NBAR conductors, while the remaining variables in part 5 are overwritten

as each successive conductor is handled. The values of the conductor current, the individual force components and the total resultant force components are all written to TAPE7 for each strip conductor.

Finally the complete set of NBAR forces in arrays FX and FY are summed to give the total resultant horizontal and vertical components of force acting on the rotor plate. This is the only output that appears on the terminal as well as on TAPE7. The option is then given to go back to stage 4 to re-evaluate the distribution of forces for a new position of the rotor, or to end the program.

At the termination of the program the output file TAPE7 contains the following output once: header, date, time, rotor parameters, initial rotor matrix, inverted rotor matrix, stator parameters and specified stator current. TAPE7 then contains the following information repeated as many times as stages 4 and 5 were executed: rotor plate position, individual rotor current loop offsets from the two stator coils, right-hand column vector RSIDE, individual strip conductor current solutions, component and resultant forces on each strip conductor, and the resultant force components on the entire plate. The output file ends with the time of program termination.

D.3.2 CONDAT - a program to use the simple strip conductor model of an expanding-geometry levitator to investigate the rotor plate in a multiplicity of different positions, and derive the resultant force components acting on it for each position.

Program FORDIS described above was written to provide an inter-active facility for obtaining a complete distribution of forces across a floating plate (hence the name - FORce DIStribution). FORDIS produces an output file containing a comprehensive listing of all parameters input to the program and most values calculated internally, in addition to the solutions for the rotor currents and

distribution of forces. As such the program is intended to be used for only a limited number of rotor plate positions, for the quantity of information output soon becomes unwieldy in its sheer volume when, say, a 40-bar rotor simulation is used to examine several positions.

A companion program, CONDAT, has been written to give a more selective output. CONDAT prompts the computer terminal for information specifying a rectangular grid of positions, and proceeds to derive the total resultant components of force acting on the rotor plate, for every position of the rotor in the grid so defined. The output file contains merely the rotor and stator parameters, the grid of rotor positions and the two resultant force components for each position.

The Fortran source code of program CONDAT is included in Appendix E. The first three parts of the program are almost identical with the corresponding parts of FORDIS, with the same objective of requesting rotor and stator parameters and performing all the computation that does not depend on rotor position. The only major differences are the default definitions of some new variables and the suppression of the rotor matrix (and inverse matrix) output to TAPE7.

The remainder of CONDAT, however, takes a different course. Part 4 asks for the left- and right-hand limits to the horizontal movement of the rotor plate and for the number of positions required within this range. It repeats the question for the lower and the upper limits to vertical movement and for the number of vertical positions. These answers define a rectangular grid of rotor positions, whose attributes are written to the output file. CONDAT then sets up two nested DO loops enclosing parts 5 and 6, in such a way as to invoke these last two parts once for every rotor position in the grid.

The extra variables introduced and their default values are:

XL	=	left limit of rotor movement	default	0
XR	=	right limit of rotor movement	"	40 mm
NUMX	=	number of horizontal positions	"	9
YB	=	bottom limit of rotor movement	"	5 mm
YT	=	top limit of rotor movement	"	20 mm
NUMY	=	number of vertical positions	"	4

Notice that these defaults give a grid of 36 positions, with intervals of 5 mm in each direction. Figures B.5 and B.6 in Appendix B (pages 289 and 291) were plotted from results calculated for such a grid. Positions for investigation have been chosen to one side only of the centre line since the system is of course symmetrical.

The last two parts of CONDAT correspond to the last two parts of program FORDIS. For each required position of the rotor, part 5 constructs the right-hand column vector RSIDE of equation 1 of Appendix B, and multiplies it by the inverted matrix BMAT (derived in part 2) to solve for the rotor loop currents RCURNT. These are combined to find the rotor bar currents BCURNT flowing in the set of equivalent strip conductors. Part 6 then evaluates the components of force on each conductor set up by reaction with the stator field and sums these to give the resultant horizontal and vertical force components acting on the rotor. These last two values are written to TAPE7 for every rotor position.

At the termination of the program the output file TAPE7 is in two sections - firstly a header giving date, time, rotor and stator parameters and the range of rotor positions, and secondly four columns giving horizontal displacement, vertical displacement, horizontal resultant force and vertical resultant force on the plate for every position specified. This information is particularly suitable for use by contouring routines (hence the name of the program - CONtour DATA), which can, for example, find a line passing through all positions for which the plate experiences an upward force equal to its own weight.

This completes the descriptions of programs FORDIS and CONDAT. They have been presented as a record of the programs which produced the theoretical results displayed in Appendix B (see Figs B.4, B.5 and B.6). They also serve as specimen programs to demonstrate the use of the strip conductor analysis of Appendices B and C, and the function and subroutine library AASORS described in section D.2. It is hoped that reference to the descriptions and source code listings of AASORS, FORDIS and CONDAT might help to ease the task of further programming involved in any future extensions to the use of the strip conductor analysis.

D.4 Keyboard commands for running FORDIS and CONDAT

This last section of Appendix D lists the keyboard commands which may need to be typed at a computer terminal in order to run programs such as FORDIS and CONDAT. The commands given are applicable only to users of the Telex sub-mode of the NOS operating system as tailored to the computer installation at Imperial College. They will be of little interest or use to users of other computer systems.

D.4.1 To insert or remove sequential line numbers.

It will be observed that the source code listings given in Appendix E do not include sequential line numbers for every line of source code. The listings are thus in keeping with the international Fortran standard and should be readily understood by all Fortran users. The Telex sub-mode of the NOS operating system, however, normally expects sequential line numbers on Fortran source code, and the resulting style of many statements becomes slightly different:

Users of the Imperial College system may be more accustomed to this modified source code style. Conversion between the two styles may be accomplished by use of the RSF (Resequencing Source File) command thus:

GET,FILE1	or an equivalent command to obtain a local file named "FILE1", which is a Fortran source code without sequential line numbers.
RSF,FILE1,FILE2,FOR,PUT	creates a second local file "FILE2" which is the equivalent Fortran source code with sequential line numbers.
RSF,FILE2,FILE3,FOR,TAK	creates a third Fortran source code "FILE3" with the numbers taken off again. FILE3 is thus the same as the original FILE1.

D.4.2 To create an object code library AALIB from the source code library AASORS .

One means to run a program such as FORDIS which makes use of routines in a separate library such as AASORS would be to append the source code of AASORS to that of FORDIS and then compile and run the entire resulting file. While this will work perfectly satisfactorily, it is nevertheless wasteful of compilation time if several different programs are required to use the same source code library. It is often preferable to maintain a ready-compiled binary library, named say AALIB, which contains the binary computer coding of the functions and subroutines in AASORS. AALIB may then be loaded together with the compiled version of any program requiring to use AASORS routines.

The creation of library AALIB from the Fortran source code AASORS may be accomplished in two stages, each requiring a single keyboard command. The first stage compiles AASORS and produces a single binary module, say AABIN, containing all the functions and subroutines in AASORS. The second stage turns this binary module into the library file AALIB. The latter stage is necessary in order to generate the kind of binary file from which the LOADER can extract only those subroutines which are required by the calling program. Single binary modules such as AABIN are not suitable for this purpose.

The sequence of keyboard commands is:

GET,AASORS	or an equivalent command to obtain the Fortran file AASORS as a local file. AASORS is assumed to have sequential line numbers throughout.
RETURN,AABIN,AALIB	ensures that there will be no clash of file names in the commands to follow.
MNF5,K,I=AASORS,B=AABIN	creates the single binary module AABIN from the input file AASORS.
LIBGEN,F=AABIN,P=AALIB	generates the binary library file AALIB from the single module AABIN.
SAVE,AALIB	- used if the resulting library file is to be made permanent for future use.

D.4.3 To run a program that uses libraries AALIB and NAG6F.

Programs such as FORDIS and CONDAT require functions and subroutines from the source code library AASORS and from the Numerical Algorithms Group library Mark 6. The previous section explained how to create a binary library AALIB from the source code AASORS. A binary library containing the NAG routines is available on the Imperial College system under the name NAG6F. It is necessary to instruct the LOADER to include these two binary libraries in its list of those to search when resolving subroutine calls.

This may be done by using the LIBRARY command thus:

X,LIBRARY,AALIB,NAG6F

The effect of this is to include libraries AALIB and NAG6F in the library search list for all subsequent program loadings until such time as another LIBRARY command may be given. Note that neither library need be available at the time that the LIBRARY command is given, though both must be available at the time of program loading. AALIB can be obtained by a GET command if it is a permanent file, or by an MNF5 / LIBGEN sequence if only AASORS is available. No commands are necessary to obtain NAG6F; it is available by default.

N.B. The initial X on the command line is essential. Its purpose is to prevent the "LIBRARY" keyword from being interpreted as a command to switch from the Telex to the Library sub-mode of the NOS operating system.

A typical sequence of commands to run program FORDIS might thus be:

GET,FORDIS,AALIB	or equivalent commands to obtain local files FORDIS (Fortran source code with line numbers) and AALIB (compiled binary library file).
RETURN,LGO	ensure default binary file LGO is not present.
MNF5,K,I=FORDIS,B	compile FORDIS, allowing the binary output file its default file name LGO.
X,LIBRARY,AALIB,NAG6F	include AALIB and NAG6F in the list of library names to be used by the LOADER.
LGO.	"Load and GO" - loads the binary file LGO together with all necessary subroutines, and runs the program. N.B. the terminating dot is essential.

Subsequent runs of program FORDIS may then be made at any time that LGO and AALIB are still local files simply by typing the "Load and GO" command again.

D.4.4 A procedure file to run programs FORDIS and CONDAT.

An alternative method of running programs such as FORDIS and CONDAT which require subroutines from AALIB and NAG6F is to use an LDSET/LOAD command sequence in place of the LIBRARY command. This method is particularly suitable for use as part of a procedure file containing an entire sequence of commands to run a program. It is not suitable for use in a sequence of individual commands to be typed at the keyboard.

The following procedure file compiles, loads and runs the local Fortran source code program with the dummy name X (the name will be replaced by the desired program name when the procedure file is called):

GET,AALIB.	ensure library AALIB is a local file,
REWIND,X,LGO.	ensure X and LGO are at start-of-file,
RFL,23000D.	allow plenty of core for compiling,
MNF5,K,I=X,B.	compile X into default binary file LGO,
RFL,20000D.	reduce core requirements for loading,
REWIND,LGO.	ensure LGO at start-of-file,
LDSET(LIB=AALIB/NAG6F)	AALIB and NAG6F to be included in LOAD,
LOAD(LGO)	LOAD the program with all subroutines,
EXECUTE.	execute the loaded program,
REWIND,TAPE7.	rewind the output file TAPE7 to start-of-file.

The above procedure file may be typed in from the terminal to a text file named, say, AARUN, as follows:

NEW,AARUN	create a new file, called AARUN.
TEXT	accept following lines as input to the new file.
Type in the above text comprising all the commands to run program X. Press "BREAK" key to finish.	all lines typed in here are passed to the file AARUN.
PACK	tidy up the new text file.
SAVE,AARUN	save AARUN as a permanent file.

Procedure file AARUN may then be used to run programs FORDIS or CONDAT by typing:

CALL,AARUN(X=FORDIS) or CALL,AARUN(X=CONDAT) as appropriate.

D.4.5 Disposing of the output file TAPE7.

Upon completion of a run of either FORDIS or CONDAT, the local file TAPE7 will be present containing all the output produced. A subsequent run of either program overwrites this file, destroying any previous information written on it. If output results are to be kept between successive runs of the program, some action is therefore necessary to preserve them.

A single local file TAPE7 may of course be saved as a permanent file by the command `SAVE,TAPE7`. This however can be done only once. If a permanent file TAPE7 already exists, a subsequent local file of the same name can be appended to the permanent file by the command:

```
APPEND,TAPE7,TAPE7 .
```

This produces a composite permanent data file containing both sets of results in succession. The process can be repeated to add yet more results up to the point where the limit of permanent file size is reached. Alternatively the local file TAPE7 can be saved under a different file name, say DATA1, thus:

```
SAVE(TAPE7=DATA1) .
```

Subsequent data files may then be saved under different names.

Finally a hard-copy listing of any TAPE7 file may be obtained by queueing the file to the line printer:

```
QUEUE(TAPE7=PS) .
```

It should be noted that the output file has been formatted for a full line printer page width of 132 characters, but no carriage control characters have been specified. TAPE7 files are therefore not suitable for output on a terminal limited to 80 characters width, although inspection of some of the results may be possible in this way. For the same reason the output file format is not immediately suitable for dumping to cards.

APPENDIX E. COMPUTER SOURCE CODE LISTINGS

E.1 Source code listing of library AASORS

C **** AASORS - Special library for Leviduction Thesis theory ****

C

C

C **** AATAN ****

C

FUNCTION AATAN (X, Y)

C

C **** Routine to compute ARCTAN (X/Y). The indefinite case

C **** X = Y = 0.0 is returned as zero.

C

DATA HALFPI, TWOPI, TINY /1.570796, 6.2831859, 1.0E-25/

AATAN = 0.0

IF (ABS(X) .LT. TINY .AND. ABS(Y) .LT. TINY) RETURN

AATAN = ATAN2 (X, Y)

IF (AATAN .GT. -HALFPI .OR. YY .GE. 0.0) RETURN

AATAN = AATAN + TWOPI

RETURN

END

C

C

C

C **** AALOG ****

C

FUNCTION AALOG (X, Y)

C

C **** Routine to compute the function 1/2 LOG (X**2 + Y**2).

C **** The infinite case X = Y = 0.0 is returned as zero.

C

DATA TINY /1.0E-25/

AALOG = 0.0

IF (ABS(X) .LT. TINY .AND. ABS(Y) .LT. TINY) RETURN

AALOG = 0.5 * ALOG (X*X + Y*Y)

RETURN

END

C

C

C

C **** TANINT ****

C

FUNCTION TANINT (X, Y)

C

C **** Routine to compute the integral of the function AATAN.

C

TANINT = X * AATAN(X, Y) - Y * AALOG(X, Y)

RETURN

END

C

C

C

C **** ALNINT ****

C

FUNCTION ALNINT (X, Y)

C

C **** Routine to compute the integral of the function AALOG.

C

ALNINT = X * AALOG(X, Y) + Y * AATAN(X, Y) - X

RETURN

END

C

C

```

C
C **** DUBINT ****
C
C      FUNCTION DUBINT (X, Y)
C
C **** Routine to compute the integral of function ALNINT.
C
C      XX = X
C      YY = Y
C      PART1 = 0.5 * (XX*XX - YY*YY) * AALOG(XX, YY)
C      PART2 = XX * YY * AATAN(XX, YY) - 0.75 * XX * XX
C      DUBINT = PART1 + PART2
C      RETURN
C      END
C
C .....
C
C **** XFLUX ****
C
C      FUNCTION XFLUX (P, Q, A, C)
C
C **** Routine to compute the horizontal flux component at position (P, Q)
C **** set up by unit current in a horizontal coil of strip conductors.
C **** Coil is at centre (0.0, 0.0), of spacings 2A and conductor width 2C,
C
C      PP = P
C      QQ = Q
C      AA = A
C      CC = C
C
C **** Sum four terms in AATAN, multiply by MU0/(4*PI), divide by width
C
C      SUM = AATAN(PP+AA-CC, QQ) - AATAN(PP+AA+CC, QQ)
C      - AATAN(PP-AA-CC, QQ) + AATAN(PP-AA+CC, QQ)
C      XFLUX = SUM * 1.0E-07 / CC
C      RETURN
C      END
C
C .....
C
C **** YFLUX ****
C
C      FUNCTION YFLUX (P, Q, A, C)
C
C **** Routine to compute the vertical component of flux at position (P, Q)
C **** set up by unit current in a horizontal coil of strip conductors.
C **** Coil is at centre (0.0, 0.0), of spacings 2A and conductor width 2C.
C
C      PP = P
C      QQ = Q
C      AA = A
C      CC = C
C
C **** Sum four terms in AALOG, multiply by MU0/(4*PI), divide by width
C
C      SUM = AALOG(PP+AA-CC, QQ) - AALOG(PP+AA+CC, QQ)
C      - AALOG(PP-AA-CC, QQ) + AALOG(PP-AA+CC, QQ)
C      YFLUX = -SUM * 1.0E-07 / CC
C      RETURN
C      END
C
C .....

```

```

C
C **** XFORCE ****
C
      FUNCTION XFORCE (P, Q, A, C1, C2)
C
C **** Routine to compute the horizontal force on unit current flowing in
C **** a horizontal strip conductor, produced by interaction with fields
C **** set up by unit current in a horizontal coil of strip conductors.
C **** The single conductor is at centre (P, Q), and is of width 2C2; the
C **** coil is centred at the origin, and is of spacing 2A and conductor
C **** width 2C1.
C
      PP = P
      QQ = Q
      AA = A
      CC1 = C1
      CC2 = C2
C
C **** Sum eight terms of AALOG integral
C
      SUM = ALNINT(PP+AA-CC1+CC2, QQ) - ALNINT(PP+AA+CC1+CC2, QQ)
C      - ALNINT(PP-AA-CC1+CC2, QQ) + ALNINT(PP-AA+CC1+CC2, QQ)
C      - ALNINT(PP+AA-CC1-CC2, QQ) + ALNINT(PP+AA+CC1-CC2, QQ)
C      + ALNINT(PP-AA-CC1-CC2, QQ) - ALNINT(PP-AA+CC1-CC2, QQ)
C
C **** Multiply by MU0/(8*PI), divide by product of widths
C
      XFORCE = SUM * 0.5E-07 / (CC1 * CC2)
      RETURN
      END
C
C .....
C
C **** YFORCE ****
C
      FUNCTION YFORCE (P, Q, A, C1, C2)
C
C **** Routine to compute the vertical force on unit current flowing in a
C **** horizontal strip conductor, produced by interaction with fields set
C **** up by unit current in a horizontal coil of strip conductors. The
C **** single conductor is at centre (P, Q), and is of width 2C2; the coil
C **** is centred at the origin, and is of spacing 2A and conductor width 2C1.
C
      PP = P
      QQ = Q
      AA = A
      CC1 = C1
      CC2 = C2
C
C **** Sum eight terms of AATAN integral
C
      SUM = TANINT(PP+AA-CC1+CC2, QQ) - TANINT(PP+AA+CC1+CC2, QQ)
C      - TANINT(PP-AA-CC1+CC2, QQ) + TANINT(PP-AA+CC1+CC2, QQ)
C      - TANINT(PP+AA-CC1-CC2, QQ) + TANINT(PP+AA+CC1-CC2, QQ)
C      + TANINT(PP-AA-CC1-CC2, QQ) - TANINT(PP-AA+CC1-CC2, QQ)
C
C **** Multiply by MU0/(8*PI), divide by product of widths
C
      YFORCE = SUM * 0.5E-07 / (CC1 * CC2)
      RETURN
      END
C
C .....

```

```

C
C **** EMLINK ****
C
C      FUNCTION EMLINK (P, Q, A1, C1, A2, C2)
C
C **** Routine to compute the mutual inductance linking two circuits each
C **** being horizontal coils of strip conductors. The coils are spaced
C **** apart by distance (P, Q); one coil has conductor spacings 2A1 and
C **** conductor widths 2C1, the other has spacing 2A2 and widths 2C2.
C
C      PP = P
C      QQ = Q
C      AA1 = A1
C      CC1 = C1
C      AA2 = A2
C      CC2 = C2
C
C **** Sum sixteen terms of double integral
C
C      SUM = - DUBINT(PP+AA1+AA2-CC1+CC2, QQ)
C      + DUBINT(PP+AA1+AA2+CC1+CC2, QQ)
C      + DUBINT(PP-AA1+AA2-CC1+CC2, QQ) - DUBINT(PP-AA1+AA2+CC1+CC2, QQ)
C      + DUBINT(PP+AA1-AA2-CC1+CC2, QQ) - DUBINT(PP+AA1-AA2+CC1+CC2, QQ)
C      - DUBINT(PP-AA1-AA2-CC1+CC2, QQ) + DUBINT(PP-AA1-AA2+CC1+CC2, QQ)
C      + DUBINT(PP+AA1+AA2-CC1-CC2, QQ) - DUBINT(PP+AA1+AA2+CC1-CC2, QQ)
C      - DUBINT(PP-AA1+AA2-CC1-CC2, QQ) + DUBINT(PP-AA1+AA2+CC1-CC2, QQ)
C      - DUBINT(PP+AA1-AA2-CC1-CC2, QQ) + DUBINT(PP+AA1-AA2+CC1-CC2, QQ)
C      + DUBINT(PP-AA1-AA2-CC1-CC2, QQ) - DUBINT(PP-AA1-AA2+CC1-CC2, QQ)
C
C **** Multiply by MU0/(8*PI), divide by product of widths
C
C      EMLINK = SUM * 0.5E-07 / (CC1 * CC2)
C      RETURN
C      END
C
C .....
C
C **** CINVRT ****
C
C      SUBROUTINE CINVRT (AMAT, BMAT, NSIZE, IFAIL)
C
C **** Subroutine to invert a complex matrix. "AMAT" is matrix to be
C **** inverted, solution is returned in "BMAT" - both complex square
C **** arrays, dimension (40, 40). NSIZE is actual size of array to be
C **** inverted (not greater than 40). IFAIL flag is returned as zero if
C **** all OK, as 1 if AMAT was ill-conditioned (solution unreliable), or
C **** as 2 if AMAT was singular (no solution possible). This routine
C **** uses the NAG library routine F04ADF.
C
C      COMPLEX AMAT(40,40), BMAT(40,40), CMAT(40,40)
C      DIMENSION SPACE(40)
C
C **** Set up parameters for NAG complex inversion routine F04ADF
C
C      IA = 40
C      IB = 40
C      N = NSIZE
C      M = NSIZE
C      IC = 40
C      IFAIL = 0

```

```

C
C **** Initialise BMAT as unit complex matrix, copy AMAT to CMAT
C
      DO 10 I = 1, N
      DO 10 J = 1, N
      BMAT(I,J) = (0.0, 0.0)
      IF (I .EQ. J) BMAT(I,J) = (1.0, 0.0)
10    CMAT(I,J) = AMAT(I,J)
C
C **** Call NAG routine, overwriting solution into BMAT
C
      CALL F04ADF (CMAT, IA, BMAT, IB, N, M, BMAT, IC, SPACE, IFAIL)
      IF (IFAIL .EQ. 0) GO TO 20
      IFAIL = 2
      RETURN
C
C **** Multiply AMAT and BMAT back into CMAT (should give unit matrix)
C
20    DO 30 I = 1, N
      DO 30 J = 1, N
      CMAT(I,J) = (0.0, 0.0)
      DO 30 K = 1, N
      CMAT(I,J) = CMAT(I,J) + AMAT(K,J) * BMAT(I,K)
30    CONTINUE
C
C **** Find RMS sum of real and imag elements of CMAT
C
      REEL = 0.0
      EMAG = 0.0
      DO 40 I = 1, N
      DO 40 J = 1, N
      REEL = REEL + ABS(REAL(CMAT(I,J)))
      EMAG = EMAG + ABS(AIMAG(CMAT(I,J)))
40    CONTINUE
C
C **** Resulting sum should equal N if all OK
C
      ISUM = REEL + EMAG
      IF (ISUM .NE. N) IFAIL = 1
      RETURN
      END

```


E.2 Source code listing of program FORDIS

```
C **** FORDIS - A program to analyse expanding-geometry levitators ****
C
      PROGRAM FORDIS (INPUT=131B, OUTPUT=131B, TAPE5=INPUT,
C          TAPE6=OUTPUT, TAPE7=131B)
      COMPLEX AMAT(40,40), BMAT(40,40)
      COMPLEX RSIDE(40), RCURNT(40), BCURNT(41)
      DIMENSION RMUT(40), FX(41), FY(41)
      COMMON AMAT, BMAT
C
C **** Initialise all variables
C
      REWIND 7
      PI      = 3.14159265
      WIDTH   = 0.1
      THICK   = 0.003
      ROE     = 2.69E-08
      OMEGA   = 2.0 * PI * 50.0
      NBAR    = 40
      SLOTW   = 0.036
      TOOTH   = 0.019
      SCURNT  = 100.0
      P       = 0.0
      Q       = 0.01
C
C **** +-----+
C **** ! Part 1 - obtain rotor parameters !
C **** +-----+
C
C **** Ask for rotor parameters
C
      10  PRINT, 'Enter width and thickness of plate (mm)',
          READ (ERR=10, END=20, 5, ) W, T
          WIDTH = W * 0.001
          THICK  = T * 0.001
C
      20  PRINT, 'Enter resistivity (<CR> for aluminium)',
          READ (ERR=20, END=30, 5, ) R
          ROE = R
C
      30  PRINT, 'Enter frequency (Hz - <CR> for 50 Hz)',
          READ (ERR=30, END=40, 5, ) F
          OMEGA = 2.0 * PI * F
C
      40  PRINT, 'Enter number of rotor current bars',
          READ (ERR=40, END=60, 5, ) N
          IF (N .GT. 2 .AND. N .LE. 41) GO TO 50
          PRINT, 'A number between 3 and 41, please.'
          GO TO 40
      50  NBAR = N
C
C **** Set coil geometry variables
C
      60  NLOOP = NBAR - 1
          WBAR = WIDTH / FLOAT(NBAR)
          RA = WBAR / 2.0
          RC = WBAR / 2.0
C
C **** Get date, time, write output header
C
```

```

      CALL DATE (ID)
      CALL TIME (IT)
      WRITE (7, 70) ID, IT
70    FORMAT ('**** OUTPUT FILE FROM PROGRAM FORDIS ****',/
C      '**** PROGRAM RUN ON ', A10, 'AT', A10)
C
C **** Write rotor parameters to TAPE7
C
      IFREQ = OMEGA / (2.0*PI)
      WRITE (7, 80) WIDTH, THICK, ROE, IFREQ, NBAR, WBAR
80    FORMAT (/, 'ROTOR PLATE ', 3PF5.1, ' MM WIDE BY ', F5.1,
C      ' MM THICK',/, 'RESISTIVITY ', 1PE9.2, ' OHM-M',/,
C      ' AT FREQUENCY ', I3, ' HZ',/, 'SIMULATION BY ', I2,
C      ' CURRENT BARS, EACH ', 3PF5.1, ' MM WIDE')
C
C **** +-----+
C **** | Part 2 - construct rotor matrix, invert it |
C **** +-----+
C
C **** Find bar resistance, set real parts of rotor matrix
C
      RESIS = ROE / (WBAR * THICK)
      DO 100 I = 1, NLOOP
      DO 100 J = 1, NLOOP
      AMAT(I,J) = (0.0, 0.0)
      IF (I .EQ. J) AMAT(I,J) = CMPLX(2.0*RESIS, 0.0)
      IF (I .EQ. J+1) AMAT(I,J) = CMPLX(-RESIS, 0.0)
      IF (I .EQ. J-1) AMAT(I,J) = CMPLX(-RESIS, 0.0)
100    CONTINUE
C
C **** Calculate set of mutual inductances across plate
C
      DO 110 K = 1, NLOOP
      X = WBAR * FLOAT(K-1)
      RMUT(K) = EMLINK (X, 0.0, RA, RC, RA, RC)
110    CONTINUE
C
C **** Set up complex elements of rotor matrix
C
      DO 120 I = 1, NLOOP
      DO 120 J = 1, NLOOP
      K = IABS(I-J) + 1
      AMAT(I,J) = AMAT(I,J) + CMPLX(0.0, OMEGA*RMUT(K))
120    CONTINUE
C
C **** Output resulting matrix to TAPE7
C
      WRITE (7, 130)
130    FORMAT (/, 'INITIAL ROTOR MATRIX :-')
      DO 150 J = 1, NLOOP
      WRITE (7, 140) J, (AMAT(I,J), I=1, NLOOP)
140    FORMAT ('R ', I2, ': ', 6(1PE9.2, ' ', E9.2, ' J '),/,
C      6(6X, 6(E9.2, ' ', E9.2, ' J ')/))
150    CONTINUE
      PRINT, '** ROTOR MATRIX COMPLETE'
C
C **** Invert matrix - check inversion succeeded
C
      CALL CINVRT (AMAT, BMAT, NLOOP, IFAIL)
      IF (IFAIL .NE. 2) GO TO 160
      PRINT, '** NAG INVERSION ROUTINE FAILED - PROGRAM ABORTED'
      STOP

```

```
C
C **** Write inverted matrix to TAPE7
C
160  WRITE (7, 170)
170  FORMAT (/, "INVERTED ROTOR MATRIX :-")
      DO 180 J = 1, NLOOP
180  WRITE (7, 140) J, (BMAT(I,J),I=1,NLOOP)
C
C **** Now check inverted matrix sensible - not ill-conditioned
C
      IF (IFAIL .EQ. 0) GO TO 220
      WRITE (7, 190)
190  FORMAT (/ "**** ILL-CONDITIONED MATRIX, IFAIL = 1")
      PRINT, "** ILL-CONDITIONED MATRIX, SOLUTION UNRELIABLE"
      PRINT, "Enter <CR> to continue or X to stop",
      READ (ERR=200, END=230, 5, ) N
200  WRITE (7, 210)
210  FORMAT (/, "**** EXECUTION TERMINATED FROM TERMINAL ****")
      STOP
220  PRINT, "** MATRIX INVERSION COMPLETE"
C
C **** +-----+
C **** | Part 3 - set stator parameters |
C **** +-----+
C
C **** Get stator geometry
C
230  PRINT, "Enter stator slot width and tooth width (mm)",
      READ (ERR=230, END=240, 5, ) S, T
      SLOTW = S * 0.001
      TOOTH = T * 0.001
240  SX = (SLOTW+TOOTH) / 2.0
      SA = SLOTW/4.0 + TOOTH/2.0
      SC = SLOTW/4.0
C
C **** Get stator current, output stator parameters to TAPE7
C
250  PRINT, "Enter stator current (amps) ",
      READ (ERR=250, END=260, 5, ) S
      SCURNT = S
260  WRITE (7, 270) SLOTW, TOOTH, 2.0*SA, 2.0*SC, SCURNT
270  FORMAT (/, "STATOR SLOT WIDTH ", 3PF5.1, " MM AND TOOTH WIDTH ",
      C          F5.1, " MM"/, "SIMULATED BY TWO COILS OF SPACING ", F5.2,
      C          " MM AND CONDUCTOR WIDTH ", F5.2, " MM"/,
      C          "STATOR CURRENT ", 0PF5.1, " AMPS"/)
C
C **** +-----+
C **** | Part 4 - set rotor offset, construct column vector, |
C **** | solve rotor loop currents and bar currents |
C **** +-----+
C
C **** Get rotor/stator offset
C
300  PRINT, "Enter P and Q displacement of rotor centre (mm)",
      READ (ERR=300, END=310, 5, ) X, Y
      P = X * 0.001
      Q = Y * 0.001
310  WRITE (7, 320) P, Q
320  FORMAT (101("."/), "ROTOR DISPLACED BY", 3PF6.2,
      C          " MM HORIZONTALLY AND ", F5.2, " MM VERTICALLY"/)
```

```

C
C **** Set up vector for RHS of equation
C
      WRITE (7, 330)
330  FORMAT ('RIGHT-HAND SIDE OF EQUATION:/', 'COIL', 9X,
C        'OFFSET L', 9X, 'OFFSET R', 15X, 'RSIDE')
      DO 350 K = 1, NLOOP
      X = P - WIDTH/2.0 + WBAR*FLOAT(K)
      X1 = X + SX
      X2 = X - SX
      RTERM = -EMLINK (X1, Q, SA, SC, RA, RC)
C      +EMLINK (X2, Q, SA, SC, RA, RC)
      RSIDE(K) = CMPLX (0.0, RTERM*SCURNT*OMEGA)
      WRITE (7, 340) K, X1, X2, RSIDE(K)
340  FORMAT (I3, 11X, 3PF5.1, 12X, F5.1, 11X, 0PF4.1, ' ', 1PE9.2, 'J')
350  CONTINUE
C
C **** Multiply inverted matrix by right-hand side to obtain vector
C **** of rotor loop currents.
C
      DO 360 J = 1, NLOOP
      RCURNT(J) = (0.0, 0.0)
      DO 360 I = 1, NLOOP
      RCURNT(J) = RCURNT(J) + BMAT(I,J) * RSIDE(I)
360  CONTINUE
C
C **** Combine loop currents to solve for bar currents
C
      BCURNT(1) = RCURNT(1)
      DO 370 K = 2, NLOOP
370  BCURNT(K) = RCURNT(K) - RCURNT(K-1)
      BCURNT(NBAR) = -RCURNT(NLOOP)
      PRINT, '** ROTOR CURRENTS SOLVED'
C
C **** +-----+
C **** | Part 5 - force calculations |
C **** +-----+
C
C **** Set up loop, take rotor bar currents one by one ...
C
      WRITE (7, 410)
410  FORMAT (/, 'SOLUTION TO ROTOR CURRENTS AND FORCES:/', ' BAR', 5X,
C        'COMPLEX CURRENT', 13X, 'LEFT FORCE', 14X, 'RIGHT FORCE',
C        14X, 'TOTAL FORCE', 33X, 'HORIZ', 7X, 'VERT', 9X,
C        'HORIZ', 7X, 'VERT', 9X, 'HORIZ', 7X, 'VERT')
      DO 430 K = 1, NBAR
C
C **** Find component forces on rotor current from each stator current
C
      X = P - WIDTH/2.0 + WBAR*(FLOAT(K)-0.5)
      X1 = X + SX
      X2 = X - SX
      SCPROD = SCURNT * REAL(BCURNT(K))
      FXL = SCPROD * XFORCE (X1, Q, SA, SC, RC)
      FYL = SCPROD * YFORCE (X1, Q, SA, SC, RC)
      FXR = -SCPROD * XFORCE (X2, Q, SA, SC, RC)
      FYR = -SCPROD * YFORCE (X2, Q, SA, SC, RC)

```

```
C
C **** Sum forces, output whole to TAPE7
C
      FX(K) = FXL + FXR
      FY(K) = FYL + FYR
      WRITE (7, 420) K, BCURNT(K), FXL, FYL, FXR, FYR, FX(K), FY(K)
420  FORMAT (I3, 3X, 1PE9.2, ',', E9.2, 'J', 5X, E9.2, 2X,
      C      E9.2, 5X, E9.2, 2X, E9.2, 5X, E9.2, 2X, E9.2)
430  CONTINUE
C
C **** Now sum forces across whole plate to get resultant
C
      FXSUM = 0.0
      FYSUM = 0.0
      DO 440 K = 1, NBAR
      FXSUM = FXSUM + FX(K)
      FYSUM = FYSUM + FY(K)
440  CONTINUE
      WRITE (6, 450) FXSUM, FYSUM
      WRITE (7, 450) FXSUM, FYSUM
450  FORMAT (/, 'RESULTANT FORCE ON PLATE : ', 1PE9.2,
      C      ' N HORIZONTALLY AND ', E9.2, ' VERTICALLY'/)
C
C **** Back for another rotor position if required
C
500  PRINT, 'Enter <CR> for new rotor position or X to stop',
      READ (END=300, 5, 510) IANS
510  FORMAT (A10)
      IF (IANS .NE. 1HX) GO TO 500
      CALL TIME (IT)
      WRITE (7, 520) IT
520  FORMAT ('**** PROGRAM TERMINATED FROM TERMINAL AT', A10)
      WRITE (6, 530)
530  FORMAT ('** END OF PROGRAM - FULL OUTPUT LISTING IS ON TAPE7.'/)
      STOP
      END
```

E.3 Source code listing of program CONDAT

```
C **** CONDAT - Program FORDIS adapted to give contouring data ****
C
      PROGRAM CONDAT (INPUT=131B, OUTPUT=131B, TAPES=INPUT,
C          TAPE6=OUTPUT, TAPE7=131B)
      COMPLEX AMAT(40,40), BMAT(40,40)
      COMPLEX RSIDE(40), RCURNT(40), BCURNT(41)
      DIMENSION RMUT(40)
      COMMON AMAT, BMAT
C
C **** Initialise all variables
C
      REWIND 7
      PI      = 3.14159265
      WIDTH   = 0.1
      THICK   = 0.003
      ROE     = 2.69E-08
      OMEGA   = 2.0 * PI * 50.0
      NBAR    = 40
      SLOTW   = 0.036
      TOOTH   = 0.019
      SCURNT  = 100.0
      XL      = 0.0
      XR      = 0.04
      NUMX    = 9
      YB      = 0.005
      YT      = 0.02
      NUMY    = 4
C
C **** +-----+
C **** | Part 1 - obtain rotor parameters |
C **** +-----+
C
C **** Ask for rotor parameters
C
      10  PRINT, 'Enter width and thickness of plate (mm)',
          READ (ERR=10, END=20, 5, ) W, T
          WIDTH = W * 0.001
          THICK  = T * 0.001
C
      20  PRINT, 'Enter resistivity (<CR> for aluminium)',
          READ (ERR=20, END=30, 5, ) R
          ROE   = R
C
      30  PRINT, 'Enter frequency (Hz - <CR> for 50 Hz)',
          READ (ERR=30, END=40, 5, ) F
          OMEGA = 2.0 * PI * F
C
      40  PRINT, 'Enter number of rotor current bars',
          READ (ERR=40, END=60, 5, ) N
          IF (N .GT. 2 .AND. N .LE. 41) GO TO 50
          PRINT, 'A number between 3 and 41, please.'
          GO TO 40
      50  NBAR = N
C
C **** Set coil geometry variables
C
      60  NLOOP = NBAR - 1
          WBAR = WIDTH / FLOAT(NBAR)
          RA   = WBAR / 2.0
          RC   = WBAR / 2.0
```

```

C
C **** Get date, time, write output header
C
      CALL DATE (ID)
      CALL TIME (IT)
      WRITE (7, 70) ID, IT
70    FORMAT ('**** OUTPUT FILE FROM PROGRAM CONDAT ****'/,
C        '**** PROGRAM RUN ON ', A10, 'AT', A10)
C
C **** Write rotor parameters to TAPE7
C
      IFREQ = OMEGA / (2.0*PI)
      WRITE (7, 80) WIDTH, THICK, ROE, IFREQ, NBAR, WBAR
80    FORMAT (/, 'ROTOR PLATE ', 3PF5.1, ' MM WIDE BY ', F5.1,
C        ' MM THICK'/, 'RESISTIVITY ', 1PE9.2, ' OHM-M,',
C        ' AT FREQUENCY ', I3, ' HZ'/, 'SIMULATION BY ', I2,
C        ' CURRENT BARS, EACH ', 3PF5.1, ' MM WIDE')
C
C **** +-----+
C **** | Part 2 - construct rotor matrix, invert it |
C **** +-----+
C
C **** Find bar resistance, set real parts of rotor matrix
C
      RESIS = ROE / (WBAR * THICK)
      DO 100 I = 1, NLOOP
      DO 100 J = 1, NLOOP
      AMAT(I,J) = (0.0, 0.0)
      IF (I .EQ. J) AMAT(I,J) = CMPLX(2.0*RESIS, 0.0)
      IF (I .EQ. J+1) AMAT(I,J) = CMPLX(-RESIS, 0.0)
      IF (I .EQ. J-1) AMAT(I,J) = CMPLX(-RESIS, 0.0)
100    CONTINUE
C
C **** Calculate set of mutual inductances across plate
C
      DO 110 K = 1, NLOOP
      X = WBAR * FLOAT(K-1)
      RMUT(K) = EMLINK (X, 0.0, RA, RC, RA, RC)
110    CONTINUE
C
C **** Set up complex elements of rotor matrix
C
      DO 120 I = 1, NLOOP
      DO 120 J = 1, NLOOP
      K = IABS(I-J) + 1
      AMAT(I,J) = AMAT(I,J) + CMPLX(0.0, OMEGA*RMUT(K))
120    CONTINUE
      PRINT, '** ROTOR MATRIX COMPLETE'
C
C **** Invert matrix - check inversion succeeded
C
      CALL CINVRT (AMAT, BMAT, NLOOP, IFAIL)
      IF (IFAIL .NE. 2) GO TO 130
      PRINT, '** NAG INVERSION ROUTINE FAILED - PROGRAM ABORTED'
      STOP

```

```

C
C **** Now check inverted matrix sensible - not ill-conditioned
C
130 IF (IFAIL .EQ. 0) GO TO 170
    WRITE (7, 140)
140 FORMAT (/'**** ILL-CONDITIONED MATRIX, IFAIL = 1')
    PRINT, '** ILL-CONDITIONED MATRIX, SOLUTION UNRELIABLE'
    PRINT, 'Enter <CR> to continue or X to stop',
    READ (ERR=150, END=200, 5, ) N
150 WRITE (7, 160)
160 FORMAT (/, '**** EXECUTION TERMINATED FROM TERMINAL ****')
    STOP
170 PRINT, '** MATRIX INVERSION COMPLETE'
C
C **** +-----+
C **** ! Part 3 - set stator parameters !
C **** +-----+
C
C **** Get stator geometry
C
200 PRINT, 'Enter stator slot width and tooth width (mm)',
    READ (ERR=200, END=210, 5, ) S, T
    SLOTW = S * 0.001
    TOOTH = T * 0.001
210 SX = (SLOTW+TOOTH) / 2.0
    SA = SLOTW/4.0 + TOOTH/2.0
    SC = SLOTW/4.0
C
C **** Get stator current, output stator parameters to TAPE7
C
220 PRINT, 'Enter stator current (amps) ',
    READ (ERR=220, END=230, 5, ) S
    SCURNT = S
230 WRITE (7, 240) SLOTW, TOOTH, 2.0*SA, 2.0*SC, SCURNT
240 FORMAT (/, 'STATOR SLOT WIDTH ', 3F5.1, ' MM AND TOOTH WIDTH ',
C      F5.1, ' MM',/, 'SIMULATED BY TWO COILS OF SPACING ', F5.2,
C      ' MM AND CONDUCTOR WIDTH ', F5.2, ' MM',/,
C      'STATOR CURRENT ', 0PF5.1, ' AMPS')
C
C **** +-----+
C **** ! Part 4 - find required set of rotor positions !
C **** +-----+
C
C **** Get rotor horizontal range and grid spacings
C
300 PRINT, 'Enter left and right limits of rotor movement (mm)',
    READ (ERR=300, END=310, 5, ) R1, R2
    XL = R1 * 0.001
    XR = R2 * 0.001
310 PRINT, 'Enter number of positions over horizontal range',
    READ (ERR=310, END=320, 5, ) NUM
    NUMX = NUM
C
C **** Get rotor vertical range and grid spacings
C
320 PRINT, 'Enter bottom and top limits of rotor movement (mm)',
    READ (ERR=320, END=330, 5, ) R1, R2
    YB = R1 * 0.001
    YT = R2 * 0.001
330 PRINT, 'Enter number of positions over vertical range',
    READ (ERR=330, END=340, 5, ) NUM
    NUMY = NUM

```



```

C
C **** Output ranges to TAPE7, also column headers
C
340  WRITE (7, 350) NUMX, XL, XR, NUMY, YB, YT
350  FORMAT ('RANGE OF ROTOR POSITIONS:', I3,
C          ' POSITIONS HORIZONTALLY FROM ', 3PF6.2, ' MM TO ',
C          F6.2, ' MM', I3, ' POSITIONS VERTICALLY FROM ',
C          F6.2, ' MM TO ', F6.2, ' MM')
      WRITE (7, 360)
360  FORMAT ('ROTOR POSITION', 6X, 'RESULTANT FORCE',
C          ' HORIZ  VERT', 6X, 'HORIZ', 7X, 'VERT')
C
C **** Set up main loops to take each position in turn
C
      DELX = (XR-XL) / FLOAT(NUMX-1)
      DELY = (YT-YB) / FLOAT(NUMY-1)
      YY = YB
      DO 460 KOUNTV = 1, NUMY
      XX = XL
      DO 450 KOUNTH = 1, NUMX
C
C **** Set up vector for RHS of equation
C
      DO 400 K = 1, NLOOP
      X = XX - WIDTH/2.0 + WBAR*FLOAT(K)
      X1 = X + SX
      X2 = X - SX
      RTERM = -EMLINK (X1, YY, SA, SC, RA, RC)
C          +EMLINK (X2, YY, SA, SC, RA, RC)
      RSIDE(K) = CMPLX (0.0, RTERM*SCURNT*OMEGA)
400  CONTINUE
C
C **** +-----+
C **** | Part 5 - solve for rotor bar currents |
C **** +-----+
C
C **** Multiply inverted matrix by right-hand side to obtain vector
C **** of rotor loop currents.
C
      DO 410 J = 1, NLOOP
      RCURNT(J) = (0.0, 0.0)
      DO 410 I = 1, NLOOP
      RCURNT(J) = RCURNT(J) + BMAT(I,J) * RSIDE(I)
410  CONTINUE
C
C **** Combine loop currents to solve for bar currents
C
      BCURNT(1) = RCURNT(1)
      DO 420 K = 2, NLOOP
420  BCURNT(K) = RCURNT(K) - RCURNT(K-1)
      BCURNT(NBAR) = -RCURNT(NLOOP)
C
C **** +-----+
C **** | Part 6 - force calculations |
C **** +-----+
C
C **** Set up loop, take rotor bar currents one by one ...
C
      FXSUM = 0.0
      FYSUM = 0.0
      DO 430 K = 1, NBAR

```

```
C
C **** Find component forces on rotor current from each stator current --
C
      X = XX - WIDTH/2.0 + WBAR*(FLOAT(K)-0.5)
      X1 = X + SX
      X2 = X - SX
      SCPROD = SCURNT * REAL(BCURNT(K))
      FXL = SCPROD * XFORCE (X1, YY, SA, SC, RC)
      FYL = SCPROD * YFORCE (X1, YY, SA, SC, RC)
      FXR = -SCPROD * XFORCE (X2, YY, SA, SC, RC)
      FYR = -SCPROD * YFORCE (X2, YY, SA, SC, RC)
C
C **** Sum forces across whole plate to get resultant
C
      FXSUM = FXSUM + FXL + FXR
      FYSUM = FYSUM + FYL + FYR
430  CONTINUE
C
C **** Write out result, back till all loops completed
C
      WRITE (7, 440) XX, YY, FXSUM, FYSUM
440  FORMAT (3PF6.2, 2X, F6.2, 3X, 1PE9.2, 2X, E9.2)
450  XX = XX + DELX
460  YY = YY + DELY
C
C **** End of run - write messages
C
      CALL TIME (IT)
      WRITE (7, 500) IT
500  FORMAT (/'**** PROGRAM COMPLETED AT', A10)
      WRITE (6, 510)
510  FORMAT (/' ** RUN COMPLETE - OUTPUT IS ON TAPE7.'/)
      STOP
      END
```